MUCUS-BACTERIA INTERACTIONS IN THE GUT: INVESTIGATING THE ROLE OF THE MUCIN MUC2 AND ITS GLYCOSYLATION IN HOST DEFENSE DURING ENTERIC BACTERIAL INFECTIONS

by

Kirandeep Bhullar

B.Sc., McMaster University, 2009

M.Sc., McMaster University, 2011

A THESIS SUBMITTED IN PARTIAL FULFILLMENT OF

THE REQUIREMENTS FOR THE DEGREE OF

DOCTOR OF PHILOSOPHY

in

THE FACULTY OF GRADUATE AND POSTDOCTORAL STUDIES

(Experimental Medicine)

THE UNIVERSITY OF BRITISH COLUMBIA

(Vancouver)

April 2016

Abstract

The intestinal mucus layer, which is largely composed of the secreted mucin Muc2 provides a first line of defense in the intestine. Muc2 is a heavily O-glycosylated protein with core 1 and core 3 derived O-glycans as primary constituents. It plays an important role in host defense against the attaching/effacing (A/E) pathogen *Citrobacter rodentium*. However whether it provides protection against the invasive human pathogen *Salmonella* is still unclear. Furthermore, the role of O-glycosylation in mediating the protective role played by the Muc2 mucin against enteric pathogens has not been investigated. Likewise, although almost all enteric bacterial pathogens must cross the overlying mucus layer to infect the intestinal epithelium, there is very little known about mucus-enteric bacterial interactions and virulence strategies used to accomplish this feat. We began our investigations by comparing *Salmonella*-induced colitis and mucus dynamics in Muc2-deficient (*Muc2* -/-), *C3GnT* -/-, and C57BL/6 (WT) mice. While absence of core 3 derived O-glycosylation only impacted epithelial barrier integrity, absence of Muc2 resulted in significantly higher barrier disruption, host mortality rates, and increased colonic and systemic *Salmonella* burdens. Likewise, absence of core 1 derived O-glycans (*C1galt1 -/-* mice) resulted in heightened susceptibility to *C. rodentium*, characterized by impaired mucus levels in the lumen, and bacterial aggregation in close proximity to the intestinal epithelial surface, phenotypes not seen in WT or *C3GnT -/-* counterparts. To understand if the non-motile pathogen *C. rodentium* used bacterial proteases/mucinases as a mucus degrading strategy to gain access to the underlying epithelium, we investigated the role of a putative mucinase and a class 2 SPATE PicC. While PicC did not affect *C. rodentium's* ability to colonize the colon, it appeared to have an unprecedented role in regulating *C. rodentium*'s activation of the innate receptor TLR2, suggesting that despite its mucinase activity, PicC's

major roles *in vivo* may be to limit *C. rodentium* aggregation and its recognition by the host's innate immune system. Overall these studies highlight a novel protective role of Muc2 and its O-linked glycosylation in host defense against enteric infections and the importance of Muc2-mediated regulation of pathogen burdens at the intestinal epithelial surface.

Preface

Chapter 3

I designed and conducted majority of the experiments, analyzed majority of the data and wrote the manuscript under the supervision of my supervisor Dr. Bruce Vallance. However, I did receive assistance from several personnel in the lab as described below: Dr. Maryam Zarepour helped me plan and execute the initial experiments of this study. She assisted me with animal experiments throughout the course of this study. Dr. Mari Montero provided useful insights and advice for the completion of this study. Caixia Ma helped with the animal infections and barrier function studies. Tina Huang helped with the immunostaining. *Muc2* -/- mice were kindly provided by Dr. Anna Velcich. *C3GnT* -/- mice were generated and kindly provided by Dr. Lijun Xia, University of Oklahoma. This study was published in the journal Infection and Immunity and is referenced by the following citation:

Zarepour M**, **Bhullar K**, Montero M, Ma C, Huang T, Velcich A, Xia L, Vallance BA.The mucin Muc2 limits pathogen burdens and epithelial barrier dysfunction during Salmonella enterica serovar Typhimurium colitis. Infect. Immun. 2013 Oct;81(10):3672-83.
**** co-first authors**

Chapter 4

I was responsible for the majority of the the experimental design and execution described in this chapter. I analyzed all the data and wrote the manuscript under the direction of Dr. Bruce Vallance. Dr. Maryam Zarepour assisted with animal experiments. Dr. Hongbing Yu helped with the optimization of biofilm formation and curli/cellulose production assays. He also assessed the T3SS profiles presented in the study. Dr. Hong Yang optimized and conducted the *in vitro* TLR2 and TLR4 activation assays. Dr. Matthew Croxen constructed all the mutant/complemented strains used in the study. Dr. Martin Stahl assisted with mucin quantification studies conducted at

University of Calgary and animal infections. Steve Cornick and Dr. Kris Chadee at University of Calgary were instrumental in conducting the mucus quantification studies. Caixia Ma assisted with initial infections and colonization studies and *in vivo* intestinal permeability assay. Tina Huang assisted with immunofluorescence staining. A version of this study was published in the journal Infection and Immunity and is referenced by the following citation:

Bhullar K, Zarepour M, Yu H, Yang H, Croxen M, Stahl M, Finlay BB, Turvey SE, Vallance BA. The Serine Protease Autotransporter Pic Modulates Citrobacter rodentium Pathogenesis and Its Innate Recognition by the Host. Infect Immun. 2015 Jul;83(7):2636-50.

Chapter 5

I was the primary contributor to this work. I designed and conducted majority of the experiments performed in this study, analyzed all the data/results and wrote this chapter with guidance from my supervisor Dr. Bruce Vallance. Dr Hyungjun Yan and Caixia Ma assisted with animal experimentation. Dr. Hongbing Yu and Caixia Ma constructed the Δ*fucK* mutant used in this study and provided the screening primer sequences. Tina Huang assisted with immunofluorescence staining. IEC *C1galt1 -/-* and *C3GnT -/-* mice were generated and kindly provided by Dr. Lijun Xia, University of Oklahoma. Dr. Martin Stahl shared useful insights regarding the fucose feeding studies. A version of this chapter will be submitted for publication.

Ethics approval

The animal research presented was conducted in accordance with guidelines provided by the Canadian Council on the Use of Laboratory Animals and approved by the UBC Animal Care Committee. UBC protocol numbers relevant to this thesis are: A09-0604 (Breeding Program),

A11-0253 (*Salmonella* Typhimurium infections) and A11-0290 (*Citrobacter rodentium* infections).

Table of Contents

List of Tables

List of Figures

List of Abbreviations

AMP	Antimicrobial peptide
AB	Alcian blue
aroA	Aromatic amino acids
AT	Autotransporters
BFP	Bundle forming protein
BSA	Bovine serum albumin
BSM	Bovine submaxillary mucin
C. jejuni	*Campylobacter jejuni*
CD	Cluster of differentiation
CFU	Colony forming units
CPM	Counts per minute
CMT	Carcinoma of mouse rectum
CpG	Cytosine triphosphate deoxynucleotide- guanine triphosphate deoxynucleotide
DAPI	4’,6’-diamidino-2-phenylindole
DC	Dendritic cells
DMEM	Dulbecco's Modified Eagle's medium
DPI	Days post-infection
DSS	Dextran sulfate sodium
E.coli	*Escherichia coli*
EAEC	Enteroaggregative *E. coli*
EHEC	Enterohaemorrhagic *E. coli*

EPEC	Enteropathogenic *E.coli*
ER	Endoplasmic reticulum
Esc	*E. coli* secretion
Esp	E. coli secreted protein
FBS	Fetal bovine serum
FITC	Fluorescein isothiocyanate
fuc	Fucose operon
Fut	Fucosyltransferases
GADPH	Glyceraldehyde 3-phosphate dehydrogenase
GI	Gastrointestinal
GRP	Glucose regulated protein
Hbp	Hemoglobin-binding protease autotransporter
HCl	Hydrochloric acid
IAP	Intestinal alkaline phosphatase
IBD	Inflammatory bowel disease
IEC	Intestinal epithelial cell
IFN	Interferon
IL	Interleukin
iNOS	Inducible nitric oxide synthase
Inv	Invasin
KC	Keratinocyte-derived cytokine
LB	Luria broth

LEE	Locus of enterocyte effacement
LER	locus of enterocyte effacement encoded regulator
LPS	Lipopolysaccharide
M cells	Microfold cells
MAP	Mitochondrial-associated protein
MCP	Monocyte chemoattractant protein-1
MLN	Mesenteric lymph nodes
MOI	Multiplicity of infection
MUC	Mucin
MyD88	Myeloid differentiation primary response gene (88)
$NaBH_4$	Sodium borohydride
NADPH	Nicotinamide adenine dinucleotide phosphate
NaOH	Sodium hydroxide
NF-κB	Nuclear factor-kappaB
NLR	Nod-like receptor
nramp	Natural resistance-associated macrophage protein
O/N	Overnight
PAS	Periodic acid schiff
PAMP	Pathogen associated molecular pattern
PBS	Phosphate-buffered saline
PCR	Polymerase chain reaction
Pet	Plasmid-encoded toxin

PGC	Porous graphitic carbon
Pic	Protein involved in intestinal colonization
PKC	Protein kinase C
PMN	Polymorphonuclear leukocytes
PMSF	Phenylmethylsulfonylfluoride
PRR	Pattern recognition receptor
PSGL	P-selectin glycoprotein ligand-1
PTS	Proline- threonine -serine
qPCR/RT-PCR	Quantitative PCR/Reverse-transcription PCR
REG	Regenerating islet- derived protein
Relm	Resistin-like molecule
RDAR	Red, dry and rough
S. flexneri	*Shigella flexneri*
*S.*typhimurium	*Salmonella enterica* serovar *Typhimurium*
Sat	Secreted autotransporter toxin
SCFA	Short chain fatty acids
SDS-PAGE	sodium dodecyl sulfate polyacrylamide gel electrophoresis
SEM	Standard error mean
SFB	Segmented filamentous bacteria
Sig	Shigella IgA-like protease
SPATE	Serine protease autotransporters of Enterobacteriaceae

SPE	Solid-phase extraction
SPF	Specific pathogen free
SPI	*Salmonella* pathogenicity island
T3SS	Type three secretion system
TFA	Trifluoroacetic acid
Tff	Trefoil factor
Th	Helper T-cells
TIR	Translocated intimin receptor
TLR	Toll-like receptor
TNF	Tumor necrosis factor
Tsh	Temperature-sensitive hemagglutinin
UC	Ulcerative colitis
UPEC	Uropathogenic *E. coli*
V. cholera	*Vibrio cholera*
VNTR	Variable number tandem repeat
WT	Wild-type

Acknowledgements

It truly is an honor to be graduating from UBC, one of the world's leading university in research and innovation. As this remarkable journey comes to an end, I would like to thank my supervisor Dr. Bruce Vallance for his tremendous support, guidance and exemplary mentorship. Bruce, it's been a great learning experience working with you. Thank you for supporting me at every step of my Ph.D. degree and for an opportunity to work in your lab. A heart-filled thank you to past and present Vallance lab members and fellow trainees for contributing towards my learning, teaching me different lab skills and adding to the breadth of my knowledge by offering their experiences and creating a positive work environment. I would like to thank my committee members Dr. Erin Gaynor and Dr. Del Dorscheid for their feedback, guidance and encouragement throughout my graduate studies. I would also like to thank the Faculty of Graduate Studies (FoGS) and the Department of Experimental Medicine for their administrative support

I would like to thank my family for providing me with endless emotional and moral support and for believing in me. My mom (Harjinder Bhullar), dad (Lachhman Bhullar) and brother (Satinder Bhullar) moved to Canada so that I could have better education opportunities. Thank you Satinder, you are an awesome brother who always supported me. Thank you mom and dad for teaching me the values of honesty, hard work, perseverance and sincerity and for all that you have done for me so that I can have a better life.

Last but not the least, I would like to thank a wonderful friend and my husband Jasmeet. With you, life is filled with positivity and happiness. Thank you for your patience, unconditional love and unreserved support. Whenever I needed to take my mind off science and talk about life,

you were there for me. Thank you for sharing my excitements and failures and for standing by me through all the ups and downs of graduate student life.

To all those who go to a great extent in their quest for knowledge and learning.

To all the women aspiring to become scientists.

Chapter 1: Introduction

1.1 The intestinal ecosystem- a primary site of host-environment interactions

The gastrointestinal (GI) tract is a complex organ system which functions primarily to digest food, absorb nutrients and expel waste [1,2]. It harbors more bacteria than the total number of cells in the human body, but surprisingly enough, hosts and their microbiota co-exist in a harmonious, mutualistic relationship under normal conditions [3,4]. The GI tract is the primary site of interactions between a host and its environment. The commensal microbiota play an important role in priming host immune responses, aid in the digestion of complex dietary fibres, help in the absorption of key vitamins and minerals, and promote colonization resistance against enteric infections [5–8]. The host in turn benefits from the carbon sources and energy produced by microbiota and correspondingly the commensal microbes are provided with a rich supply of mucus-associated glycans, diet-dependent nutrients (e.g. undigestable polysaccharides) and metabolites (bile acids, lipids, amino acids) and a favourable, anoxic environment [6,9].It is intriguing that despite such an abundance of microbial antigens and their immunogenic potential, the GI tract remains in a relatively hypo-responsive and tolerogenic mode, by keeping a constant check on the immune responses triggered by the commensal microflora, meaning that in a healthy individual the host immune system tolerates the presence of commensal microbiota without any overt or undesirable activation of the immune system [10–13].The physical and biochemical segregation of the commensal microbes from the host intestinal surface is mediated by a thick, complex mucus layer, also containing antibodies (IgA, IgG) and antibacterial factors such as lysozyme and high concentrations of antimicrobial peptides in close proximity to the epithelial surface. These factors restrict bacteria to the lumen and protect the underlying epithelium from unnecessary exposure to the commensals[14]. Likewise the spatial and temporal regulation of innate immune signalling, anatomical segregation and reduced expression and

sequestering of sensing receptors helps in maintaining the state of hyporesponsive immune signalling at the intestinal surface[15]. While intestinal epithelial cells provide a protective barrier against luminal bacteria, there are specialized sites in the GI tract (Peyer's patches) which constantly sample commensal microbes and luminal contents allowing their uptake by antigen presenting dendritic cells (DC). These DC promote the differentiation of naïve CD4+ T cells into regulatory T cells and the maturation of B cells, priming the immune system for antigenic encounter[16]. Therefore, the presence of commensals promotes the development of tightly controlled and regulated innate and adaptive immune responses and results in heightened inflammatory tone within the GI tract, also known as "physiological inflammation"[12]. Therefore, the GI tract offers a unique environment that exists in a state of "armed peace" where constant interactions between the intestinal epithelium and commensals prepare the immune system to defend against pathogenic bacteria and other intruders. Unlike commensal microbes, enteric bacterial pathogens are capable of subverting the various protective intestinal barriers, ultimately infecting and causing damage to the intestinal epithelium[17]. Infection by enteric bacterial pathogens typically breaches the intestinal protective barriers and causes excessive stimulation of the innate immune signalling pathways within intestinal epithelial cells and underlying inflammatory/immune cells, resulting in increased production of proinflammatory cytokines and increased recruitment of immune cells to the site of infection. The interactions between the intestinal epithelium and enteric pathogens are primarily mediated by virulence effectors secreted into the host cells[18]. This represents a state of "war" where the fate of infection is determined by the host (mounting inflammatory responses) and the pathogen (exploiting host signalling pathways and subverting the function of epithelial cells).The GI tract, therefore, provides an important site for studying the interactions between the host and its environment and

different aspects of the complex interplay between host intestinal epithelial cells, host mucus layer and enteric pathogens will be explored in the following chapters.

1.1.1 The intestinal epithelium

The intestinal epithelial cells (IEC) lining the GI tract play a critical role in providing host defense against foreign agents, including toxins and bacterial products[19]. IEC in the colon are organized in a monolayer and consist of columnar epithelial cells, held together by tight junctions. IEC are further classified into secretory IEC consisting of enteroendocrine cells (secrete hormones such as serotonin and vasoactive intestinal peptide), goblet cells (secrete mucin Muc2), Paneth cells (secrete antimicrobial peptides) and absorptive enterocytes, which on their own, constitute more than 80% of all IEC[20–22]. Hormone-secreting enteroendocrine cells play an important role in gut motility and digestive physiology but compromise only a small percentage (< 1%) of the overall epithelial cell population[23]. Paneth cells are specialized in producing a wide variety of AMPs but are only found at the base of the small intestinal crypts[24]. Mucus-producing goblet cells are the second most abundant IEC subtype present in an increasing gradient from small intestine to the descending colon, where they can make upto 20% of the total IEC population[25,26]. Enterocytes possess a greater surface area due to the presence of dense microvilli on their apical surface and are largely responsible for absorption and transport of nutrients across the intestinal mucosal surface, aiding in digestion[27].

Pluripotent epithelial stem cells are localized at the base of crypts and are important for renewal, proliferation and differentiation of IEC into different cell lineages[20,28,29]. Intestinal epithelial stem cells are identified by the presence of the Lgr5 marker (Leucine-rich repeat-containing G protein-coupled receptor 5)[30,31]. Differentiated IEC migrate up the crypt-villus axis, ultimately resulting in terminal differentiation into one of the four principle cell lineages. Notch

and Wnt signalling pathways play an important role in specifying the fate of the epithelial stem cells and in maintaining the cells at a proliferative stage in the transient amplifying zone, a region found in the bottom portion of the crypts[31]. Disruption of Notch signalling pathway results in the conversion of proliferative cells into secretory cell lineages of the intestine such as, goblet cells and enteroendocrine cells[32,33], whereas inhibition of Wnt signalling drives the fate of proliferating cells towards enterocytes (absorptive cells)[34,35], suggesting that the undifferentiated, proliferative state is maintained by the concerted actions of both pathways. Although there are multiple factors involved in determining the fate of specific cell types, signalling cascades involving the transcription factors Hes1 (Notch pathway) and Math1 (Wnt pathway) regulate the secretory and absorptive cell fates respectively[36–38].

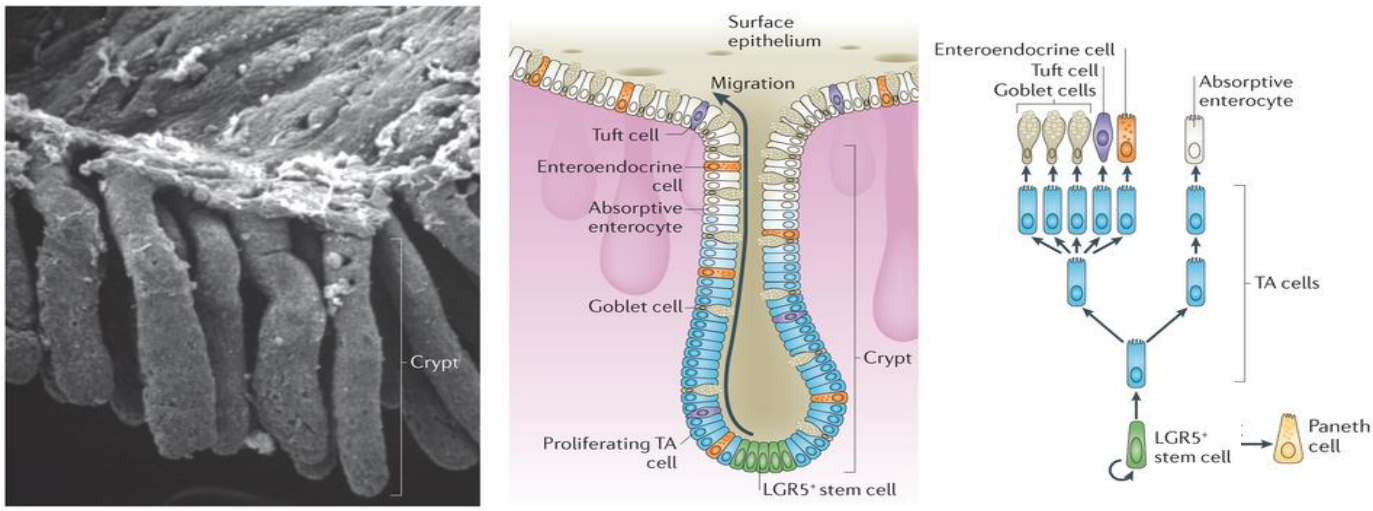

Figure 1.1 The intestinal colonic crypt structure and lineages of the intestinal tract.
Left panel shows the structural organization of intestinal crypts, as depicted through scanning electron microscopy (SEM). The Lrg5+ stem cells are found at the base of crypts and rapidly proliferate to generate epithelial progenitor cells, also known as proliferating transit-amplifying (TA) cells. TA cells undergo terminal differentiation to generate the various functional IEC subsets (enteroendrocrine cells, enterocytes, goblet cells, tuft cells, found in both the small intestine and colon) and paneth cells (found at the base of the crypt only in the small intestine, not shown). Image reproduced from reference [28] with permission.

Secretory IEC (goblet cells and paneth cells) provide the first line of defense against microbial intrusion by forming a protective barrier overlying the IEC[39,40]. Goblet cells secrete mucins, which is critical for flushing bacteria away from the intestinal surface. The intestinal mucus layer, largely composed of the mucin Muc2 also provides a thick physical and biochemical barrier to protect the underlying intestinal epithelium from intruding commensal and pathogenic microbes[39,41]. Furthermore, the gel-like consistency of the mucus layer facilitates the constant movement and passage of luminal contents through the GI tract[25]. The goblet cell mediators, Trefoil-like factor 3 (Tff3) and Resistin-like molecule-β (Relm-β) provide additional layers of host defense. Tff3 promotes epithelial cell migration over sites of mucosal injury, thereby stimulating healing of the intestinal mucosa and providing structural integrity and stability to the mucus layer[42,43]. Furthermore, Tff3 and mucin glycoproteins display synergistic protection against bacterial toxins by reducing epithelial permeability[44]. Relm-β has been shown to regulate host-protective adaptive CD4 (+) T cell responses promoting parasite-infection induced intestinal inflammation[45]. In a DSS-colitis model, Relm-β was shown to exert pro-inflammatory responses by inducing TNF-α production in a dose-dependent manner[46]. A recent study revealed an unexpected role of Relm-β in host defense against enteric pathogens by recruiting CD4 (+) T cells to the site of *C. rodentium* infection and promoting intestinal epithelial cell proliferation through the production of IL-22[45]**.** Secretion of antimicrobial peptides (AMP) such as α- defensins, lysozyme, C-type lectins and phospholipases by small intestinal Paneth cells into the crypt lumen is thought to prevent invasion of crypts by enteric pathogens. Most of the secreted AMP have broad spectrum activity against most pathogenic as well as commensal microbes. Secreted AMP can also migrate to the large intestinal mucus layer, largely driven by the diffusion of these bactericidal components down the GI tract through intestinal contractions

and motility where they provide an antimicrobial defense barrier of the intestinal mucosa against microbial attachment and invasion[14,47–49]. Epithelial cells are sealed by tight junctions which connect adjacent IEC and regulate intestinal permeability, thereby offering an impervious layer of defense against penetration by bacterial antigens[50–52]. Tight junctions are largely composed of a family of transmembrane proteins- claudins, zonula occludens 1 (ZO1) and occludin. Associated with cellular cytoskeletal components, including actin and myosin, tight junctions protect the basolateral surface of enterocytes from antigen exposure and other unwanted toxins and are critical determinants of epithelial barrier integrity[53].

Furthermore, even under the "normal - uninflamed" state, IEC are protected by the of several types of immune cells such as lymphocytes, natural killer cells, innate lymphoid cells (ILCs) and CD4 (+) T cells in the underlying lamina propria. The lamina propria is located beneath the basement membrane of the epithelial cells. Subepithelial dendritic cells constantly sample bacterial antigens and transfer antigenic signals (e.g. bacterial products) to lamina propria lymphocytes and these signals are important for the development of appropriate tolerogenic or host defense immune responses[5455]. Dendritic cells sample both enteric pathogens and non-invasive commensal bacteria[55]. In conclusion, IEC are crucial in the promotion of intestinal homeostasis and produce multiple layers of host-defenses to ensure that IEC sustain an appropriate physical and biochemical barrier between the host and its luminal environment.

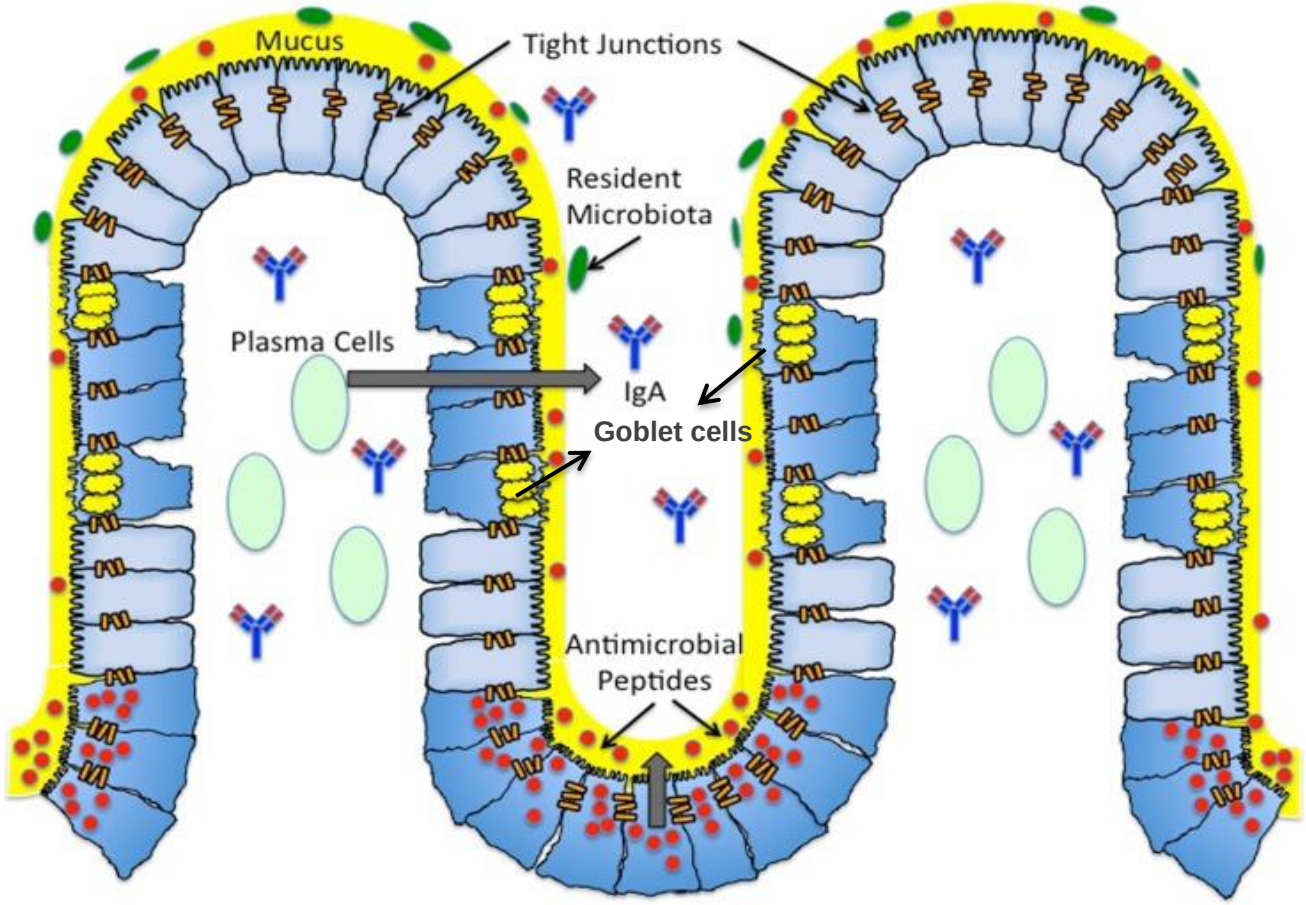

Figure 1.2 The architecture of the intestinal mucosa.
This image represents different epithelial cell types that contribute to the host-defense layers of the intestinal mucosa. The mucus layer (yellow) is primarily composed of the mucin Muc2 which is released by goblet cells (yellow granules) and is a frontline defense barrier, protecting the underlying epithelium from commensal microbes and enteric pathogens. Secreted antimicrobial peptides (defensins, lysozyme) reside in the mucus layer and provide further host defense through broad spectrum anti-bacterial activity. Commensal microbiota promotes colonization resistance to intestinal pathogens by competing for nutrients and space and is crucial in preventing rapid colonization of IEC by enteric pathogens. Furthermore, secreted IgA, produced by plasma B cells and concentrated in the thick mucus layer provides additional host defense by removing antigens and preventing pathogens from adhering to the mucosa. Interactions between epithelial cells through tight junctions form a protective barrier by sealing the epithelial layer against bacterial penetration. This figure was reproduced from reference [56] under the Creative Commons Attribution License.

1.1.2 Innate immune signalling in the intestinal epithelium

In addition to promoting host defense, IEC act as frontline sensors for microbial encounters. IEC express a variety of pattern recognition receptors (PRR), which consist of toll-like receptors (TLR) and nucleotide olgomerization domain-like receptors (NLR). These receptors sense PAMPS (pathogen associated molecular patterns) triggering cytokine production and other pro-inflammatory responses as well as activation of adaptive immune responses[56–58]. While TLRs are found associated with cell-surfaces and in endosomes, NLRs consists of soluble proteins that detect the presence of intracellular pathogens. TLR are the best studied innate immune receptors and their importance in stimulating host innate and adaptive immune responses and contributing to host defense is now well established[59]. To date, 10 TLR have been identified in humans and 12 TLRs have been reported in mice. Despite some notable differences between mice and human TLRs, much of our understanding in the field of innate immunology comes from the use of various mouse models[60,61]. Polarized expression of TLRs is thought to be important for maintaining epithelial barrier function and controlling development of host immune responses by enhancing the ability of DC to emit projections between IEC for luminal sampling[62]. IEC TLR signalling has also been implicated in the production of antimicrobial peptides (stimulating Paneth cell to release AMP) and Tff3 to repair intestinal injury damage[63–65]. In mice, TLR2 is expressed on the apical side of epithelial cells, facing the intestinal lumen where it recognizes lipopeptides found on the surface of many bacteria. TLR2 can also form heterodimers with TLR1 and TLR6. TLR2-TLR1 and TLR2-TLR6 heterodimers recognize triacylated (Gram-negative) and diacylated (Gram-positive) lipopeptides, respectively[57]. More recent studies have shown that TLR2 can also interact with curli fibrils (bacterial surface structures) produced by *Enteriobacteriaceae* as they form biofilms[66]. TLR4

and its co-receptor MD-2 are also expressed on the apical side of IEC (but at very low levels) and recognize lipopolysaccharide (LPS)[57,67]. TLR5 is found on the basolateral surface and recognizes flagellin[68,69]. TLR9 is found on both the apical and basolateral sides of IEC and recognizes the unmethylated CpG motifs found in the DNA from viruses and bacteria[70]. Stimulation of TLR signalling facilitates the activation of the MyD88 (myeloid differentiation primary-response protein 88) (TLR1, TLR2, TLR4, TLR5, TLR6, TLR9) pathway or the MyD88 independent pathway (TLR4). Activation of the signalling cascade leads to translocation of nuclear factor-kappaB (NF-kb) to the nucleus and induces expression of pro-inflammatory cytokines. In addition to the intestinal epithelium, TLR are also expressed in other host cells, such as monocytes, macrophages and dendritic cells. It is important to note that there are differences in the spatial distribution, expression and functionality of TLRs in IEC. This selectivity allows the intestinal epithelium to remain in a generally hypo-responsive state, despite their constant exposure to microbial ligands from commensal microbiota[57,61,67,71].

Specialized IECs called the microfold cells (M cells) are important for sampling of luminal antigens by dendritic cells which are the key antigen presenting cells in the gut. The recognition of antigens and invading microbes by TLRs on dendritic cells stimulates the production of pro-inflammatory cytokines and enhances antigen presentation to naïve T cells, which is essential for activating adaptive immune responses[7273]. While TLR help maintain gut homeostasis, during an enteric infection, PAMP ligand mediated activation of TLR can mount a pro-inflammatory response which results in culmination of inflammatory mediators (cytokines, chemokines) essential for host defense. Enteric pathogens contain pathogenicity islands within their genomes and have altered biological interactions with epithelial cells (can hijack cell signalling pathways and inject virulence factors into the host cytoplasm). As enteric pathogens

colonize, attach and invade the mucosal surface, strong innate immune responses are activated by several PAMPs associated with the invading pathogen[60,62]. For example, *C. rodentium* infection activates both TLR2 and TLR4 responses, leading to the increased recruitment of inflammatory cells (macrophages, neutrophils) to the infection site. MyD88 dependent signalling plays a critical role in resolving *C. rodentium* infection (discussed later)[74,75].

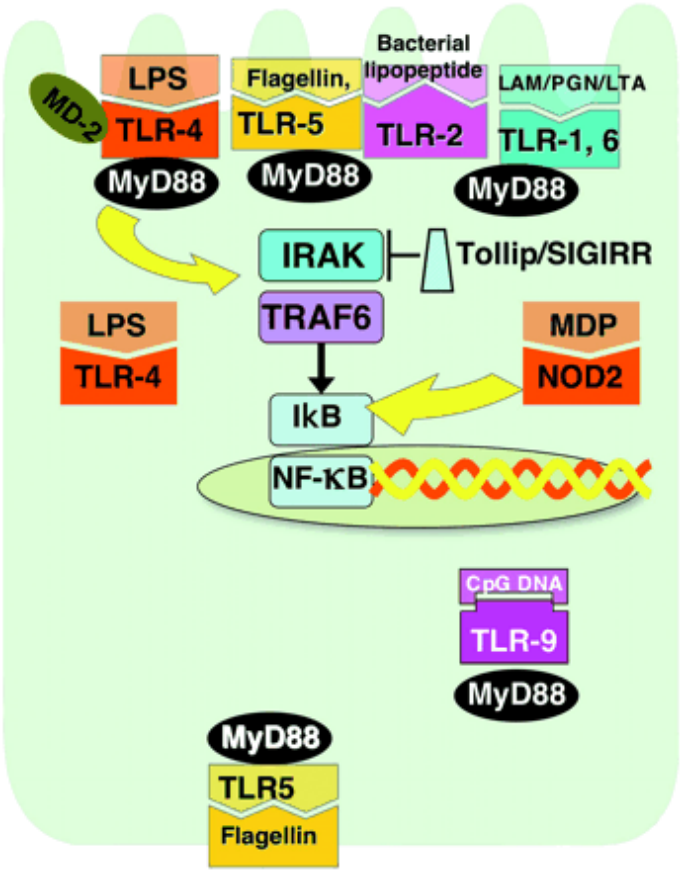

Figure 1.3 Toll-like receptors (TLR's) and the intestinal epithelium

(A) TLR are activated by specific bacterial ligands in intestinal epithelial cells. Polarized (apical/ basolateral surface) expression, (spatial and temporal segregation), limited TLR expression, PAMP-induced tolerance and presence of inhibitors play a role in tightly regulating the TLR expression in IEC. TLR are also expressed in several other host cells, including macrophages and dendritic cells. Certain TLRs can also be found sequestered in endosomes. Image reproduced with permission from reference [57].

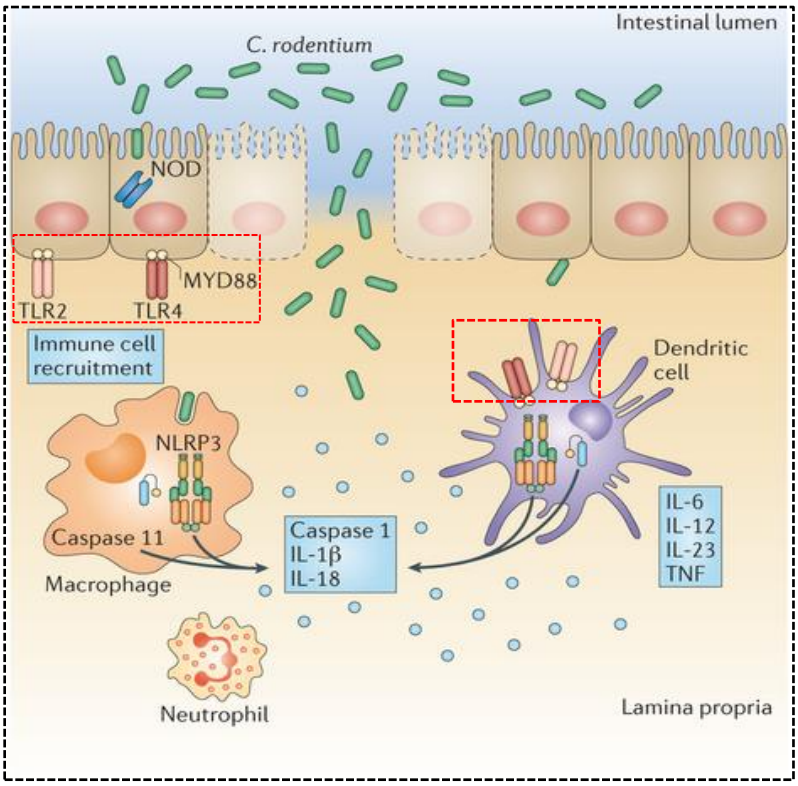

(B) TLR signalling induced during infection by an enteric pathogen, *C. rodentium*. TLR2 and TLR4 play a crucial role during *C. rodentium* infection (boxed). TLR2 is activated by *C. rodentium* surface structures (ie. lipopeptides) and TLR4 is activated by LPS. Activation of these TLRs results in immune cell recruitment and production of pro-inflammatory cytokines. Tissue damage results in production of DAMPS (damage associated molecular patterns) which further heightens the induction of pro-inflammatory responses. Reproduced from reference [74], with permission from Macmillan Publishers Limited.

1.1.3 Attaching and effacing *E. coli* and subversion of host cellular responses

Despite the fact that there are multiple ways the intestinal epithelium contributes to host defense, it remains an important site of infection by pathogenic bacteria. An important aspect of enteric bacterial infection is how these pathogens circumvent intestinal defense barriers to cause infection. Attaching and effacing (A/E) enteric pathogens like enteropathogenic *E. coli* (EPEC), a leading cause of infantile diarrhea and enterohemorrhagic *E. coli* (EHEC), which causes diarrhea, hemorrhagic colitis, and hemolytic uremic syndrome – infect their hosts by targeting

the intestinal epithelium and subverting host cellular processes. EPEC and EHEC are the most prevalent and the best studied clinically important A/E pathogens[76]. Using EPEC as an example of how enteric pathogens can subvert host defense mechanisms, EPEC contains the locus of enterocyte effacement (LEE), a pathogenicity island needed for the formation of A/E lesions on the surface of IEC[77]. In a three-step process, EPEC forms dense microcolonies, resulting in local adherence. The initial attachment of EPEC comes through the bundle forming pillus (BFP) which attaches to IEC. At the second stage, EPEC produces bacterial effectors which are translocated into the host cytoplasm through the Type III secretion system, a complex bacterial virulence system which allows Gram-negative enteric pathogens to directly inject their virulence effectors into the host cytoplasm. EPEC-secreted protein A (EspA) forms the translocation tube; EspA and EspD are thought to be important for forming pore- like structures in the host membrane, thereby allowing the translocation of virulence proteins into the host cell. The last step is the formation of pedestal- like structures and bacterial attachment through the bacterial membrane protein, intimin and the concurrent effacement of microvilli. The entire process is defined as the formation of "attaching and effacing" lesions, a defining characteristic of A/E enteric pathogens[78]. Translocated-intimin receptor (Tir) (an effector synthesized by EPEC and translocated into host cells, where it is inserted into the host cytoplasmic membrane) binding to initimin triggers a cascade of events, including cytoskeleton rearrangements and signalling pathways such as activation of MAP and PKC kinases[79–81]. EPEC induces tyrosine phosphorylation of host proteins resulting in cytoskeletal rearrangements and facilitating bacterial attachment to the IEC. Several non-LEE encoded effectors specifically target components of inflammatory signalling and thereby suppress host pro-inflammatory responses, thus contributing to EPEC pathogenesis[82]. EPEC effector proteins have been implicated in

altering gut homeostasis through their ability to disrupt ion transport in the gut and by weakening epithelial integrity through the subversion of tight junctions, which has been implicated in the development of watery diarrhea[83,84]. EPEC's ability to manipulate these IEC functions, along with its intimate attachment to the host epithelial cells ultimately results in the activation of host immune responses.

From the host perspective, EPEC associated PAMP's such as LPS (TLR4) and flagellin (TLR5) are recognized by the TLRs, thus activating proinflammatory responses. EPEC associated activation of several MAP kinases has been implicated in modulating translocation and transcriptional activity of NF-kB to the nucleus, ultimately resulting in the production of IL-8 and increased recruitment of neutrophils to the site of infection[85]. It has been hypothesized that this plays a role in resolving the infection[83]. Notably, the final outcome of an infection is dictated by bacterial surface structures, secreted bacterial factors, the stage and intensity of infection (infectious dosage), as well as the expression and activation of PRR (inflammatory responses), host cell death and IEC proliferation. EPEC pathogenesis provides a good example of the complexity of host-pathogen interactions and how constant warfare between the host and pathogen ultimately determines the fate of the pathogen and the host.

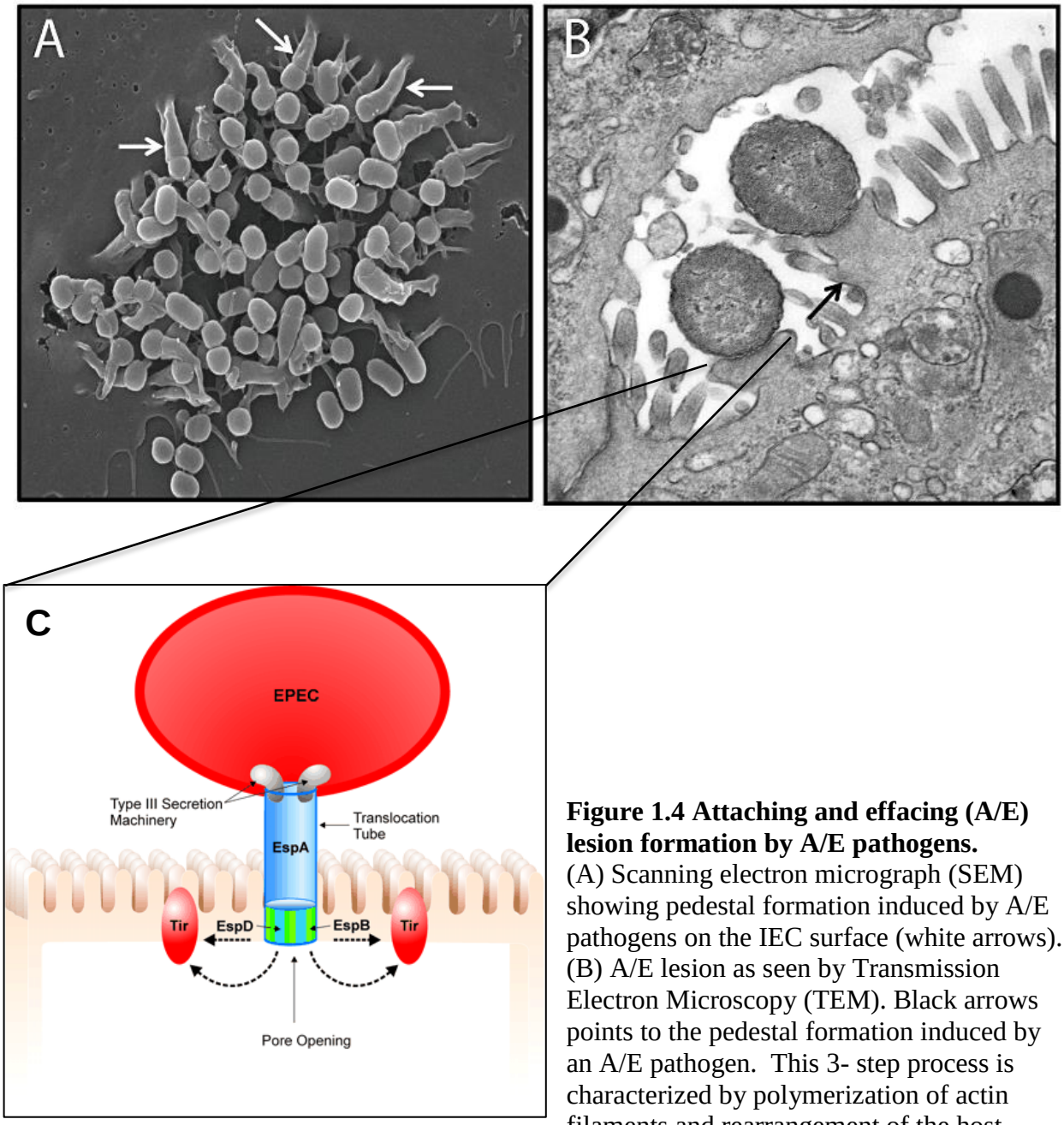

Figure 1.4 Attaching and effacing (A/E) lesion formation by A/E pathogens. (A) Scanning electron micrograph (SEM) showing pedestal formation induced by A/E pathogens on the IEC surface (white arrows). (B) A/E lesion as seen by Transmission Electron Microscopy (TEM). Black arrows points to the pedestal formation induced by an A/E pathogen. This 3- step process is characterized by polymerization of actin filaments and rearrangement of the host cytoskeleton proteins, resulting in the formation of pedestal- like structure underneath the bacteria. Molecular mechanisms of T3SS effector translocation used by A/E pathogen, EPEC to inject effector proteins into the host cell cytoplasm. This figure is an adaption of figures from [76] and [78], reproduced with permission.

1.2 Microbiota and intestinal homeostasis

The healthy human gastrointestinal tract (GI) contains trillions of microorganisms. In fact the number of microbes within and on the typical human body vastly exceeds the total number of eukaryotic cells, emphasizing the importance of prokaryotic cells in the function and health of the human body[4]. Most of these microbes reside in the GI tract and the bacterial communities in the intestine are highly diverse and complex. The majority of the intestinal bacteria belong to the Bacteriodetes and Firmicutes phyla, whereas other phyla such as Actinobacteria, Proteobacteria, Fusobacteria and Cyanobacteria are also represented in the gut[3]. These microbes, also known as intestinal microbiota influence normal gut physiology and functions, ranging from metabolism to immune homeostasis and are thought to be important players in determining disease susceptibilities, hence resulting in their recent classification as a " virtual organ"[2,86]. In a healthy gut environment, a symbiotic relationship exists between microbes and humans where microbes aid in the digestion/fermentation of complex carbohydrates, as well as the production of vitamins and ion absorption[1,87]. Commensal microbes are also an important source of short-chain fatty acids (SCFAs) such as butyrate, which provides energy to the host cells, including colonocytes[88]. Colonization resistance refers to the ability of the commensal microbiota to provide a certain degree of protection against rapid colonization by enteric pathogens. Intestinal microbiota confer direct colonization resistance by competing for essential nutrients (e.g. monosaccharides) and intestinal niches, resulting in the competitive expulsion of invading pathogens[7,8,89,90]. Furthermore, certain commensal species secrete antibacterial molecules and factors that can enhance protection against enteric pathogens. For example, *Bacteriodes thetaiotaomicron* produces bacteriocin which has targeted bactericidal effects on the enteric pathogens *Clostridium difficle* and *E. coli*[91]. Commensal microbiota can also provide host defense indirectly, by

activating the innate immune system by PAMPs, with the downstream inflammatory effects ultimately targeting invading pathogenic microbes (immune-mediated colonization resistance)[8]. Commensal microbiota (e.g. Bacteroidetes) induce the production of peptides such as REGIIIγ which has antibacterial activity. Furthermore, commensal microbial products can stimulate TLRs present on the surface of enterocytes as well as in dendritic cells to produce cytokines (e.g. IL-18) which further upregulate the production of REGIIIγ. Interestingly, a recent study showed that REGIII-γ production was upregulated by the presence of the probiotic *Bifidobacterium breve*, not by non-probiotic commensal *E. coli* suggesting that the composition, richness and diversity of commensal microbiota could play a role in regulating the expression of certain AMP in the intestine[92–94]. Segmented filamentous bacteria (SFB) are closely associated with the small bowel intestinal epithelium and stimulate B cells to produce IgA, hence promoting mucosal immunity. SFB also induce antigen specific-intestinal Th17 responses locally in the lamina propria[95,96]. Furthermore, SFB colonization confers Th17- mediated mucosal protection against *C. rodentium* through production of pro-inflammatory cytokines such as IL-17 and IL-22[97]. In addition to production of antimicrobial factors and regulating immune responses, commensals directly compete with pathogenic bacteria for nutrients and cause pathogen displacement providing an important "physical" barrier to prevent pathogenic colonization in the intestine. The intestinal microbiota occupies a wide range of available intestinal niches, forming complex, tightly-interlinked unique metabolic niches where metabolic by-products by one species provide a food source for another species. Rapid consumption of liberated monosaccharides by commensals creates an environment of nutrient depletion for the invading enteric pathogens[90]. It has now well established that antibiotic treatment that can deplete (or shift the makeup of) the commensal microbiota increases host susceptibility to enteric pathogen infections. Rapid depletion of

commensals results in a transient increase in the free monosaccharides found in the gut lumen, and thus opens up intestinal niches, allowing for efficient colonization by enteric pathogens[98,99]. Germ-free mice (no commensal populations) display greater susceptibility to enteric pathogens, such as *Salmonella typhimurium* than specific pathogen free (SPF) and conventional mice, and also display impaired immune systems as gut microbiota play a key role in development of the immune system[100,101]. Furthermore, loss of microbiota diversity and an increased abundance of *Enterobacteriaceae* has been shown to contribute to increased susceptibility to intestinal colonization by enteric pathogens like *C. rodentium* and *S. typhimurium*[102]. In recent years, there has been an increasing appreciation for the role that microbiota play in health and disease and the fact that perturbations/changes in the gut microbiota (dysbiosis) can trigger intestinal inflammation, thereby contributing to immune disorders like Inflammatory Bowel Disease (IBD)[103–105].

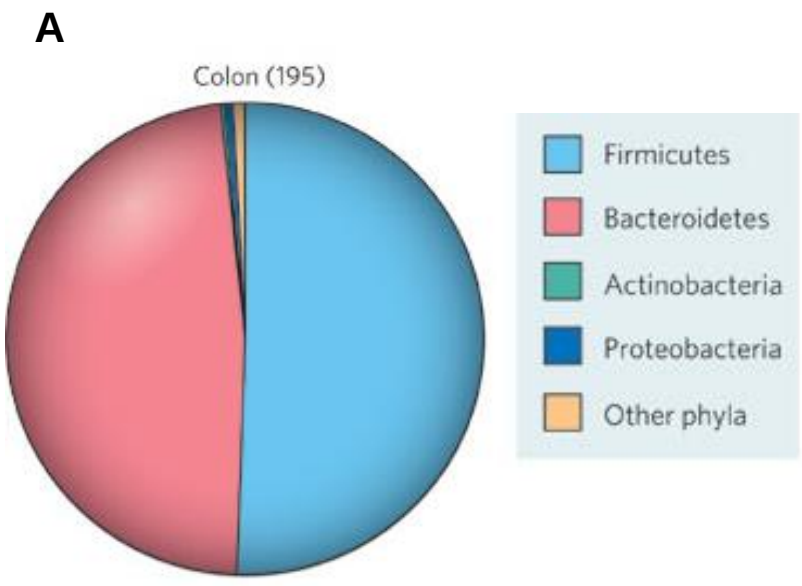

B

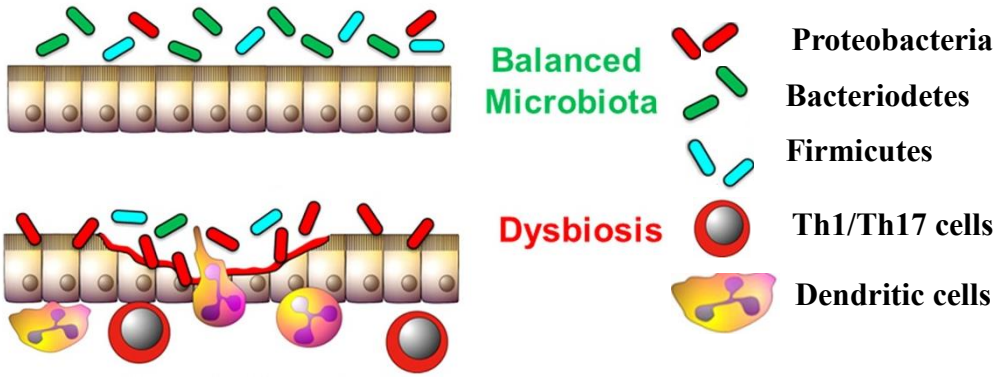

C

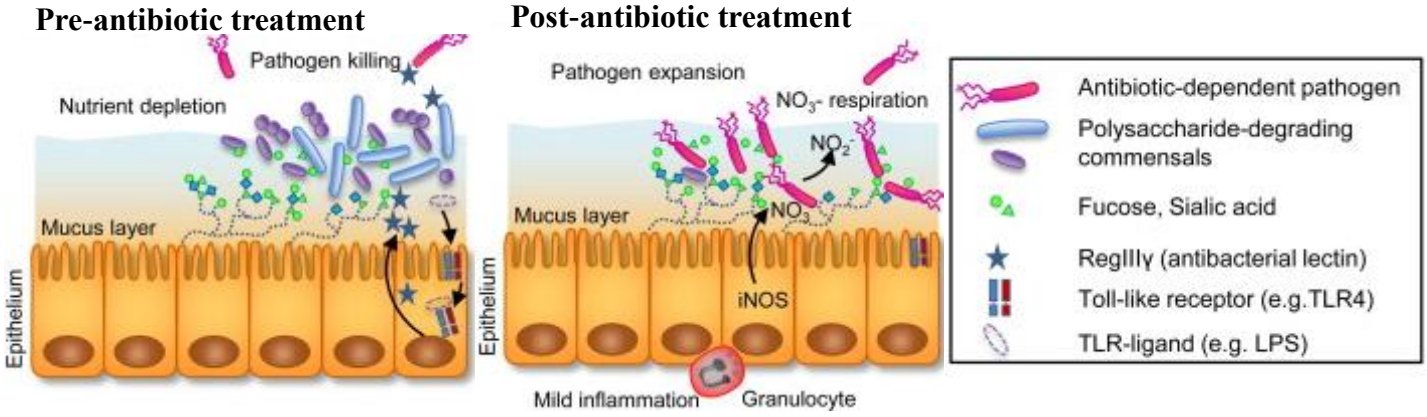

Figure 1.5 Microbiota and intestinal homeostasis.
(A) Relative abundance of different microbial phylas in the mammalian colon. Bacteroidetes and Firmicutes are the predominant phyla in the gut. Image reproduced with permission from [3].
(B) Balanced microbiota represents a balanced state in the gut- diverse and abundant bacteria with dominance of Firmicutes and Bacteriodetes. Reduced microbial diversity and an increased percentage of pathobionts and/or proteobacteria represent a state of intestinal dysbiosis. Increased bacterial contact with the mucosal surface results in intestinal inflammation, accompanied by the increased recruitment of T effector cells.
(C) Under homeostatic conditions, commensals offer colonization resistance as well as induce production of antibacterial lectins, including RegIII-γ. Commensals also contribute to the development of immune tolerance through the accumulation of Th17 cells which increases resistance to pathogens via secretion of pro-inflammatory cytokines. Antibiotic treatments can deplete the majority of the commensal microbiota, disrupting innate defense responses. In the absence of commensals, pathogens exploit free monosaccharides for their own growth while they are also known to be able to utilize nitrates for anaerobic respiration. Image reproduced and adapted with permission from [98].

1.3 Mucus layer- a frontline defense barrier

As discussed above, the intestinal surface is protected by several active (innate and adaptive immune system) as well as perceived passive barriers (mucus layer). The mucus layer overlying the IEC is one of the first sites of direct contact between the host and the gut bacteria and acts as a protective barrier against commensals and enteric pathogens reaching the IEC[106,107]. The protective role of mucus layer is largely due to its chemical and physical properties[25], although in recent years, it has become apparent that the functional properties of mucus layer are not restricted to it being just a physical barrier. Mucus thickness varies throughout the GI tract, although the mechanisms defining the thickness of the mucus layer yet remain to be elucidated[108,109]. There are two mucus layers in the colon- a firmly adherent inner mucus layer (attached to the intestinal surface) and a loosely attached outer mucus layer. The inner mucus layer is largely devoid of bacteria whereas the outer mucus layer is heavily colonized by commensals[110]. Underneath the mucus layer, a dense network of highly diverse glycoproteins and glycolipids form a layer called glycocalyx which is directly attached to the IEC. Membrane/cell-associated (transmembrane) mucins are a major constituent of this layer[111]. The organization of the mucus layers thus ensures that commensals are well-separated from the IEC surface and the immune system which thereby limits unnecessary stimulation of the host immune system.

Mucins are further classified into secreted mucins and transmembrane mucins. The secreted mucins (Muc2, Muc5AC, Muc6), are released from the apical surface of IEC/goblet cells and forms a protective, gel-like mucus layer[112]. The secreted mucus layer is found throughout the gastrointestinal tract. Transmembrane mucins (Muc1, Muc4) are membrane-associated glycoproteins, abundantly expressed and found attached to the apical surface of the

epithelial cells. In addition to hydrating and lubricating the epithelial surface, they provide defense against enteric pathogens (anti-adhesive) and participate in inducing host-signalling pathways[113].

The intestinal mucus layer is largely composed of the gel forming mucin Muc2[114–116]. Muc2 mucin is stored in granules within goblet cells and once released/secreted, it expands dramatically in volume to form the mucus gel. Mucin molecules are highly condensed inside the intracellular granules and are held together by the neutralizing force of Ca^{2+} ions. The release of mucin molecules is followed by the rapid dissociation of the Ca^{2+} unshielding the overall anionic surface. The repulsive forces of negative charge mediates the expansion of mucins and upon their hydration, the mucus layer is formed. HCO_3^- (bicarbonate) plays an important role in removing positively charged Ca^{2+} cations from mucin molecules and unshielding the polyanionic surface of mucin molecules[117]. In fact, it has been recently shown that the basolateral side of goblet cells contains a bicarbonate transporter, termed Bestrophin-2, which is hypothesized to secrete HCO_3^- into the colonic lumen[118]. Once secreted and formed, the inner and outer mucus layer have different physical properties, the outer mucus layer being readily soluble whereas the inner mucus layer is insoluble and shares the solubility properties with the Muc2 mucin stored in secretory granules (i.e. Muc2 stored in the secretory vesicles and the inner mucus layer are insoluble in the chaotropic salt guanidinium chloride)[119]. Additional proteolytic cleavage at the C-terminus (cysteine rich regions) is thought to be an important factor in generating the increased solubility and loose structure of the outer mucus layer[110].

1.3.1 Structure and biosynthesis of the mucin Muc2

The Muc2 protein is organized into cysteine rich N and C- terminus regions and a central Variable Number of Tandom Repeats (VNTR) region which is rich in tandem repeats of proline,

threonine and serine residues. Flanking the central PTS region, there are four complete von Willebrand D domains (3 at N-terminus and 1 at C-terminus) and one incomplete von Willebrand D domain at N-terminus. von Willebrand domains are rich in cysteine residues and form disulphide linkages between mucin monomers and play an important role in mucin polymerization[110,120,121]. Muc2 dimers (dimerization) are formed in the endoplasmic reticulum through disulphide linkages (head to head) between the cysteine knot domains at the C-terminus. After their dimerization in the ER, Muc2 dimers pass into the Golgi apparatus, where the PTS regions get heavily O-glycosylated, facilitated by several glycosyltransferases such as (Polypeptide N-acetylgalactosaminyltransferase, Core 1 β1-3 galactosyltransferase, Core 2 β1-6 N-acetylglucosaminyltransferase, Core 3 β1-3 N-acetylglucosaminyltransferase, Core 2/4 β1-6 N-acetylglucosaminyltransferase) that are found in Golgi apparatus, resulting in Muc2 being ~ 5MDa in size. In the trans-Golgi network, disulphide bridges are formed between N- terminus D domains, forming a polymer- like structure. Muc2 polymers are packed into secretory granules until they are released into the intestinal lumen. Once released, Muc2 becomes hydrated and forms an organized sheet that provides the structural basis of the intestinal mucus layer[122].

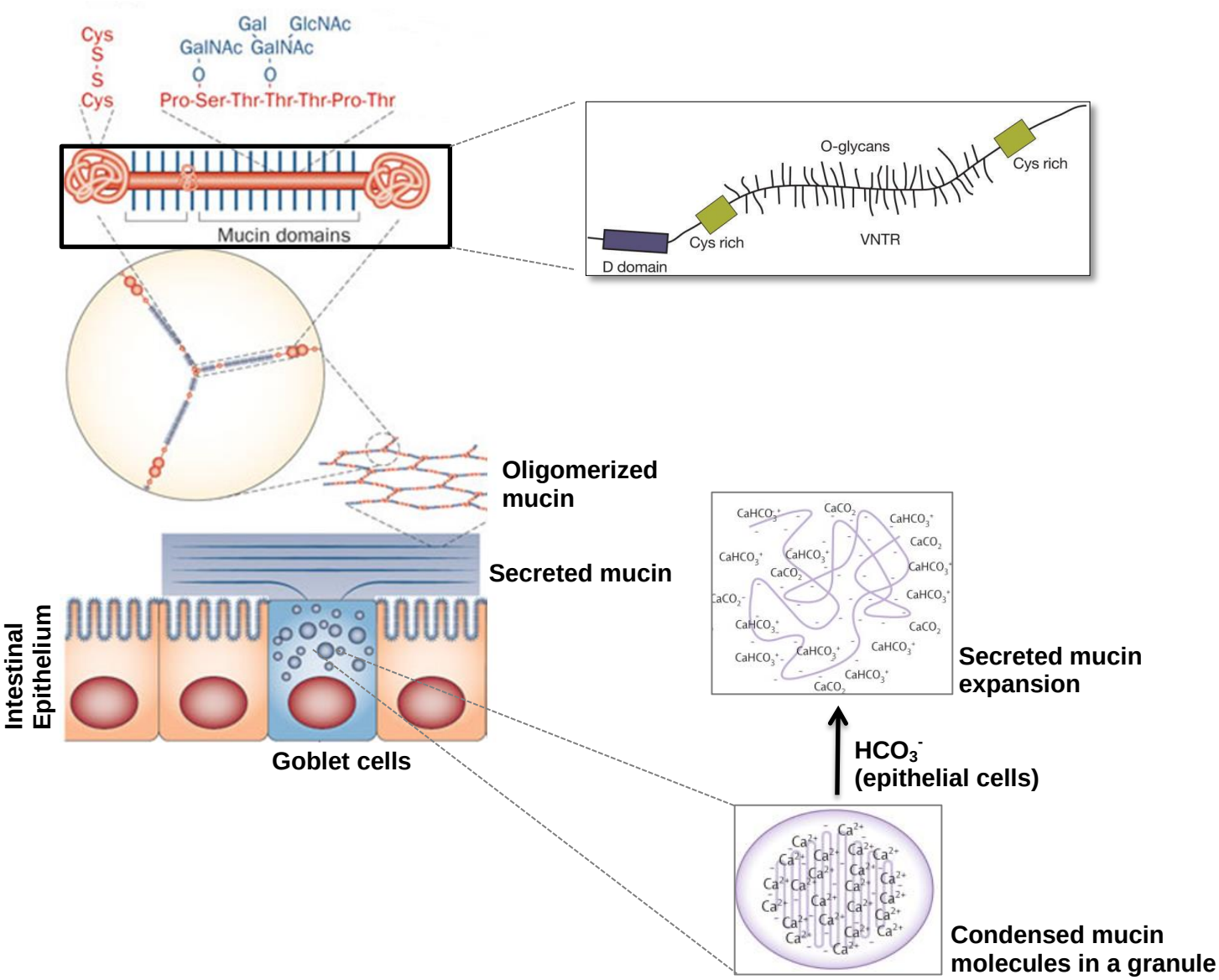

Figure 1.6 Structural organization of the gel-forming mucin Muc2 in the intestine. Following O-glycosylation in the golgi apparatus, secreted mucins are packed into the granules of the goblet cells. Secreted mucins are oligomeric in nature and upon secretion into the extracellular milieu, form a complex network. The interactions between mucin molecules are mediated by N- and C-linked cysteine residues found on D domains (also known as von Willebrand factor type D domain) which form disulphide bonds, resulting in formation of large, complex polymers. The central region of the Muc2 mucin is the variable number of tandem repeat (VNTR) region, which is heavily O-glycosylated. O-GalNac residues with several different structures can be attached to the repeats of Serine/Threonine/Proline residues found in the VNTR region, adding to the structural integrity and complexity of the secreted mucin Muc2. (INSET-Top) Structural organization of Muc2 mucin. (INSET-Bottom)- Negatively charged mucin molecules are tightly packed with the help of positively charged Ca^{2+} ions and H^{+} ions (not shown). Upon secretion, HCO_3^- from the epithelial cells sequesters Ca^{2+} ions, causing the rapid expansion of mucin molecules due to electrostatic repulsion. This figure is an adaptation of figures from references [123], [117], and [124] (with permission).

1.3.2 Glycosylation of the mucin Muc2

As discussed in the previous section, the Muc2 mucin is heavily O-glycosylated, where glycans comprise upto 80% of the mucin mass, while the remaining 20% is the protein mass[123,124]. Mucin type O- linked glycosylation begins with the addition of N-acetylgalactoseamine (GalNac) on Ser/Thr residues, resulting in the formation of the "Tn antigen" which is further modified by downstream glycosyltransferases to generate a series of core O-linked glycans. The most common O-glycan is Galβ1-3GalNAc, also known as core-1 O glycan, which is generated after the addition of a galactose residue to the Tn antigen by the glycosyltransferase, core 1 β1,3-galactosyltransferase (C1galt1, also known as T-synthase) . Core 2 O-glycans are generated after the addition of N-acetylglucosamine to the core 1 structure. Addition of N-acetylglucosamine to the Tn antigen by core 3 beta1, 3-N-acetylglucosaminyltransferase (C3GnT) forms core 3 O-glycans. Further addition of N-acetylglucosamine to core-3 structure results in formation of core 4 O-glycans. The addition of core 2 and core 4 monosaccharaides to the precursor core 1 and core 3 structures respectively is facilitated by tissue specific glycosyltransferases[125,126]. Although there are 8 different core structures that can be modified by the addition of sugars, core glycans 1-4 seem to be the most important for mucin structure and are the most abundant structures. Detailed glycomics analysis has revealed that the majority of the oligosaccharides in human colonic Muc2 are based on core 3 and core 4 structures whereas murine colonic Muc2 is predominantly characterized by the presence of core 1 and core 2 based glycans[124,127]. O-linked glycans can become further modified and elongated adding to the complexity of the mucus layer. Some of the commonly found terminal modifications are fucosylation, sialylation and sulfation. Complex O- glycosylation of the mucin structure provides protection against protease degradation. O- linked glycans are

hydrophilic and negatively charged, and hence are essential for the ability of Muc2 to hydrate through the binding of water and salts[126].

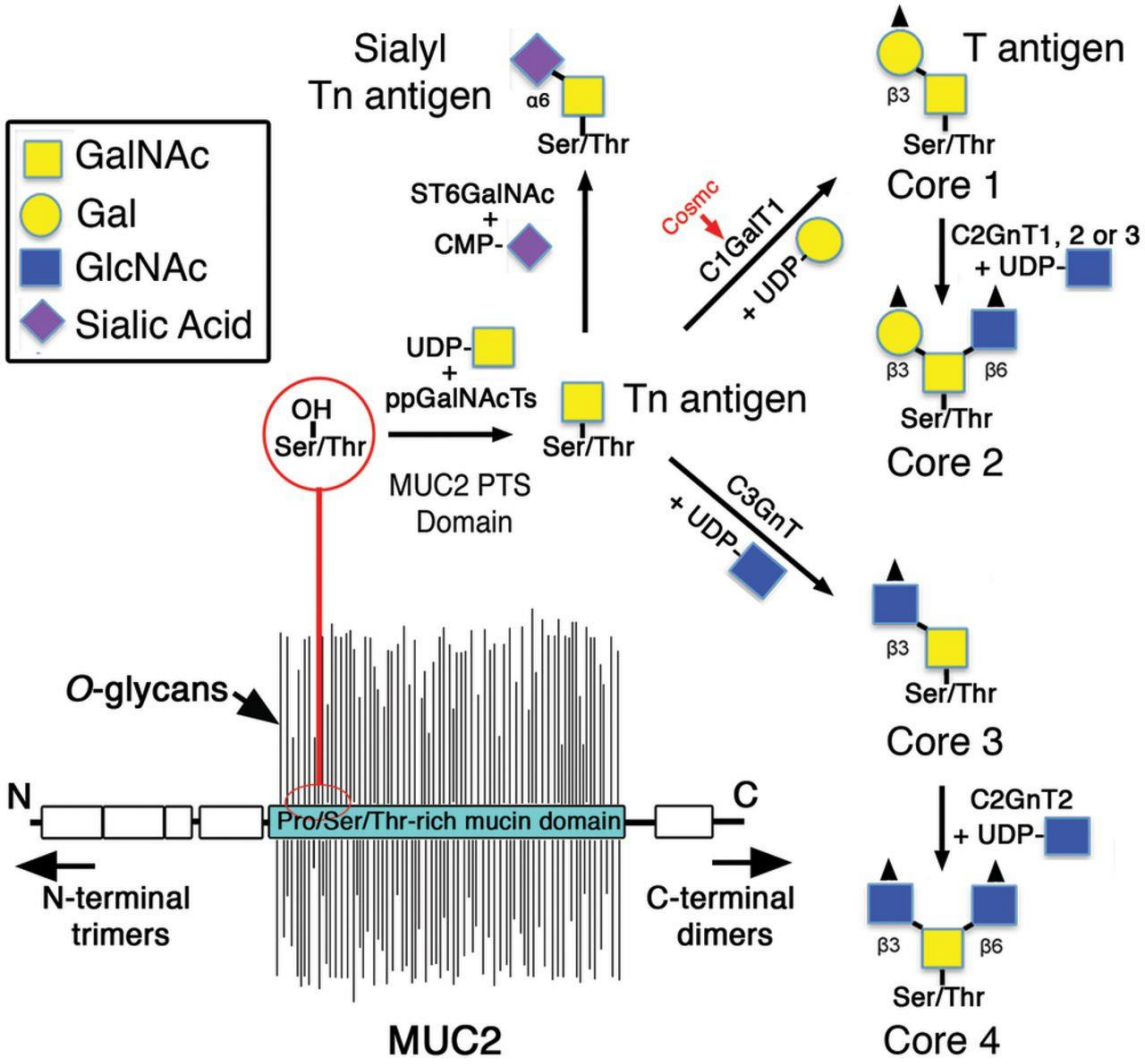

Figure 1.7 O-linked glycosylation of the mucin Muc2.
Muc2 glycosylation begins with the addition of GalNac on the hydroxyl group of PTS (proline, threonine, serine) amino acids, generating a Tn antigen. Tn antigen can be further modified by the addition of galactose by core 1 glycosyltransferase (*C1galt1*) generating core 1 O-glycans. Similarly, addition of a GlcNac residue to the Tn antigen by core 3 glycosyltransferase results in the formation of core 3 structures. Core 1 and core 3 glycans can be further modified to generate Core 2 and Core 4 O-linked glycans respectively. Addition of sialyl by sialyltransferase forms sialylated Tn antigen which cannot be modified further. Each core structure can undergo terminal modifications such as fucosylation, sialylation or sulfation. Image was reproduced from reference [128] with permission.

1.3.3 Mucus and disease

The intestinal mucus barrier is protective and any breach affecting the integrity of the mucus layer can potentially allow luminal bacteria to come in direct contact with the underlying epithelial surface and trigger inflammatory and/or immune responses. Mucin-secreting goblet cells are thought to be key players in innate host defense via the formation of the mucus layer that protects the mucosal surface. A few studies have indicated that in ulcerative colitis patients, the number and size of goblet cells seemed to be reduced/altered. Ultimately this contributes to a thinner mucus layer barrier which can be more easily breached by commensal microbes as well as by enteric pathogens[39,128]. The degree of sulphation, sialylation, the rate of glycosylation and the length and complexity of mucin oligosaccharides are also altered in IBD patients. Generally speaking, in IBD patients there is evidence showing reduced mucin sulphation, increased mucin sialylation and decreased acetylation[129,130]. In a normal healthy human gut, sialylated mucins are O-acetylated which makes them highly resistant to degradation. Reduced acetylation of mucins may contribute to their increased proteolytic degradation, affecting the mucus viscosity and thickness[131]. As previously discussed, recent studies looking at mouse models of colitis have shown the importance of the mucus barrier in protecting the host against colitis[132–134]. Another contributing factor implicated in the development of IBD is commensal microbial dysbiosis. A relative shift in the proportions of protective (Firmicutes, Bacteriodetes) and potentially pathogenic commensal microbes (Proteobacteria and Actinobacteria) as well as changes in the functional diversity of commensal microflora could all be involved in the pathogenesis of IBD[104,135]. Since the outer mucus layer is heavily colonized by commensals[110], the role of this microbial ecology in maintaining gut homeostasis and colonization resistance and in part, regulating complex mucin glycan metabolism cannot be underestimated.

Since IBD patients are at higher risk of developing colorectal cancer[136], extensive work has been done looking at the mucin glycosylation changes that occur during colorectal cancer and the potential of using these changes as biomarkers for early prognosis of cancer as well as targets of cancer therapy. During malignant transformation, mucins exhibit some cancer specific modifications including (i) reduced core 3 and core 4 structures (ii) increased expression of C1GALT1, resulting in increased production of " Tn" antigens associated with cancer metastasis (iii) the increased presence of sialylated Tn antigens resulting in the production of truncated O-glycans (iv) reduced sulfation and increased sialylation[137,138]. C3GnT activity has been shown to be downregulated in colorectal cancer tissues and is thought to be protective against cancer metastasis[138–140]. Furthermore, mucinous carcinomas express high levels of the *Muc2* mucin gene and are characterized by the presence of abundant extracellular mucins (> 50% of the tumor mass)[141]. Mucin abnormalities and ER stress associated with aberrant changes in Muc2 processing and assembly can initiate colitis in mice and share similar pathology to human ulcerative colitis[132,142]. For example, presence of misfolded Muc2 protein and the accumulation of non-O-glycosylated precursors are concomitant with the positive staining for protein misfolding and ER stress marker, GRP78 in the tissues collected from UC patients[132].

The intestinal goblet cells and mucins thus form a frontline defense barrier for host protection. The mucus layer serves as an important interface for complex host-microbiota interactions, regulating host innate and adaptive immune responses, host physiology and is a site of complex glycan metabolism. Research into intestinal mucus has evolved from initially viewing the mucus layer as a static, physical barrier to a more recent understanding of its complex and dynamic functional nature. In recent years, several studies have shown the protective role played by the gut mucus barrier against enteric infections, spontaneous intestinal

inflammation and experimentally-induced colitis. Further elucidation of the mechanisms underlying the mucin changes involved in cancer and intestinal inflammation will be crucial for development of novel therapeutic approaches.

1.3.4 Mucus and host defense

The role of the intestinal mucus layer in providing host defense has gained much appreciation in recent years. There are at least 3 possible ways the gut mucus layer provides host defense against enteric pathogens. The mucus layer acts as an important physical barrier to protect the underlying intestinal epithelium from intruding pathogens/commensal bacteria. It has been reported that in the absence of the Muc2 mucin, a key component of intestinal mucus in mice (Muc2 deficient mice, *Muc2 -/-),* commensal bacteria could be seen in close proximity to the colonic epithelial surface and were detected within the intestinal crypts[143]. We showed that in *Muc2 -/-* mice, the enteric bacterial pathogen *S. typhimurium* was found in a close proximity to the epithelial surface whereas in WT mice, the Muc2-dependent mucus layer provided a distinct barrier, keeping *Salmonella* distant from the epithelial surface[144]. The absence of the intestinal mucus layer thus increases host susceptibility to *S. typhimurium* and as shown in other studies, to the A/E pathogen, *C. rodentium*[145]. Overall, these *in vivo* studies have revealed the significance of the mucus layer in providing a physical barrier that limits the ability of commensal and enteric pathogens to reach the epithelial surface. This becomes important in preventing activation of the innate immune system as well as overt intestinal inflammation and is thus critical for keeping a check on the host immune system and maintaining intestinal homeostasis.

The intestinal mucus layer also acts to retain (and prolong the activity of) antimicrobial peptides produced by host epithelial cells[14,48,49]. Some of the important AMP with broad-spectrum activity against a variety of microbes include defensins, C-type lectins, the REG family

of lectins and lysozyme[24]. Secretory IgA is also thought to be anchored in the outer mucus layer through interactions with mucus proteins and commensal microbiota where it provides immune protection against pathogens[146]. Intestinal alkaline phosphatase (IAP), a brush border enzyme expressed by enterocytes (and thought to be released into the mucus layer) is important for detoxification of the microbial ligands, LPS, CpG and flagellin through dephosphorylation which alters the interactions of these PAMPS with TLR receptors and protects the host against TLR induced inflammation[147,148]. It has been shown that the absence of an intestinal mucus layer alters the expression of several enzymes in the intestinal epithelium, IAP being one of them[149]. A recent study of *Muc2 -/-* mice showed reduced expression of IAP in their intestinal tissues compared to WT mice and reduced LPS dephosphorylation activity against *Salmonella* and *E. coli* LPS[144]. Although the mechanisms dictating IAP and mucus layer interactions are not well defined, perhaps intestinal mucus layer plays a role in retaining secreted IAP in close proximity to IEC rather than allowing IAP to be flushed out of the GI tract. Overall, these studies provide an intriguing link between IAP, intestinal mucus and host defense.

Muc2 -/- mice have proven crucial in understanding the role of the intestinal mucus layer in host defense as the absence of Muc2 disrupts intestinal homeostasis. Gene mutations affecting Muc2 processing, assembly or production predispose mice to intestinal inflammatory disease and increase their susceptibility to experimental colitis[132,134,149]. In recent years, there has been an increased interest in exploring the role of individual glycosylations of the Muc2 mucin in protecting the host against enteric pathogens. Studies with mice lacking core 3 beta1,3-N-acetylglucosaminyltransferase (C3GnT), an important enzyme for the synthesis of core 3 derived O-glycans, shares ~70% homology to human C3GnT, showed that *C3GnT -/-* mice displayed increased susceptibility to experimental colitis, along with an impaired mucus barrier and

increased permeability of their intestinal barrier[140]. Since core 3-O derived glycans are the primary constituent of human Muc2, this study has relevance in understanding the etiology of intestinal inflammation in humans (Inflammatory Bowel Disease). The role of core 1 derived O-glycans, a major component of the murine intestinal mucus was examined using core 1 β1,3-galactosyltransferase KO mice (*C1galt1 -/-*). C1galt1 enzyme controls the biosynthesis of core 1 O-glycans, so the deletion of C1galt1 abolishes core 1 derived O-glycans. *C1galt1 -/-* mice developed spontaneous colitis, showed greater proportions of mucosa associated bacteria, an overtly diminished mucus layer and overt intestinal inflammation as compared to WT counterparts[150]. Similar results were seen with the target deletion of core 2 beta1,6-N-acetylglucosaminyltransferase-2 (C2GnT2), a glycosyltransferase expressed in the digestive tract that initiates core 2 derived O-glycan branching. C2GnT2 deficiency resulted in alterations in the overall mucin composition as core 2-glycans form the basis of core 2 and core 4 structures[151]. These mice also had defects in their intestinal barrier function and heightened susceptibility to DSS colitis. Therefore, it is evident that different forms of Muc2 linked O- glycosylation have an important protective role in maintaining intestinal homeostasis by maintaining the integrity of mucus barrier and the barrier function of the intestine.

The mechanisms regulating the post-transcriptional modifications of O-linked glycans on the intestinal mucins (fucosylation, sialylation, sulfation) are not well understood. The terminal modifications are potentially important for the physiological and biological functions of the intestinal mucins[152]. For example, acidic mucins consist of sulfo- and sialo-mucins and are predominantly found in the large intestine (distal colon). The most commonly found mucin O-glycan modification is sulfation. The addition of negatively charged sulfate groups to O-glycans found on intestinal mucins are primarily mediated by the N-Acetylglucosamine 6-O-

sulfotransferase, GlcNAc6ST-2[153]. Reduced sulfation has been implicated in increased susceptibility to experimental colitis[154]. The Tn antigen is a common primary structure found in all O-linked glycans (GalNAcα-O-Ser/Thr) and is usually a hidden substrate as it is highly modified through the addition of several monosaccharides. Sialylated Tn antigen is further modified to form core1/core 3 O- linked glycans[155]. The absence or impaired activity of certain glycosyltransferases can expose Tn antigens on the epithelial surface. In a few studies, Tn antigens have been detected in IBD patients which indicates an impairment of O-glycosylation in some IBD patients, which could play a potentially causal role in these conditions[156–158]. These findings emphasize the complex dynamics underlying how the mucin Muc2 creates the intestinal mucus layer, along with its glycosylations and terminal modifications in determining whether intestinal disease will be averted or exaggerated.

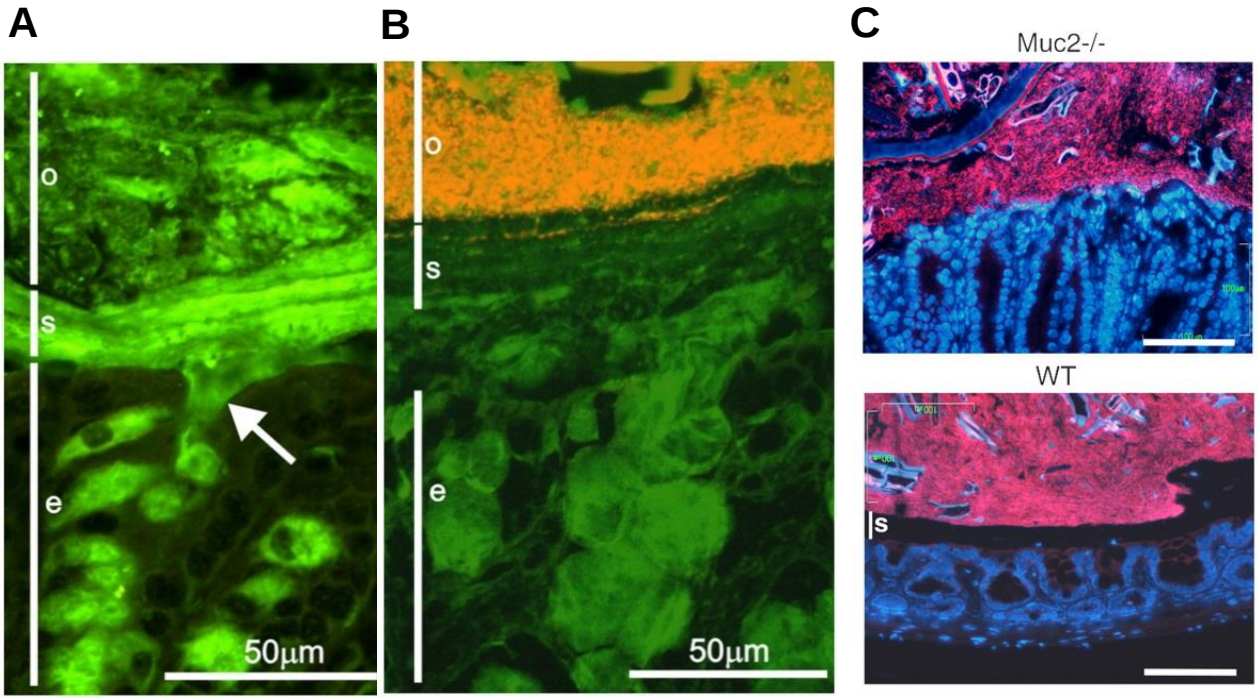

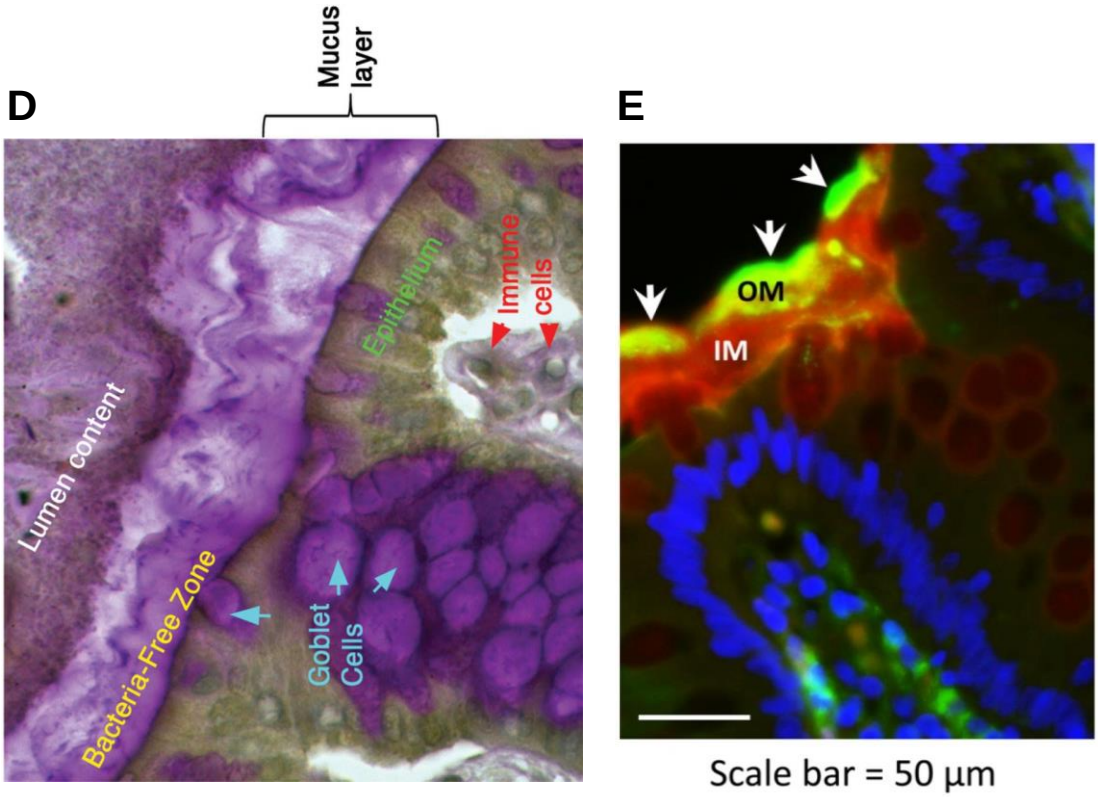

Figure 1.8 Mucus layer in the distal colon.
(A) Muc2 (green) is organized into 2 layers over the top of intestinal epithelial cells (e) - a firmly attached inner mucus layer (s), a loose, non-firmly attached outer mucus layer (o). Image reproduced with permission from [110].
(B) Commensal bacteria colonization is restricted to the outer mucus layer (as seen by the general bacterial FISH probe, EUB568) whereas the inner mucus layer is largely devoid of any bacteria. Image reproduced with permission from [110].
(C) In the absence of Muc2 and the resulting mucus layer, commensals can be seen in close proximity to the epithelial surface whereas in WT mice, the mucus layer provides a physical barrier to prevent bacteria from contacting the epithelial surface. Image reproduced with permission from [143].
(D) Periodic Acid-Schiff staining showing the release of mucin Muc2 from the goblet cells, which proceeds to form the mucus layer. The mucus layer protects the underlying intestinal epithelium from luminal contents such as bacterial antigens and hence prevents the overt activation of immune responses. This figure was reproduced with permission from [128].
(E) Co-localization of secretory IgA and Muc2 in the outer mucus layers adds a further layer of defense against enteric pathogens. Image reproduced with permission from reference [146].

1.3.5 Fucose- an important sugar at the host-pathogen interface

In the mammalian gastrointestinal tract, fucose is the most abundant sugar found on glycan structures (O-linked and N-linked), proteins and lipids. α (1, 2) fucosylation is predominant in the GI tract and the majority of this fucosylation is mediated by α(1,2)-fucosyltransferase (Fut2)[159]. It has been shown that Fut2 activity is associated with secretory cell-types in the GI tract, including goblet cells of distal colon, caecum and Brunner's glands in the duodenum[160]. Once released from mammalian glycoconjugates (fucosylated intestinal glycans, ABO blood antigens, glycolipids), fucose provides an important food source for microbes. *B. thetaiotaomicron* produce multiple fucosidases to cleave fucose from host glycans, predominantly found in the mucus layer, mucosal secretions and on the surface of epithelial cells facing the lumen[91]. Depending on the nutrient availability, gut homeostasis and colonization densities, *B. thetaiotaomicron* can induce host fucosylation to increase the levels of available fucose in the intestine by sensing the levels of L-fucose in the GI tract. L-fucose acts through FucR (a molecular sensor of L-fucose availability) as a inducer of the fucose utilization pathway (*fucRIAK*) and as a co-repressor of transcription at the control of signal production (*csp)* locus. Low levels of L-fucose decreases the L-fucose binding to *csp*, signalling the host to increase production of hydrolysable fucosylated glycoconjugates[161,162]. Fucose enhances the beneficial activity of host symbionts through the production of metabolites (e.g the SCFA propionate) for the host or other microbes and contributes to increased colonization resistance against enteric bacterial pathogens by acting as an energy source for commensal microbiota[163]. Systemic exposure to bacterial ligands such as LPS induces rapid α (1, 2) fucosylation of small intestinal IEC. Fucosylated proteins are then shed into the intestinal lumen where fucose is released and

metabolized by commensals, indicating that fucosylation is a host protective mechanism to restore intestinal homeostasis under infection-induced stress[163161].

Notably, enteric bacterial pathogens (*E. coli* serovars, *C. rodentium, S. typhimurium*) also rely on simple monosaccharides, such as fucose as an important food source[164,165]. However, pathogens lacking the α-fucosidase enzyme are unable to release fucose from complex dietary and host glycans. A recent study showed that intestinal fucose released from the mucus layer through the metabolic activity of commensals inhibits virulence gene expression by the pathogen EHEC[166]. Downregulating virulence in a highly competitive and nutrient poor environment i.e the mucus layer where commensals are utilizing the majority of the available monosaccharides and then turning on the virulence and metabolic genes in close proximity of the epithelial surface likely confers a competitive advantage to EHEC. In contrast, a low fucose environment (such as in close proximity of the epithelial surface) represses *fusKR* (fucose sensing system) resulting in de-repression of the LEE (locus of enterocyte effacement) pathogenicity island. This process activates the expression of ler regulated genes involved in bacterial virulence, thereby promoting EHEC's ability to infect the epithelium. Furthermore, *B. thetaiotaomicron* was shown to repress LER (transcriptional regulator of LEE) expression in EHEC when incubated with fucosylated mucin, as the presence of *B. thetaiotaomicron's* fucosidases cleaved fucose from the fucosylated mucin, directly repressing the LEE expression which is necessary for bacterial virulence. This provided further evidence to support the importance of fucose in modulating bacterial pathogenesis in response to *B. thetaiotaomicron* mediated release of mucin-derived fucose[167]. Overall, this highlights the complexity of L-fucose dynamics in the GI tract where host-commensal interactions dictate the availability and status of L-fucose which can also affect the pathogenesis of enteric pathogens.

Enteric pathogens entering the gastrointestinal tract must consume energy-rich substrates to replicate and colonize the host. Pathogens have evolved a number of strategies to exploit the various nutrients available in the intestine[168,169]. *S. typhimurim* colonization of the ceca of mice requires antibiotic-mediated depletion of commensals to perturb microbiota dependent colonization resistance[170]. As previously discussed in the section *Microbiota and intestinal homeostasis,* in a normal gut, commensal microbes offer colonization resistance by occupying most of the intestinal niches and consuming most of the available monosaccharides (and other nutrients) in the intestinal lumen[8]. Antibiotic treatment results in a significant reduction in the numbers and diversity of the commensal microbiota (reduced colonization resistance) which results in a transient increase in the amount of available monosaccharides such as fucose and sialic acid due to a significant reduction in the proportions of commensals which can metabolize them[98–100,171]. Antibiotic resistant enteric pathogens like *S. typhimurium* can therefore exploit the monosaccharide pool, to expand their numbers in the gut, colonizing and establishing an infection[98,99]. Furthermore, in the presence of the commensal *B. thetaiotaomicron*, *S. typhimurium* is known to significantly upregulate the genes involved in fucose metabolism, suggesting that *Salmonella* uses microbiota-liberated sugars such as fucose for growth[163,172,173]. Therefore, L-fucose availability in the gut plays an important role in regulating virulence, nutrient utilization as well as in maintaining host-commensal symbiosis.

1.4 Dynamics of mucus and enteric pathogen interactions

1.4.1 Quantitative and qualitative changes in the mucus layer during inflammation

In order to protect the underlying intestinal epithelium, the protective mucus blanket is maintained through slow, constitutive secretion of mucins from goblet cells, a process called baseline secretion. The movement of secretory granules to the epithelial surface is in part mediated by microtubule contractions within the goblet cells, through the cytoskeleton[174,175]. Accelerated goblet cell secretion, on the other hand, is commonly seen during enteric pathogen infections and is usually due to the action of receptor mediated secretagogues. It is characterized by the rapid discharge of mucus stored in intracellular granules in goblet cells through exocytosis[25]. Microbial products (LPS), bacterial effectors (SPATES), pro-inflammatory cytokines, physical injury and cholinergic stimulation can all induce accelerated mucin secretion into the intestinal lumen. This results in goblet cell depletion (cavitation), a hallmark characteristic of mucus hypersecretion[41,176–178]. Furthermore, expression of secreted and cell-surface mucins can be upregulated by a wide spectrum of pro-inflammatory cytokines such as interferons, TNF-α and IL-1β as a potential host defense mechanism[41,179,180]. There can also be qualitative changes in mucins during a diseased state. Qualitative changes are characterized by changes in the biochemical and physical properties of the mucus layer and its associated mucins[181,41]. Sulphation and sialylation protect the intestinal mucins from bacterial degradation[182,129]. Terminal sulfation of the mucin Muc2 has been shown to have a protective role against the massive leukocyte infiltration that can occur during DSS-induced experimental colitis as mice lacking N-Acetylglucosamine 6-O-sulfotransferase-2 (GlcNAc6ST-2) (enzyme catalyzing the sulfation of colonic mucus) showed significantly greater leukocyte infiltration[154]. Interestingly, reduced sulfation and increased sialylation of mucus have been reported during

intestinal inflammatory conditions. The length of the oligosaccharide chains and mucus viscosity also vary between the inflamed and normal gut. Altered mucus glycosylation during inflammation can affect microbial adhesion as well as the ability of pathogens to degrade the mucus (e.g. increased sulfation)[129,183,184]. Overall, intestinal inflammation results in dynamic and complex quantitative and qualitative changes in the mucus composition and structure.

1.4.2 How do pathogens subvert the intestinal mucus barrier?

As discussed above, when an enteric pathogen comes in contact with the epithelial cell surface, it stimulates the secretion of stored mucins in intracellular granules inside the goblet cells. Mucin hypersecretion is thought to flush the pathogenic bacteria away from the intestinal surface and may represent an important host defense mechanism. Secreted mucins are thought to act as decoys for the adhesins used by pathogens to bind to cell-surface mucins, as mucins possess most of the oligosaccharide structures present on the epithelial cell surface. Mucins are constantly being produced in large quantities and are washed away from the mucosal surface, also removing pathogenic bacteria[121,165,185]. Cell-surface mucins can shed their extracellular domains following bacterial adherence as well as act as releasable decoy ligands for bacterial adhesins. Subsequently, this limits the ability of enteric pathogens to bind other ligands and invade the intestinal epithelium. For example, *Helicobacter pylori* binds to the extracellular domain of the mucin Muc1 through adhesins/lectin interactions, upon which Muc1 is released from the epithelial surface[186,187]. Not surprisingly, *H. pylori* infection also results in the depletion of Muc1 mucin[188]. A similar mechanism is observed during *Campylobacter jejuni* infection where Muc1 was shown to protect epithelial cells from the effects of cytolethal distending toxin by acting as a releasable decoy[189]. This is yet another way for the host to prevent pathogen invasion of IEC. A recent study showed that *C. rodentium* infection induced substantial changes

in the amount of intestinal mucins, including Muc2 and demonstrated Muc2 binding to *C. rodentium*, reflecting on the ability of secreted mucins to remove pathogenic bacteria from near the epithelial surface[190]. *S. typhimurium* also binds to a neutral intestinal mucin, ~250kDa which serves as a receptor for *Salmonella* binding. This may provide an initial attachment site on the mucus layer for *S. typhimurium* and may contribute to *Salmonella's* ability to successfully colonize the intestinal surface[191].

Despite the complex nature of the mucus layer and the multiple levels of protection it offers, enteric pathogens have evolved a number of strategies to subvert or avoid the mucus barrier and directly access the intestinal epithelium. The commonly used strategies for subversion of the host mucus barrier are (1) degradation and penetration of the mucus (2) avoidance of the mucus layer (3) alterations in the host cells (e.g. disruption of the epithelial integrity)[121]. For the majority of pathogenic bacteria, flagella-mediated motility and chemotaxis are important routes for navigating the mucus layer. Flagella are the primary motility organelle which helps to propel the bacteria through the mucus layer and access the intestinal surface to permit colonization[192]. Some enteric pathogens like *Vibrio cholera* and *Helicobacter pylori* rely on flagella-mediated motility to get through the mucus layer[193,194] whereas for some enteric pathogens such as *C. jejuni*, motility combined with chemotaxis is crucial for accessing unique colonization niches on the epithelial surface[195,196]. *C. jejuni* also uses the Muc2 mucin as an environmental cue to modulate the expression of genes involved in its pathogenicity and colonization[197]. In addition, enteric pathogens have evolved an array of enzymes to degrade intestinal mucins. It is important to note that mucus degradation is not limited to enteric pathogens, since commensal bacteria also harbour enzymes to digest complex mucins as a means to provide food for themselves and other resident bacteria in the gut[198–200]. Interestingly,

microbes are able to switch between different food sources, depending on their availability. *Bacteroides thetaiotaomicron*, a glycophile normally digests a broad range of polysaccharides found in plant fibre, as well as on the surface of sloughed epithelial cells but in conditions where these food sources are limited, it turns to glycan-forging in the mucus[172]. However, the colonization and mucolytic activity of commensals is limited to the outer mucus layer, unlike enteric pathogens which are able to penetrate the mucus layer barrier, as a prerequisite to colonize and infect the underlying epithelium. Degradation of mucus is a complex process mediated by several enzymes. It usually begins with the proteolysis of the non-glycosylated protein backbone of Muc2 by host and microbial proteases. This decreases the viscosity of mucus layer, accompanied by the accumulation of highly glycosylated mucin subunits which are resistant to proteolytic degradation. Mucin glycopeptides are further degraded by bacterial enzymes which include glycosidases, sulphatases, sialidases, fucosidases, cysteine proteases and mucinases, corresponding to the complexity and the type of oligosaccharide chains[201–203]. Enteric pathogens like *C. rodentium*, EPEC, and *Shigella flexneri* secrete mucin serine proteases through Type V secretion systems into the extracellular milieu. These proteases recognize O-glycosylated serine residues on the mucin molecules and cleave the peptide backbone, potentially decreasing the viscosity of the mucus layer and hence are classified as mucinases[204–206].

Another strategy commonly used by enteric pathogens is to avoid the mucus barrier. Intestinal M cells are found in the follicle-associated epithelium and act as part of an antigen sampling system. M cells allow microorganisms to cross through them and be captured by the underlying antigen presenting cells like dendritic cells and thus play a role in promoting mucosal defense (previously discussed). However, compared to the surrounding enterocytes, M cells have a poorly organized brush border membrane, no glycocalyx layer and a thin mucus layer, and

therefore, they provide an easy route for infection of the intestinal mucosa and systemic spread by enteric pathogens, such as *Salmonella, S. flexneri*, *Yersinia enterocolitica* and *V. cholera*[54,207,208]. Some of these pathogens can then spread laterally, through other IEC, thereby disrupting the integrity of intestinal epithelium by accessing the basolateral surface of other IEC. Enteric pathogens can also modulate the mucin biosynthesis pathways. *H. pylori* decreases gastric mucin synthesis by directly inhibiting one of the precursor glycosyltransferases required for mucin biosynthesis, UDP-galactosyltransferase[188]. *Shigella* activated bone morphogenetic protein (BMPs) modulates the transcription of the CDX2 transcription factor which is needed for Muc2 and Muc5AC mucin expression by epithelial/goblet cells[209]. Likewise, *Salmonella* induced IFN-γR signalling controls mucus secretion by goblet cells as infected IFN-γR-/- mice displayed significantly greater numbers of mucus-filled goblet cells in their intestinal tissues[210]. Overall this suggests that in addition to avoiding the mucus barrier, enteric pathogens can regulate/modulate mucin expression and secretion responses in the host. In summary, some pathogens use mucins as receptors and these carbohydrate moieties on the mucus layer acts as "anchors" for enteric pathogens and are likely important for initial colonization.

However, mucins may also act as decoys by binding bacteria through lectin interactions and through this binding, the mucins prevent the pathogens from penetrating the mucus layer. Once the pathogen infects the intestinal epithelium, host mucin hypersecretion responses likely flush many of the pathogenic bacteria away from the intestinal surface and/or trap the bacteria within the mucus, by which they are removed through peristaltic actions of the intestine. On the other hand, pathogens may subvert the mucus defense by triggering signalling pathways that inhibit mucin synthesis and secretion or cause apoptosis of mucus producing goblet cells.

Therefore, the dynamics of interactions between enteric pathogens and mucus are complex as goblet cell functions are probably modulated by both the pathogen and the host[121].

Much of our understanding of the interactions between enteric pathogens, IEC and host responses come from *in vivo* studies (animal models). Enteric bacterial infection models offer a powerful tool to address how goblet cells respond to a noxious stimulus and to examine dynamic changes in the host immune responses as well as different epithelial cell responses. *Citrobacter rodentium* and *Salmonella enterica* serovar Typhimurium are the two widely used bacterial infection mouse models and will be the focus of the following discussion.

1.5 Mouse models of infectious colitis

1.5.1 *C. rodentium*- a model for A/E bacterial infections

C. rodentium is a widely used *in vivo* model for understanding the pathogenesis of A/E pathogens (such as EPEC and EHEC). *C. rodentium* is a naturally occurring mouse pathogen causing transmissible murine colonic hyperplasia, which is characterized by colonic crypt elongation and a decrease in the number of goblet cells along with intestinal inflammation. It initially colonizes the caecum at earlier stages of infection (1-3 days) and is predominantly localized to the distal colon at later stages of infection[74,211]. *C. rodentium* has been shown to intimately attach to the intestinal epithelial surface, causing effacement of the brush border microvilli and forming pedestal-like structures, also known as A/E lesions. At the peak of infection, *C. rodentium* usually sheds from its host in the stool where it is hyperinfectious and can effectively transmit to new hosts via coprophagy (oral-fecal route). There are striking similarities between the virulence genes found on the LEE pathogenicity island needed for A/E pathology in terms of genetic organization and gene function between *C. rodentium*, EPEC and EHEC, making *C. rodentium* an ideal *in vivo* model to study the role of these genes in bacterial

pathogenesis[77,212]. In addition to LEE effectors, there are other virulence factors (non-LEE encoded effector genes) that play a role in *C. rodentium* pathogenesis. In our experience, *C. rodentium* infection (ie. pathogen burdens) peaks at days 6-10 post infection (dpi). This time frame also marks the induction of adaptive immune responses by the host, through cytokine production characterized by Th1 and Th17 immune responses, i.e. (IFN)-γ-producing T helper (Th)1 and IL-17-producing $CD4^+$ effector cells that orchestrate the host immune response to *C. rodentium* infection. *C. rodentium* infection is self-limiting and usually clears from the host between 14-21 days post-infection and is completely resolved by 28 dpi[213,214].

MyD88, a signalling adaptor molecule used in TLR/IL-1R pathways plays a key protective role against *C. rodentium* infection. While it plays an essential role in promoting epithelial homeostasis, it also protects the host through the induction of several pro-inflammatory cytokines, e.g IL-6 and TNF-α and by upregulating the production of inducible nitric oxide synthase (iNOS) and NADPH oxidase 1. Upregulation of these enzymes can produce large quantities of reactive nitrogen and reactive oxygen species, respectively, which can exert antimicrobial activity against *C. rodentium*[215,216]. *C. rodentium* activated TLR receptors, TLR2 and TLR4 seem to be the key players in exerting MyD88 dependent protective innate responses. TLR2 deficient mice suffer from exaggerated colitis, increased mortality, disrupted mucosal integrity and impaired production of IL-6, a cytokine important for epithelial cell repair. However, *Tlr2 -/-* mice surviving the *C. rodentium* infection ultimately cleared the infection, suggesting that TLR2 is not needed for *C. rodentium* clearance[217]. Interestingly, TLR4 is also dispensable for the clearance of *C. rodentium* infection. Infected TLR4 deficient mice are attenuated in infection induced inflammation and colonic pathology and have carry lower pathogen burdens, suggesting that TLR4 promotes early colonization of *C. rodentium* in the

colon and surprisingly, does not play a critical role in host defense[218]. Although the exact mechanisms responsible for this phenotype are not well-known, the ability of an enteric pathogen to benefit from host innate receptors triggering low level inflammation is intriguing. In addition to innate immune responses, adaptive immune responses mediated by B cells (IgG production) and CD4+ T cells are thought to play an important role in *C. rodentium* clearance from the host[213,219,220].

Another characteristic of *C. rodentium* infection is that it causes a significant reduction in the total commensal population of the host. Several studies have shown that *C. rodentium* induced intestinal inflammation results in a ~60% depletion of the commensal population by day 6-7 post infection, coinciding with increased *C. rodentium* colonization in the intestine. These changes were accompanied by 3 fold-reduction in the total number of bacterial cells (compared to uninfected controls) and significant alterations in the intestinal microbiota composition (overgrowth of Enterobacteriaceae, relative reduction in Bacteroidales). Overall, this suggested that host-mediated inflammation during *C. rodentium* infection caused commensal depletion/ alterations in the commensal composition, compromising colonization resistance and ultimately opening niches for *C. rodentium* colonization[221].

1.5.2 *S. typhimurium*- a model for enterocolitis

Salmonella enterica species are facultative Gram-negative anaerobes and a leading cause of food-borne and water-borne diarrheal diseases. The common clinical symptoms associated with *Salmonella* infection in humans are typhoid fever (commonly caused by serovar *S. typhi*) and a self-limiting gastroenteritis/intestinal inflammation (caused by S. *typhimurium* and other serovars). While serovar typhi is largerly restricted to humans, other serovars can cause natural animal infections. *S. typhimurium* is a widely used model organism for understanding the

pathogenesis of typhoid fever and gastroenteritis. While *S. typhimurium* infection can cause typhoid-like pathology in mice, it does not cause them to suffer any significant intestinal disease, likely due to colonization resistance by commensal microbiota[170,222,223].

Pretreatment of mice with streptomycin offers a unique infection model where exposure to streptomycin removes competing commensal microbes from the intestine, and allows *S. typhimurium* colonization in the large intestine (cecum), resulting in the development of enterocolitis (dramatic intestinal inflammation)[170]. However, some mouse strains including C57BL/6 mice have a natural mutation in their nramp1 gene and thus lack a functional NRAMP1 protein in their macrophages. As a result, they succumb to *Salmonella* at very early stages of the infection due to exaggerated proliferation of the microbe at systemic sites[224]. To circumvent this limitation, an attenuated strain (*S. typhimurium* Δ*aroA*) that does not kill C57BL/6 mice, has been widely used for studying enterocolitis *in vivo*[225]. Mice infected with *S. typhimurium ΔaroA* develop significant mucosal damage in addition to inflammatory cell recruitment and edema without suffering from any unnecessary mortality due to infection[226].

1.5.2.1 *Salmonella* virulence

S. typhimurium can actively invade IEC using one of two type III secretion systems it possesses[227]. Invasion of enterocytes is promoted by effectors encoded in the *Salmonella* Pathogenicity Island 1 (SPI-1), which encodes *Salmonella* T3SS1. Several SPI-1 virulence effectors induce actin rearrangement essential for cell invasion and almost all other SPI-1 effectors have been implicated in modulating host immune responses and host cell survival as well as disrupting host cell integrity. SPI-2 effectors are needed for intracellular survival of *S. typhimurium* inside macrophages, and they play a critical role in systemic infection[228]. The induction of SPI-1 expression takes place in the gut lumen where it is regulated in response to

osmolarity and oxygen availability whereas SPI-2 gene expression is upregulated inside infected host cells due to Mg2+ deprivation and phosphate starvation[228,229]. SPI-2 mutants have been shown to be impaired in systemic spread and show a reduced ability to survive inside macrophages[230].

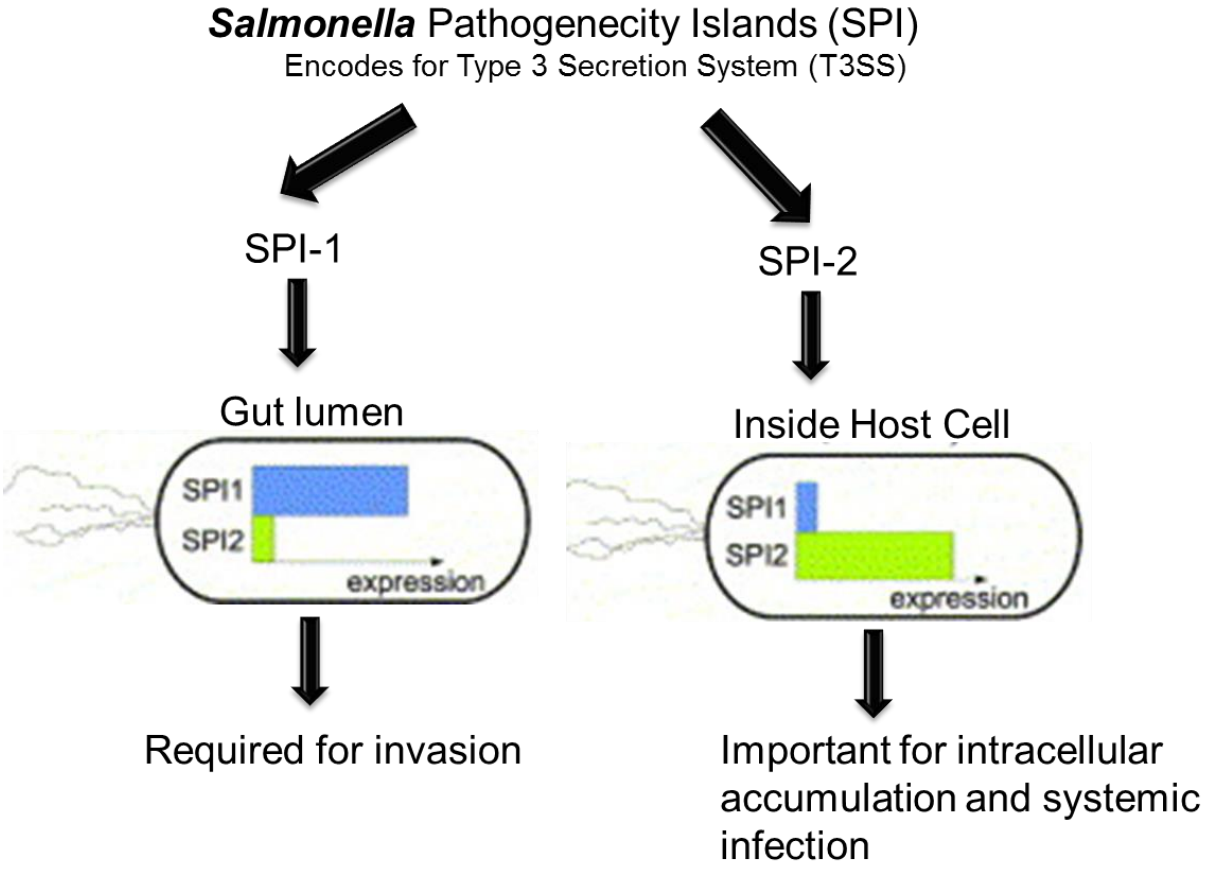

Figure 1.9 Expression and roles of SP1-1 and SPI-2 in *Salmonella* pathogenesis.
SPI-1 expression (blue bar) is upregulated in the gut lumen in response to high osmolarity and low oxygen environment. SPI-1 function is required for the initial phase of Salmonella infection (i.e. invading and penetrating the host cells). SPI-2 expression is upregulated (green bar) once *Salmonella* is inside the host cells in response to environmental cues such as Magnesium and Phosphorous levels. SPI-2 function is critical for later stages of the infection (i.e. systemic spread and intracellular replication). Image adapted from reference [229] with permission.

1.5.2.2 *Salmonella* and immune activation

Salmonella associated PAMPs activate a number of innate immune receptors, including TLRs[231]. The activation of TLR4 in response to *Salmonella* LPS is essential for triggering innate immune responses resulting in activation of NF-kB, as a result, *Tlr4-/-* mice display heightened susceptibility to *Salmonella* infection. Furthermore, TLR4 dependent activation of macrophages and natural killer cells in response to *Salmonella* LPS drives the production of a number of pro-inflammatory cytokines[232]. Another important innate receptor during *Salmonella* infection is TLR5, stimulated by *Salmonella* flagellin. Flagellin-mediated activation of TLR5 on the IECs is a potent activator of NF-kB resulting in the production of pro-inflammatory cytokines and chemokines[69,233,234]. Increased secretion of the chemokine IL-8 by IEC recruits neutrophils to the site of infection which are important for the clearance of *Salmonella* infection, because *Salmonella* can be killed by neutrophils through the formation of neutrophil extracellular traps which traps and kill bacteria due to the presence of several proteins such as lysozyme, proteases, antimicrobial peptides, ion chelators (calgranulin) and degradation of virulence factors by the protease activity of neutrophil elastase[235–237].

In addition to IL-8, the SPI-1 effector SipA serves as a pathogen elicited neutrophil chemoattractant, recruiting neutrophils to infected IEC where they can transmigrate out of the mucosa to the apical side of IEC, and then into the gut lumen, where they can damage luminal *Salmonella*. SPI-1 and SPI-2 effectors have both been shown to modulate host immune responses[238]. *Salmonella* SPI-1 effectors activate intracellular signalling cascades and induce membrane ruffling, thereby promoting the uptake of *Salmonella* and activating MAPKs which can also induce the NF-kB signalling cascade[239]. The SPI-1 effector SopE has been shown to activate Cdc42 and downstream MAPK signalling, ultimately resulting in the transient SPI-1

dependent activation of NF-kB signalling during *Salmonella* infection providing an example of how enteric pathogens can engage with the host cell signalling machinery[240,241]. In conclusion, enteric-pathogen induced intestinal inflammation is a double edge sword where the outcome of the infection is dictated by host immune responses triggered by bacterial PAMPS as well as by a pathogen's ability to engage the signalling machinery within the host cell for its own benefit.

As previously discussed, most enteric pathogens must cross the mucus barrier to colonize and infect the intestinal epithelium. While flagellated pathogens like *Salmonella* and *C. jejuni* can propel through the mucus layer with flagella-mediated motility and chemotaxis[195,242,243], it is not entirely clear how non-flagellated pathogens like *C. rodentium* penetrate and cross the mucus layer. Class 2 SPATES, a family of serine proteases belonging to Autotransporter (AT) secretion pathway has come into light for the presence of several annotated/characterized mucinases and for their ability to digest intestinal mucins *in vitro*[244–247]. Furthermore, their high prevalence in clinically important enteric pathogens suggests a potential link between the ability of these pathogens to cross the mucus layer and their pathogenesis. The following discussion will focus on further understanding the role of these SPATES in enteric bacterial pathogenesis.

1.6 Bacterial virulence- a paradigm shift

The Type III secretion system (T3SS), also known as the injectisome provides many enteric bacterial pathogens with an effective system allowing them to inject virulence factors directly into their host cell's cytoplasm. This virulence strategy has emerged as a hallmark for Gram-negative bacterial pathogenesis[248]. However, in recent years, other bacterial secretion systems have come to light for their role in bacterial pathogenesis, type V secretion being one of them[249]. The type V secretion system is one of the simplest protein secretion pathways, found in the outer membrane of a majority of Gram-negative bacteria, also known as the autotransporter

secretion pathway. Autotransporter proteins consist of three distinct domains- (1) N terminus region/amino terminus consisting of a signal peptide sequence important for translocation of the immature protein peptide across the inner membrane. The N-terminus signal peptide is cleaved by signal peptidases, releasing the protein into the periplasm. (2) The carboxy-terminal β-barrel-forming domain (β-domain) structure inserts into the outer membrane and translocates (3) the passenger domain through the β barrel pore to the cell surface. Once at the cell surface, the passenger domain can either stay attached to the cell surface or it gets cleaved and released into the extracellular milieu through its autoproteolytic activity or the activity of other proteases[250–253]. SPATES (Serine Protease Autotransporters of Enterobacteriaceae) consist of a large family of proteases secreted by enteric pathogens (such as *Shigella*, *E. coli* strains such as EPEC, EHEC and *C. rodentium*), where they are implicated in bacterial virulence. As the name implies, SPATES are secreted through the Type V secretion pathway. The passenger domain consists of a characteristic GDSGS domain, where a serine is the residue responsible for proteolytic activity. The active site of serine proteases is also dependent on histidine (H) and aspartic acid (D), which form a catalytic triad along with serine (S)[244–246].

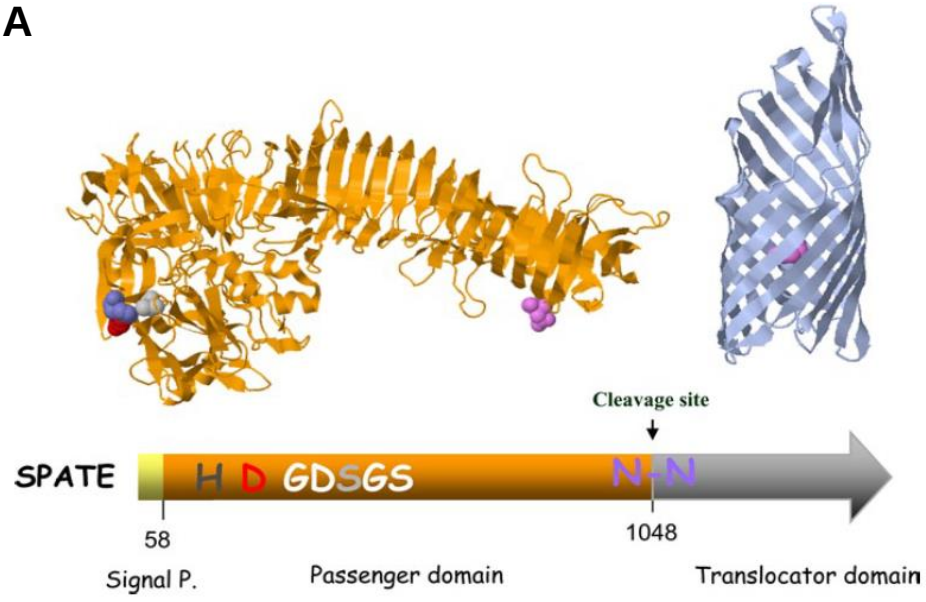

B

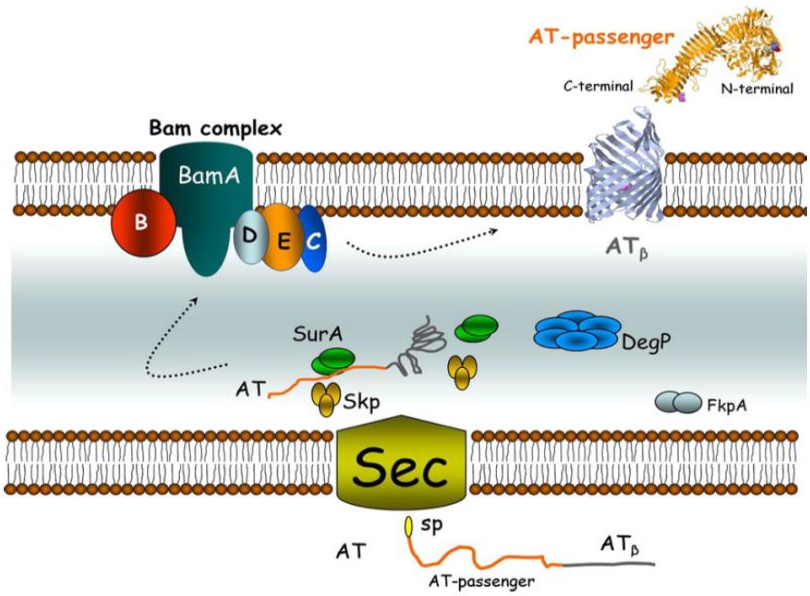

Figure 1.10 Structural organization and biogenesis of SPATES.
(A) SPATE autotransporters consist of three functional domains, signal peptide sequence, N terminus passenger domain and C terminus translocator domain. The passenger domain is responsible for the biological activity of SPATES. SPATES are characterized by the presence of the GDSGS domain, where serine is the catalytic residue. Passenger domain crystal structure (orange) shows the catalytic traid consisting of histidine (H), aspartic acid (D) and serine (S). The cleavage site (asparagine residues N, violet) represents the site of cleavage between the passenger domain and β-barrel translocator domain (grey). (B) Autotransporters are translocated into the periplasmic space through the Sec dependent pathway. Once in the periplasm, they become associated with chaperones to prevent aggregation and premature folding. Translocation of the AT passenger domain through the outer membrane occurs through the C-terminus β-barrel domain. Once at the surface, ATs can stay associated with the outer membrane or undergo intra-barrel cleavage at the N-N cleavage site where they are then secreted into the extracellular milieu (as in case of SPATES). Image reproduced with permission from reference [254].

Based on their functional activity, SPATES are further classified into two categories (i) Class 1 SPATES and (ii) Class 2 SPATES. Class 1 SPATES exert cytotoxic effects on host cells and have been shown to target several host cytoskeleton proteins such as α-spectrin through an unknown mechanism. Targeting host cytoskeleton proteins alters the integrity of the host cells through the disruption of their tight junctions[254,255]. Some of the best studied Class 1 SPATES include EspC (EPEC), Pet (enteroaggregative *E. coli*, EAEC), SigA (*Shigella*, EAEC) and Sat (uropathogenic *E.coli* UPEC, *Shigella*, EAEC). Class 1 SPATES have host intracellular targets

and can cause significant mucosal damage by exerting enterotoxin activity on intestinal tissues. The major substrate for Class 2 SPATES is mucins as these SPATES possess mucinase activity. Class 2 SPATES generally have extracellular targets not limited to glycoproteins found in the mucus layer, but have a much broader range of targets, for example, glycoproteins found on hematopoietic cells and leukocytes which have diverse roles in cellular and innate and adaptive immune functions. Therefore, Class 2 SPATES are classified as immunomodulators. Most of our understanding of Class 2 SPATES comes from studies of Tsh/Hbp (*E.coli*) and the Pic protease (*Shigella*, EAEC, UPEC, *C. rodentium*)[245,255].

1.6.1 Protein involved in intestinal colonization, Pic

Pic homologs have been identified in several enteric pathogens such as *Shigella flexneri*, EAEC, UPEC and *C. rodentium*. Initial characterization of Pic, a secreted protease showed it posseses multifunctional roles, as it was shown to have mucinase activity, it conferred serum resistance and caused red blood cell (RBC) agglutination[204]. Pic binds to the monosaccharide constituents of the oligosaccharide chains of the mucin molecules (such as GlcNac, GalNac and sialic acid), displaying lectin-like activity. This binding is thought to be important for Pic-mediated degradation of the protein backbone of mucins. Preincubation of Pic with monosaccharides reduced Pic binding to BSM (bovine submaxillary mucin). Interestingly, pretreatment of BSM with neuraminidase (removes terminal sialic acid residues from the mucin) resulted in a significant reduction in Pic's mucinase acitivity, compared with untreated mucin, providing further evidence to suggest that Pic's ability to bind and interact with monosaccharides is an important factor for its binding to mucins and its mucinase activity[256].

Pic is thought to be important for promoting intestinal colonization of enteric pathogens by cleaving complex mucins and providing a nutritional advantage to enteric pathogens once

readily available food sources are exhausted, presumably due to the competing commensal microflora or the absence of preferred substrates in the intestine. In EAEC, the Pic mutant (PicS258A, serine replaced with alanine hence abolishing the mucinase activity of Pic) was shown to be impaired in intestinal colonization and was outcompeted by a WT EAEC Pic construct in competition studies[206]. Interestingly, WT EAEC Pic and Pic mutant (PicS258A) strains entered the stationary phase of growth around the same time when grown in the presence of crude cecal mucin, however, at later time points, the growth of the Pic mutant was attenuated whereas WT Pic continued steady growth for several more hours. Furthermore, Pic enhanced the growth of a WT EAEC construct upon addition of mucin to M9 minimal media whereas the Pic mutant's growth remained uniform even in the presence of mucin. It has also been shown that Pic degrades intestinal mucins and BSM in a dose dependent manner and this activity is dependent on its serine protease motif. Preincubation of Pic with phenylmethane sulfonyl fluoride (PMSF) , a protease inhibitor or site directed mutagenesis of the catalytic serine residue abolished Pic's ability to cleave mucin[204]. Overall, these studies helped define the metabolic role of Pic in intestinal colonization[206,256].

Pic homologs found in EAEC, UPEC and *S. flexneri* have also been shown to induce mucin hypersecretion in a rat ileal loop model, characterized by luminal fluid accumulation, an increase in the number of mucus-producing goblet cells and increased cavitation of goblet cells. Rapid mucin secretion was quantified using a Periodic acid–Schiff (PAS) calorimetric assay (detects neutral mucins) as well as histological quantification of acidic mucins using Alcian Blue staining. Interestingly, mucin hypersecretion was independent of the Pic serine protease motif[176]. The ability of Pic to induce mucin hypersecretion but also degrade mucus due to its mucinase activity appears to suggest contradictory functions. We hypothesize that mucus colonizing

enteric pathogens may use Pic to induce mucus secretion, but also use it to prevent their rapid expulsion from the intestine by degrading the secreted mucus, thereby remaining within the gut, but also obtaining a rich nutrient source for the bacteria in the mucus layer.

Finally the most recent reported function of Pic is its ability to act as an immunomodulator. The ability of Pic to cleave O-linked glycoproteins was found to extend to CD43 (a sialomucin and a predominant membrane associated glycoprotein on the surface of leukocytes), CD44 (multifunctional cell surface glycoprotein), CD45 (receptor-linked protein tyrosine phosphatase), CD93 (glycoprotein), fractalkine/CX3CL1 (membrane bound chemokine) and PSGL-1 (glycoprotein found on hematopoietic cells). Cleavage of the O-linked glycan PSGL-1 by Pic inhibited PMN chemotaxis, migration and the oxidative burst reaction in neutrophils. Likewise, crosslinking of surface O-linked glycoproteins by Pic induced cell death through apoptosis[257]. Overall, Pic's ability to cleave O-linked glycans present on the surface of several leukocyte populations (granulocytes, monocytes, T-lymphocytes and B- lymphocytes) as well as other substrates appears to impair the ability of the host to mount an effective leukocyte and lymphocyte-mediated response. A recent study expanded on Pic's proteolytic activity against O-linked glycoproteins found on hematopoietic cell lineages, including leukocytes and lymphocytes, suggesting it plays an important role in modulating innate and adaptive immune responses and hence it acts as an immunomodulator[258]. This finding has important implications for our understanding of the roles played by SPATES in modulating the host immune system.

The majority of our understanding of the role played by Pic in bacterial virulence comes from *in vitro* and *ex vivo* analysis, making it hard to make conclusions in the context of a natural intestinal infection. Although Pic appears to have multifaceted roles in the pathogenesis of several clinically important human enteric pathogens such as EPEC, EAEC, UPEC,

Shigella[204,247,259], the role of Pic *in vivo* during an enteric infection is unknown due to the lack of an appropriate animal model. Given that *C. rodentium* contains Class 2 SPATE homologs (e.g. Pic) and colonizes and infects mice, it provides an excellent model to study the role of these SPATES in bacterial colonization and pathogenesis and will be the focus of our next discussion section. Lack of in depth studies investigating the role of Pic in bacterial virulence prompted us to examine its role using *C. rodentium* model (Chapter 4).

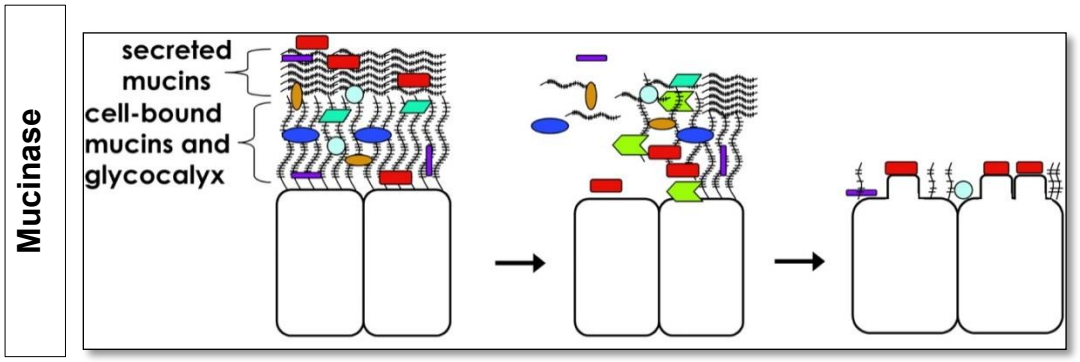

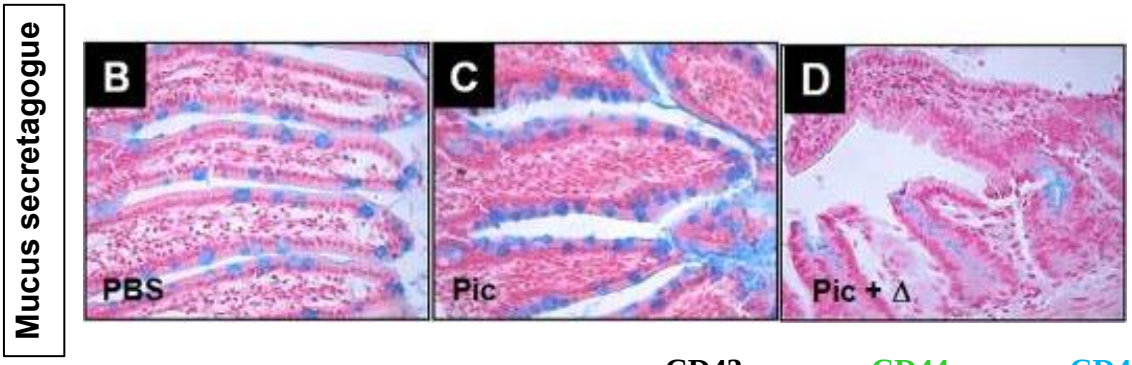

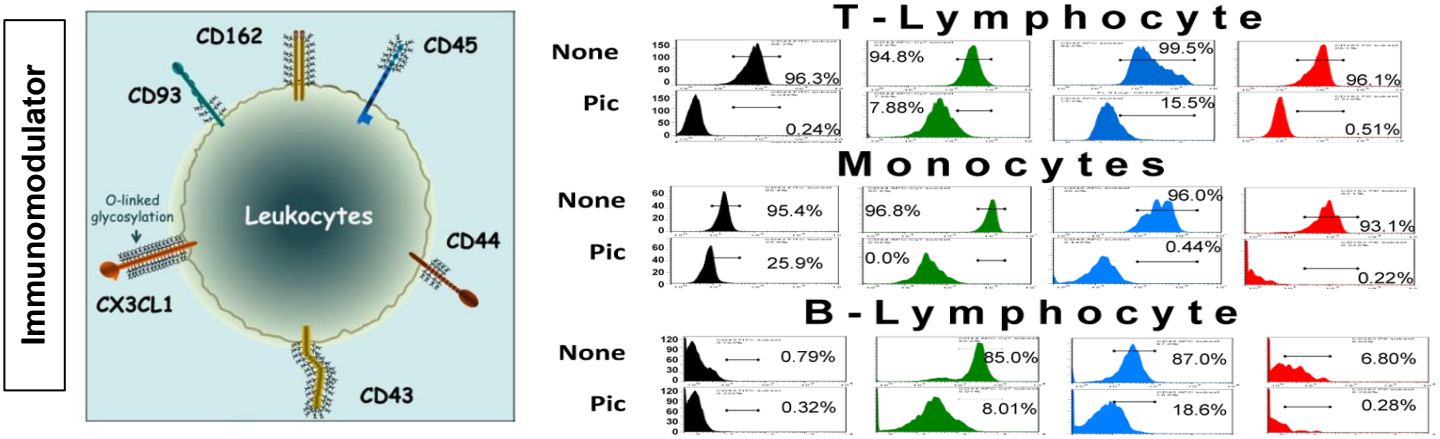

Figure 1.11 Proposed roles of Pic (protein involved in intestinal colonization), a multifunctional class 2 SPATE expressed by several enteric pathogens.
(A) Proposed model for Pic's mucinase activity in promoting intestinal colonization. Pic's ability to cleave O-glycans found in the mucus layer (mucinase activity) is thought be important for helping enteric pathogens cleave complex glycans and penetrate the mucus layer. This ultimately plays a role in bacterial colonization. As depicted in Panel A, serine proteases like Pic (green) are secreted by enteric pathogens (such as *E. coli*, *Shigella*, *Citrobacter*) (red) and can cleave heavily glycosylated proteins of the mucus layer thereby allowing the pathogens to access the intestinal surface. Image reproduced from reference [260].
(B) Pic has been shown to be a potent mucin secratagogue. As shown in the middle image (C), through Alcian Blue staining, purified Pic induced mucin hypersecretion in the intestinal lumen, whereas no mucin secretion was noted in the absence of Pic. Image reproduced from [176].
(C) A more recent role identified for Pic is its ability to act as an immunomodulator. Pic has been shown to cleave O-linked glycoproteins present on the surface of leukocytes, such as CD43, CD44, CD45 and CD162.When incubated with purified naïve human leukocytes, purified Pic was shown to cleave the extracellular domain of mucin type O-linked glycoproteins present on monocytes, granulocytes, B- and T- lymphocytes, as seen through flow cytometry analysis. Image reproduced/adapted from [257] under Creative Commons Attribution License.

1.6.2 *C. rodentium*- a model for studying the role of autotransporters in bacterial pathogenesis

The *C. rodentium* genome has been annotated as containing 20 different autotransporter genes, 3 of which are predicted to belong to the SPATE family, which have been shown to contribute towards bacterial virulence and are multifunctional[212]. Based on the sequence alignment and homology analysis, 2 out of the 3 SPATE homologs belong to the family of Class 2 SPATES and share more than 80% homology to Tsh and Pic homologs respectively, found in pathogenic *E. coli*. One homolog is a Class 1 SPATE, sharing 84% homology to EspC secreted by EPEC. The remaining ATs are thought to be involved in bacterial adhesion, agglutination of red blood cells and recruitment of host factors to the outer membrane of the invading pathogen. One of these autotransporters is a pseudogene, resulting from a frame shift mutation[260].

The majority of the characterization of the role of SPATES in bacterial virulence has been based on *in vitro* or *ex vivo* studies. Previously used rat ileal loop model[254] and the

streptomycin pretreatment *Salmonella* model[256] offer great potential but have their own limitations. As previously discussed, *C. rodentium* is a natural mouse pathogen and infects mice without any need for prior perturbation of the commensal microbiota and is a well-defined model for assessing enteric disease pathology in a natural environment. Recent identification of some key SPATES in *C. rodentium* makes it an excellent model for investigating the role of these SPATES in bacterial virulence and pathogenesis in *vivo*[260]. In fact, a recent study looked at the role of the Class 1 SPATE named as Crc1 (YP_003368469, shares homology to cytotoxic autotransporter, EspC). Upon infection of C57BL/6 mice with the Δ*crc1* mutant, the mice displayed a hyperinflammatory phenotype within their GI tracts with increased infiltration of immune cells and increased production of several pro-inflammatory cytokines in the distal colon, suggesting a novel immunomodulatory role for Class 1 SPATES[261].

1.6.3 Research objectives

The intestinal mucus layer and the glycosylation of its main constituent – Muc2, have been implicated in providing host defense. The mucus layer sits at the host-microbe interface and offers the first line of defense against enteric pathogens. However, very little is known about how enteric pathogens interact with the mucus layer, and the role played by Muc2 glycosylation in protecting the intestinal epithelium from invading pathogens. Furthermore, although the mucus layer has largely been viewed as a passive physical barrier, this underestimates its multi-faceted roles in host defense. Equally intriguing is the ability of enteric pathogens to cross the mucus barrier and subvert this barrier. Despite the ability of the mucus layer to largely segregate commensal microbes away from the epithelium, almost all enteric pathogens do ultimately cross the mucus barrier and infect the underlying epithelial cells, raising the question of how this subversion occurs, and whether bacterial pathogens ultimately use the mucus layer as part of

their pathogenic strategy. Even though the mucus layer acts as a frontline defense barrier against bacterial infections, there has been little characterization of the interactions that must occur between intestinal mucin (Muc2) and enteric pathogens using *in vitro* approaches. Moreover, the *in vivo* dynamics of pathogen-mucus interactions and the impact of these interactions on bacterial pathogenesis have not been assessed. Looking from the bacterial perspective, enteric pathogens like *C. rodentium* are known to secrete serine proteases into the extracellular milieu, however very little is known about the role of these SPATES, as putative virulence factors, in modulating bacterial virulence as well as innate immune responses.

General Hypothesis: The intestinal mucus layer is a dynamic, complex layer which, in addition to providing a physically protective barrier, also provides a niche for complex interactions with enteric pathogens, ultimately impacting host defense and bacterial pathogenesis. My work explores enteric microbe-mucus interactions from both the host and pathogen perspective and is among the first to explore how mucus and its glycosylation can impact on bacterial pathogenesis *in vivo*.

Using two different models of infection, I studied (i) how the invasive enteric pathogen *Salmonella typhimurium* interacts with and ultimately crosses the intestinal mucus layer to infect the underlying intestinal epithelium (ii) how the A/E enteric bacterial pathogen *C. rodentium* that is related to human *E. coli* pathogens uses the SPATE/mucinase Pic to modulate its pathogenesis and regulates host innate immune responses through TLR2 stimulation (iii) how glycosylation of Muc2 plays a role in host defense again enteric pathogens and the role of fucosylation, a terminal modification of Muc2 and other proteins adds to the functionality of the mucus layer as a barrier. Overall the body of work I performed during my Ph.D. provides a novel understanding of the functional dynamics of mucus-enteric pathogen interactions and sheds light on the complexity of

these interactions, viewed as a constant struggle between the host and the pathogen. My work also highlights the importance of the mucus layer in maintaining host-microbial homeostasis and highlights the significance of the mucus barrier in the initiation and resolution of intestinal disease caused by enteric pathogens.

Chapter 2: Materials and methods

2.1 Animals

Six to eleven week old C57BL/6, *Muc2 -/-* and *Tlr2 -/-* mice were bred in-house at the Child and Family Research Institute. *C3GnT-/-* (core 3 β1,3-N-acetylglucosaminyltransferase) mice (on the C57BL/6 background) and intestinal epithelial cell (IEC) specific knockout mice IEC *C1galt1 -/-* (core 1 β1,3-galactosyltransferase) (on the C57BL/6 and 129 genetic background) were generated in Dr. Lijun Xia's laboratory (University of Oklahoma) as previously described [140,150] and bred in our animal facility for more than 2 years for the infection studies. Briefly, *C3GnT -/-* mice were genereated by by targeted homologous recombination in mouse embryonic stem cells. Targeted deletion mice, IEC *C1galt1 -/-* (lacking *C1galt1 -/-* specifically in IEC) were generated by crossing mice with loxP sites flanking *C1galt1* with an intestinal epithelium-specific Cre-expressing transgenic line (VillinCre mice). Mice were kept in sterilized, filter-topped cages, handled in tissue culture hoods, and fed autoclaved food and water under specific-pathogen-free conditions (Child and Family Research Institute). The protocols used in the study were approved by the University of British Columbia's Animal Care Committee and were in direct accordance with guidelines provided by the Canadian Council on the Use of Laboratory Animals.

2.2 Bacterial strains

The *S. Typhimurium* wild-type (WT) strain SL1344, the SL1344 *ΔinvA* strain, and the SL1344 *ΔaroA* strain were grown, with shaking (200 rpm), at 37°C in Luria-Bertani (LB) broth supplemented with 100 μg/ml streptomycin. Approximately 24 h prior to infection, 6 to 8 week-old mice were treated with 20 mg of streptomycin by oral gavage. 24 h after streptomycin treatment, mice were infected with the strains mentioned above at a dose of 3×10^7 CFU in 100 μl of phosphate-buffered saline (PBS; pH 7.2) by oral gavage.

For *C. rodentium* infections, *C. rodentium* DBS100 and *C. rodentium* mutants were grown with shaking overnight at 200 rpm at 37°C in Luria-Bertani (LB) broth. For studies in Chapter 5, a streptomycin resistant derivative of *C. rodentium* DBS100 was used (grown in LB broth supplemented with 100 μg/ml streptomycin). Mice (6 to 8 weeks old) were infected with 0.1 ml of the O/N cultures (~2.5×10^8 CFU) by oral gavage.

2.3 Tissue collection and histology

Mice were monitored for mortality and morbidity throughout the course of infection and were euthanized when they showed >15% body weight loss compared to their starting body weight. Uninfected and infected mice were anesthetized using isoflurane and were euthanized by cervical dislocation. For bacterial enumeration, tissues (colon, cecum, liver, spleen, mesenteric lymph nodes [MLN]) and luminal contents were collected in preweighed 2.0-ml tubes containing 1.0 ml of phosphate-buffered saline, pH 7.2 (PBS), and steel beads (Qiagen) and homogenized with a Mixer Mill 301 homogenizer (Retsch, Newtown, PA). For enumeration of bacterial counts within the tissue (adherently attached) versus in the intestinal luminal contents, the ceca and colon were opened longitudinally, and luminal contents (stool) were transferred into 2 ml tubes. Cecal and colonic tissues were washed 2X in PBS and placed into additional tubes. CFU were determined by serial dilutions of homogenized samples that were plated on the appropriate media plates (LB agar plates supplemented with 100 μg/ml streptomycin for *S.* typhimurium and streptomycin resistant *C. rodentium* DBS100) and MacConkey agar for *C. rodentium* DBS100. Plates were incubated O/N at 37°C. Colony counts were normalized to the weight of the tissue collected to obtain CFU/gram. For histology, cecal tissues were fixed in 10% neutral buffered formalin (Fisher Scientific) overnight and were then transferred to 70% ethanol. Fixed tissues were embedded in paraffin and were cut into 5-μm sections. Tissues were stained with

hematoxylin-eosin (H&E) according to standard techniques by the University of British Columbia Histology Laboratory (Vancouver, BC, Canada). To preserve the mucus layer, sections of cecal tissue were fixed in water-free ethanol-Carnoy's fixative (60% ethanol, 30% chloroform, and 10% acetic acid) (all reagents were purchased from Fisher Scientific), and after 3 h of storage at 4°C, samples were transferred to 100% ethanol for subsequent processing. Fixed tissues were embedded in paraffin and cut into 5-μm sections.

2.4 Assessing commensal translocation during *C. rodentium* infection

For assessing commensal translocation to MLN during *C. rodentium* infections, reinforced clostridial agar (Oxoid, Thermo Scientific) and anaerobe basal agar (Oxoid, Thermo Scientific) were used. MLN were harvested and transferred into 1 ml sterile PBS. CFU were determined by serial dilutions of homogenized samples and that were plated on the above-mentioned media. Plates were incubated in an Oxoid Anaerojar, where a CampyGen 2.5-liter atmosphere generation system sachet was used to create an oxygen-depleted environment for 2 days. Colony counts were normalized to the weight of the tissue collected to obtain CFU/gram.

2.5 Tissue pathology scoring

2.5.1 *Salmonella* induced gastroenteritis

Hematoxylin-eosin-stained (H&E) cecal tissues were assessed for mucosal pathology, including polymorphonuclear leukocyte (PMN) infiltration (scores 0 to 4), goblet cell numbers/depletion (scores 0 to 3), epithelial integrity (scores 0 to 3), and submucosal edema (scores 0 to 3) by two blinded observers as previously described. PMN infiltration was scored at a magnification of ×400 (10 high-power fields), and the average number of cells per high-power field was calculated. Scores were defined, as described previously[170,226], as follows: 0, <5 cells/high-power field; 1, 5 to 20 cells/high-power field; 2, 21 to 60 cells/high-power field; 3, 61

to 100 cells/high-power field; 4, >100 cells/high-power field. The average number of goblet cells per high power field (x 400 magnification) were determined and used for scoring as follows: 0= no goblet cell depletion (> 28 goblet cells/crypt), 1 = 11 to 28 goblet cells/high-power field (mild depletion); 2 = 1 to 10 goblet cells/high-power field (moderate depletion) and 3 = <1 goblet cell/high-power field (severe goblet cell depletion). Epithelial integrity was scored as: 0= no damage, 1 = epithelial desquamation; 2 = erosion of the epithelial surface (shedding of 1-10 epithelial cells/lesion); and 3 = epithelial ulceration (gaps of >10 epithelial cells/lesion and severe crypt destruction). Submucosal edema was scored as: 0 = no pathological changes; 1 = mild edema, 2 = moderate edema 3 = profound edema. The maximum possible score was 13.

2.5.2 *C. rodentium* induced colitis

Hematoxylin-eosin-stained (H&E) distal colon tissue sections were assessed for submucosal edema (0, no edema; 3, profound edema), epithelial hyperplasia (scored based on the percent change in crypt height compared to that of the control crypts; 0, no change; 1, 1 to 50% change; 2, 51 to 100%; 3, >100%), PMN infiltration (0, none; 3, severe), epithelial integrity (0, no damage; 1, <10 epithelial cells shedding per lesion; 2, 11 to 20 epithelial cells shedding per lesion; 3, maximum damage to epithelial surface as noted by crypt destruction and epithelial ulceration) and goblet cell depletion (0, no depletion, > 28 goblet cells/high power field, 3, maximum depletion, i.e. <1 mucus-filled goblet cells/high-power field). The maximum possible score was 15. Scoring was done by 2 blinded observers.

2.6 Immunohistochemistry

Unless indicated otherwise, formalin fixed sections were used for immunostaining. For immunohistochemical detection of Muc2, periodic acid-Schiff/alcian blue (PAS/AB) and IAP (intestinal alkaline phosphatase) staining, Carnoy's fixed tissues were used. For immunostaining,

deparaffinized sections were boiled for 20 min in citrate buffer (10 mM sodium citrate, 0.05% Tween 20, pH 6.0) for antigen retrieval. The sections then were blocked for 20 min using blocking buffer (2% goat serum, 1% bovine serum albumin [BSA], 0.1% Triton X-100, 0.05% Tween 20 in 0.1 M PBS, pH 7.2) to prevent nonspecific antibody binding. Sections were incubated overnight at 4°C with one of the following primary antibodies: rabbit anti-Muc2 (1:200; Santa Cruz Biotechnologies), an anti-LPS antibody (1:50; Salmonella O antisera; BD Biosciences), a rabbit anti-IAP antibody (1:200; Abcam), rat derived *C. rodentium*-specific Tir (1:5,000; gift from W. Deng), rat derived anti-F4/80 (1:200; AbD Serotec), rabbit derived polyclonal anti-CD3 (1:100; Abcam), rabbit derived monoclonal anti-Ki67 (1:100, Abcam), rabbit derived polyclonal anti-Relmβ (1:100,Abcam), rabbit derived polyclonal anti-Tff3 (1:200; a gift from D. Podolsky). Staining for fucosylated residues was carried out using biotinylated-Ulex europaeus agglutinin-1 (2µg/ml; Vector Labs). The following secondary antibodies were used: Alexa Fluor 568-conjugated goat anti-rabbit IgG (1:2,000 dilution; Molecular Probes) or Alexa Fluor 488-conjugated goat anti-rabbit IgG (1:2,000 dilution; Molecular Probes). Tissues were mounted using ProLong gold antifade (Molecular Probes) containing 4′,6-diamidino-2-phenylindole (DAPI) for DNA staining. Images were captured using a Zeiss AxioImager microscope equipped with an AxioCam HRm camera operating through AxioVision software.

2.7 Fluorescence in situ hydridization (FISH) staining

Formalin fixed tissues (distal colon) were deparaffinized and incubated with Texas red-conjugated EUB338 general bacterial probe (5′-GCTGCCTCCCGTAGGAGT-3′) and an AlexaFluor 488 conjugated GAM42a probe (5′-GCCTTCCCACATCGTTT-3′) that recognizes bacteria that belong to the γ-Proteobacteria class (37°C, O/N, in the dark). Tissue samples were washed with hybridization buffer (0.9 M NaCl, 0.1 M Tris pH 7.2, 0.1% SDS). This step was

repeated with FISH Washing Buffer (0.9 M NaCl, 0.1 M Tris pH 7.2) with gentle shaking for 15 minutes. Sections were washed with water and mounted using GOLD Prolong with DAPI (Molecular Probes) and imaged using AxioImager microscope equipped with an AxioCam HRm camera operating through AxioVision software.

2.8 *In vivo* intestinal permeability measurement

Uninfected or infected mice at day 6 post infection (day 6 PI/ 6DPI) used in the study were administered 150 µl of 80 mg/ml fluorescein isothiocyanate (FITC)-dextran (FD4; Sigma-Aldrich) by oral gavage 4 h prior to euthanizing the mice. Mice were anesthetized using isoflurane, and blood samples (~500 µl/mouse) were collected using cardiac puncture. The collected samples were immediately transferred to 3% acid-citrate dextrose (ACD) containing 20 mM citric acid, 110 nM sodium citrate, 5 mM dextrose (protocol provided by Harald Schulze, Shivdasani Laboratory, DFCI). The serum concentration of the FITC-dextran was measured using a fluorometer (PerkinElmer Life Sciences) (excitation wavelength of 490 nm and emission wavelength of 530 nm).

2.9 RNA extraction and quantitative PCR

Immediately after euthanization of mice, colonic tissues were collected and stored in RNAlater Buffer (Qiagen) at -80 °C. Total RNA was extracted using a Qiagen RNeasy kit as per manufacturer's instructions. Total RNA was quantified using a NanoDrop spectrophotometer (ND1000). One microgram of RNA was reverse transcribed using an Omniscript reverse transcription (RT) kit (Qiagen). For quantitative PCR, cDNA was diluted 1:5 in RNase- and DNase-free water, and 5 µl of diluted cDNA was added to a PCR mixture (10 µl of Bio-Rad SYBR green supermix, primers at a final concentration of 300 nM; final reaction volume, 20 µl). Quantitative PCR was carried out using a Bio-Rad MiniOpticon or Opticon 2 system. Data was

analyzed/quantified using Gene Expression Macro OM 3.0 software (Bio-Rad). Expression levels were normalized by the respective housekeeping gene expression/transcription. PCR primers (sequences) and PCR cycling conditions used are listed below:

Table 2.1 Murine qPCR primer sets and PCR conditions used in this study.
[##] House-keeping genes

Target mRNA	Primer Sets	PCR cycling conditions (denature, anneal, extend)
TNF-α	F: 5'CATCTTCTCAAAATTCGAGTGACAA 3' R: 5'TGGGAGTAGACAAGGTACAACCC 3'	94°C, 30s/ 55°C, 30s/ 72°C, 45s
IL-1β	F: 5'CAGGATGAGGACATGAGCACC 3' R: 5'CTCTGCAGACTCAAACT CAC 3'	94°C, 30s/ 65°C, 30s/ 72°C, 45s
IFN-γ	F: 5' TCAAGTGGCATAGATGTGGAAGAA 3' R: 5' TGGCTCTGCAGGATTTTCATG 3'	94°C, 30s/ 60°C, 30s/ 72°C, 30s
IL-17A	F: 5' GCTCC GAAGGCCCTCAGA 3' R: 5'CTTTCCCTCCGCATTGACA 3'	94°C, 30s/ 60°C, 30s/ 72°C, 30s
IL-10	F: 5' GTTGCCAAGCCTTATCGGAA 3' R: 5'CCAGGGAATTCAAATGCTCCT 3'	94°C, 30s/ 55°C, 30s/ 72°C, 30s
IL-6	F: 5' GAGGATACCACTCCCAACAGACC 3' R: 5'AAGTGCACTACTGTTGTTCATACA 3'	94°C, 30s/ 60°C, 30s/ 72°C, 30s
MCP-1	F: 5' TGCTACTCATTAACCAGCAAGAT 3' R: 5'TGCTTGAGGTGGTTGTGGAA 3'	94°C, 30s/ 59°C, 15s/ 72°C, 90s +78°C, 5s
KC	F: 5' TGCACCCAAACCGAAGTCAT 3' R: 5'TTGTCAGAAGCCAGCGTTCAC 3'	94°C, 30s/ 57°C, 30s/ 72°C, 45s
Core 1 Synthase	F: 5'GTGGGACTGAAAACCAA 3' R 5'AGATCAGAGCAGCAACCA 3'	94°C, 30s/ 56°C, 30s/ 72°C, 29s
Core 3 Synthase	F: 5′ AGCACTGCAGCAGTGGTTC 3′ R 5′ GAGGAAGGTGTCCGCGAAG 3′	94°C, 30s/ 56°C, 30s/ 72°C, 30s
Fut1	F: 5'CAAGGAGCTCAGCTATGTGG 3' R: 5'GACTGCTCAGGACAGGAAGG 3'	94°C, 30s/ 57°C, 30s/ 72°C, 45s
Fut2	F: 5'ACAGCCAGAAGAGCCATGGC 3' R: 5'TAACACCGGGAGACTGATCC 3'	94°C, 30s/ 57°C, 30s/ 72°C, 45s
18s rRna[##]	F: 5' GTAACCCGTTGAACCCCATT 3' R: 5'CCATCCAATCGGTAGTAGCG 3'	94°C, 30s/ 55°C, 30s/ 72°C, 30s
β-actin[##]	F: 5'CAGCTTCTTTGCAGCTCCTT 3' R: 5'CTTCTCCATGTCGTCCCAGT 3'	94°C, 30s/ 55-60°C, 30s/ 72°C, 30s

GADPH[##]	F: 5′ CCTGGCCAAGGTCATCCATGACA 3′ R: 5′ATGAGGTCCACCACCCTGTTGCT 3′	94°C, 30s/ 56°C, 30s/ 72°C, 30s

2.10 LPS dephosphorylation activity analysis

To assess the crude LPS detoxification activity, cecal tissues from uninfected and infected mice were homogenized in 500 µl of homogenization buffer containing 150 mM NaCl, 0.1% Triton X-100, 0.5% sodium deoxycholate, 0.1% SDS and 50 mM Tris pH 8.0, followed by the addition of 5 µl of phenylmethylsulfonyl fluoride (PMSF), a protease inhibitor. Homogenates were centrifuged at 13,200 rpm (4°C for 15 min) to remove the insoluble contents. Bradford analysis was conducted according to the manufacturer's instructions to determine the protein concentrations in the lysates. Eighty microliters of the lysate was incubated with 30 µl of 2.5-mg/ml *Escherichia coli* 055:B5 LPS (L2880; Sigma) or *Salmonella enterica* serotype Typhimurium LPS (L6511; Sigma) at room temperature for 2 h. A malachite green solution was prepared to the final concentration of 0.1% malachite green, 16% concentrated sulphuric acid, 1.5% ammonium molybdate, 0.18% Tween-20. Forty microliters of the malachite green solution was added to the reaction mixture, which was then incubated for 10 min. The reaction of malachite green dye with free phosphate released by the dephosphorylation of LPS by intestinal alkaline phosphatase (IAP) present in the tissues resulted in a color change (colorometric assay). Green color developed in proportion to the amount of inorganic phosphate released by the IAP activity. The plates were read at an absorbance of 595 nm, and data were analyzed using Microsoft Excel.

2.11 Construction of *C. rodentium* mutant strain *ΔpicC*

To generate the *C. rodentium ΔpicC* strain (on DBS100 background), the *C. rodentium picC* gene (ROD_p1411) was replaced using the lambda red system[262]. Briefly, primer pair ROD_p1411 Fwd (5′-GTGAATAAAATATACTCGCTGTGTAGGCTGGAGCTGCTTC-3′) and ROD_p1441 Rev (5′-TCAGAACATATAACGGAAGTTCGCATTCCGGGGATCCGTCGACC-3′) was used to amplify the FLP recombination target (FRT)-flanked kanamycin resistance gene (kan) from the plasmid pKD13 with PFU Turbo (Promega)[262].These two primers included sequences homologous to the flanking regions of *picC*. The resulting PCR fragment was electroporated (Bio-Rad Micropulser) into wild-type *C. rodentium* DBS100 carrying the pSIM9 recombineering plasmid[263].The recombinant genes carried by the plasmid pSIM9 catalyzed the exchange of picC with the FRT-flanked kan gene. Recombinants were selected on LB agar containing kanamycin (50 μg/ml) by incubation overnight (O/N) at 37°C, followed by removal of the kan gene from kanamycin-resistant clones with the pCP20 plasmid as described previously[262,264]. To verify the deletion of picC, colony PCR was performed using primers external to picC (ROD_p1411comp Fwd and ROD_p1411comp Rev; see below). The resulting amplicon was also confirmed by Sanger DNA sequencing at the NAPS Unit (UBC).

2.12 Construction of plasmids to complement the *C. rodentium ΔpicC* strain

Primer pair ROD p1411comp Fwd (5′-TGACCTCGAGACACATACACCGCGGAAATAG-3′) and ROD_p1411comp Rev (5′-AGCTGGATCCGTCCTTTGATAACGCCCTGAC-3′) was used to amplify the region containing the native promoter and coding sequence of *picC*. The resulting PCR product was cloned into the XhoI/BamHI restriction sites of pZA31MCS which harbours the p15A origin of

replication, and chloramphenicol resistance (Expressys, Ruelzheim, Germany)[265] to generate the plasmid pPic containing wild-type picC. This plasmid also was used as a template to construct a site-directed catalytic mutant named pPicS258I. Using a QuikChange site-directed mutagenesis kit (Agilent Technologies), site-directed mutagenesis was performed with primer pair Fwd (5′-CGGCGTCCCCGGAGACATTGGTTCCCCTCTTTTTG-3′) and Rev (5′-CAAAAAGAGGGGAACCAATGTCTCCGGGGACGCCG-3′). Following mutagenesis, the S258I mutation was confirmed using double strand sequencing of the sequence flanking GDSGS serine protease motif. Plasmids pPic and pPicS258I then were electroporated into the *C. rodentium ΔpicC* strain to produce *C. rodentium ΔpicC* + pPicC (complemented) and *C. rodentium ΔpicC* (pPicS258I) strains, respectively.

2.13 Construction of *C. rodentium ΔfucK* mutant

Overlap extension PCR was used to generate in-frame deletion of *fucK* on the chromosome of *C. rodentium* (streptomycin resistant derivative of DBS100)[266]. To generate the *ΔfucK* construct, two PCR fragments were amplified using *C. rodentium* genomic DNA as the template. Primer pairs used to amplify the PCR fragments are Fuck-P1 (5'-GACTAGGTACCGAATCCCTCGGCTATAACGCCATAGT-3') plus Fuck-P2 (5'-CATAATGACTCTCCGGCCTGCGTCGTATCT-3'), and Fuck-P3 (5'-CCGGAGAGTCATTATGAGAGAACAGGTGCGCTATCAGTA-3') plus Fuck-P4 (5'-GACAGTGAGCTCGATCGATCTCCAGCGCTTTAAGCT-3'), respectively. This resulted in a 944-bp fragment containing the upstream region of the *fucK* gene and a 1026-bp fragment containing the downstream of the *fucK* gene respectively. These two PCR fragments were then mixed and used as the template for a secondary PCR (with primer pairs Fuck-P1 containing a KpnI restriction enzyme site and Fuck-P4 containing a SacI restriction enzyme site). The 16-bp

overlapping sequence in primers Fuck-P2 and Fuck-P3 allows the amplification of a 1,956-bp PCR product. This PCR product was digested with KpnI and SacI, and directly cloned into a suicide vector pRE112 (chloramphenicol resistance)[267]. DNA sequencing was performed to confirm the *ΔfucK* construct. This pRE112-based *ΔfucK* construct was then transformed into *E. coli* SM10λ pir. The single-crossover mutants were obtained by conjugal transfer into *C. rodentium*. Double-crossover mutants were obtained by plating onto LB agar plates containing 5% sucrose. The deletion mutants were confirmed by PCR with primers Fuck-check-F (5'-GCATTCCGGTCTGTATGCACAA-3') and Fuck-check-R (5'-GCGTAGCTGTCGAGTTCAAACA-3'). The predicted size of WT and mutant bands is 1768-bp and 423-bp, respectively.

2.14 Mucinase activity assay analysis

WT *C. rodentium* DBS100, *ΔpicC*, complemented *ΔpicC* + pPicC, and *ΔpicC* (pPicS258I) *C. rodentium* strains were grown O/N in 5 ml LB culture. Bacterial cultures were spun down at 4,000 rpm for 30 min to remove bacterial cells. Supernatants were filtered through Amicon Ultra 15 (100-kDa cutoff; Millipore) filters to concentrate the samples to a final volume of ~50 µl. Crude supernatants (30 µl) were incubated for 24 h at 37°C in a medium containing 5 µl of bovine submaxillary mucin (BSM; Sigma) and 15 µl of water. Treated (BSM and crude supernatants) and untreated (BSM alone) mucin samples were electrophoresed on an 8% SDS-PAGE gel. The gel was developed using a Pierce glycoprotein staining kit (Thermo Scientific).

2.15 Mucin quantification analysis

As previously described[145,268], uninfected (only LB treated) and infected (WT *C. rodentium* and Δ*pic C. rodentium*) C57BL/6 mice (6 DPI) were injected intraperitoneally with 20 µCi of [3H] glucosamine (Amersham) and left for 4 hours for the metabolic labelling of mucins

in the intestine. After 4 hours, mice were euthanized and colon sections were scraped with a glass slide to remove mucins and they were collected in PBS. Collected scrapings were vortexed for 10 minutes and the supernatants were spun down (1,000 g for 10 minutes) to remove any cells/tissue debris. The glycoproteins were precipitated using 10% trichloroacetic acid and 1% phosphotungstic acid (PTA) (1:1 by volume). Precipitated glycoproteins were suspended in the column buffer and neutralized to a pH of 7.0. 5 ml of scintillation fluid (UniverSol) was added to the samples and a scintillation counter was used measure the total radioactivity in the samples. To separate the high molecular weight mucin pool (glycoproteins) from the non mucin pool, collected samples were loaded onto Sepharose 4B column (calibrated with blue dextran (BD; 2,000 kDa), thyroglobulin (669 kDa) and BSA (67 kDa) (Amersham). Approximately 1 ml fractions were collected (column volume 40 ml) and radioactivity for all the fractions was measured using scintillation counter. The results were analyzed using GraphPad Prism Version 5.0.

2.16 Congo red assay and cellulose production assay

To visualize the RDAR (red, dry, aggregative) phenotype (an indicator of the production of extracellular matrix components, such as curli and cellulose) 5 µl of O/N bacterial cultures were inoculated onto LB-agar (no salt) plates containing 40 µg/ml of Congo red dye and 20 µl/ml of Coomassie blue R-250. Plates were incubated at 25°C for 5 days. Cellulose production assays using Congo red and calcofluor were performed. Briefly, bacteria were streaked out for single colony isolation. Single colonies were inoculated in LB-media and cultures were grown at 25°C O/N (14-15 hours). Bacterial cells from 2 ml of O/N culture were centrifuged and resuspended in 1ml of LB media (no salt) containing 0.004% Congo red or 1.6% Calcofluor and grown shaking for 2 hours. Bacteria cultures were centrifuged for 10 minutes at ~ 17 000 g to

remove the bacterial bound Congo red or calcofluor. The amounts of unbound Congo red or calcofluor were measured by reading the absorbance of the supernatants at 490 nm for Congo red and at 350 nm for calcofluor, as previously described[269].

2.17 Crystal violet biofilm formation assay

Biofilm formation *in vitro* was assessed using the crystal violet assay. Briefly, bacteria were grown at 25°C for 5 days in LB media (no salt) in a 96-well plate. Cultures were decanted and washed 3× with water. Plate Crystal violet dye (0.1%) was added to the plate and eluted with 100% ethanol after 1 h of incubation with crystal violet dye. The optical density at 595 nm (OD_{595}) was used to measure biofilm formation.

2.18 Profiling T3SS effectors in *C. rodentium* WT and mutant strains

As previously described[270,271], WT *C.rodentium, C. rodentium* mutant strains and Δ*escN C. rodentium* (T3SS deficient control) were streaked onto LB-Agar plates for single colony isolation. 5 ml LB media was inoculated with a single colony of the above mentioned strains and grown shaking O/N at 37° C. After O/N growth in LB, the strains were subcultured (1:50 dilution) into Dulbecco's modified Eagle's medium (DMEM, Life Technologies). Cultures were incubated standing (no shaking) at 37° C, 5% CO_2 until the optical density of the cultures reached 0.7(OD_{600} ~0.7). Bacteria were pelleted and removed (13, 200 rpm, 4 °C, 10 minutes) and the supernatant proteins were precipitated using 10% Trichloroacetic acid (TCA, Sigma) O/N at 4 °C. Precipitated proteins were pelleted by centrifugation (13, 200 rpm, 4 °C, 10 minutes) and resuspended in Laemmli sodium dodecyl sulfate-polyacrylamide gel electrophoresis buffer (SDS-PAGE Buffer). Samples were resolved on 12% polyacrylamide gel and visualized by Coomasie R-250 Blue Staining.

2.19 Cell adhesion assay

CMT-93 (mouse rectal epithelial) cells (ATCC CCL-223) were seeded at a density of 1 × 10^5 cells/well (12-well plate) and grown until >90% confluence in DMEM supplemented with 10% fetal bovine serum (FBS; Life Technologies) (37°C, 5% CO2). Before bacterial infection, cells were washed twice with prewarmed DMEM supplemented with 2% FBS (2×). Cells were infected with an overnight culture of *C. rodentium* WT or *ΔpicC* strains (multiplicity of infection [MOI] of 1:10 and 1:100) for 4 h. Cell monolayers then were washed three times with prewarmed Dulbecco's PBS (Life Technologies) to remove any non-adherent bacteria. To quantify adherent bacteria, 500 µl of PBS was added to the wells and cells were scraped off (using a cell scraper) and thoroughly mixed by pipetting. Samples were serially diluted in PBS and plated onto MacConkey plates (O/N at 37°C).

2.20 Commensal microbe enumeration by DAPI DNA staining

Stool samples were collected from uninfected mice (baseline) and from mice infected with the *C. rodentium* WT or *ΔpicC* strain (days 2, 4, 6, and 8). Samples were homogenized and transferred to 10% neutral buffered formalin to a final concentration of 3.7%. Stool samples were further diluted (1/100 in PBS) and filtered through an Anodisc 25 filter (Whatman International Ltd.) with a pore size of 0.2 µm. Filter discs were thoroughly dried and stained using Gold antifade reagent containing DAPI (Molecular Probes). DAPI-positive microbes (average of 6 randomly chosen fields/slide) were counted (×630 magnification). The percentage of commensals remaining following infection was calculated based on the commensal numbers recovered from infected mice divided by the numbers recovered from uninfected controls.

2.21 Measuring *in vitro* TLR2 and TLR4 activation through TLR reporter cells and colorimetric assay

HEK (human embryonic kidney)-TLR reporter cell lines, HEK-BlueTM hTLR2, HEK-BlueTM hTLR4 and HEK-BlueTM hTLR9, were purchased from InvivoGen (San Diego, CA, USA). HEK-BlueTM hTLR2 were obtained by co-transfection of hTLR2 and hCD14 co-receptor genes into HEK 293 cells, while HEK-BlueTM hTLR4 were obtained by co-transfection of hTLR4 and hMD-2/CD14 co-receptor genes. HEK-BlueTM hTLR9 was generated by transfection of the hTLR9 gene into HEK293 cells. These cells were also transfected with the secreted embryonic alkaline phosphatase (SEAP) gene and stably express SEAP under the control of a promoter inducible by NF-κB and activator protein 1 (AP-1). Thus, stimulation of hTLR2, hTLR4 and hTLR9 leads to the production of extracellular SEAP in the culture medium that is proportional to the level of NF-κB/AP-1 activation. Cells were grown in High Glucose DMEM (HyClone, Logan, UT, USA) with 2mM L-glutamine, 10% heat-inactivated FBS (HyClone), 100 µg/ml Normocin (InvivoGen) and selective antibiotics (1x HEK-Blue selection for TLR2 and 4, 10 µg/ml Blasticidin and 100 µg/ml Zeocin for TLR9, InvivoGen) according to the manufacturer's instructions.

The activation of TLR2, TLR4 and TLR9 was assessed by measuring the SEAP activity using the QUANTI-Blue (InvivoGen) colorimetric assay. The reporter cells were seeded in a 96-well plate (BD Bioscience, Mississauga, ON, Canada) at the density of 5×10^4 cells per well in 100 µL medium. The next day, cells were treated with fresh media (without selective antibiotics) containing WT, Δ*picC* mutant, complemented *ΔpicC* + pPicC or *ΔpicC*(pPicS258I) *C. rodentium* strains for 4 h. Cells treated with culture medium only, TLR2 ligand Pam3CSK4 (10 ng/mL, InvivoGen), TLR 4 ligand lipopolysaccharide (LPS, *Escherichia coli* K-12, 100 ng/mL,

InvivoGen) served as the negative and positive controls for each corresponding TLR stimulation, respectively. The experiments were carried out three times independently and all conditions in each experiment were tested in triplicate. After 4 h incubation, culture media was collected and centrifuged to remove bacteria. The supernatants (20 µl) were then incubated with QUANTI-Blue solution (180 µl) in a 96-well flat-bottom plate at 37°C for 16-18 h. The color change of the substrate solution was quantified by optical density (wavelength = 655 nm) measurement using a SpectraMax 384 Plus plate reader (Molecular Devices, Sunnyvale, CA, USA), which corresponds to the activation of NF-κB/AP-1 by specific TLR stimulation.

2.22 Transmission experiments

To examine the ability of WT and *ΔpicC* strains of *C. rodentium* to transmit between hosts, index mice were infected with 0.1 ml of the O/N cultures (~2.5×10^8 CFU) by oral gavage. On 6 DPI, index mice were transferred to a clean cage and secondary (naive) mice were added. After 48 h of cohousing, all mice were euthanized and *C. rodentium* counts in the formerly naive mice were enumerated in the distal colon (primary site for *C. rodentium* infection). Distal colon colonization was used to assess the transmission success of each strain from index to naive mice.

2.23 Commensal analysis using qPCR

Fecal pellets were collected from uninfected (baseline) and *C. rodentium* infected mice (day 6 post-infection). Total DNA was isolated using QIAamp DNA stool kit (Qiagen) as per manufacturer's instructions. Following DNA extraction, 50 ng DNA /reaction was used for quantitative PCR using 16s RNA group specific primers. Quantitative PCR (qPCR) was performed using Mini-Opticon Real Time PCR system (Bio-Rad). The relative abundance of each taxonomic group was determined by normalizing the respective average Ct values to the

average Ct value corresponding to the universal Eubacteria (total bacterial 16s RNA) and is expressed as a relative abundance.

Table 2.2 Bacterial qPCR primers

Primer Name	Sequence
Eubacteria	UniF340 F: 5' ACTCCTACGGGAGGCAGCAGT 3' UniR514 R: 5'ATTACCGCGGCTGCTGGC 3'
γ-Proteobacteria	1080γ F: 5' TCGTCAGCTCGTGTYGTGA 3' γ1202 R: 5'CGTAAGGGCCATGATG 3'
Bacteriodetes	AllBac296 F: 5' GAGAGGAAGGTCCCCCAC 3' AllBac412 R: 5'CGCTACTTGGCTGGTTCAG 3'
Firmicutes	Firm934 F: 5'GGAGYATGTGGTTTAATTCGAAGCA 3' Firm1060 R: 5'AGCTGACGACAACCATGCAC 3'

2.24 *In vivo* competitive assay

The ability of *C. rodentium* mutants (*ΔpicC* and Δ*fucK*) to compete with WT *C. rodentium* was tested *in vivo*. 6-8 week old mice were infected with 1:1 mixture of WT *C. rodentium* and the respective mutant strain (~10^8 CFU). Samples of the inoculum were serially diluted and plated to confirm the input ratio of mutant: WT *C. rodentium.* Mice were euthanized on day 6 post-infection and distal colon tissues were collected in pre-weighed tubes containing 1X sterile PBS. Tissues were homogenized, serially diluted and plated. To calculate CI, single colonies were picked and used as a template for colony PCR with deletion screening primers (FucK Fwd 5'- GCATTCCGGTCTGTATGCACAA- 3', FucK Rev 5'-TGTTTGAACTCGACAGCTACGC- 3') from the generation of Δ*fucK* mutant and (ROD_p1411 Fwd 5' GTCTGATTATGGTGCGGTCAT 3', ROD_p1411int Rev 5' CCATATTGCCATTAAGCTGGC 3') from the generation of Δ*picC* mutant CI was calculated as the ratio of output ratio (mutant divided by WT) over the input ratio (mutant divided by WT).

2.25 Fucose feeding studies

To determine whether L-fucose supplementation was capable of affecting *C.rodentium* virulence *in vivo*, mice were gavaged with 200 µL of 25mM L-fucose twice daily at 12 hour intervals during the course of infection. Mice were euthanized at day 6 post-infection and pathogen counts were enumerated in colonic sites (caecum, distal, lumen) and systemic sites (liver, spleen, MLN) by plating on LB- Streptomycin places. Histological and pathological analysis was performed, as described before.

2.26 O-glycan structure analysis in the murine intestine

The protocol for extraction and purification of O-glycans was provided by Dr. Jianjun Li (National Research Council of Canada, Ottawa). Briefly, to release O-glycans, mucins (~ 2 mg) were scrapped from the distal colon using a glass slide and resuspended into a small volume of cold 1X sterile PBS. Mucin samples were collected from both uninfected and *C. rodentium* infected (day 6) mice. Mucin samples were dissolved in 500 µl of solution containing 1M $NaBH_4$ and 0.1M NaOH (freshly prepared) and incubated for 12-16 hours at 42 ºC. Samples were placed in an ice bath and 1M HCl was slowly added to destroy the excess $NaBH_4$. C18 SPE cartridges (Thermo Scientific) were conditioned by flowing through 2 x 1 mL of 80% acetonitrile/0.1% TFA and then 2 x 1 mL of 0.1% TFA. Each sample was loaded into a separate C18 port and the flow-through was collected. PGC cartridges (Extract CleanTM Carbo, All-Tech) were pre-conditioned with 3.0 mL of 80% (v/v) acetonitrile containing 0.1% TFA, followed by 3.0 mL water. Flow-through from C18 SPE cartridges was loaded onto pre-conditioned PGC column and then washed with water (3.0 mLx3) to remove buffer and salts. O-glycans were eluted with 50% acetonitrile in 0.1% TFA. Each fraction was collected and dried for MS analysis using a lyophilizer.

2.27 Statistical analysis

Survival data from *in vivo* infection studies was analyzed using Log-rank (Mantel-Cox) on the curves generated using GraphPad Prism. All the results shown in this study are plotted as mean values with standard errors of the means (SEM). Statistical analysis was performed with GraphPad Prism, version 4.00 for Windows (GraphPad Software, San Diego, CA, USA), using nonparametric Mann-Whitney t tests. A P value of ≤ 0.05 was indicative of statistical significance.

Chapter 3: The mucin Muc2 limits pathogen burdens and epithelial barrier dysfunction during *Salmonella enterica* serovar Typhimurium colitis

3.1 Introduction

Salmonella enterica subspecies 1 serovar Typhimurium is a Gram-negative enteric bacterial pathogen that is a leading clinical cause of food-borne and waterborne diarrheal disease[223]. An intracellular pathogen, *S. Typhimurium* is known to use virulence factors encoded on *Salmonella* pathogenicity island 1 (SPI-1), such as invA, to infect and/or translocate across the epithelial cells that line the luminal surface of the mammalian intestine. This virulence strategy has been studied extensively *in vitro* and is also known to be involved in the ability of *S. Typhimurium* to cause both mucosal inflammation and diarrhea in infected hosts[272,273]. Despite our detailed understanding of this aspect of *S. Typhimurium* pathogenesis, much less is known about how orally delivered *S. Typhimurium* circumvents the various luminal defenses and intestinal barriers that protect the targeted epithelium, such as the overlying mucus layer.

In large part, the dearth of knowledge in this area reflects the inability of oral *S. Typhimurium* infection of mice to provide a relevant model for the enterocolitis caused by *Salmonella* species[274]. Despite the rapid invasion of intestinal epithelial cells in tissue culture by *S. Typhimurium*, very few orally gavaged *S. Typhimurium* bacteria are found to directly infect the intestinal epithelium *in vivo*, resulting in minimal intestinal inflammation. Recently, recognition that the resistance of mice to oral *S. Typhimurium* infection might reflect commensal-microbe-based colonization resistance led to testing of the impact of antibiotic pretreatment. Prior exposure to the antibiotic streptomycin was found to remove competing commensal microbes within mice, facilitating heavy *S. Typhimurium* colonization of the murine large bowel, leading to increased contact with the intestinal epithelium and dramatic cecal and colonic inflammation[170]. However, the two mouse strains most commonly used for the *Salmonella* enterocolitis model (C57/BL6 and BALB/c) are known to possess a mutation in their

nramp1 genes, leaving these mice highly susceptible to *S. Typhimurium* and succumbing rapidly to infection[224].

To circumvent this limitation, we have recently described a model using the attenuated *S. Typhimurium ΔaroA* mutant strain, which still causes severe colitis but typically causes no mortality, even in highly susceptible mouse strains[226]. Most studies employing the enterocolitis model have focused on dissecting the virulence strategies of *S. Typhimurium* or exploring the specific host factors that drive the resulting inflammation. In contrast, studies have yet to address how *S. Typhimurium* interacts with, and ultimately crosses, the intestinal mucus layer to reach the underlying epithelium. The mucus barrier is formed predominantly by Muc2, a prominent secretory mucin that overlies the intestinal epithelium. Produced within specialized goblet cells, Muc2 possesses a protein core that is heavily O-glycosylated, with its numerous carbohydrate chains making up 80% of its mass[110]. In large part, the function of Muc2 depends on its glycosylation patterns[275–277]. Among the most abundant of these oligosaccharides are the core 3-derived O-glycans, which are synthesized by β1,3-N-acetylglucosaminyltransferase (C3GnT)[278]. While loss of C3GnT does not prevent Muc2 from forming the mucus layer, C3GnT-deficient (*C3GnT* -/-) mice produce a thinner mucus layer than normal, leaving them more susceptible to chemically induced forms of colitis[140].

Once secreted by goblet cells, Muc2 undergoes rapid and dramatic expansion, forming a gel-like layer on the intestinal epithelial surface. This insoluble layer provides a physical barrier that appears to protect the underlying epithelium from direct contact with commensal microbes as well as from many pathogenic insults[39]. In addition to secreted mucins, the mucus barrier also contains carbohydrates, antimicrobial peptides, immunoglobulins, electrolytes, lipids, and other intestinal proteins, making it a complex biochemical matrix acting as an important host defense

barrier. Recently, intestinal alkaline phosphatase (IAP), a brush border enzyme expressed on the apical sides of enterocytes (and thus at the base of the mucus layer), has emerged as an important gut mucosal defense factor due to its ability to detoxify bacterial lipopolysaccharide (LPS) by removing the phosphate group from LPS and limiting LPS-mediated activation of the innate immune receptor Toll-like receptor 4 (TLR4). Furthermore, IAP-mediated LPS detoxification plays a role in preventing systemic translocation of LPS across the intestinal barrier[67,148,279–283]. In the absence of this detoxification, systemic translocation of LPS triggers exaggerated inflammatory responses that can ultimately prove fatal to the host through proinflammatory cytokine-induced septic shock[284–286].

The mucus barrier provides partial protection against several enteric bacterial pathogens, including *Yersinia enterocolitica*, *Shigella flexneri*, and *Citrobacter rodentium*[145,287,288]. Despite this protection, these and other microbes do ultimately cross the mucus barrier and infect the underlying epithelial cells, raising the questions of how this subversion occurs and whether bacterial pathogens ultimately use the mucus layer as part of their pathogenic strategies. To better define *S. Typhimurium* interactions with the intestinal mucus layer, we infected *Muc2 -/-* and *C3GnT -/-* mice with *ΔaroA S. Typhimurium*. We found that Muc2 plays an important role in limiting the extent of *Salmonella* colonization of the intestinal lumen, the subsequent mortality of infected hosts, the interactions of *S.* Typhimurium with the intestinal epithelium, and its translocation across the intestinal epithelium. Furthermore, *Muc2 -/-* mice had less IAP expression and significantly less LPS detoxification activity in their cecal tissues than WT mice. We suggest that LPS-triggered inflammatory responses at systemic sites, such as the liver, could be a potential basis for the increased mortality seen in *Muc2 -/-* mice. We noted that lack of core 3 derived O-glycosylation (*C3GnT -/-* mice) did not impact the pathogen burdens but resulted in

epithelial barrier dysfunction, whereas lack of the entire mucus layer (*Muc2 -/-* mice) caused increased epithelial barrier dysfunction as well as heavier colonization. We also found that in the absence of the mucus layer, as seen in *Muc2 -/-* mice, the barrier dysfunction was dramatically more *invA* dependent than in WT mice. Our study thus demonstrates not only the protective nature of intestinal mucus but also surprising interactions with *S. Typhimurium* that have an impact on its virulence characteristics.

3.2 Results

3.2.1 *S.* Typhimurium infection of WT mice alters expression of intestinal glycans and the major secretory mucin Muc2

To investigate intestinal mucin dynamics and glycosylation patterns over the course of *S.* Typhimurium infection, we infected wildtype (WT) mice with *ΔaroA S.* Typhimurium since we have previously shown this strain of *S.* Typhimurium causes significant colitis but does not kill even susceptible murine hosts[226]. We collected cecal tissues over a seven day time course, and stained them with Periodic Acid-Schiff's reagent (PAS) as well as Alcian blue. PAS stains neutral carbohydrates (pink/magenta) whereas Alcian blue stains acidic carbohydrates (deep blue), while tissues containing both acidic and neutral mucins stain dark blue/purple (31). Assessment of uninfected tissues identified distinct pink staining (neutral carbohydrates) on the epithelial surface (presumably secreted mucins) and blue staining (acidic carbohydrates) within the goblet cells. In contrast, cecal tissues collected at day 3 post-infection (DPI) and 7 DPI revealed significant changes in mucin staining, with dark blue/purple coloration throughout the tissues, indicative of changes in the distribution and expression pattern of neutral and acidic mucins during *Salmonella* infection. Specifically on 3 DPI, we noted an increase in PAS/Alcian blue staining in goblet cells as well as within the cecal lumen, suggesting mucin levels were increased both in tissues as well as secreted into the cecal lumen. Interestingly, by 7 DPI, the PAS/Alcian blue staining of goblet cells was dramatically reduced, suggesting mucin content within goblet cells was reduced. In contrast, staining of mucus was primarily seen in the cecal lumen, suggesting a relative increase in the proportion of secreted versus goblet cell contained mucins by this stage of the infection (Figure 3.1a).

Since Muc2 is the major secreted mucin within the colon, and has previously been shown to protect against enteric bacterial infections[145], we wondered if *Salmonella* infection induced any changes in Muc2 expression. As assessed by immunostaining, we noted that by 3 DPI, there was a relative increase in secreted Muc2 as compared to uninfected mice. Muc2 was seen on the mucosal surface and within the lumen and an increase in Muc2 staining intensity was also noted inside goblet cells. On 7 DPI, we found more Muc2 within the cecal lumen (secreted) and an increase in the number of Muc2-positively staining goblet cells within the cecal crypts compared to 3 DPI (Figure 3.1b). We also assessed *Muc2* gene transcription and noted a significant increase over the course of infection (Figure 3.1c). These results suggest that *Salmonella* infection leads to an increase in the expression and secretion of Muc2 glycoprotein in WT mice, potentially as a host defense mechanism. Furthermore, there were notable changes in the gene transcription of cell surface mucins such as Muc1 and Muc3, as well as secreted gel-forming salivary and gastric mucins Muc19 and Muc5AC (Figure 3.1d), suggesting that major changes in both the cell-surface and secreted mucins occur in response to intestinal *Salmonella* infection.

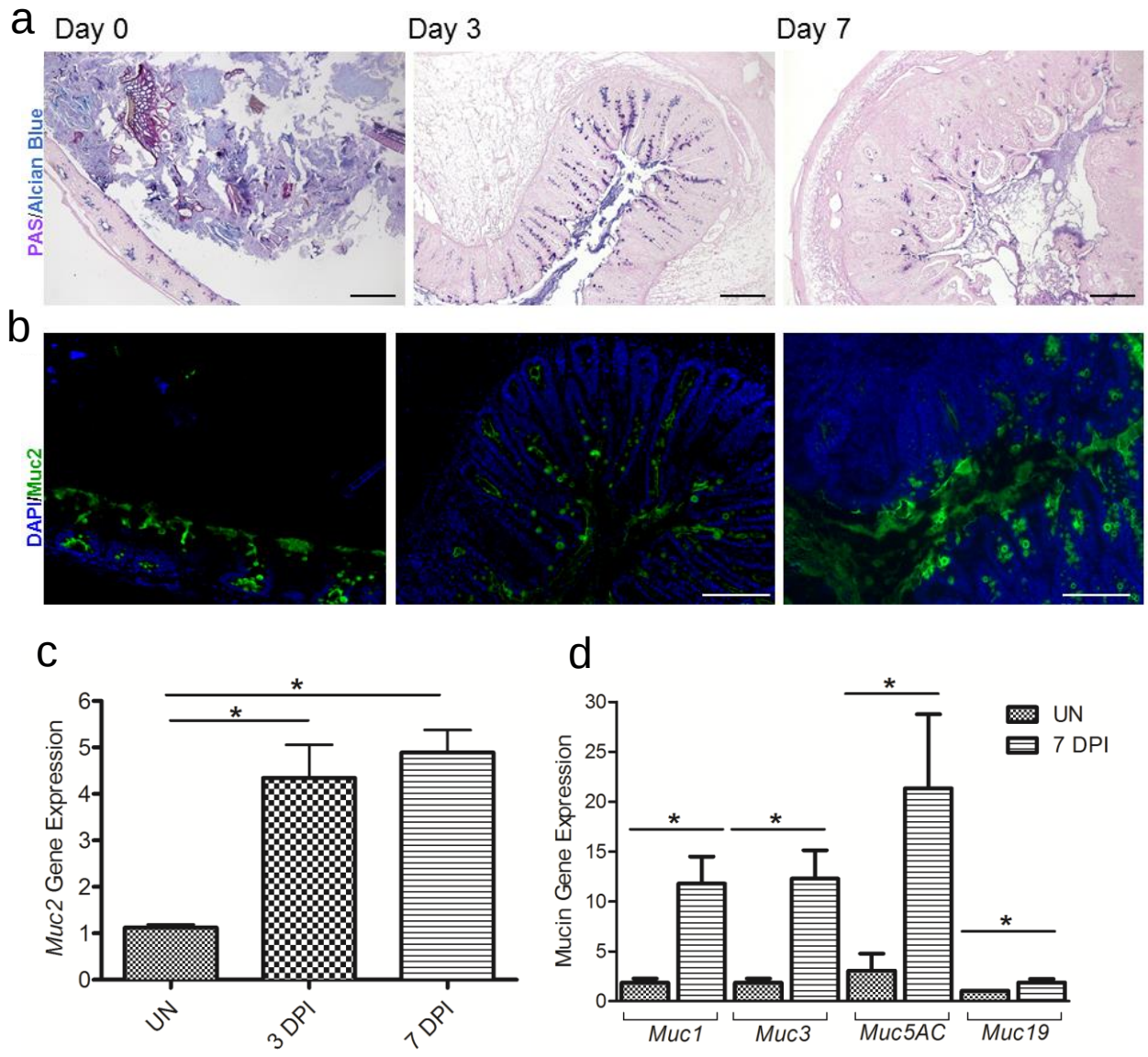

Figure 3.1 Δ*aroA S.*Typhimurium infection results in increased mucin secretion in WT mice.

(a) Representative PAS/Alcian Blue Staining of Carnoy's fixed cecal tissues at day 0 (un-infected), 3 DPI and 7 DPI. (Original magnification 100x, scale bar 100 µm). (b) Representative Muc2 immunostaining in cecum using Muc2 antibody (green) and DAPI counterstain (cellular DNA, blue) at day 0 (un-infected), 3 DPI and 7 DPI. (Original magnification 200x, scale bar 50 µm). (c) *Salmonella* infection induced significantly higher transcription of Muc2 mucin in the cecal tissue of WT mice. (d) Transcription of several other mucin genes encoding various Muc family members in the cecal tissues of *Salmonella* infected WT mice under uninfected and infected conditions (7DPI). Overall, under infected conditions, there is higher transcription of Muc family genes. All samples were normalized to the transcription of housekeeping genes, β-actin. Error bars represent Standard Error of the Mean (SEM) from three independent

experiments (n=9 per group). Asterisks indicate significant differences (*, $P < 0.05$) by the Mann-Whitney test.

3.2.2 *Muc2 -/-* mice display increased susceptibility to *S.* Typhimurium infection

It has been previously reported that Muc2 plays a protective role against *Citrobacter rodentium* and DSS-induced colitis[134,145]. To assess whether Muc2 protects against *S.* Typhimurium infection, we infected WT and *Muc2 -/-* mice with *ΔaroA S.* Typhimurium and compared body weights and survival over the following nine days. While the infected WT mice showed only a modest weight loss and ultimately none of the WT mice succumbed to infection, exposure to *S.* Typhimurium was more damaging to the *Muc2 -/-* mice. Between 6 and 7 DPI, 50% of the *Muc2 -/-* mice succumbed to infection, and by 7 DPI, the remaining mice had lost 15-20% of their starting body weight, and displayed other signs of morbidity such as hunched posture, inactivity and piloerection of their fur (Figure 3.2a). As a result, all the remaining infected *Muc2 -/-* mice were euthanized on 7 DPI (Figure 3.2b).

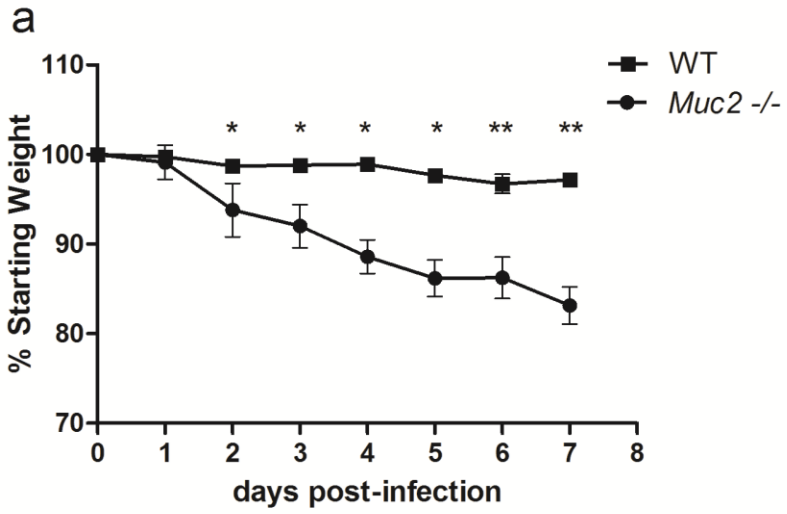

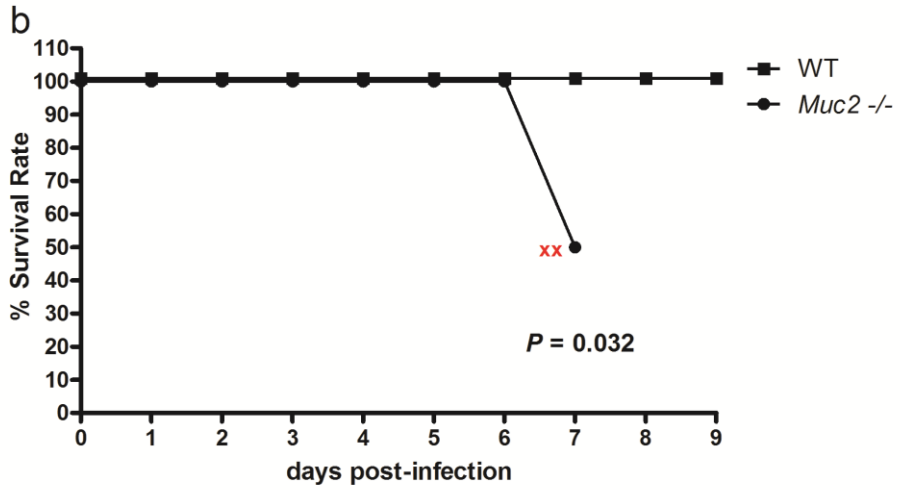

Figure 3.2 *Muc2 -/-* mice exhibit dramatic susceptibility to Δ*aroA S.*Typhimurium infection compared with WT mice.
(a) Body weights of WT and *Muc2 -/-* mice from 0 to 7 DPI, plotted as % starting weight, normalized to day 0 weight. *Muc2-/-* mice exhibited rapid weight lost following *Salmonella* infection. Results are representative of three independent infections. Asterisks indicate significant differences (*, P < 0.05, **, P < 0.01) by the Mann-Whitney test. (b) Survival curve of WT and *Muc2 -/-* mice following *Salmonella* infection. Red (xx) indicates the humane end point for remaining *Muc2 -/-* mice. P values (0.032) are from the log-rank test and indicate a statistically significant difference between the survival curves. Error bars represent SEM from three independent experiments with 9 mice per group.

3.2.3 *Muc2 -/-* mice carry increased *S.* Typhimurium burdens compared to WT mice

Based on the increased Muc2 immmunostaining (Figure 3.1a) noted in infected WT mice, we speculated that increased Muc2 secretion during *Salmonella* infection might play a role in controlling pathogenic bacterial burdens. We therefore enumerated the *S.* Typhimurium within cecal tissues and within the cecal lumen, while also assessing pathogen translocation and/or replication outside of the gut, by collecting liver, spleen and MLN tissues. We observed a significantly higher pathogen load in the ceca of *Muc2 -/-* mice compared to WT mice. Similarly we recovered higher pathogen burdens from the cecal contents (lumen) of *Muc2 -/-* mice compared to WT mice (Figure 3.3a). We also noted higher pathogen burdens in the livers of

Muc2 -/- mice compared to WT mice suggesting the higher intestinal burden also impacted on microbial numbers reaching (or proliferating within) the liver. Conversely, *S.* Typhimurium was recovered from the spleen and MLN at levels comparable to WT mice, (Figure 3.3b), suggesting that *Muc2 -/-* mice do not suffer any overt or widespread defects in controlling *S.* Typhimurium burdens at other systemic sites.

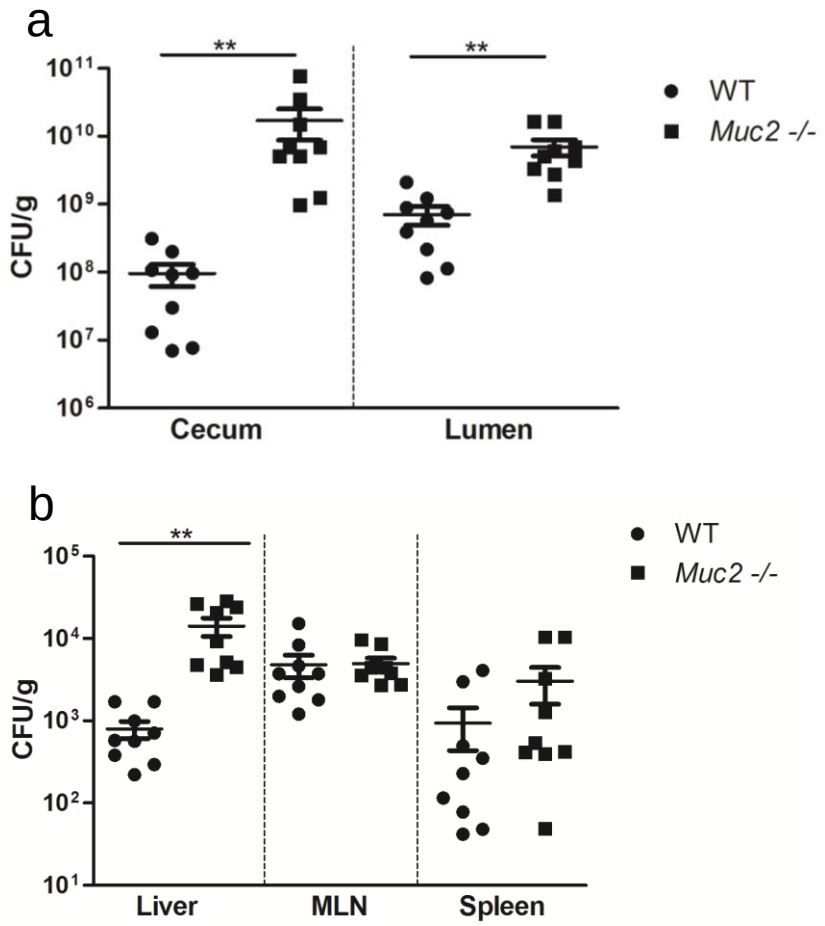

Figure 3.3 Δ*aroA S.*Typhimurium recovered from the cecum, intestinal lumen, liver, MLN and spleen of WT and *Muc2 -/-* mice respectively.
Bacterial burdens carried at 7 DPI in WT and *Muc2 -/-* mice. *Muc2 -/-* mice carried significantly higher pathogen burdens that WT mice in cecum and lumen. (b) *Salmonella* burdens enumerated in systemic sites. *Muc2 -/-* had significantly greater pathogen burdens in liver and comparable burdens in MLN and spleen to WT mice. Each data point represents one animal and the results are pooled from 3 independent experiments (n=9). Data is shown as mean ± SEM. (**, $P < 0.01$, Mann-Whitney Test).

3.2.4 *Muc2 -/-* mice exhibit a similar level of colitis to WT mice but suffer exaggerated epithelial barrier disruption

Next we sought the cause of the heightened mortality seen in *Salmonella* infected *Muc2 -/-* mice. We undertook histological analysis and pathology scoring to see if in addition to higher pathogen burdens, these mice suffered more severe tissue damage, potentially explaining their dramatically higher rates of mortality. Intestinal pathology was evaluated using previously described histopathological scoring methods (5, 7) and surprisingly, no significant differences were observed in the cecal histopathology of infected *Muc2 -/-* mice when compared to WT mice. Histological analysis revealed that *Salmonella* infection elicited pronounced inflammation within the cecal tissues of both WT mice and *Muc2 -/-* mice (Figure 3.4a). We observed profound edema and PMN infiltration into the cecal submucosa and mucosa along with significant damage to epithelial integrity, marked by erosions, crypt loss and damage to crypt structure by 3 DPI. This pathology was found to be modestly worse by 7 DPI in both mouse strains, resulting in slightly higher pathology scores than those seen at 3 DPI (Figure 4b). Since tissue damage was comparable between WT and *Muc2 -/-* mice, we next tested if the lack of mucus led to increased damage to the intestinal epithelial barrier in *Muc2 -/-* mice. Using oral FITC-dextran gavage, we found that FITC-dextran translocation in uninfected *Muc2 -/-* mice was modestly, but not significantly greater than that seen in WT mice. In contrast, while *S.* Typhimurium infection did not cause any significant impairment in epithelial barrier function in WT mice, infected *Muc2 -/-* mice demonstrated significantly higher (3-fold) intestinal permeability ($P < 0.01$) (Figure 3.4c).

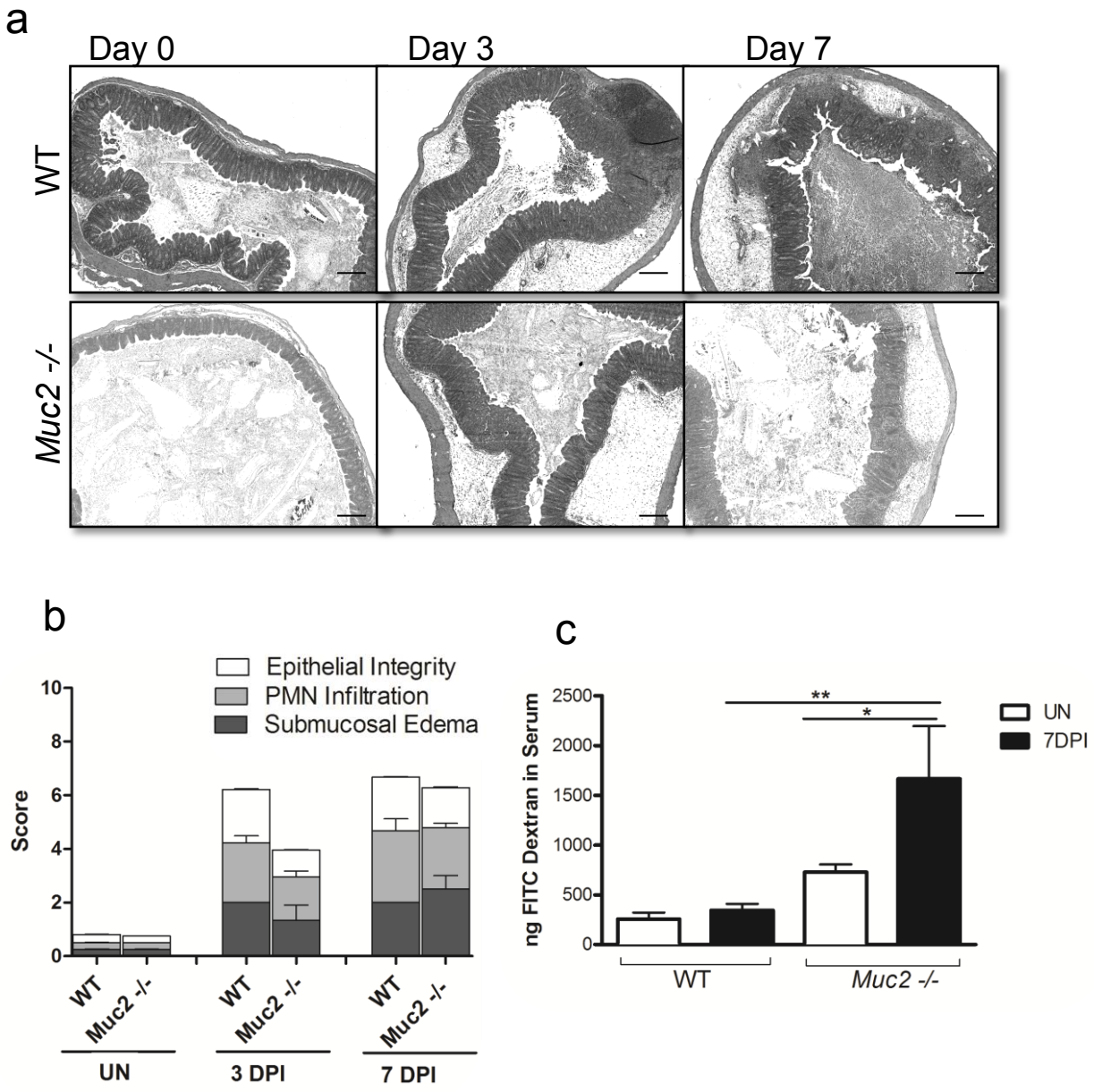

Figure 3.4 Histology, tissue pathology and epithelial barrier integrity assessment of Δ*aroA S.*Typhimurium infected WT and *Muc2 -/-* mice.
(a) H&E stained cecal sections (original magnification 50x, scale 100 µm) of WT mice and *Muc2-/-* mice at day 0 (un-infected) as well as 3 DPI and 7 DPI. (b) Tissue pathology scores. Mucosal pathology scoring includes epithelial barrier integrity, PMN infiltration and submucosal edema. Each bar represents the average scores of 6-7 tissues, scored under blinded conditions. No significant difference was noted between groups. (c) FITC- Dextran intestinal permeability assay for WT and *Muc2 -/-* mice, un-infected (UN) and 7 DPI. *Muc2 -/-* display significantly greater intestinal permeability compared to WT counterparts. Bars represent the average value of 9 mice per group, pooled from 3 independent experiments. (*, $P < 0.05$, Mann-Whitney Test).

3.2.5 *S.* Typhimurium infected *C3GnT -/-* mice show impaired epithelial barrier integrity, but comparable bacterial burdens to WT mice

Since Muc2 is a heavily O-glycosylated glycoprotein, we next sought to test whether its critical role in host defense against oral *S.* Typhimurium reflected the Muc2 protein itself, or instead some aspect of its glycosylation. Core 3 derived O-glycans are one of the major glycans found in the murine intestine and core 3 β1,3-N-acetylglucosaminyltransferase (C3GnT) is the enzyme responsible for synthesis of core 3 derived O-glycans. We noted that there were elevated gene transcript levels for *C3GnT* during *Salmonella* induced infection (Figure 3.5a). It was therefore of interest to investigate the importance of core 3 derived-O glycans during *Salmonella* infection. We infected mice lacking core 3 derived O-glycans (*C3GnT -/-* mice) to determine if these mice had a similar phenotype (i.e. increased pathogen burdens and barrier disruption) to infected *Muc2 -/-* mice. Since *C3GnT -/-* mice still produce intestinal mucus, we noted that like WT mice, they displayed an increased accumulation of luminal mucus following their infection by *S.* Typhimurium (Figure 3.5b). Despite this response, we also noted that *Salmonella* infected *C3GnT -/-* mice showed 8-10% greater weight loss over the course of infection compared to WT mice (Figure 3.5c). To address the basis for their increased weight loss, we looked at intestinal and systemic *S.* Typhimurium burdens. Surprisingly, the pathogen burdens were comparable (no statistically significant difference) between *C3GnT -/-* mice and WT mice (Figure 3.5d) suggesting that the loss of core 3-O glycosylation did not significantly affect *Salmonella* colonization. Interestingly, the *C3GnT -/-* mice did display significantly impaired epithelial integrity compared to infected WT mice, as assessed by the FITC-Dextran assay (Figure 3.5e), suggesting core 3 derived O- glycans do play a significant role in protecting intestinal barrier function. However, corresponding to the pathogen burdens, histological analysis (Figure 3.6a)

and pathology scoring (Figure 3.6b) also did not reveal any significant differences between *C3GnT -/-* mice and WT mice. *Salmonella* infected *C3GnT -/-* mice displayed a similar level of infiltrating inflammatory cells, damage to epithelial structure and submucosal edema to that seen in WT mice.

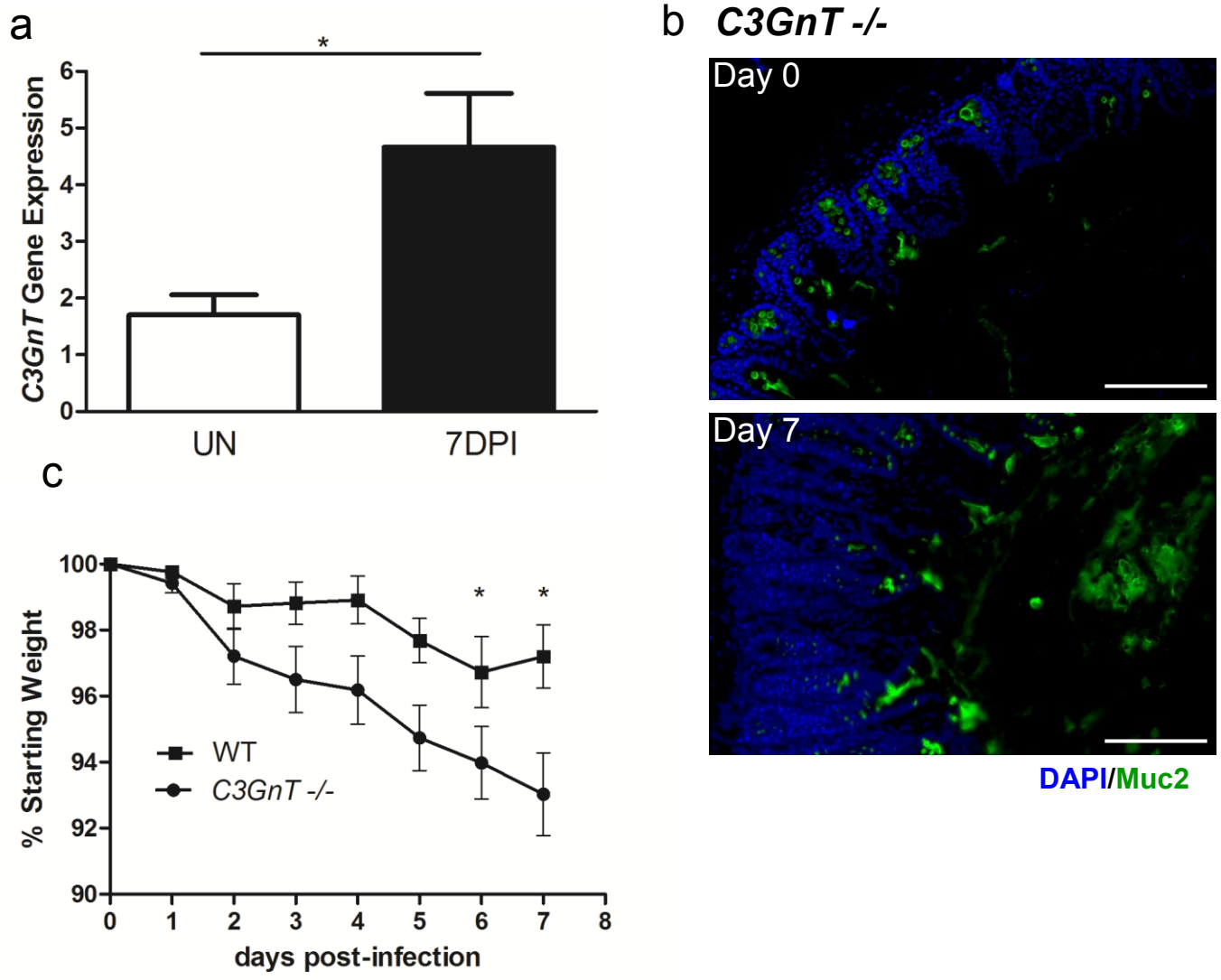

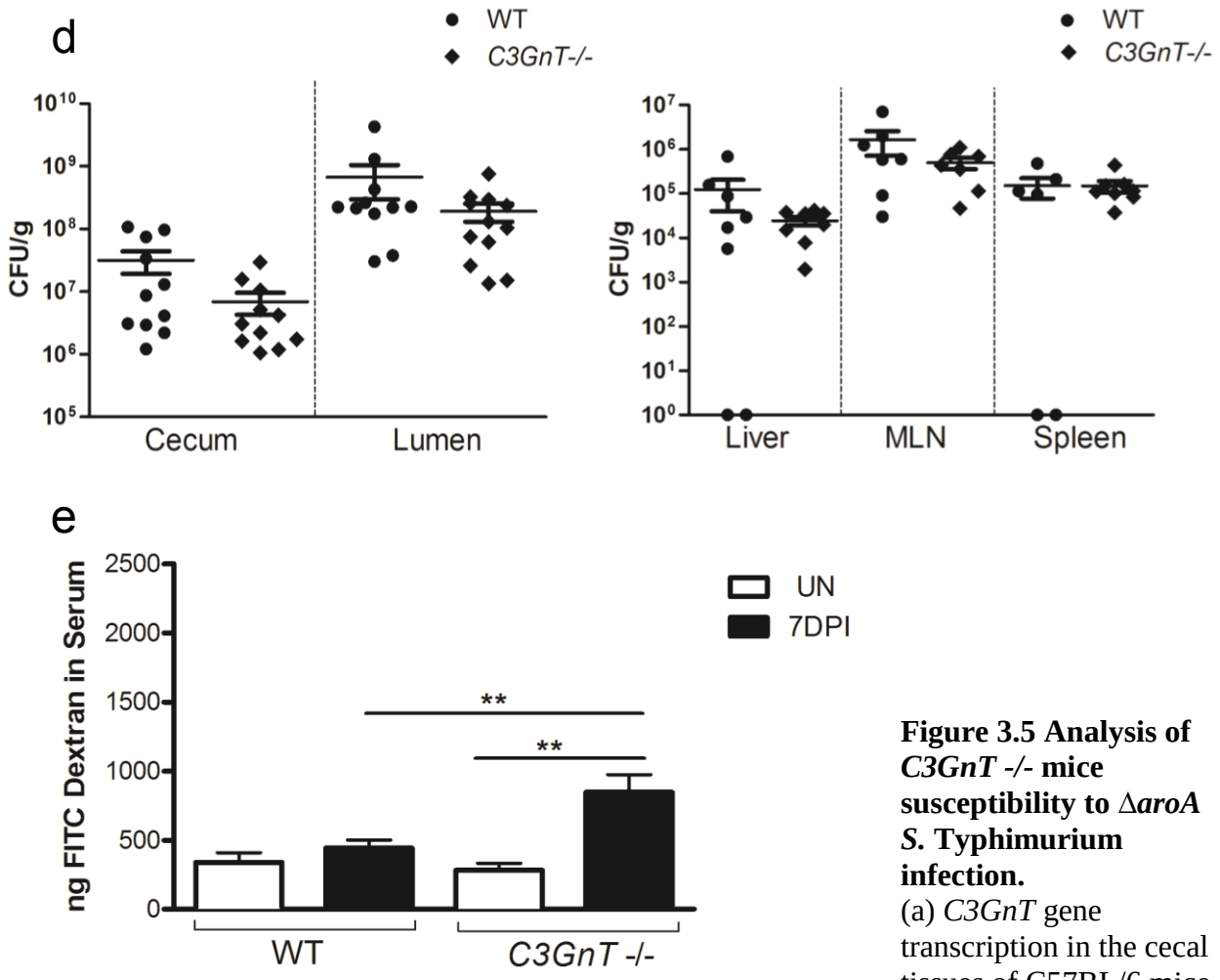

Figure 3.5 Analysis of *C3GnT* -/- mice susceptibility to Δ*aroA S.* Typhimurium infection.
(a) *C3GnT* gene transcription in the cecal tissues of C57BL/6 mice, as assessed by qPCR. Data was normalized to the housekeeping gene, GADPH. (b) Muc2 immunostaining profile in *C3GnT* -/- mice after Δ*aroA S.* Typhimurium infection. Representative Muc2 immunostaining in cecum using Muc2 antibody (green) and DAPI counterstain (cellular DNA, blue) at day 0 (un-infected) and 7 DPI. (Original magnification 200x, scale bar 50 μm). (c) Body weight of WT and *C3GnT* -/- mice followed until 7 DPI. *C3GnT*-/- mice lost ~8-10% of their starting body weight post *Salmonella* infection. (d) Colonization of *Salmonella* infected WT and *C3GnT* -/- mice. No significant differences were noted in colonization levels. (e) FITC-dextran intestinal permeability assay of WT mice and *C3GnT* -/- mice, un-infected (UN) and 7 DPI. Damage to the intestinal barrier was assessed by measuring FITC Dextran in serum, collected by cardiac puncture, 4 hours following oral administration (**, P< 0.01, Mann-Whitney Test). (8-10 mice/group, 3 independent experiments, mean ± SEM are indicated on the graphs).

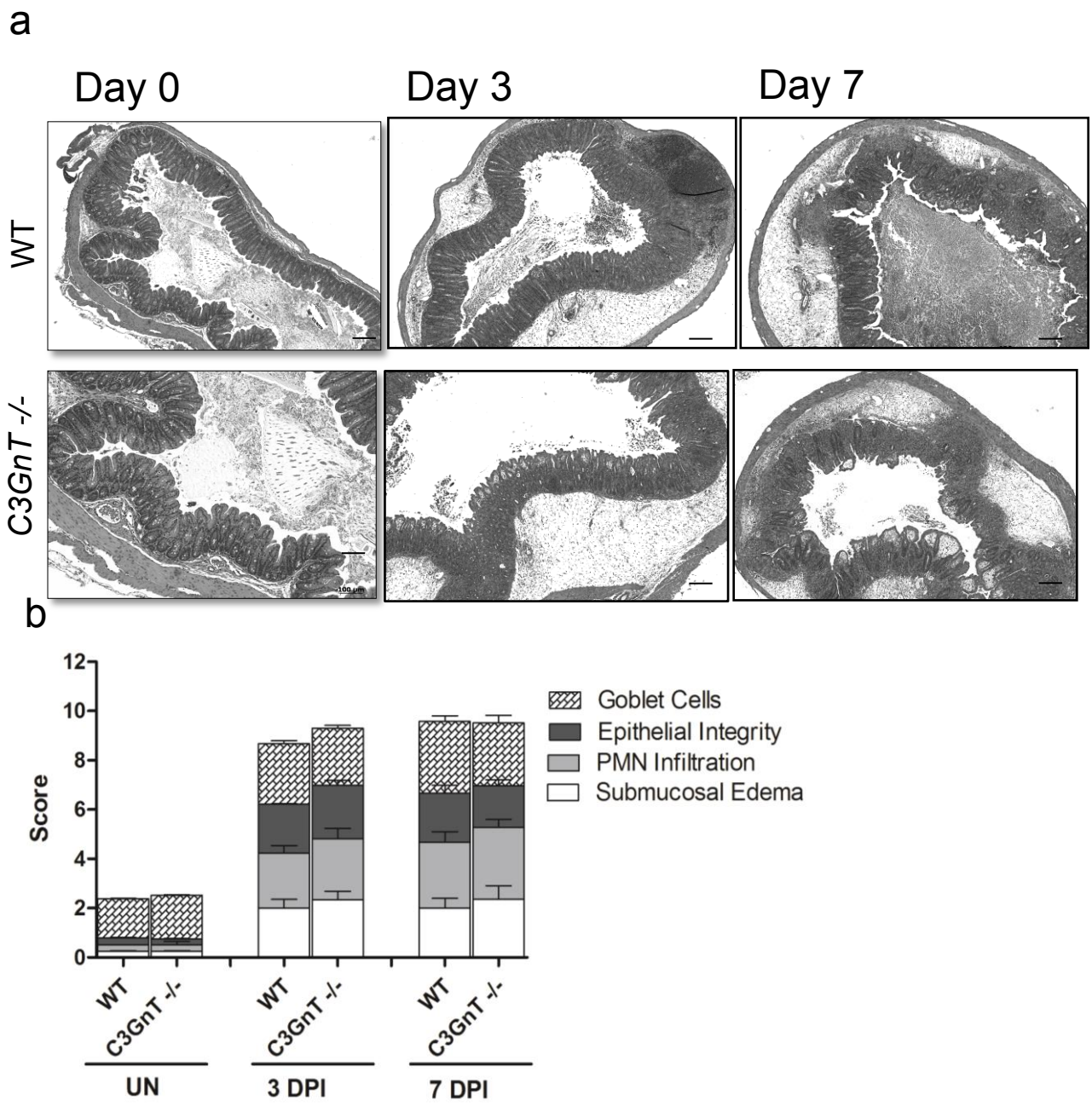

Figure 3.6 Histological and pathological comparison of WT and *C3GnT -/-* mice infected with Δ*aroA S.* Typhimurium.
(a) H&E stained cecal sections (original magnification 50x, scale 100 μm) of WT mice and *C3GnT -/-* mice at 3 DPI and 7 DPI. (b) Tissue pathology score. Pathology scores included assessment of epithelial integrity, goblet cell depletion, PMN infiltration and submucosal edema. There were no significant differences in pathological scores between the two groups. Each bar represents the average of 9 cecal tissues.

3.2.6 Muc2 layer acts as a physical barrier to limit *Salmonella* contact with the intestinal epithelium

Based on the impact of Muc2 on both *S.* Typhimurium pathogen burdens and the protection of intestinal barrier function, we hypothesized that Muc2 provides a physical barrier to limit *Salmonella* interactions with underlying epithelium. To investigate *S.* Typhimurium localization relative to the mucus layer and epithelium, we fixed tissues with Carnoy's fixative and stained serial sections for Muc2 and *Salmonella* LPS. Immunostaining revealed that in WT mice, the mucus layer provided a distinct barrier, keeping the vast majority of the *S.* Typhimurium within the cecal lumen and distant from the epithelial surface. In contrast, in *Muc2 -/-* mice, *Salmonella* were seen in close proximity, and even adherent to the epithelial surface (Figure 3.7).

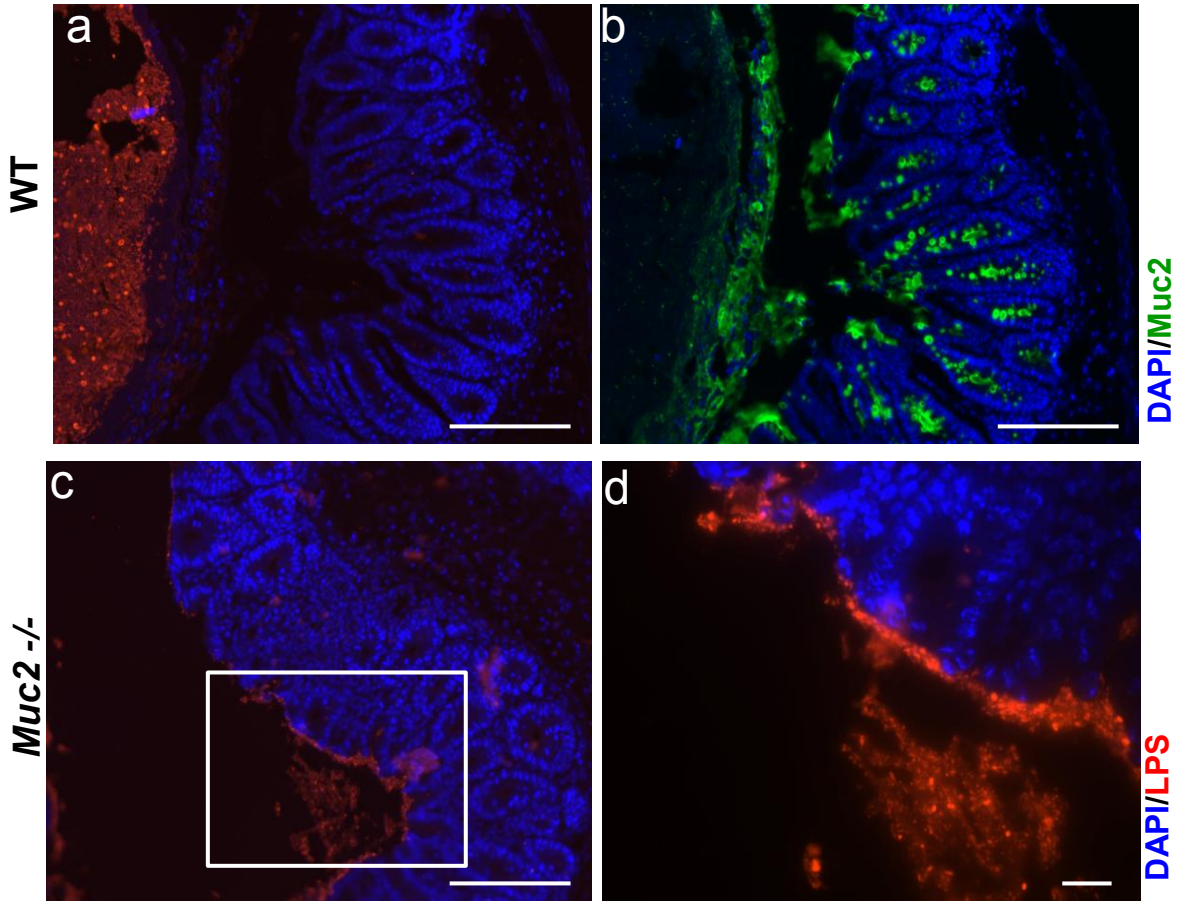

Figure 3.7 Muc2 provides a physical barrier between the host epithelial surface and *S.* Typhimurium.
(a) *Salmonella*-LPS staining in red and DAPI (counterstain) in blue, showing *Salmonella* localized to the cecal lumen. (b) Muc2 immunostaining in green and DAPI counterstain in blue. The thick mucus layer can be seen between the epithelial surface and the lumen. Immunostaining for both markers was done on serial sections of cecal tissue collected from WT mice infected with *Salmonella* (original magnification 200x, scale 50 μm). (c) In contrast to panel a, *Salmonella* can be seen in close proximity to the epithelial surface in the cecal tissues of *Muc2 -/-* mice (original magnification 200x, scale 50 μm). (d) Magnified image from inset shown in panel c, (original magnification 630x, scale bar 5μm).

3.2.7 Increased intestinal barrier dysfunction in *S.* Typhimurium infected *Muc2 -/-* mice is *invA* dependent

Cell culture studies have previously shown that *S.* Typhimurium uses its SPI1 pathogenicity island, including *Salmonella* invasion gene invA, an inner membrane protein component of the SPI-1 T3SS, to infect intestinal epithelial cells and cause barrier disruption [272,273]. Since infected *Muc2 -/-* mice suffered from exaggerated barrier disruption, we wondered if this was dependent on the actions of invA, one of the more important proteins involved in *Salmonella* virulence. To test this hypothesis, we infected WT and *Muc2 -/-* mice with wildtype and Δ*invA Salmonella* (on the wildtype background) and euthanized the mice at 3 DPI. Interestingly, wildtype *S.* Typhimurium caused severe cecal pathology and inflammation in both mouse strains, and similar to our findings with Δ*aroA S.* Typhimurium, *Muc2 -/-* mice carried heavier pathogen burdens than WT mice. Moreover infection caused significant barrier disruption in *Muc2 -/-* mice whereas no disruption was seen in WT mice (Figure 3.8a). When WT mice were infected with Δ*invA Salmonella*, the resulting pathogen burdens in the cecal lumen were similar to those seen with wildtype *Salmonella*, whereas Δ*invA Salmonella* numbers in the cecal tissues, as well as within systemic tissues were modestly but significantly lower than those seen with wildtype *Salmonella* (Figure 3.8b, 3.8c). Interestingly the resulting cecal

pathology was only modestly reduced, and no intestinal barrier disruption was noted.

Infected *Muc2 -/-* mice were found to carry higher Δ*invA Salmonella* burdens in their cecal lumens, albeit significantly reduced from the levels seen with wildtype *Salmonella*. Pathogen translocation into cecal tissues was dramatically reduced while *Salmonella* numbers at systemic sites such as the liver and spleen were also reduced, to roughly the same degree as that seen in Δ*invA Salmonella* infected WT mice (Figure 3.8b, 3.8c). Notably, in contrast to the cecitis suffered by WT mice, no significant cecal pathology was seen in Δ*invA* infected *Muc2 -/-* mice and despite their high luminal pathogen burdens; Δ*invA S.* Typhimurium did not cause any barrier disruption (Figure 3.8d, 3.8e). Taken together, these findings suggest that although *S.* Typhimurium's ability to cause cecal pathology in WT mice is partially dependent on invA, the dependence on invA for inducing cecal pathology is dramatically greater in the absence of a mucus layer (*Muc2 -/-* mice), suggesting that *Salmonella's* interactions with the mucus layer may play a modulatory role in its pathogenesis. Furthermore, while *Muc2 -/-* mice infected with wildtype *S.* Typhimurium showed *Salmonella* in close proximity or adherent to the cecal epithelial surface, mice infected with Δ*invA S.* Typhimurium showed few if any of these bacteria adherent to the epithelial surface (Figure 3.8f). Moreover, *Muc2 -/-* mice showed no mortality over the infection time course with Δ*invA S.* Typhimurium suggesting that pathogen translocation out of the cecum likely plays an important role in the high mortality rates suffered by these mice.

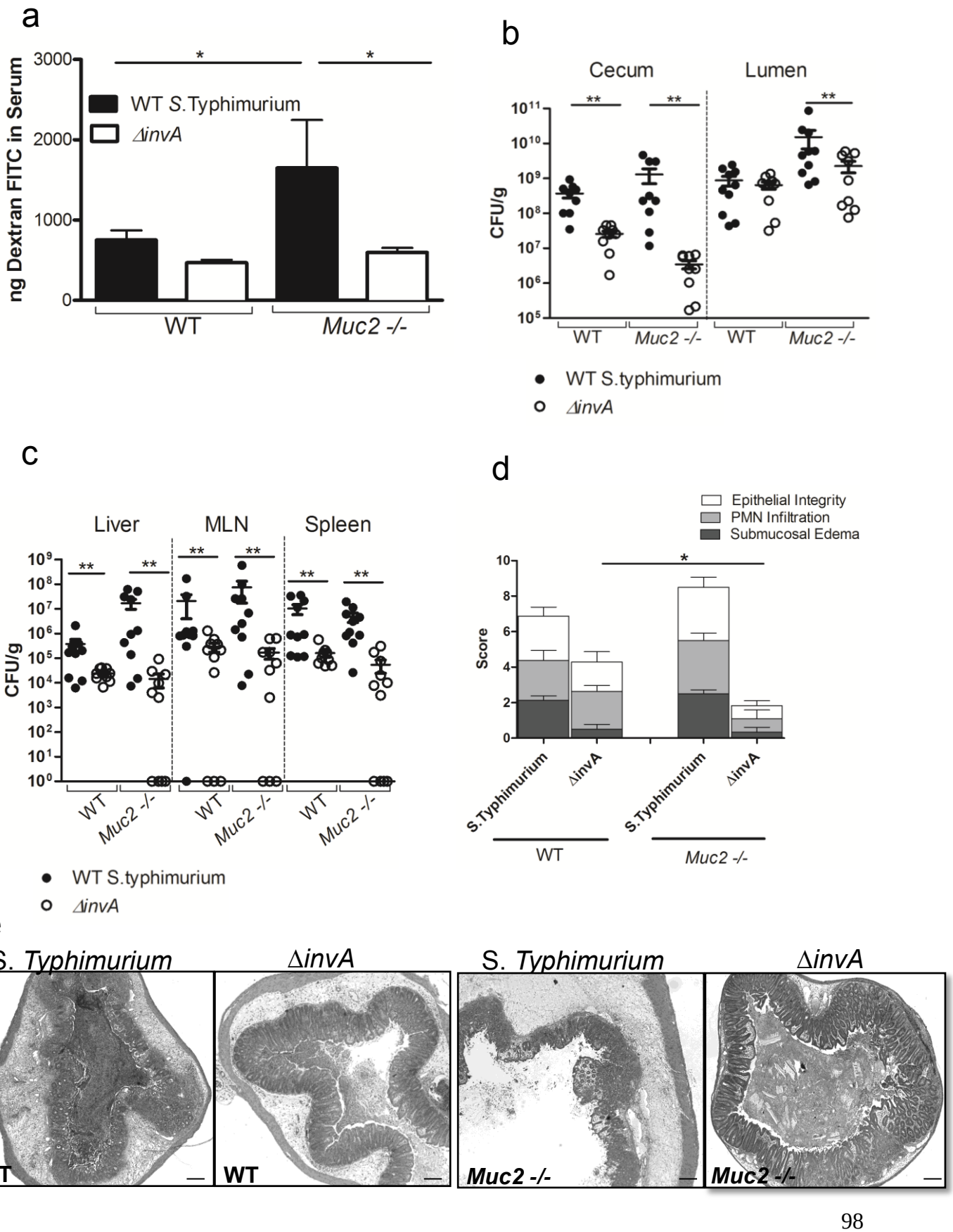
a
ng Dextran FITC in Serum
3000
2000
1000
0
*
*
WT S.Typhimurium
ΔinvA
WT
Muc2 -/-
b
Cecum
Lumen
CFU/g
**
**
**
WT
Muc2 -/-
WT
Muc2 -/-
WT S.typhimurium
ΔinvA
c
Liver
MLN
Spleen
CFU/g
WT S.typhimurium
ΔinvA
d
Epithelial Integrity
PMN Infiltration
Submucosal Edema
Score
*
S.Typhimurium
ΔinvA
S.Typhimurium
ΔinvA
WT
Muc2 -/-
e
S. Typhimurium
ΔinvA
S. Typhimurium
ΔinvA
WT
WT
Muc2 -/-
Muc2 -/-

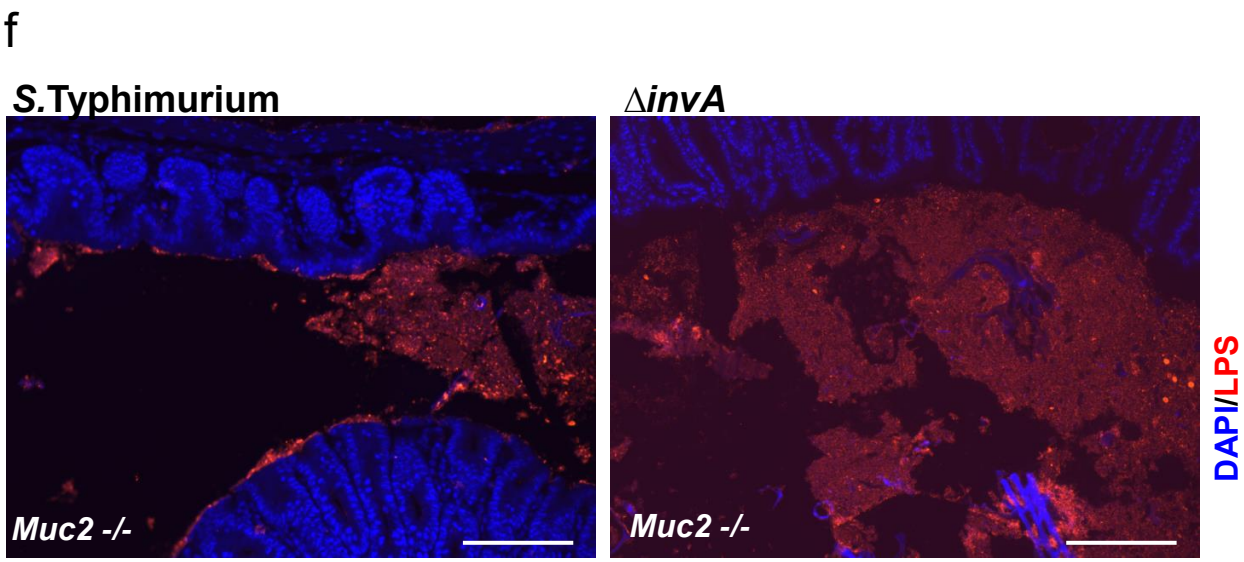

Figure 3.8 Analysis of *invA*-dependent susceptibility of *Muc2 -/-* mice.
(a) FITC-Dextran intestinal permeability assay for WT mice and *Muc2 -/-* mice infected with wild-type *Salmonella* SL1344 and *ΔinvA Salmonella* (SL1344 background). (b/c) Colonization after infection with wildtype *Salmonella* and *ΔinvA* infected WT mice and *Muc2 -/-* mice is shown for cecum and lumen (panel b), and for liver, spleen and MLN (panel c). (d) Tissue Pathology score in WT and *Muc2 -/-* mice upon infection with wild-type *Salmonella* and *ΔinvA Salmonella*. Pathology scoring included damage to epithelial integrity, PMN infiltration and submucosal edema. Asterisks indicate significant difference (*, P< 0.05, **, P< 0.01, Mann-Whitney Test, n=9 mice, 3 independent experiments). (e) Representative H&E stained images for WT and *Muc2 -/-* mice infected with wildtype and *ΔinvA Salmonella* (original magnification 50x, scale bar 100 µm). (f) *Salmonella*-LPS immunostaining profile in *Muc2 -/-* mice infected with WT *S.* Typhimurium and Δ*invA S.* Typhimurium Representative *Salmonella*- LPS staining images in cecum using *anti-Salmonella*-LPS antibody (red) and DAPI counterstain (cellular DNA, blue) are shown. WT Salmonella can be seen clustering and adherent to cecal epithelial cells whereas Δ*invA* is mostly seen in the lumen, away from the epithelial surface. (Original magnification 200x, scale bar 50 µm).

3.2.8 Infected *Muc2 -/-* mice display enhanced liver damage and inflammatory responses following *Salmonella* infection

It was surprising that *Muc2 -/-* mice succumbed to *ΔaroA S.* Typhimurium, considering that infection by this pathogen is not normally lethal to even severely immunodeficient mice [226,289]. Considering that their symptoms (hunched appearance, piloerection, and reduced activity) observed during *Salmonella* infection are typically signs of a systemic disease[290], we decided to compare inflammatory responses within the livers of WT and *Muc2 -/-* mice. Interestingly, the

production of the cytokines IL-6, TNF-α and IL-1β were significantly elevated in *Muc2 -/-* mice compared to WT mice (Figure 3.9a) while histologically, the livers of *Muc2 -/-* mice displayed much greater signs of inflammation and tissue damage, as seen by higher numbers of inflammatory foci as compared to their WT counterparts. Aggregates of inflammatory cells (inflammatory infiltrate) were more pronounced in *Muc2 -/-* mice. Overall, based on the histological and qPCR analysis, there appeared to be more evidence of hepatocellular injury in *Muc2 -/-* mice due to inflammatory responses induced by *Salmonella* (Figure 3.9b).

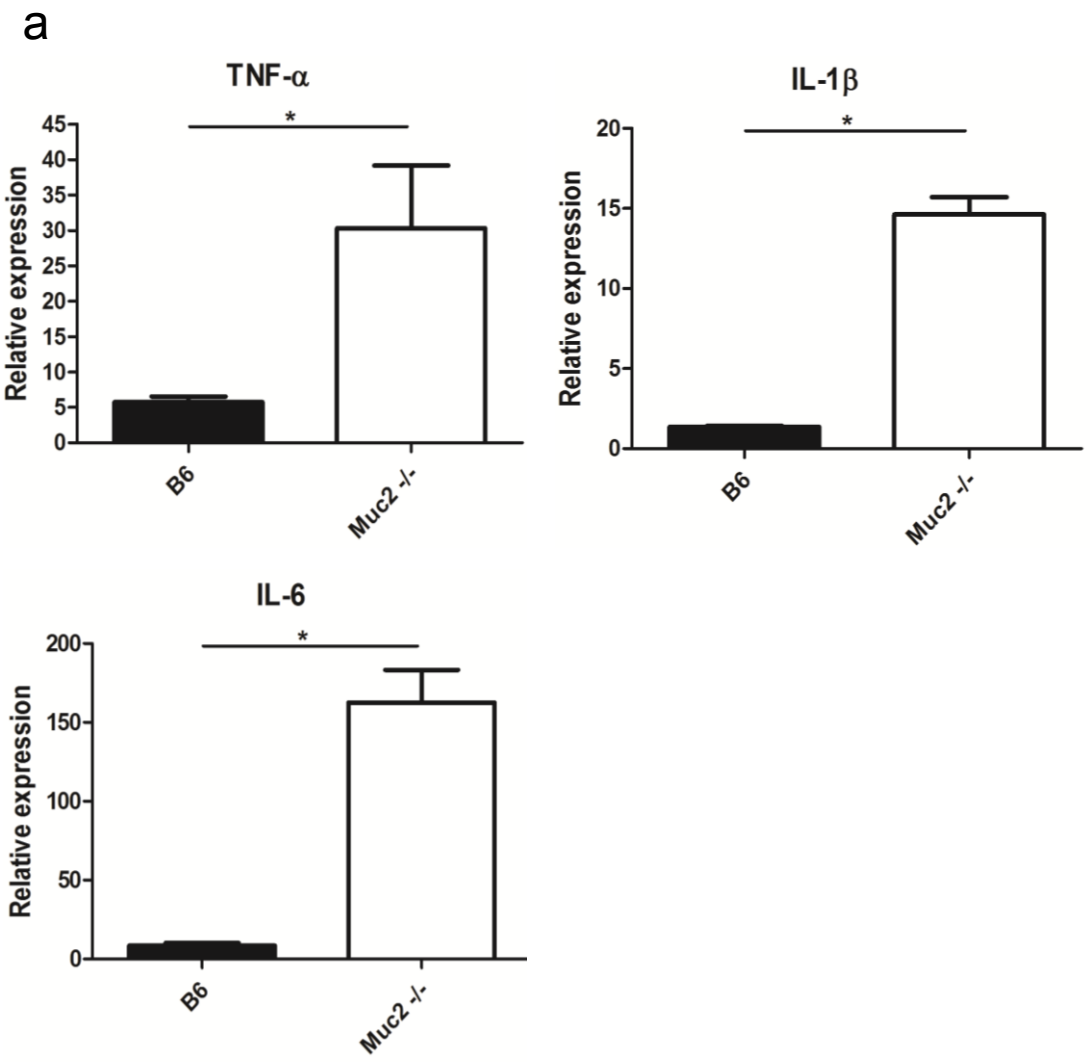

b

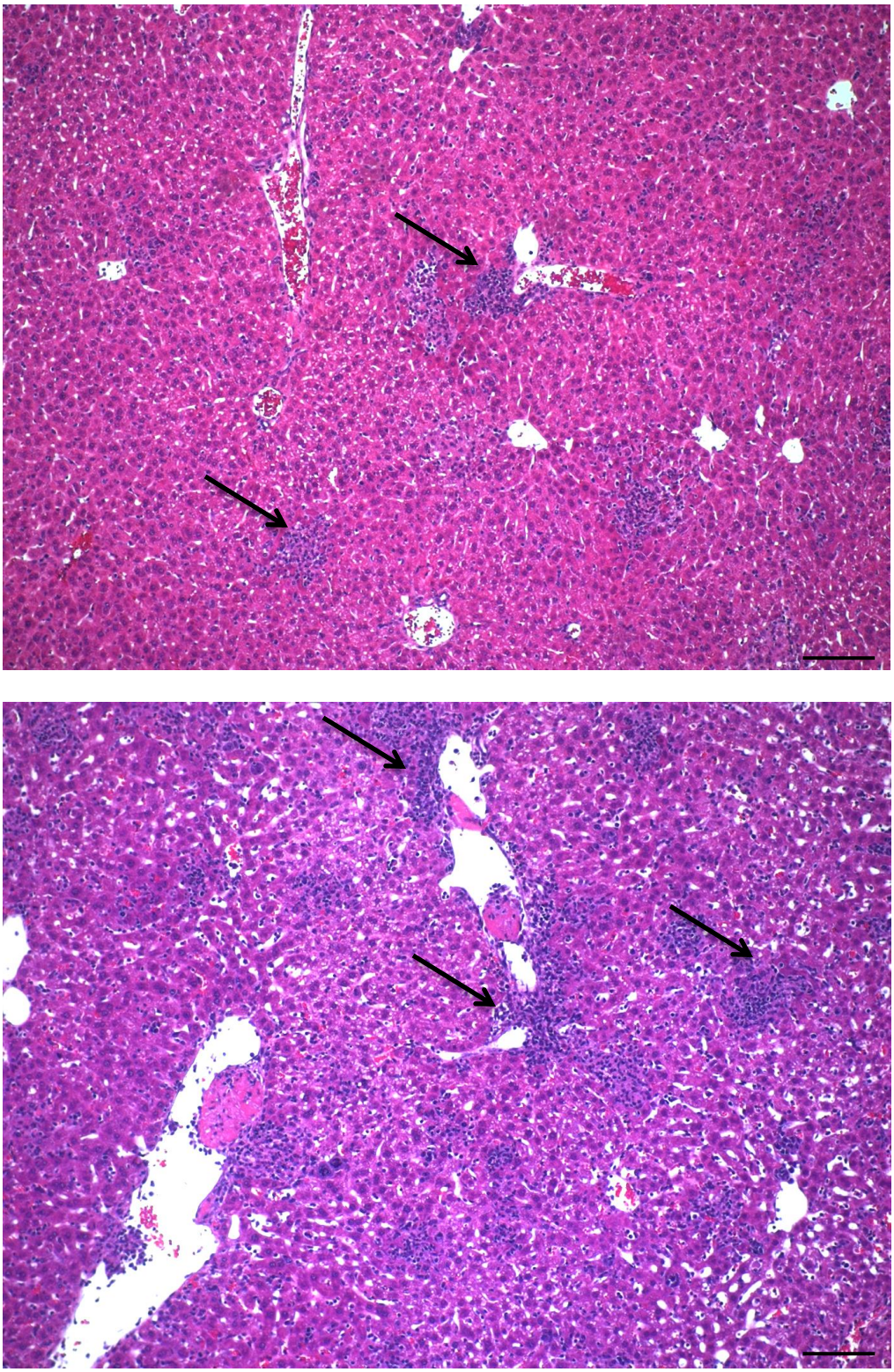

Figure 3.9 *Muc2 -/-* mice suffer from exaggerated liver damage and liver inflammatory responses during *ΔaroA Salmonella* infection.
(a) Pro-inflammatory cytokine analysis in the liver tissues of WT and *Muc2 -/-* mice as determined through quantitative PCR. Note – infection in both mouse strains leads to increased TNF-α, IL-6 and IL-1β gene transcription, as compared to uninfected mice of the same strain (data not shown), however gene induction in infected *Muc2 -/-* mice is significantly elevated compared to infected WT mice. (b) Histological analysis of liver in WT mice and *Muc2 -/-* mice. H&E stained liver tissues (Original magnification 100x, 100 μm) are shown. Arrow points to the representative inflammatory foci in the liver of each mouse, largely composed of neutrophils.

3.2.9 IAP expression and LPS detoxification are impaired in *Muc2 -/-* mice

We previously noted that liver injury during *S.* Typhimurium infection is largely mediated by LPS based activation of the innate receptor TLR4[291]. LPS produced by gram-negative bacteria within the intestine is typically detoxified by intestinal alkaline phosphatase (IAP), an enzyme expressed by enterocytes[279,282–284]. We therefore wondered if there were any differences in IAP expression or function between WT and *Muc2 -/-* mice that could lead to exaggerated inflammatory signalling in response to *S.* Typhimurium that translocate out of the gut and reach the liver. We found IAP positive staining on much of the intestinal epithelium of infected WT mice, whereas the staining was comparatively reduced on the epithelial surface of *Muc2 -/-* mice (Figure 3.10a). To address whether this reduced staining had any functional impact, we assessed the capacity of cecal tissues from the two mouse strains to detoxify LPS. Strikingly, we identified significantly reduced LPS dephosphorylation activity in the caecal tissues of *Muc2 -/-* mice compared to WT mice (Figure 3.10b), suggesting impaired LPS detoxification could underlie the high mortality rates suffered by infected *Muc2 -/-* mice.

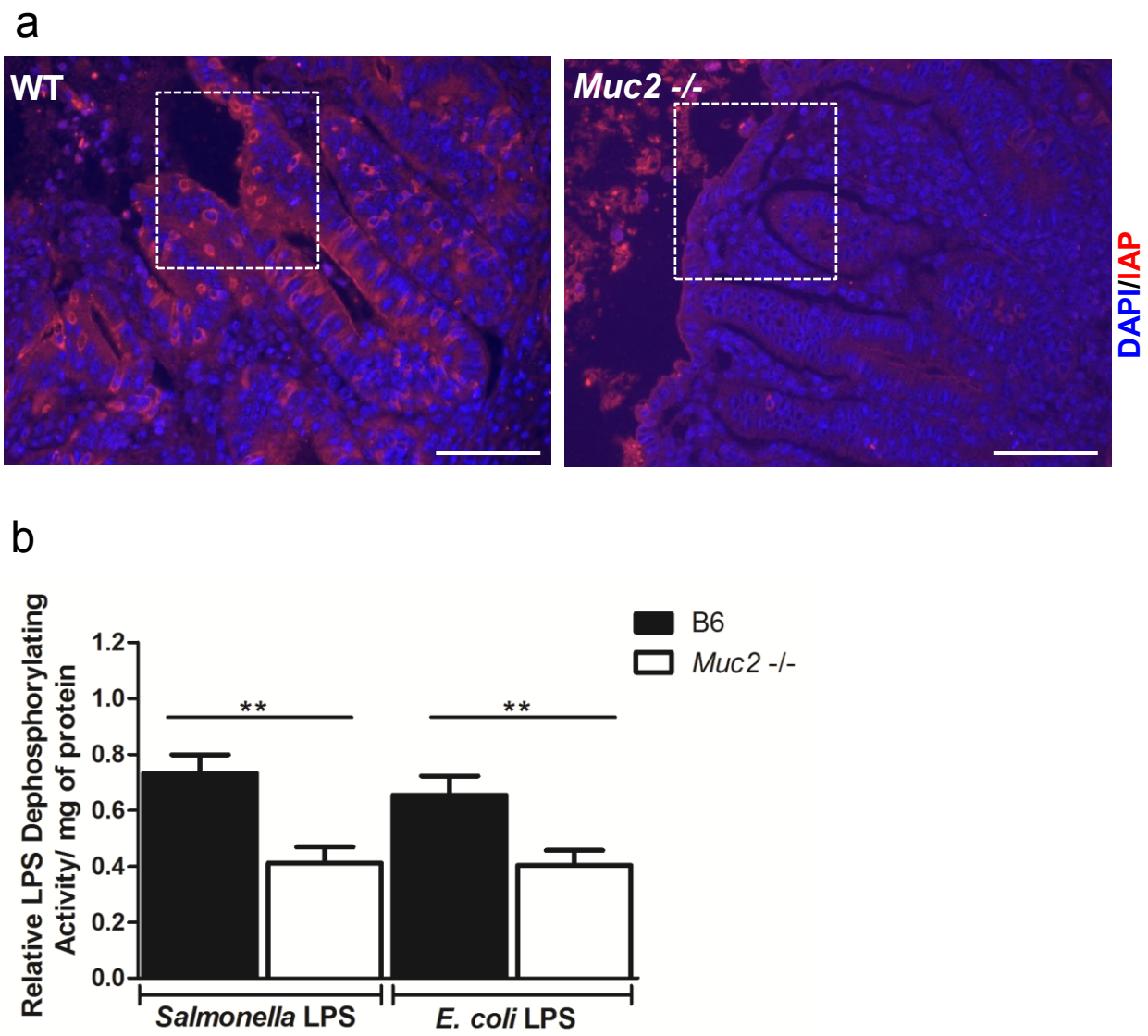

Figure 3.10 *Muc2 -/-* mice are impaired in intestinal alkaline phosphatase (IAP) staining and activity.
(a) Representative IAP immunostaining (red) in the cecum of WT mice and *Muc2 -/-* mice infected with Δ*aroA S.* Typhimurium at 7DPI. DAPI counterstain is shown in blue. (Original magnification 400x, scale 20 μm). Note the IAP positive staining along the intestinal surface and at the crypt tops (boxed area) in WT mice, but missing in *Muc2 -/-* mice. (b) Analysis of ex-vivo LPS dephosphorylation activity in the cecal tissues of WT mice and *Muc2 -/-* mice infected with Δ*aroA S.* Typhimurium (assessed at 7 DPI). Homogenized cecal tissues were incubated with *Salmonella* LPS and *Escherichia coli* LPS for 2 hours and the malachite green assay was used to measure the activity (absorbance at 595 nm). The activity was calculated as relative LPS dephosphorylation activity/mg of protein (normalized to uninfected controls in each group). (n=9 mice for each group, **, P< 0.01, Mann-Whitney Test).

3.3 Discussion

The intestinal mucus layer is predominantly comprised of the secreted mucin Muc2. Synthesized and secreted by goblet cells. Muc2 is a heavily O-glycosylated glycoprotein that forms a gel-like and viscous mesh-like layer overlying the intestinal epithelium. Intestinal mucus is the initial structural barrier encountered by enteric bacterial pathogens and as such, provides the first line of defense for the host against these and other infectious agents. The presence of the mucus layer has thus necessitated the development of specific virulence strategies allowing enteric pathogens to cross the mucus layer and reach the epithelium, such as flagella based motility and even mucus degradation[121]. Aside from functioning in host defense, over the course of the evolutionary dialogue between pathogens and the mucus layer, the mucus layer has also been subverted by some microbes, to aid in their pathogenesis. For example, mucus can provide attachment sites for pathogenic bacteria[292,293], as well as provide an energy/food source for adherent bacteria[198,294]. However, despite our growing understanding of the strategies used by enteric pathogens to cross the mucus barrier, it is not entirely clear how they physically interact with the mucus layer.

S. Typhimurium is a leading cause of enterocolitis in humans and is used as a model organism for studying bacterial pathogenesis and host responses to intracellular bacterial infections[223]. Streptomycin pretreatment of mice followed by infection with S. Typhimurium provides a relevant model for studying *Salmonella*-induced intestinal disease in humans[170]. The two most commonly used mouse strains are C57BL/6 and BALB/c, but since these strains suffer from a loss of function mutation in their *nramp1* gene, they are extremely susceptible to *Salmonella* infection[224]. Recently we have shown the applicability of using the attenuated Δ*aroA* strain of *S.* Typhimurium for studying colitis in these mouse strains[226]. Our present studies found

that Muc2 plays a critical role in host defense against *S.* Typhimurium. *Muc2 -/-* mice showed a dramatically heightened susceptibility to *Salmonella* infection compared to WT mice, carrying much heavier pathogen burdens, both in their intestinal lumens and in mucosal tissues. Our results recall earlier studies with the bacterial pathogen *C. rodentium,* where the loss of Muc2 also led to dramatically heavier intestinal pathogen burdens. In both infection models, Muc2 expression/secretion in WT mice was increased during infection, potentially promoting host defense by removing bacteria from the mucosal surface[145]. In *Muc2 -/-* mice, numerous *S.* Typhimurium were seen in close proximity (or adherent) to the intestinal epithelium, whereas in WT mice, the majority of the *Salmonella* were segregated from the epithelial surface by the overlying mucus layer, suggesting that aside for being a physical barrier, mucus-mediated flushing can play an important role in controlling pathogen burdens in the gut.

The exaggerated pathogen burdens carried by *Muc2 -/-* mice were accompanied by significant weight loss and other signs of morbidity, requiring the euthanization of all *Muc2 -/-* mice by 7 DPI. This severe response was unexpected since Δ*aroA S.* Typhimurium typically does not cause serious morbidity or any mortality in other mouse strains, including severely immunodeficient *RAG1 -/-* mice that can carry very high systemic burdens of this mutant strain[289]. We however hypothesize that the susceptibility of the *Muc2 -/-* mice to this mutant reflects not only their heavy pathogen burdens, but also the exaggerated barrier dysfunction they suffer during infection. A number of studies have shown that *S.* Typhimurium can cause tight junction disruption in infected epithelial cells, resulting in increased epithelial permeability[50,238,295,296]. Despite this *in vitro* phenotype, we and others have not been able to detect overt intestinal barrier dysfunction in other mouse strains orally infected by *S.*

Typhimurium. The current findings thus indicate that loss of Muc2 leaves the intestinal epithelium unusually susceptible to *S.* Typhimurium driven barrier disruption.

To better define the mechanisms behind the barrier disruption seen in the infected *Muc2 -/-* mice, we infected WT and *Muc2 -/-* mice with a *Salmonella* strain lacking *Salmonella* Pathogenicity Island 1 (SPI 1) dependent type III secretion. *InvA* is the first gene in the *inv*ABC operon and is located in the SPI1 pathogenicity island 1 (SPI 1) and is required, at least *in vitro* for *S.* Typhimurium*'s* invasion of epithelial cells[273,297]. When *Muc2 -/-* mice were infected with the *ΔinvA* mutant, barrier function was not disrupted and very minor histological damage was observed. Taken together with the observation that systemic *ΔinvA* pathogen burdens were dramatically reduced in the *Muc2 -/-* mice, these data suggest that the susceptibility of the *Muc2 -/-* mice was dependent on *invA*. In contrast, the *ΔinvA* mutant was still able to cross the intestinal epithelium of WT mice and cause significant cecal pathology, albeit less than that seen with wildtype *Salmonella*. These results suggest that potential interactions with intestinal mucus permit *Salmonella* (in this case an *invA* mutant) an increased opportunity for uptake and translocation out of the gut lumen, potentially by dendritic cells or macrophages through pathogen driven, but non-SPI1 dependent mechanisms[298,299]. In contrast, in the absence of mucus (*Muc2 -/-* mice), SPI1 dependent mechanisms appear to play a more important role for *Salmonella* to cross the intestinal epithelial barrier. These results may suggest that *S.* typhimurium adherent to the mucosal surface are expressing the genes involved in SPI-1 virulence system and there may be differential expression of this system in *Muc2 -/-* mice vs WT mice, dictated by the direct interactions between *Salmonella* and epithelial surface and/or by interactions with the mucus layer.

Aside from the mucus layer, there are other factors that determine host-susceptibility to an enteric bacterial pathogen, including the enzyme intestinal alkaline phosphatase (IAP). Recently there has been renewed interest in IAP activity and its role in promoting intestinal mucosal defense[279]. Several studies have shown that LPS dephosphorylation mediated by IAP protects the host against LPS-induced inflammation as well as reduces the systemic translocation of enteric bacteria[148,283,284]. To investigate if IAP activity was playing a role in the increased susceptibility/ morbidity of *Muc2 -/-* mice in our model, we stained for IAP and found that *Muc2 -/-* mice had reduced IAP expression as well as reduced LPS dephosphorylation activity (a measure of activity of IAP) within their cecal tissues. While the basis for this impairment is unclear, a recent study has reported an altered expression of other enzymes within the intestinal epithelium of *Muc2 -/-* mice[149]. However, it is unclear at this point if these changes in epithelial cell function reflect a direct role for Muc2 mucin, or alternatively, are the result of increased microbial interactions with the epithelium.

Interestingly, we also noted a dramatic increase in pro-inflammatory cytokine gene levels within the livers of the *Muc2 -/-* mice. We speculate that impaired intestinal barrier function in concert with reduced LPS detoxification within the cecum of *Muc2 -/-* mice leads to the translocation of *Salmonella* carrying highly pro-inflammatory LPS to the liver, resulting in increased inflammation (through TLR4-LPS signalling) and exaggerated damage to the liver, ultimately contributing to the higher mortality observed in these mice. These results are in line with our previous studies showing the importance of TLR4 signalling in mediating inflammatory responses in the liver[291].Our study also sheds light on the complex interactions between host factors (mucus layer, IAP) and pathogen factors (virulence genes) that ultimately determine the outcome of an infection.

To better define how Muc2 plays such a critical role in controlling *S.* Typhimurium pathogenesis; we infected mice lacking different components of this glycoprotein. Muc2 is a heavily O-glycosylated mucin and the impact of its glycosylation was noted by a recent study examining different glycosylation patterns of Muc2 in mice and humans[127,130]. Consistent with previous findings[140], we found that core 3 O-glycosylation plays a major role in protecting intestinal barrier function. Mice lacking core 3 derived O-glycans possess a thinner intestinal mucus layer and although they do not develop any spontaneous gut diseases, they do show increased susceptibility to DSS-induced colitis[140]. Infecting these *C3GnT -/-* mice, we found no significant differences in infection induced histology, pathology or *S.* Typhimurium burdens compared to WT mice. However these mice still suffered from increased epithelial barrier disruption during infection when compared to WT mice. This suggests that the core 3 glycosylation component of the mucus layer may play a role in controlling *Salmonella* driven disruption of epithelial barrier integrity, whereas the Muc2 protein, and/or its remaining glycosylation are the key factors in controlling *S.* Typhimurium burdens and overt intestinal pathology.

Increased release of mucus into the intestinal lumen, as seen during *Salmonella* infection in WT mice and *C3GnT -/-* mice, may help protect the epithelium by limiting pathogen contact and barrier disruption. This may reflect a unique action of secreted mucins, since it has been previously shown that *Muc1 -/-* mice showed no increased susceptibility to *S.* Typhimurium infection[189] whereas in this study, we show increased susceptibility of *Muc2-/-* mice to *S.* Typhimurium infection. We believe that such a protective role may be a generalized defense against many enteric bacterial pathogens. Indeed, there have been reports of Muc2 interactions

with other enteric pathogens, including *Campylobacter jejuni*[197]and the A/E pathogen *C. rodentium*[190].

There has been a growing recognition of the important role played by the mucus barrier in regulating the severity of infectious diseases but the specifics of how enteric bacterial pathogen interact with mucus/mucus components remains unclear. This study unravels the importance of Muc2, a major secreted mucin, during yet another enteric pathogen infection, *S.* Typhimurium and is the first study to provide insight into the importance of core 3 derived-O glycosylation during *Salmonella* infection. This study also provides insights into the potential role of mucus in modulating *Salmonella* pathogenesis. Considering that the mucus layer acts as a frontline defense barrier, further investigation of interactions between enteric pathogens and mucus layer may aid in the development of therapeutic strategies.

Chapter 4: The serine protease autotransporter Pic modulates *Citrobacter rodentium* pathogenesis and its innate recognition by the host

4.1 Introduction

Citrobacter rodentium is a natural attaching and effacing (A/E) mouse pathogen, widely used to model the pathogenesis of the human-specific bacterial pathogens enteropathogenic *Escherchia coli* (EPEC) and enterohemorrhagic *E. coli* (EHEC). *C. rodentium* has been widely used to explore the innate and adaptive immune responses elicited during A/E bacterial infections[211,300–302] For example, studies by our group and others have shown that *C. rodentium* based activation of toll like receptors 2 (TLR2) and 4 (TLR4) drive much of the inflammation and tissue pathology seen during infection[217,218]. Studies of *C. rodentium* infection have also helped characterize the *in vivo* role of T3SS effector proteins such as translocated intimin receptor (Tir) in pathogenesis, since there is strong homology between the translocated effector proteins produced by EPEC/EHEC and those produced by *C. rodentium*[303]. While the impact of less defined virulence factors, such as serine protease autotransporters of *Enterobacteriaceae* (SPATES) has received less attention, recent identification of three SPATES (one Class 1 SPATE and two Class 2 SPATES) as well as 17 other autotransporters encoded within the *C. rodentium* genome has opened the potential for investigating the role of these proteins *in vivo*[260]. For example, a recent study examining the role of *C. rodentium*'s Class 1 SPATE *crc1* showed it played an unexpectedly important immunomodulatory role. Deletion of *crc1* resulted in a hyper-inflammatory phenotype during infection, leading to exaggerated colitis, as measured by increased pathology, cytokine levels and inflammatory cell infiltration within the infected colon of C57BL/6 mice[261].

Pic (protein involved in intestinal colonization) is a Class 2 SPATE produced by several enteric pathogens including *Shigella flexneri*, enteroaggregative *E. coli* (EAEC) and uropathogenic *E. coli* (UPEC)[204,206,255,259,304]. A homologue of this protein was recently found

encoded within the *C. rodentium* genome (YP_003368482.1)[260], which we have termed PicC. So far, several *in vitro* or *ex vivo* functions have been attributed to Pic, including mucinolytic activity, thought to be important for enteric pathogens to colonize the intestines of their hosts by helping them penetrate the mucus layer that coats the intestinal epithelium. Curiously, several homologues of Pic have also been shown to induce rapid and exaggerated mucus secretion in rat ileal loop models, suggesting that Pic can also act as a mucus secretagogue[258]. More recent studies have also shown that Class 2 SPATES, like Pic possess immunomodulatory properties, by cleaving the O-glycosylated molecules found on the surface of immune cells, chemokines and complement proteins[257,258]. Despite these varied functions, the potential impact of Pic in bacterial virulence *in vivo* has yet to be defined.

Considering that *C. rodentium* is a non-motile pathogen, yet crosses the intestinal mucus layer to infect the underlying epithelium of its murine hosts, we were interested in testing whether PicC possessed mucinolytic activity, and if it played a critical role in *C. rodentium* pathogenesis. We constructed a PicC mutant (Δ*picC*), demonstrating that much of the *in vitro* mucinolytic activity of *C. rodentium* was dependent on the presence of PicC. Surprisingly, upon infection of mice, Δ*picC* exhibited a hypervirulent phenotype with infected mice carrying dramatically heavier intestinal pathogen burdens and suffering more severe colitis than mice infected with wild-type *C. rodentium*. Notably the virulence of Δ*picC* was normalized when the *picC* gene was restored, however a PicC point mutant causing loss of mucinase activity did not replicate the Δ*picC* phenotype. Further evaluation of the Δ*picC* mutant revealed that *in vitro*, it showed an increased propensity to develop an aggregative, red, dry and rough (RDAR) morphology, while it was found to form mixed pathogen-commensal microcolony-like structures *in vivo*. Interestingly, compared to wild-type, Δ*picC C. rodentium* showed increased *in vitro*

activation of the innate receptor TLR2, but not TLR4. Moreover, wild-type and *ΔpicC C. rodentium* caused comparable damage in TLR2 deficient mice. While this, in part, reflected increased damage caused by wild-type bacteria, the ability of *ΔpicC* to cause greater damage than wild-type *C. rodentium* was lost in the TLR2 deficient mice. Thus, despite its mucinase activity, PicC's major roles *in vivo* may be to limit *C. rodentium* aggregation as well as limit its recognition by the host's innate immune system.

4.2 Results

4.2.1 Characterization of *C. rodentium* mucinase activity - involvement of the Pic homolog, PicC

Bioinformatic analysis of the *C. rodentium* genome revealed the presence of a gene closely related to that encoding *S. flexneri* Pic. Sequence alignment showed the presence of a conserved GDSGS serine protein domain, N-terminus sequences and high sequence homology (~80% to *S. flexneri* Pic) so we named this homolog PicC (Figure 4.1). Since previously reported Pic homologs have been shown to possess mucinase activity[204,256,259], concentrated supernatants from WT *C. rodentium*, *C. rodentium* Δ*picC* and complemented *C. rodentium* Δ*picC* + pPicC were tested for potential mucinase activity. The samples were incubated with bovine submaxillary mucin (BSM), loaded onto 8% SDS-PAGE gels and stained using a PAS Glycoprotein Staining Kit. As shown in Figure 4.2A, while the lane carrying untreated BSM showed high molecular weight bands indicating intact mucin, these bands were absent following treatment with WT *C. rodentium* supernatant, suggesting the supernatant contained significant mucinase activity. Notably, when BSM was treated with *C. rodentium* Δ*picC* supernatant, high molecular weight bands were still evident suggesting that the majority of the mucinase activity observed following treatment with WT *C. rodentium* supernatant could be attributed to the presence of Pic. Correspondingly, restoration of Pic in supernatants collected from *C. rodentium* Δ*picC* + pPicC again led to the loss of high molecular weight mucin bands, similar to that seen with WT *C. rodentium*, indicating a restoration of mucinase activity. Interestingly, the mucinase activity of PicC was significantly attenuated upon treatment with the protease inhibitor phenylmethylsulfonylfluoride (PMSF) suggesting that the serine protease motif was involved in the mucinolytic digestion of the mucin. To further assess the role of the serine protease motif on

the mucinase activity of PicC, we generated a S258I mutant (catalytic residue serine changed to isoleucine through site directed mutagenesis) and confirmed that the mutation caused the loss of mucinase activity *in vitro* (Figure 4.2B).

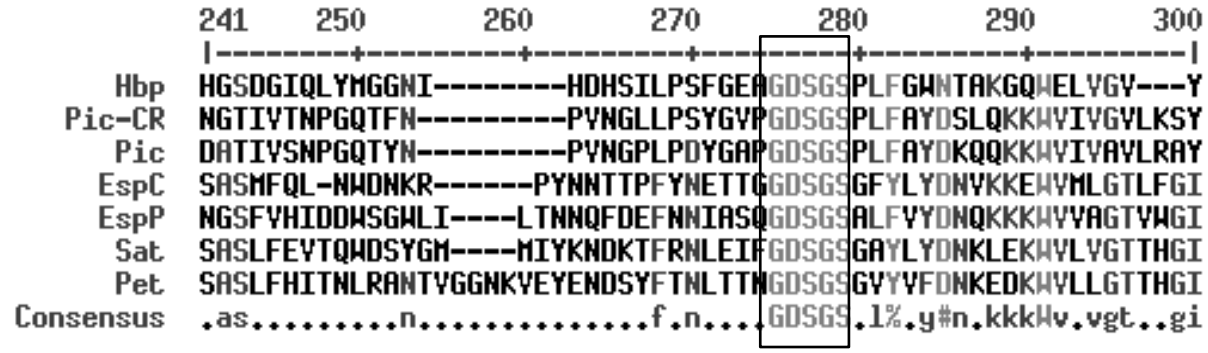

Pic- CR- pic homolog from *C. rodentium*
Pic- well characterized Pic homolog in *S. flexneri*
Hbp- Haemoglobin binding protease
EspC-EPEC Secreted Protein C
EspP- Extracellular serine protease plasmid
Sat- Secreted autotransporter toxin
Pet- Plasmid encoded autotransporter toxin

Figure 4.1 Clustal alignment of SPATES found in several enteric pathogens.
The conserved serine protease "GDSGS" domain is shown in black box. *C. rodentium* PicC homolog (labelled as Pic-CR) contains this domain. Overall, Pic homolog from *S. flexneri* and *C. rodentium* show > 80% identity at amino acid level. Note that amino acid numbering is assigned by Clustal alignment program and doesn't reflect the numbering of PicC sequence.

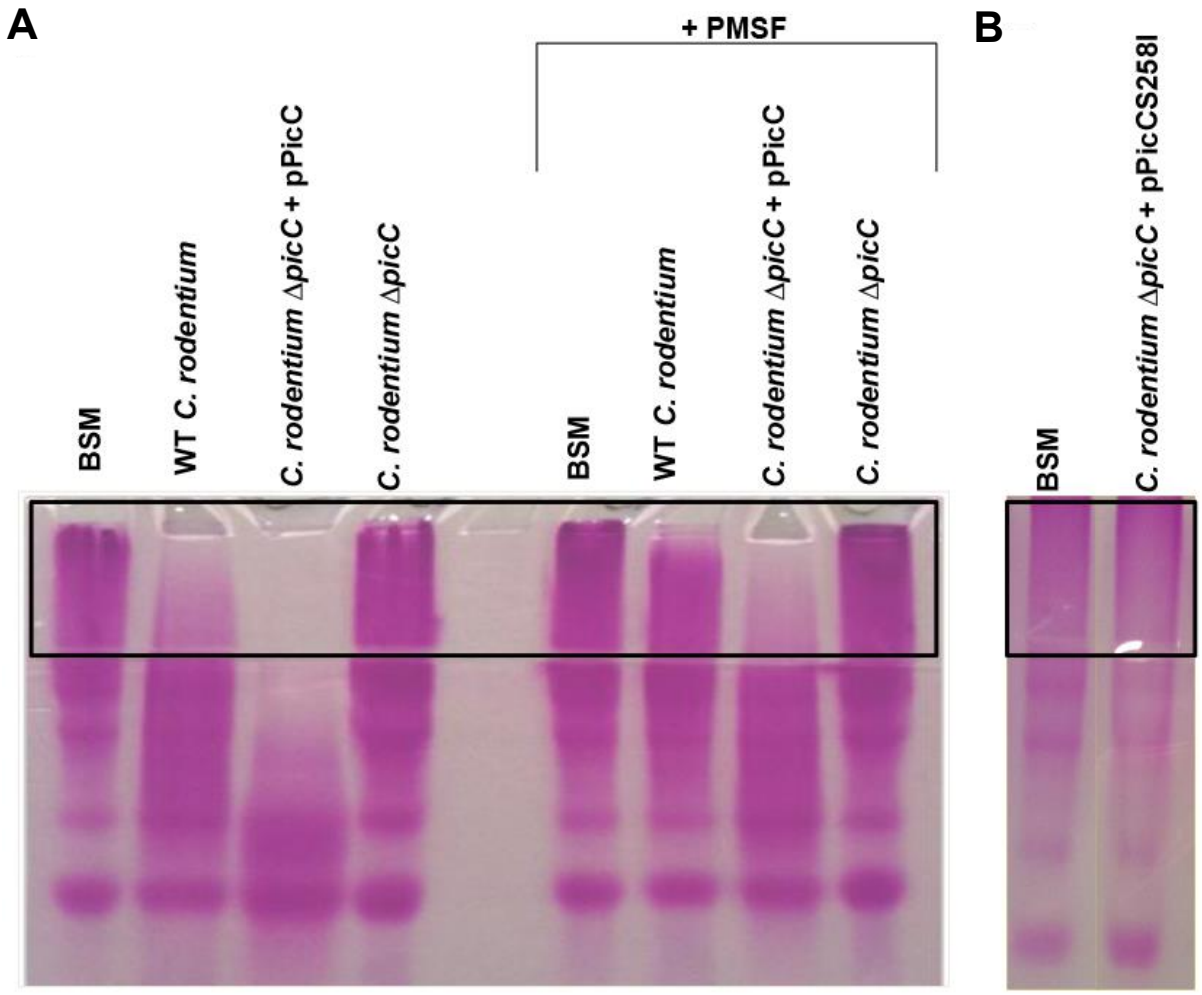

Figure 4.2 Characterization of mucinase activity of *picC* in *C. rodentium*.
Zones of mucin (bovine submaxillary mucin, BSM) clearance are visible in the stacking region of the SDS-PAGE gel (boxed area), indicative of mucinase activity. Deletion of *picC* (*C. rodentium* Δ*picC*) results in loss of mucinase activity, which is restored after complementation of *picC* (*C. rodentium* Δ*picC* + pPicC). Incubation of samples with PMSF significantly reduced mucinase activity, with the exception of *C. rodentium* Δ*picC* (no mucinase activity). (B) Reduced mucinase activity was also seen with a *C. rodentium* strain expressing a PicC protein containing a mutation in the serine protease active site S258I. Lane labelled as 'BSM' represents untreated mucin. The gels are stained with PAS.

4.2.2 *C. rodentium* Δ*picC* is highly virulent in infected mice

Since most bacterial pathogens that express *pic* homologs (e.g., *S. flexneri*, EAEC, UPEC)[204,259]are human-specific, the lack of appropriate animal models has until now prevented the investigation of the *in vivo* biological role of Pic. Since *C. rodentium* is a natural mouse pathogen, we decided to investigate the biological role of PicC, anticipating that the reduced mucinase activity of the Δ*picC C. rodentium* strain would dramatically impair its pathogenesis. Surprisingly when we compared C57BL/6 mice orally infected with WT *C. rodentium* as well as mice infected with Δ*picC C. rodentium* and monitored their body weights and survival rates over a 2 week infection period, we discovered that Δ*picC C. rodentium* was strikingly virulent in infected mice.

Interestingly, Δ*picC C. rodentium* infected mice steadily lost weight starting by day 8 post-infection (8 DPI) and their weight loss continued until 14 DPI (Figure 4.3A). In contrast, WT *C. rodentium* infected mice displayed only a modest weight loss between 2 and 4 DPI, following which their weights stabilized and remained stable throughout the remaining infection time course. While all mice survived WT *C. rodentium* infection until they were euthanized at 14 DPI, Δ*picC C. rodentium* proved much more virulent. Depending on the infection, 50-80 % of Δ*pic C. rodentium* infected mice required early euthanization between 10-13 DPI, due to significant weight loss, as well as other signs of morbidity such as hunched posture, inactivity and piloerection of the fur (Figure 4.3B). Based on the severe disease suffered by Δ*picC C. rodentium* infected mice from 10 DPI onward, further studies focused on 6 and 8 DPI.

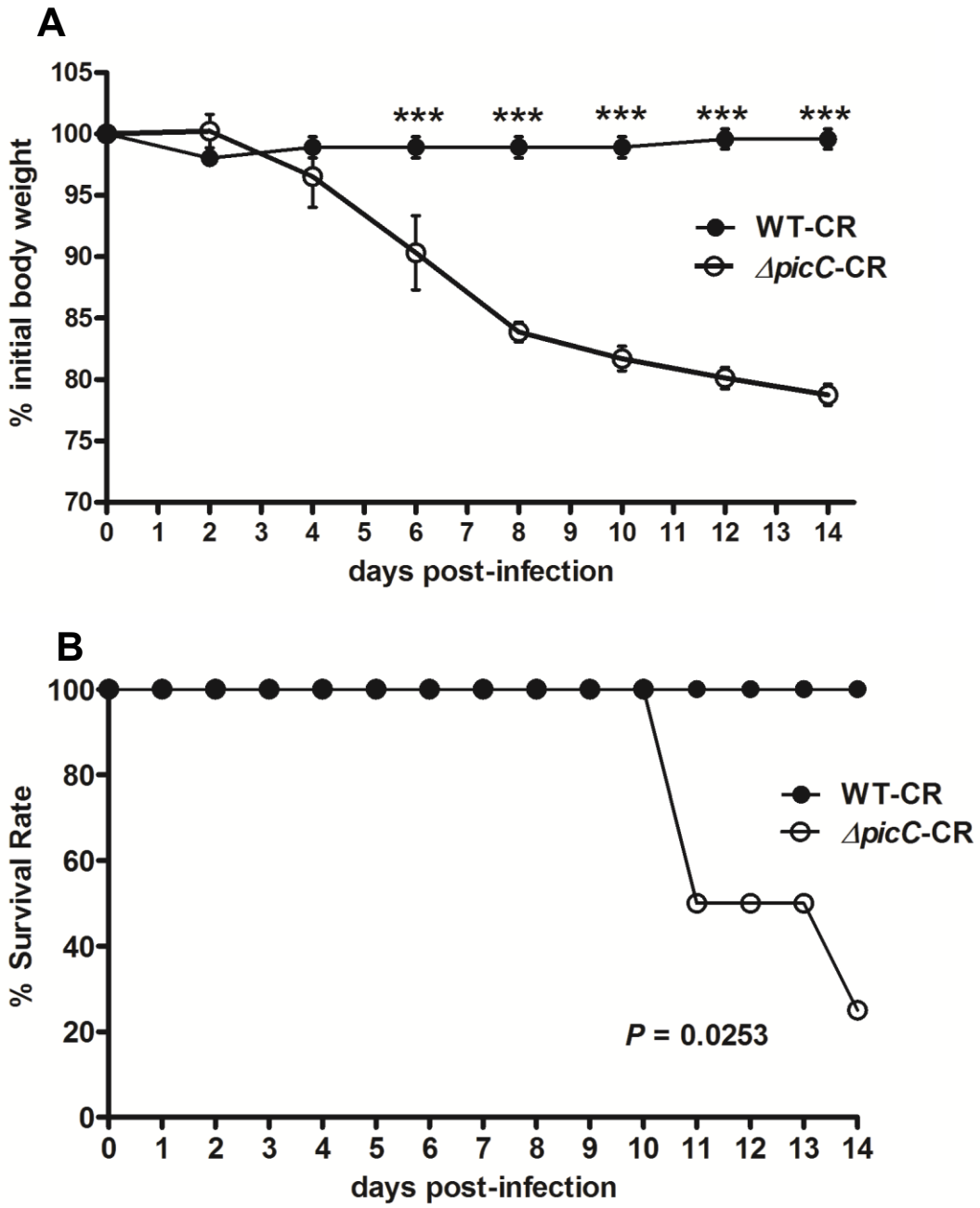

Figure 4.3 C57BL/6 mice exhibit dramatic susceptibility to Δ*picC C. rodentium*.
(A)Weight loss of WT *C. rodentium* and Δ*picC C. rodentium* infected mice, plotted as % of initial body weight and normalized to day 0 body weight. Error bars represent SEM and asterisks indicate significant differences (***, p< 0.0005) by the Mann-Whitney test. (B) Survival curve of C57BL/6 mice following WT *C. rodentium* and Δ*picC C. rodentium* infection. A *P* value (0.0253) is from the log-rank test and indicates a statistically significant difference between the survival curves. Results are representative of 3 independent experiments (12 mice per group).

4.2.3 Δ*picC C. rodentium* colonizes the mouse intestine more heavily than WT *C. rodentium*

To better define the basis for the exaggerated lethality of the Δ*picC C. rodentium* strain, we enumerated pathogen burdens in the colon and cecal tissues (considered adherent or directly infecting the epithelium) as well as those *C. rodentium* found in the luminal contents of both mouse groups at 8 DPI, as this timepoint was just prior to the exaggerated morbidity seen in the Δ*picC C. rodentium* infected mice. We found that *C. rodentium* Δ*picC* infected mice carried significantly greater pathogen burdens in their cecal and distal colon tissues (5-20 fold higher), as compared to mice infected with WT *C. rodentium*. Interestingly, the luminal pathogen burdens were not significantly different between groups suggesting that the increased Δ*picC C. rodentium* burdens were predominantly tissue adherent (Figure 4.4A). Since *C. rodentium* infection is most prominent in the distal colon, we examined pathogen localization at this site by staining for the Translocated Intimin Receptor (Tir). Tir is a T3SS effector that is injected into infected epithelial cells and is therefore a selective marker of *C. rodentium* infection[303]. As expected, WT *C. rodentium* colonization was found predominantly localized to the mucosal surface of the distal colon with a patchy localization. In contrast, staining for Tir in mice infected with Δ*picC C. rodentium* revealed more positive staining that was continuously distributed over a greater mucosal surface. Interestingly, Δ*picC C. rodentium* also showed deeper penetration into colonic crypts as compared to WT *C. rodentium* (Figure 4.4B, 4.4C), with significant staining not only directly adherent to the epithelium, but also within the crypt lumen. Thus, despite losing the mucinase activity of PicC, Δ*picC C. rodentium* appeared to reach the intestinal epithelium and colonize the intestinal crypts of infected mice even better than wild-type.

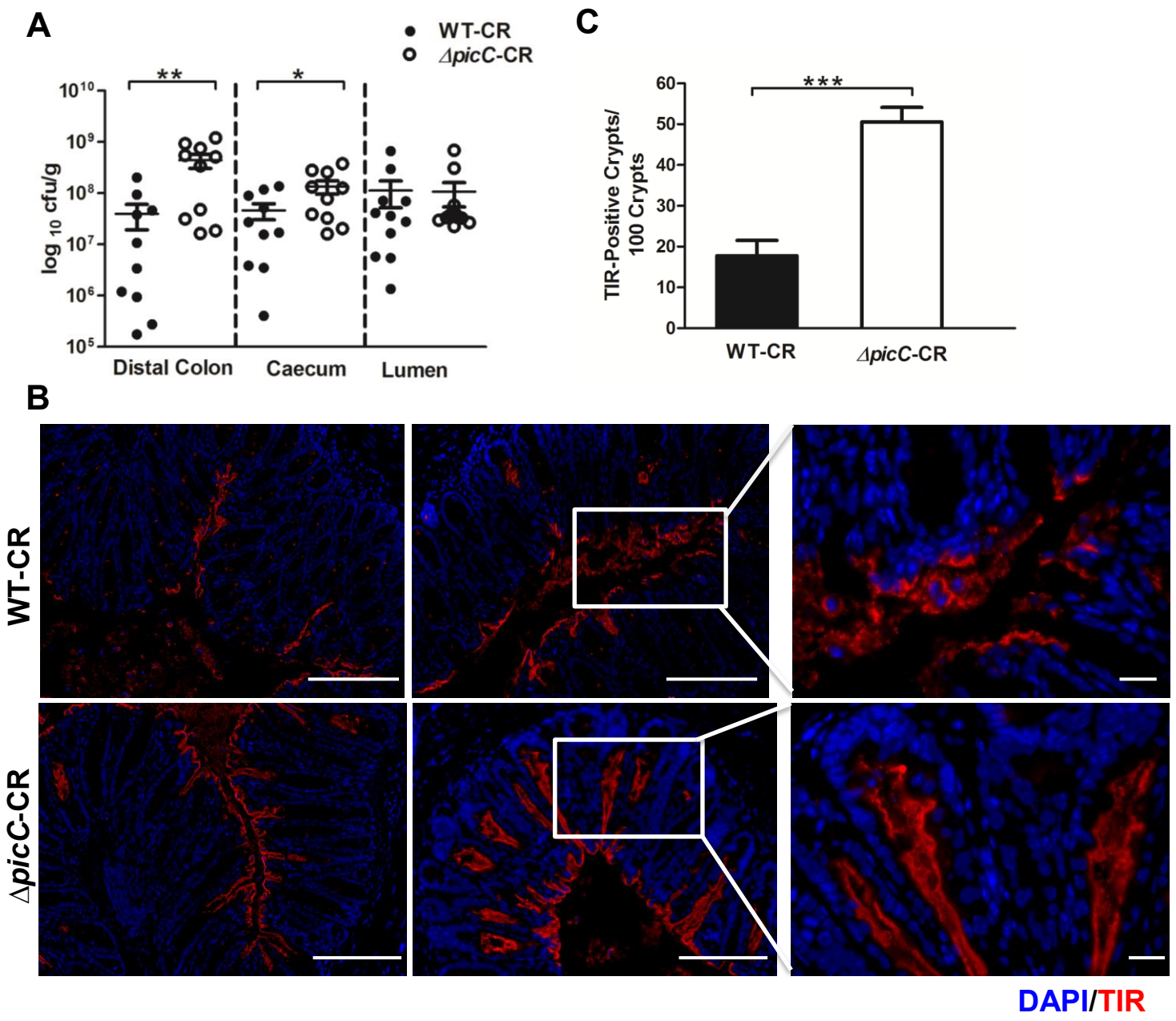

Figure 4.4 Δ*picC C. rodentium* infected mice carry heavier pathogen burdens.
(A) Adherent (distal and cecal tissues) and non-adherent luminal *C. rodentium* burdens at day 8 PI. (B) Representative images from distal colon showing *C. rodentium* localization as seen via Tir (*C. rodentium* specific effector; red) and DAPI (counterstain; blue) staining. Original magnification 200X. WT *C. rodentium* is mostly seen on the epithelial surface (inset, top panel, 630X) whereas Δ*picC C. rodentium* penetrates deeper into the crypts (inset, bottom panel, 630X). (C) Quantitative analysis looking at Tir-positive crypts/100 crypts. Analysis was done at original magnification 200X and represents an average of distal colons from at least 9 different mice/group. Error bars represent SEM and asterisks indicate significant difference (***, $p < 0.0005$) by the Mann-Whitney test.

4.2.4 *C. rodentium* Δ*picC* infected mice exhibit exaggerated mucosal damage and inflammation

Next we investigated the intestinal pathology that developed in mice infected with Δ*picC C. rodentium* as compared to WT *C. rodentium*. We noted that Δ*picC C. rodentium* infected mice suffered significantly higher intestinal pathology scores compared to WT *C. rodentium* infected mice, as reflected by increased crypt epithelial cell hyperplasia, inflammatory cell infiltration and greater damage to the epithelial surface in the distal colon (Figure 4.5A and B). As expected, WT *C. rodentium* infection led to elevated gene transcript levels of several pro-inflammatory cytokines (IL-17A, IFN-γ, IL-10, TNF-α, IL-6, IL-1β) and chemokines (MCP-1, KC) in the distal colon, however consistent with their worsened pathology, the transcript levels for these genes were significantly higher in tissues from Δ*picC C. rodentium* infected mice (Figure 4.5C). In concert with the increased cytokine gene transcripts, we also noted increased inflammatory and immune cell infiltration (macrophages (F4/80 +ve) and T lymphocytes (CD3 +ve) in the tissues of the Δ*picC C. rodentium* infected mice (Figure 4.6A, 4.6B) suggesting that Δ*picC C. rodentium* infected mice developed exaggerated intestinal inflammation as compared to WT *C. rodentium* infected mice.

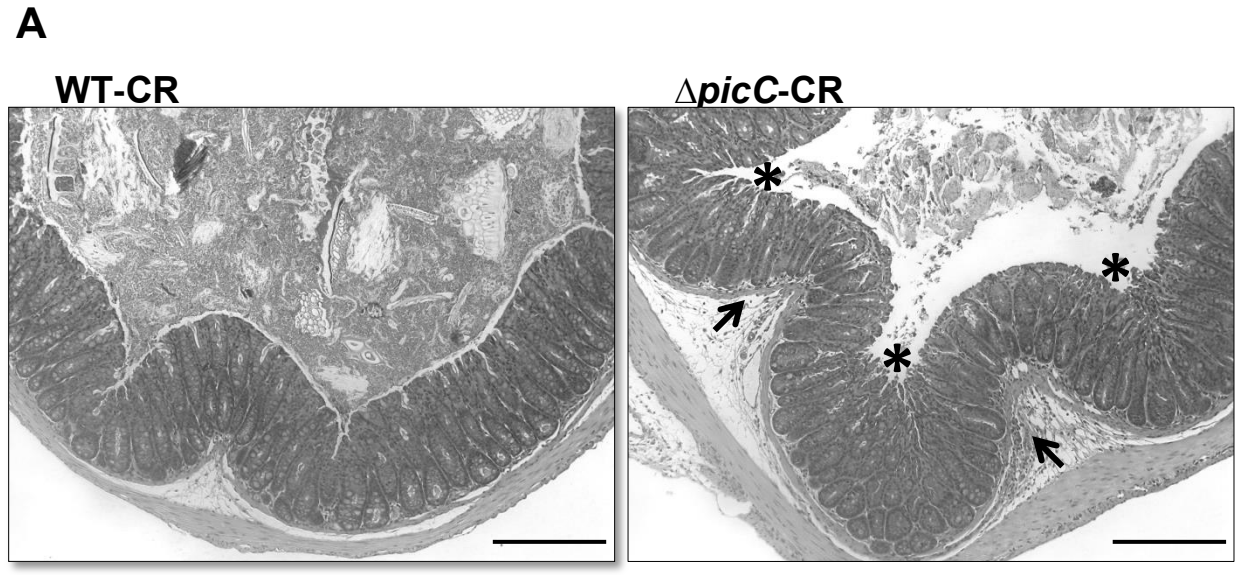
A
WT-CR
ΔpicC-CR

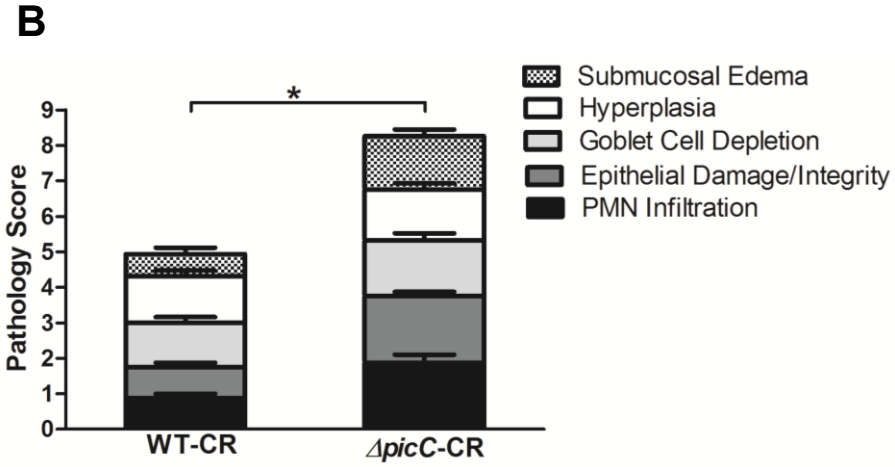
B
Submucosal Edema
Hyperplasia
Goblet Cell Depletion
Epithelial Damage/Integrity
PMN Infiltration
Pathology Score
WT-CR
ΔpicC-CR

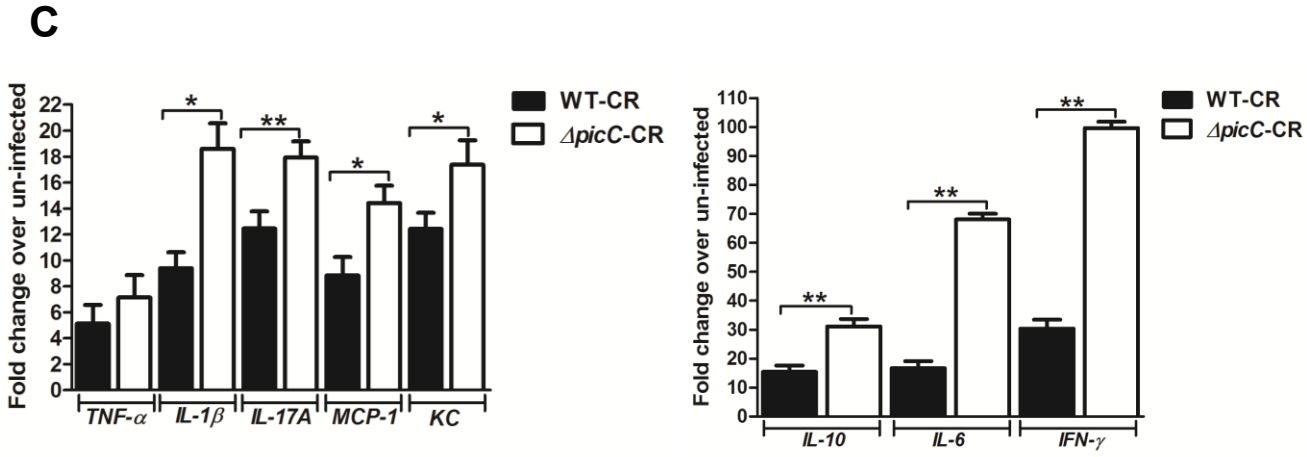
C
WT-CR
ΔpicC-CR
Fold change over un-infected
TNF-α
IL-1β
IL-17A
MCP-1
KC
IL-10
IL-6
IFN-γ

Figure 4.5 Heightened histopathological damage and increased pro-inflammatory cytokines in Δ*picC C. rodentium* infected mice.
(A) Representative H&E stained distal colon (original magnification 100X) at day 8 PI for WT *C. rodentium* and Δ*picC C. rodentium* infected mice. Asterisks (*) represent damage to the intestinal epithelial surface, as seen by ruffling and loss of crypt structure and/or epithelial integrity. Arrows point to increased edema and infiltration of immune/inflammatory cells. (B). Cumulative tissue pathology damage scores from distal colon of WT and Δ*picC C. rodentium* infected mice. Scoring was done by blinded observers and represents an average of 9 mice/group. (C) Quantitative PCR of proinflammatory cytokine and chemokine genes in the distal colon of the WT and Δ*picC C. rodentium* infected mice. Note that WT *C. rodentium* infection resulted in increased gene transcript levels of tested chemokines and cytokines, however there was a greater induction seen with Δ*picC C. rodentium* infection, indicative of hyper-inflammatory responses. Errors bars represent SEM from three independent experiments and at least 9 mice/group. ** $p < 0.01$; * $p < 0.05$, Mann-Whitey test.

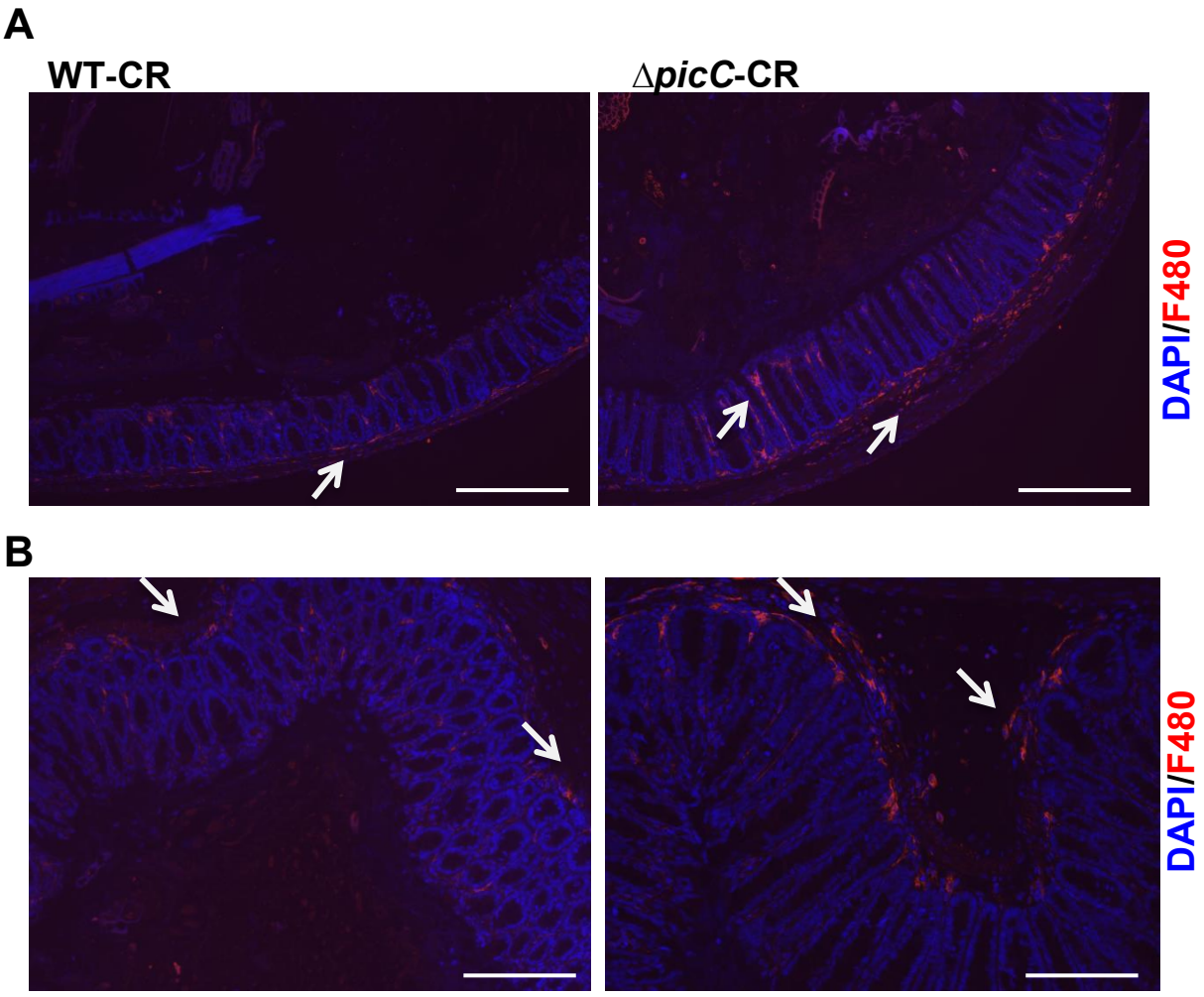

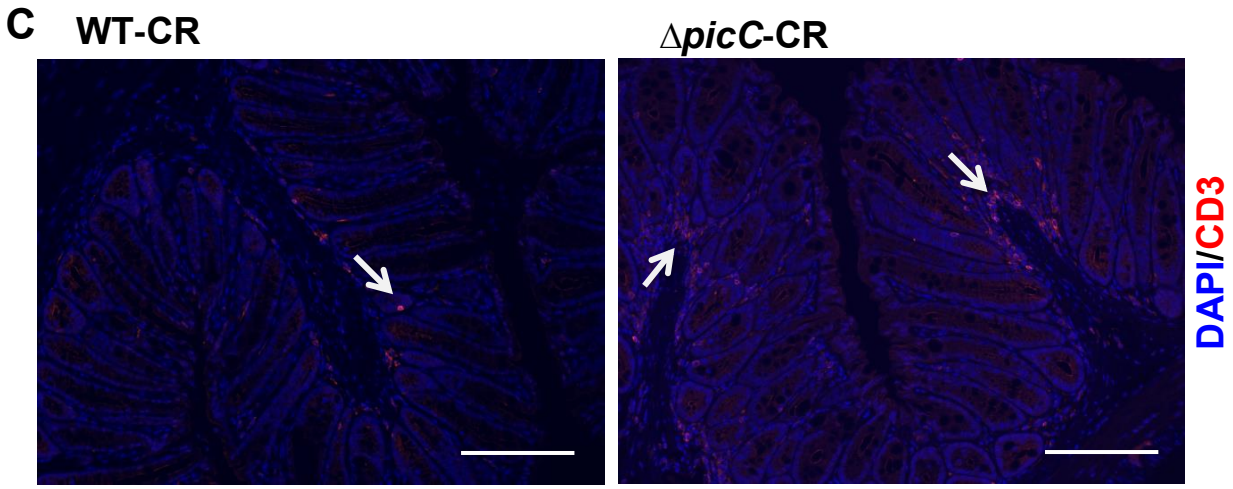

Figure 4.6 Characterization of immune cell infiltration in WT and Δ*picC C. rodentium* infected distal colons.
(A/B) Immunostaining for infiltrating macrophages (F4/80- red, DAPI-blue, counterstain). Arrows point to F4/80 positive staining seen in the mucosa and submucosa of the representative sections. (C) CD3+ T lymphocytes (red) seen infiltrating the distal colons of infected mice (white arrow). Original magnification 200X. White arrows- CD3+ cells.

Upon complementation of *picC* into Δ*picC C. rodentium* (Δ*picC* + pPicC), the WT *C. rodentium* infectious phenotype was restored for body weight loss, mortality, pathogen burdens/location, and tissue pathology (Figure 4.7). There were no notable differences in the above mentioned parameters between WT *C. rodentium* and complimented strain, suggesting that the deletion mutation was in frame and the observed phenotype in the deletion mutant was not caused by a polar effect. It also confirmed the specific role of PicC protein in the observed phenotypes.

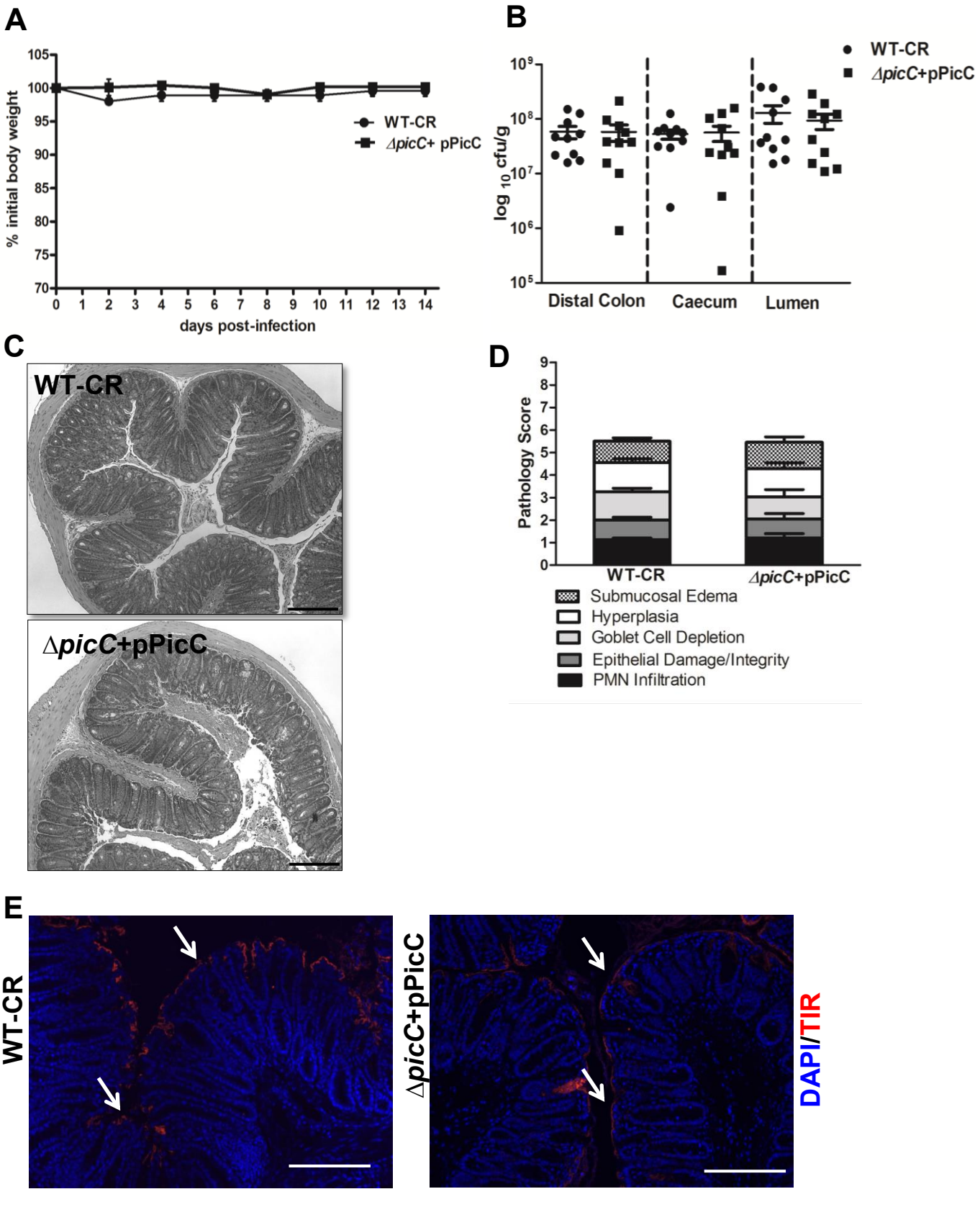
A
% initial body weight
days post-infection
WT-CR
ΔpicC+ pPicC
B
log 10 cfu/g
WT-CR
ΔpicC+pPicC
Distal Colon
Caecum
Lumen
C
WT-CR
ΔpicC+pPicC
D
Pathology Score
WT-CR
ΔpicC+pPicC
Submucosal Edema
Hyperplasia
Goblet Cell Depletion
Epithelial Damage/Integrity
PMN Infiltration
E
WT-CR
ΔpicC+pPicC
DAPI/TIR

Figure 4.7 Complementation of Pic into Δ*picC C. rodentium* restores the WT phenotype. (A) Body weights of C57BL/6 mice infected with WT *C. rodentium* and *picC* complemented *C. rodentium* (Δ*picC* + pPicC). (B) Pathogen burdens enumerated day 8 PI in distal colon, cecum and lumen from mice infected with WT *C. rodentium* and *picC* complemented *C. rodentium.* No significant differences were seen between the two strains. (C) Histopathological analysis of H&E stained distal sections collected from WT *C. rodentium* and *picC* complemented *C. rodentium* (Δ*picC* + pPicC) infected C57BL/6 mice. (D) Cumulative histology damage scores from distal colon of C57BL/6 mice infected with WT *C. rodentium* and *picC* complemented *C. rodentium* respectively. Data shown represents an average of 9 mice/group. (E) *C. rodentium* specific Tir staining (red) showing *C. rodentium* localized to epithelial surface of distal colons of WT and complemented strain (white arrows). There were no overt differences in *C. rodentium* localization between the two strains. DAPI- nuclei, counterstain. Original magnification 200X.

4.2.5 *C. rodentium* infected mice display exaggerated epithelial barrier disruption and increased translocation of pathogenic and commensal bacteria

To explore the basis for the exaggerated inflammation, pathology and increased morbidity/mortality seen in mice infected by Δ*picC C. rodentium*, we assayed epithelial barrier function in the two groups of infected mice. FITC Dextran was orally administered to WT *C. rodentium* and Δ*picC C. rodentium* infected mice, at 6 DPI, with the levels of FITC-Dextran translocated into the serum measured. Δ*picC C. rodentium* infected mice had significantly higher levels of FITC Dextran in their serum, compared to WT *C. rodentium* infected mice, indicating increased damage to the intestinal epithelial barrier following infection with Δ*picC C. rodentium* (Figure 4.8A). To assess the impact of the exaggerated barrier disruption suffered by Δ*picC C. rodentium* infected mice, we examined pathogen burdens at systemic tissue sites (liver, spleen, MLN). While there was a trend towards higher burdens in the spleens of mice infected with Δ*picC C. rodentium* as compared to WT *C. rodentium,* significantly more *C. rodentium* were recovered from the liver and MLN of Δ*picC C. rodentium* infected mice (Figure 4.8B). We also assessed whether infection with Δ*picC C. rodentium* impacted the translocation of commensal microbes to the MLN of infected mice. We collected MLN from mice at 8 DPI and enumerated

the commensal colony forming units (CFUs) by plating on commensal specific media under controlled anaerobic conditions. Notably, there were significantly higher commensal numbers recovered from the MLN of Δ*picC C. rodentium* infected mice (Figure 4.9C). Collectively, our data indicates that infection with Δ*picC C. rodentium* not only leads to increased epithelial barrier dysfunction, but also results in higher systemic translocation of both pathogenic and commensal bacteria, potentially contributing to the increased mortality rates in these mice.

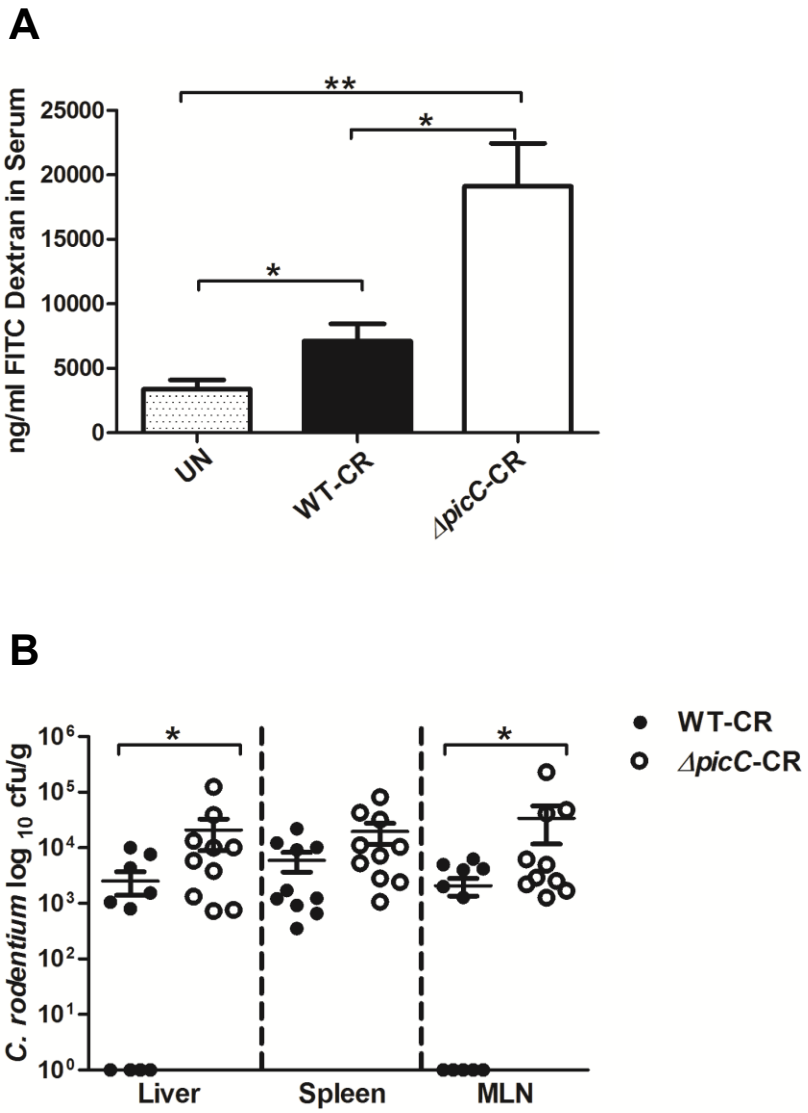

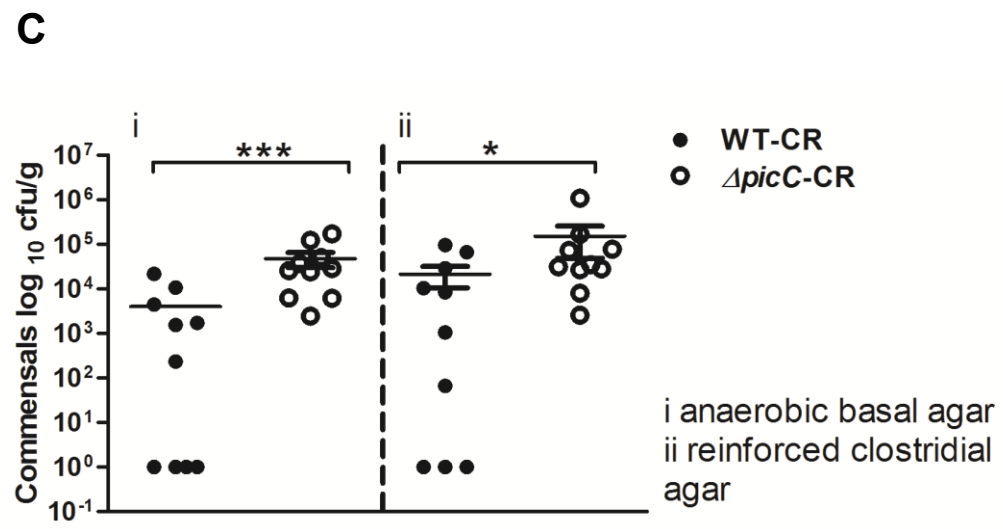

Figure 4.8 *C. rodentium* Δ*picC* infected mice have impaired epithelial barrier integrity and increased translocation of pathogenic and commensal bacteria.
(A) Δ*picC C. rodentium* infected mice display greater FITC-Dextran flux across their intestinal barrier on day 6 PI as compared to WT *C. rodentium*. Bar graph shows the quantity of FD4 in serum and represents an average of 9 mice/group, UN- uninfected C57BL/6 mice. (B) Quantification of *C. rodentium* burdens recovered from systemic sites (liver, spleen, MLN) day 8 PI. Δ*picC* infected mice had significantly greater translocation of pathogenic *C. rodentium* to the systemic sites. (C) Recovery of viable commensal bacteria from MLN, harvested from mice infected with WT *C. rodentium* or Δ*picC C. rodentium*, under controlled anaerobic conditions and commensal specific media (i- anaerobic basal agar; ii-reinforced clostridial agar). Errors bars represent SEM from 3 independent experiments. ***, $p < 0.0005$, ** $p < 0.01$; * $p < 0.05$ by the Mann-Whitney test.

4.2.6 The *in vivo* impact of PicC on *C. rodentium* virulence does not reflect its effects on mucins

While the mucinase activity of PicC did not appear to be required for *C. rodentium* to colonize the murine intestine, we decided to clarify whether the loss of its serine protease activity was the basis for the exaggerated pathology suffered during infection by Δ*picC C. rodentium*. We confirmed that the S258I mutation caused the loss of mucinase activity *in vitro* (Figure 4.2A). However when we tested the point mutant *in vivo*, we noted a similar phenotype to that seen with WT *C. rodentium*, with roughly similar pathogen burdens (Figure 4.9A,4.9B), tissue pathology (Figure 4.9C, 4.9D) and epithelial barrier dysfunction (Figure 4.9E). These results

indicate that the exaggerated pathology seen in the absence of PicC reflects other actions of Pic than its serine protease activity.

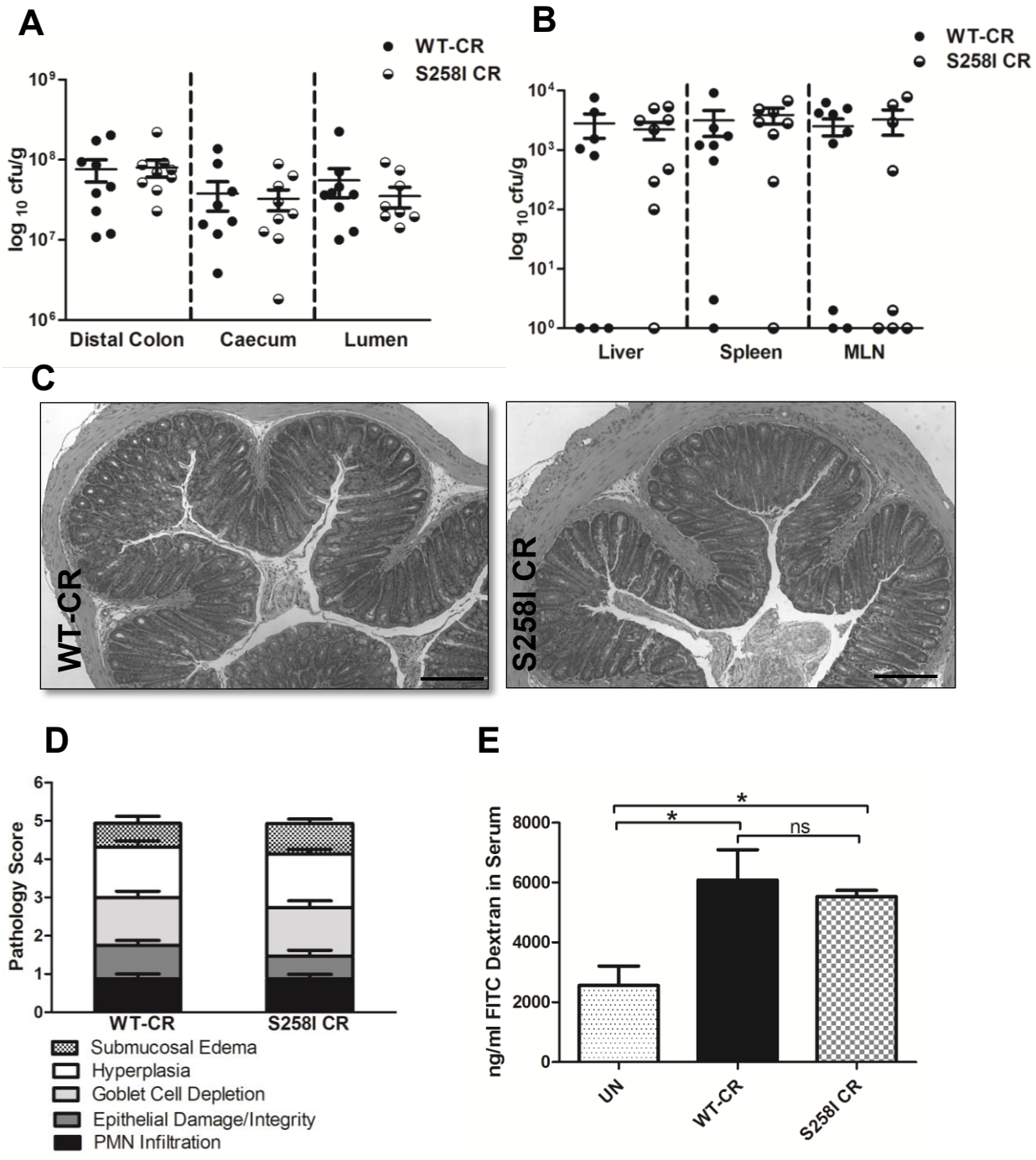

Figure 4.9 Mucinase activity of PicC is not essential for intestinal colonization.
(A) *C. rodentium* burdens enumerated at day 8 PI from distal colon, cecum and lumen for WT *C. rodentium* and S258I *C. rodentium* (catalytic mutant with no mucinase activity) infected mice. (B) WT *C. rodentium* and S258I *C. rodentium* burdens recovered from systemic sites, i.e. liver, spleen and MLN at day 8 PI. (C) Representative H&E stained distal colon (original magnification 100X) at day 8 PI. (D) Histologic damage scores from distal colon of WT *C. rodentium* and S258I *C. rodentium* infected mice. Pathology scoring included submucosal edema, hyperplasia, goblet cell depletion, damage to epithelial integrity and PMN infiltration. Scores were determined by 2 independent observers under blinded conditions. (E) FITC-Dextran intestinal permeability assay for WT *C. rodentium* and S258I *C. rodentium* infected C57BL/6 mice respectively. Baseline FITC-Dextran flux for uninfected C57BL/6 mice is also shown. Uninfected and infected mice were gavaged with FITC-Dextran and serum was collected using cardiac puncture. Serum FD4 levels were measured. Asterisks represent statistically significant difference (* $p < 0.05$ by the Mann-Whitney test); ns- not significant. Errors bars= SEM; 3 independent infection and 9 mice/group.

Aside from mucinase activity, Pic proteins from several pathogens (EAEC, UPEC, *Shigella flexneri*) act as mucin secretagogues[258]. To test whether the loss of PicC from *C. rodentium* impacted on mucus secretion during infection, we measured mucin production/release during infection. As shown in Figure 7A and 7B, while *C. rodentium* infection was associated with an increase in mucin secretion, the quantitative levels did not significantly differ between mice infected with WT *C. rodentium* and mice infected with Δ*picC C. rodentium* (Figure 7C), indicating that in our model system, PicC did not exhibit significant mucin secretagogue activity.

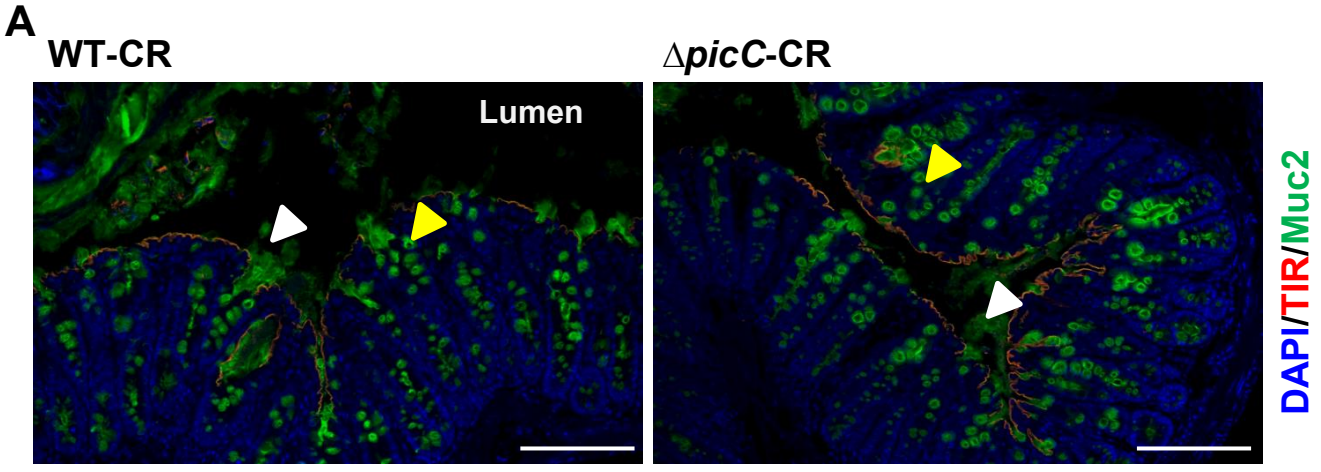

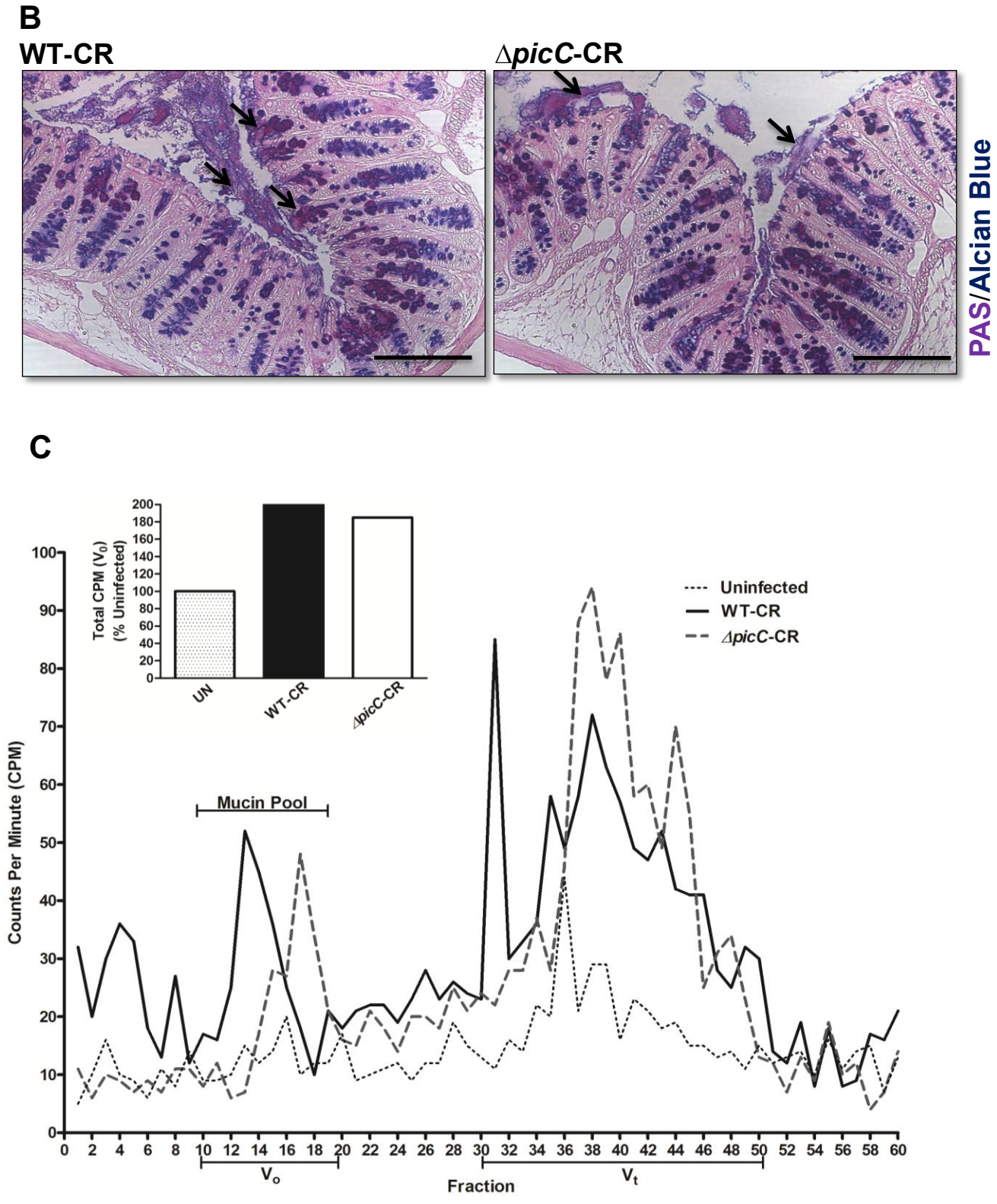
B
WT-CR
ΔpicC-CR
PAS/Alcian Blue
C
Total CPM (V0)
(% Uninfected)
UN
WT-CR
ΔpicC-CR
Uninfected
WT-CR
ΔpicC-CR
Mucin Pool
Counts Per Minute (CPM)
Vo
Fraction
Vt

Figure 4.10 *C. rodentium* PicC is not a potent mucus secretagogue *in vivo*.
(A) Representative dual immunofluorescence staining in Carnoy's fixed distal colon at day 8 PI. Mucin Muc2 (green), Tir (red- shows the association of *C. rodentium* with Muc2-positive crypts) and DAPI (nuclei, counterstain). White arrowhead indicates secreted/luminal mucus, yellow arrowhead shows representative Muc2-filled goblet cells. (B) Representative PAS/AB staining of Carnoy's fixed distal colon collected from WT *C. rodentium* and Δ*picC C. rodentium* infected mice. Arrows point to the secreted mucus. (C) Quantification of total mucus secretion in WT *C. rodentium* and Δ*picC C. rodentium* infected mice day 6 PI. Plot shows the counts per minute (CPM) in individual column fractions containing radioactive ^{3}H activity after total secretions were subjected to gel filtration chromatography (Sepharose 4B column). This plot represents an average of 6 mice/group and 2 independent infections. Inset shows a bar graph representation of total CPM in void (V_o) volume fractions (#10-20, large, mucin glycoproteins) plotted as % of uninfected samples. V_t represents fractions eluting non-mucin glycoproteins.

4.2.7 Δ*picC C. rodentium* shows increased aggregation *in vivo*

Considering our data indicating that PicC modulates *C. rodentium* pathogenesis, but not through its impact on the host, at least in terms of mucin degradation or release, we considered literature indicating that autotransporters can also impact on the structure and function of the bacteria that express them[305–308]. We therefore tested whether PicC altered the structure and/or function of *C. rodentium*, starting with a functional assessment of its type three secretion system. Secretion deficient mutant *C. rodentium* Δ*escN* was used as a control. Lysates of WT and Δ*picC C. rodentium* looked similar, as did the profile of the T3SS effectors secreted by these strains when grown in DMEM media (Figure 4.11A). We also tested if there were any differences in epithelial adherence of WT and Δ*picC C. rodentium* using the CMT93 mouse rectal epithelial cell line. Confluent CMT93 cells were infected (MOI 10 and 100) with the above-mentioned strains and adherent bacteria counts enumerated through plating. No differences were seen between WT and Δ*picC C. rodentium* suggesting that there were no intrinsic differences in the *in vitro* infectivity of these strains that could account for the increased virulence displayed by Δ*picC C. rodentium* (Figure 4.11B).

We next investigated the status of Δ*picC C. rodentium in vivo.* It was notable that despite the heavier adherent burdens seen in Δ*picC C. rodentium* infected mice, their luminal burdens were not increased to a similar degree. Upon examination of infected tissues using immunostaining for Tir and Muc2, the Δ*picC* strain was found abnormally clustered within the adherent mucus layer and in the colonic crypts, as though they were aggregating together to form microcolonies. In contrast, WT *C. rodentium* were primarily observed directly adhering to the mucosal surface, without any signs of aggregation (Figure 4.12).

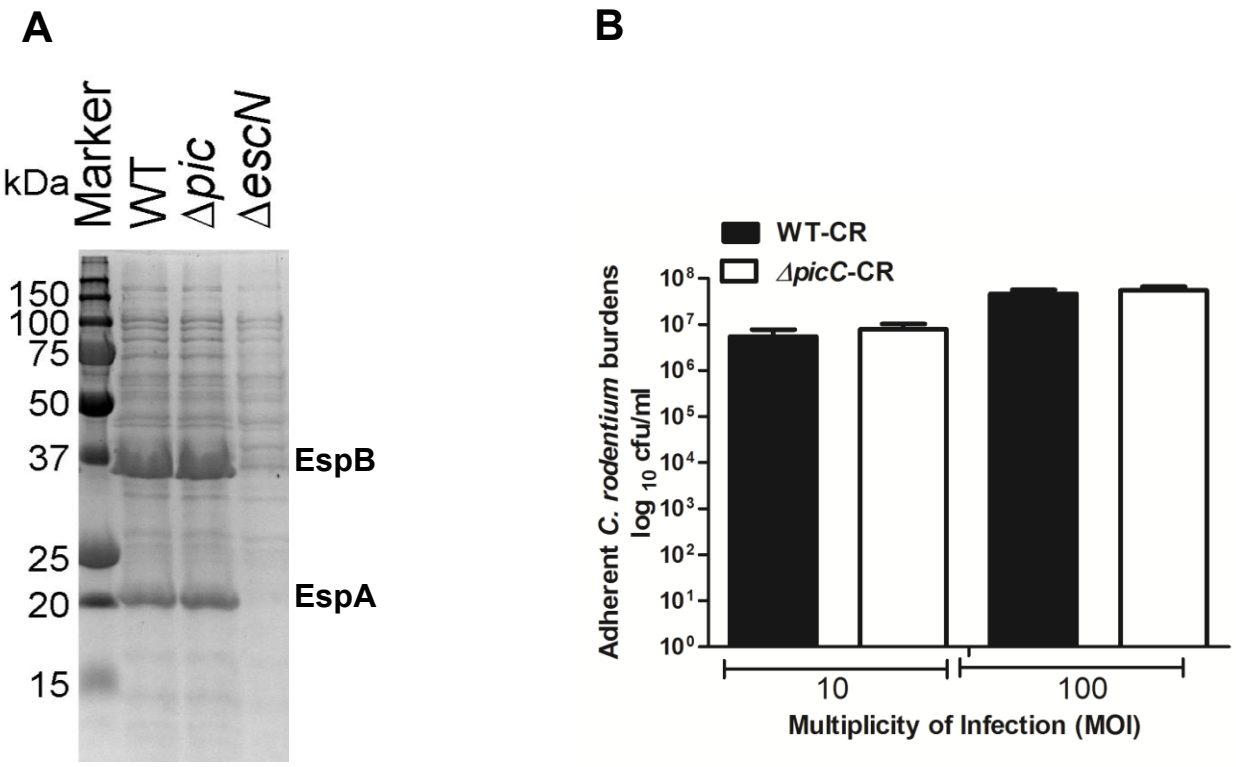

Figure 4.11 Assessing the impact of PicC on *C. rodentium* structure and function.
(A) T3SS effector secretion profile for WT *C. rodentium* and Δ*picC C. rodentium*. Δ*escN C. rodentium* was used as a negative control since it is T3SS deficient. Bacteria were grown in DMEM and secreted proteins were precipitated using 10% TCA. Samples were visualized on 15% SDS-PAGE gel through Coomassie staining. (B) *In vitro* adherence assay examining adherence of WT *C. rodentium* and Δ*picC C. rodentium* using CMT-93 murine rectal cell line. CMT-93 cells were infected with the O/N bacterial cultures for 4 hours and adherent bacteria counts were enumerated on MacConkey plates.

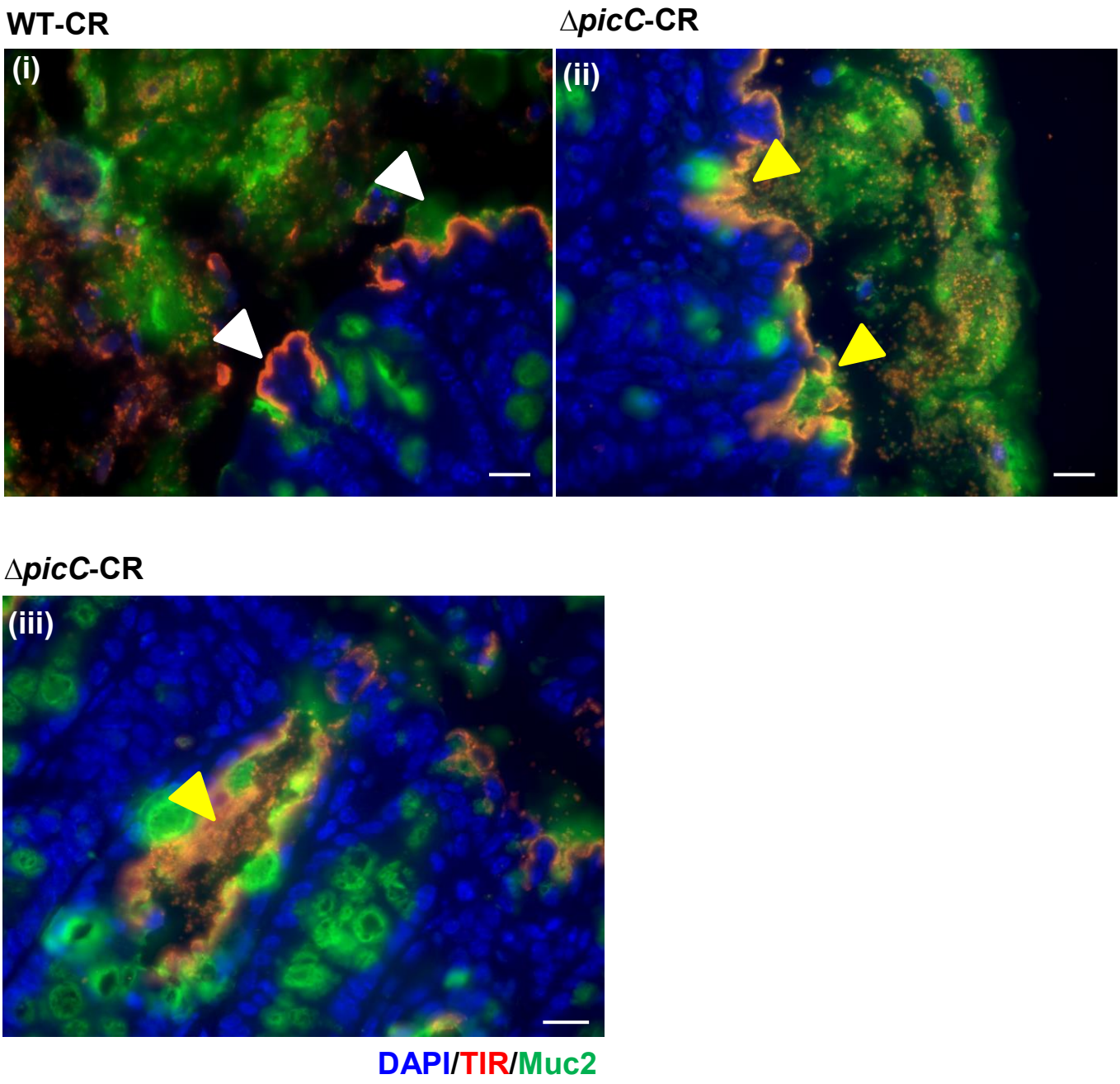

Figure 4.12 Δ*picC C. rodentium* form microcolony-like structures *in vivo.*
Representative Muc2/Tir dual staining profile in distal colon. White arrowheads show localization of WT *C. rodentium* mostly on the epithelial surface in a single layer (i). Yellow arrowheads point to clustering of Δ*picC C. rodentium* close to epithelial surface (ii) and within the colonic crypts (iii). Image description/presentation is in clockwise direction from the first image Original magnification 630X. Blue- DAPI counterstain.

To investigate if the Δ*picC C. rodentium* infected mouse tissues might also show abnormal pathogen-commensal interactions, we conducted dual FISH staining on infected tissues. We used a Texas-Red conjugated EUB338 probe that recognizes the majority (99%) of gut bacteria, and an AlexaFluor 488-conjugated GAM42a probe that detects γ-Proteobacteria, which in infected tissues, are almost entirely *C. rodentium*. Consistent with Tir and Tir/Muc2 dual staining, there was patchy distribution of WT *C. rodentium* on the epithelial surface (yellow, EUB338+ GAM42a+) whereas commensal microbes (red, EUB338+ GAM42a -) could be seen in the lumen, distant from the epithelial surface. In contrast, dual FISH staining on Δ*picC C. rodentium* infected tissues revealed multispecies microcolonies comprising commensal (non-*C. rodentium*) bacteria (stained red) mixed with *C. rodentium* (yellow) in close proximity to the mucosal surface (Figure 4.13).

Based on this finding, we assessed commensal microbe numbers in the colons of WT and Δ*picC C. rodentium* infected mice. As previously shown [221], commensal microbes were rapidly depleted from the colon during infection by WT *C. rodentium*. In contrast, this depletion was significantly impaired in mice infected with Δ*picC C. rodentium* (Figure 4.14A), with the increased commensal numbers potentially explaining the increased translocation of commensal microbes seen in these mice (Figure 4.8C). We also noted reduced *C. rodentium* shedding in the stool samples collected from Δ*picC C. rodentium* infected mice, in comparison to WT *C. rodentium* infected mice (Figure 4.14B). Taken together, these results indicate that PicC potentially impacts on bacteria-bacteria interactions, such that in its absence, there is increased aggregation of *C. rodentium* with itself as well as commensal microbes.

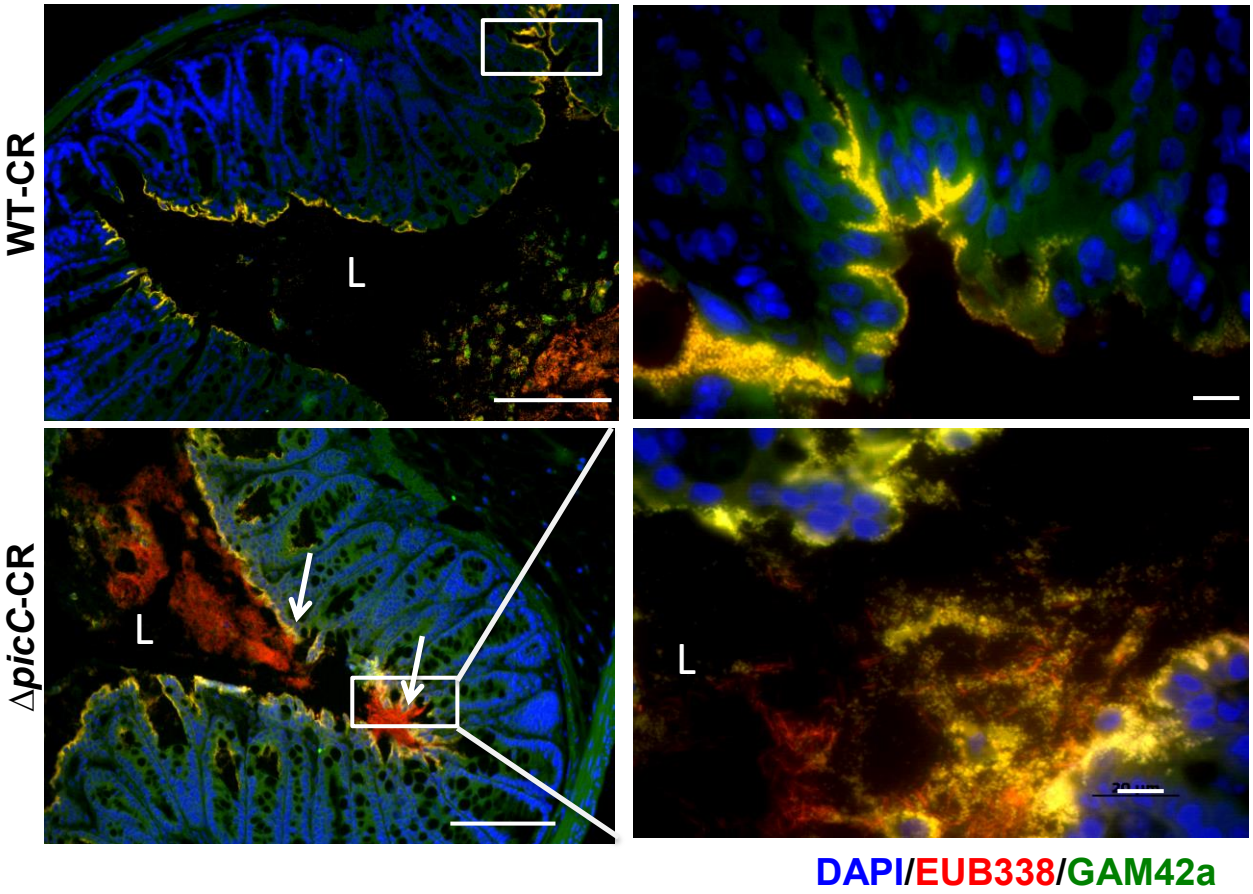

Figure 4.13 Δ*picC C. rodentium* form aggregates with commensal bacteria *in vivo.*
Dual FISH staining in distal colon using EUB338 DNA probe (stains all bacteria red) and GAM42 DNA probe (stains γ-Proteobacteria green, *C. rodentium* belongs to this family). Yellow-*C. rodentium*, red- commensals, L- lumen. (Top panel) WT *C. rodentium* (yellow) can be seen on the epithelial surface where majority of commensals (red) can be seen in the intestinal lumen, isolated from the epithelial surface. White boxed region is shown as a magnified image (630X), showing *C. rodentium* interacting with the epithelial surface. (Bottom panel) White arrows point to microcolony-like structures on mucosal surface in Δ*picC C. rodentium* sections, not seen in WT *C. rodentium* sections. Original magnification 200X. Last panel is a magnified image (630X) of white boxed area showing a microcolony intermixed with commensals and Δ*picC C. rodentium.*

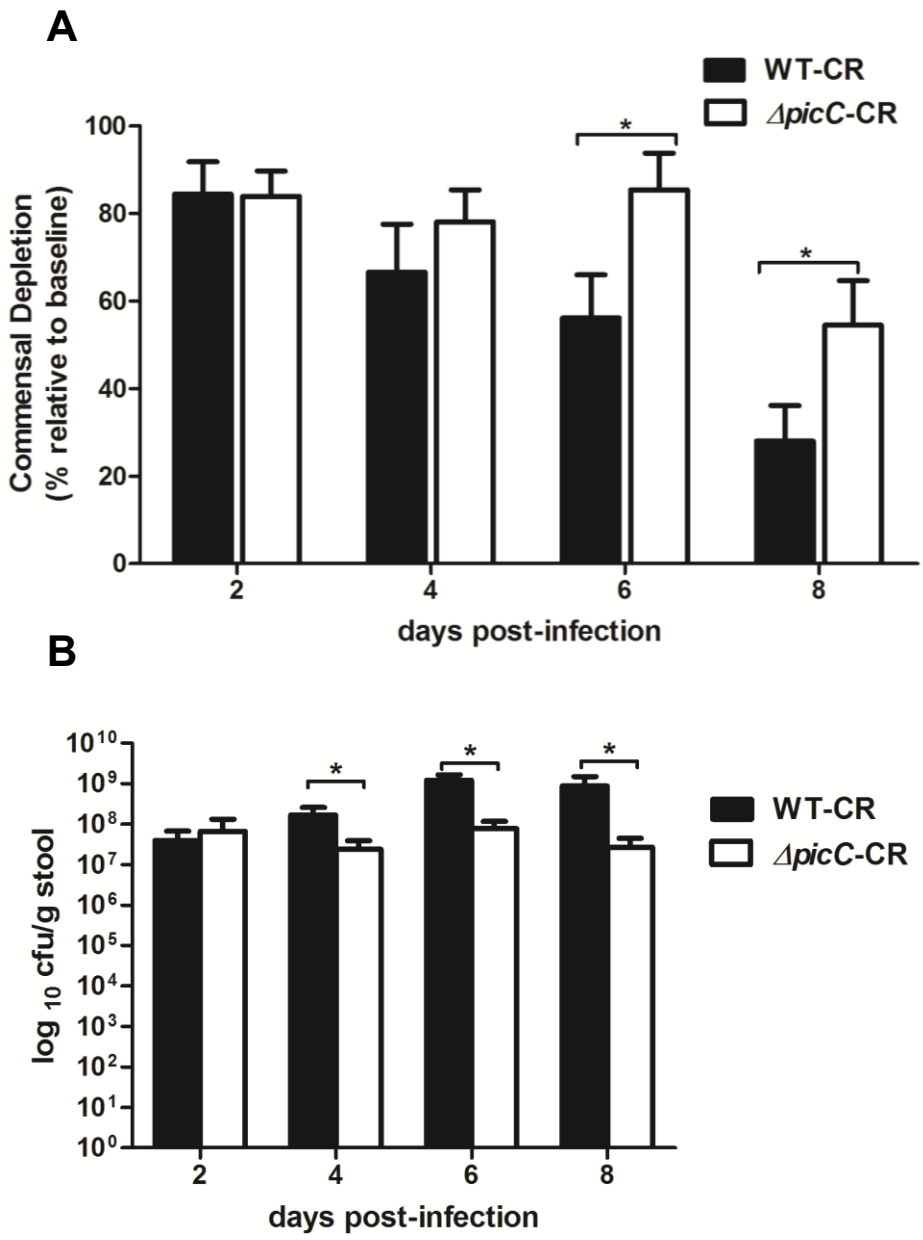

Figure 4.14 Δ*picC C. rodentium* infected mice have greater commensal and pathogen numbers in the colon.
(A) Δ*picC C. rodentium* infected mice are impaired in commensal depletion in comparison to WT *C. rodentium* infected mice Commensal bacteria in stool samples were enumerated using the DAPI DNA staining method. (B) Δ*picC C. rodentium* infected mice show reduced pathogen shedding in stool compared to WT *C. rodentium* infected mice. Stool samples were collected at several time points during the course of the infection and *C. rodentium* burdens were enumerated by plating onto MacConkey Agar. Errors bars= SEM; * $p < 0.05$ by the Mann-Whitney test, 9 mice/group.

4.2.8 Δ*picC C. rodentium* is impaired in transmitting their infection to naïve mice

Interestingly, as previously mentioned, despite their heavier intestinal burdens, mice infected with Δ*picC C. rodentium* showed reduced pathogen numbers in their stool (Figure 4.13B). Speculating that the heightened aggregation seen with Δ*picC C. rodentium* might impact their ability to exit the intestine and spread to new hosts, we next analyzed the ability of Δ*picC C. rodentium* to transmit to new hosts using a strategy previously outlined by Wickham et al[309]. To examine this, transmission experiments were conducted (as described in materials and methods section). Briefly, index mice were orally infected with WT *C. rodentium* or Δ*picC C. rodentium* for 6 days. At day 6, index mice were added to a cage containing naïve (uninfected) mice and were co-housed for 2 days prior to euthanization (Figure 4.15A). Transmission was defined as the % of naïve mice that were infected/colonized upon exposure to infected index mice. Interestingly, we noted that Δ*picC C. rodentium's* ability to transmit to new hosts (secondary mice) was much lower than WT *C. rodentium* (~11% versus ~67% respectively) (Figure 4.15B). Furthermore, secondary mice that were colonized by Δ*picC C. rodentium* consistently carried lower pathogen burdens in comparison to mice exposed to WT *C. rodentium* (Figure 4.15C). Examining distal colon colonization, we found that 5 out of 8 naïve (secondary) mice exposed to WT C. *rodentium* infected index mice showed distal colon colonization (~10^6 cfu/g) whereas with only 1 out of 8 secondary mice exposed to a Δ*picC C. rodentium* infected index mouse were colonized. Overall these findings suggested that Δ*picC C. rodentium* is impaired in successfully transmitting to new hosts.

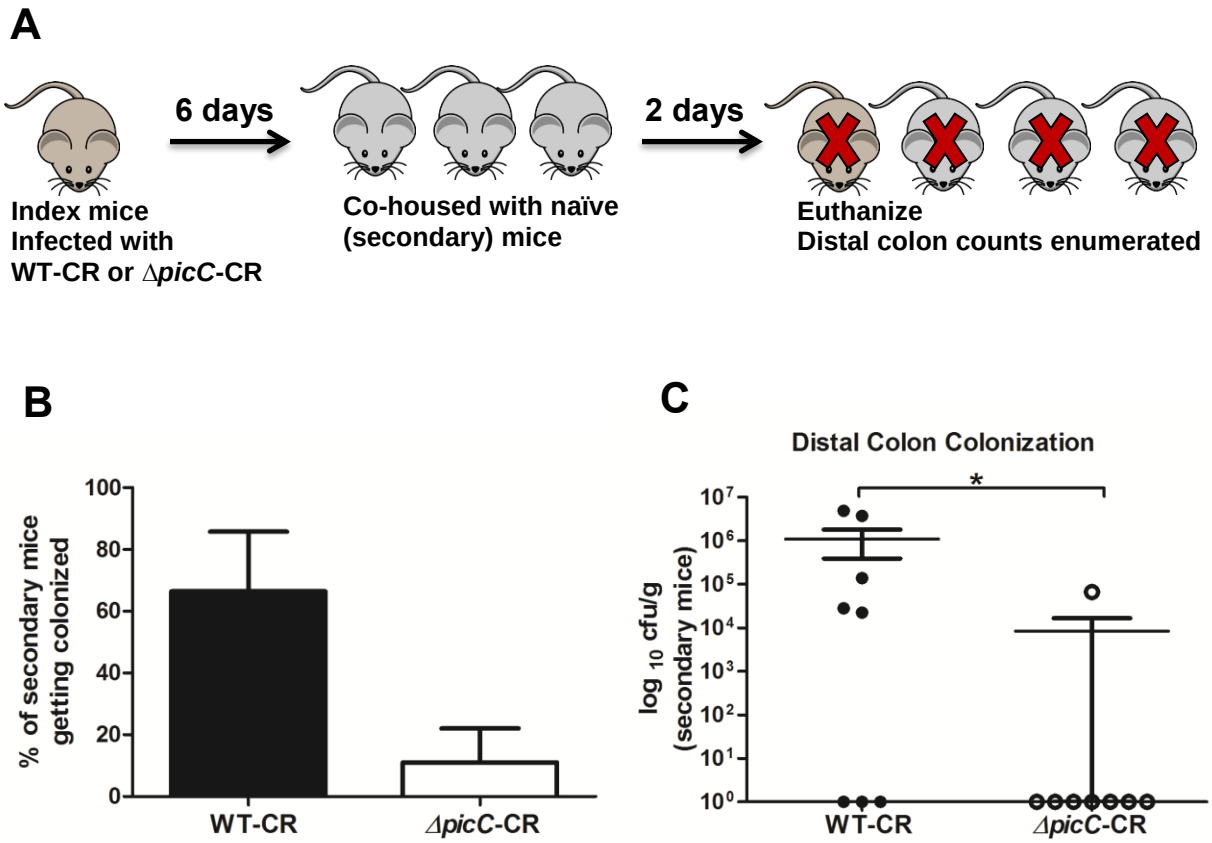

Figure 4.15 Δ*picC C. rodentium* shows reduced transmission to new hosts.
(A) Schematic representation for *C. rodentium* host to host transmission experiments. (B) Bar graph showing % transmission (i.e. % of naïve secondary mice getting colonized from exposure to index mice) infected with WT or Δ*picC C. rodentium.* Δ*picC C. rodentium* displayed reduced transmission to new hosts compared to WT *C. rodentium.* (B) Viable *C. rodentium* (CFU) recovered from distal colon of secondary mice. Note that index mice were mixed with naïve (secondary) mice on day 6 PI and co-housed for 48 hours, after which all mice were euthanized. Results shown are representative of 2 independent infections. Asterisk indicates statistical significance (* $p < 0.05$ by the Mann-Whitney test).

4.2.9 Δ*picC C. rodentium* exhibits a pronounced RDAR morphotype *in vitro*

To further explore the impact of PicC on *C. rodentium* structure and function, we tried growing the *C. rodentium* strains on Congo red plates (LB- agar plates lacking salt but supplemented with congo red dye). This media allows the assessment of bacterial growth under limiting nutrient conditions and the production of what is termed the red, dry and rough (RDAR)

morphotype. This phenotype reflects an aggregative and resistant physiology that has been linked to survival in nutrient-limited environments, and previously shown to indicate the production of extracellular components, such as curli fimbriae and cellulose[310–313]. Notably, the Δ*picC C. rodentium* exhibited a more pronounced RDAR morphotype than the WT strain (Figure 4.16A). While this phenotype is best known and studied outside of hosts, its expression within the gut could explain the aggregative nature of Δ*picC C. rodentium in vivo*. We also examined *in vitro* biofilm formation and cellulose production in WT *C. rodentium* and Δ*picC C. rodentium* and found that Δ*picC C. rodentium* displayed moderate but significantly higher biofilm formation (Crystal violet dye assay) (Figure 4.16B) and cellulose production (as assessed by Congo red binding assay and the calcofluor binding assay) compared to WT *C. rodentium* (Figure 4.16C, 4.16D). While there are other bacterial products, such as curli that could be differentially expressed by Δ*picC C. rodentium* that could explain their aggregative nature, rather than examining each one, we decided to instead focus on the effects such changes might have on the ability of the host's immune system to recognize *C. rodentium.*

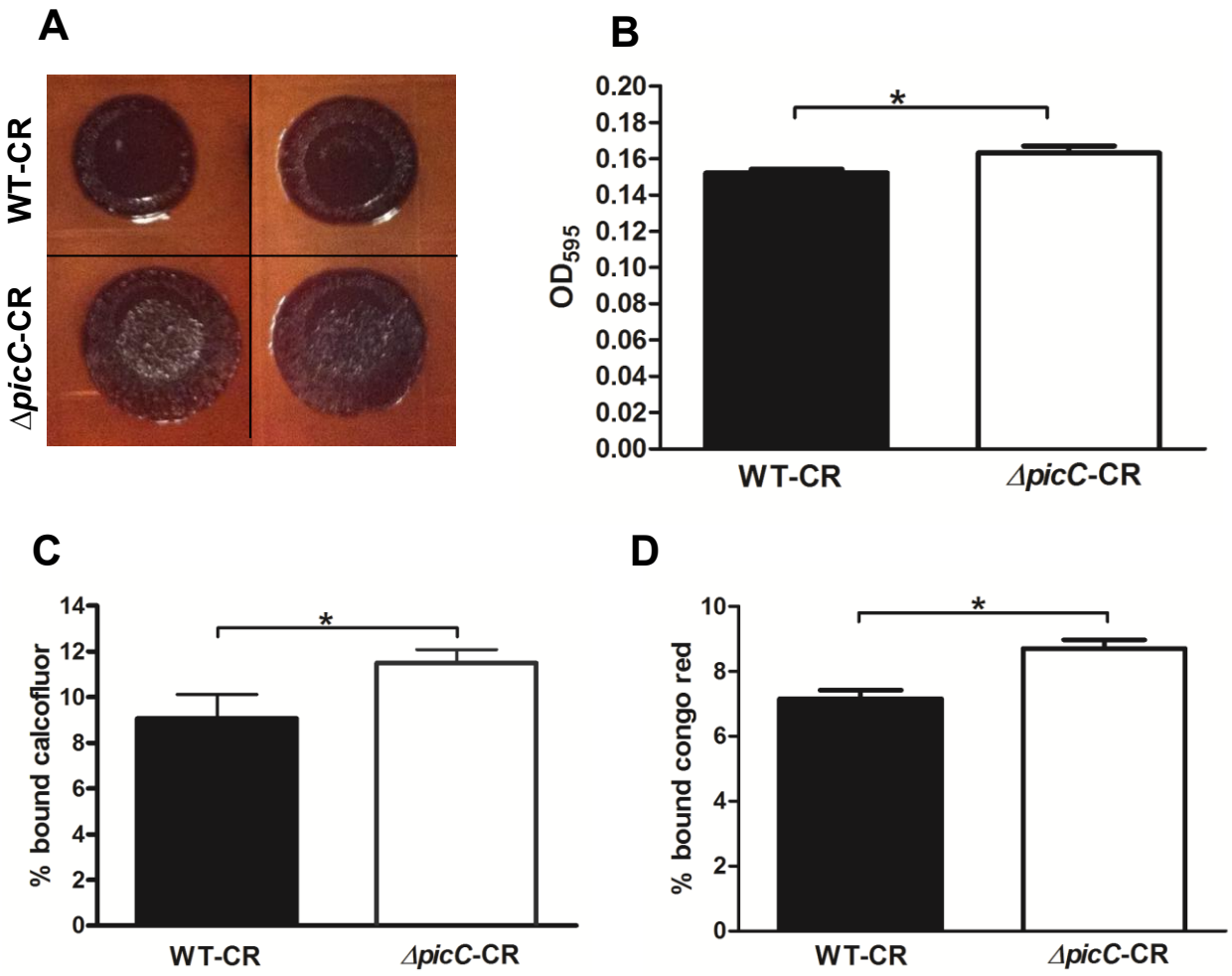

Figure 4.16 Assessing the impact of PicC on *C. rodentium* surface structures.
(A) RDAR colony morphology of WT *C. rodentium* (top) and Δ*picC C. rodentium* (bottom) on Congo red plates incubated at 25 °C for 5 days. Note the differences in colony morphology between WT *C. rodentium* and Δ*picC C. rodentium* and the dry, rough phenotype localized in the central region of Δ*picC C. rodentium* colonies. (B) Biofilm formation in LB (no salt) at 25° C for WT *C. rodentium* vs Δ*picC C. rodentium* as measured using the Crystal violet assay. (C) Cellulose production assessed using the calcofluor assay for WT *C. rodentium* and Δ*picC C. rodentium* at 25° C in LB (no salt). (D) Cellulose production from WT *C. rodentium* and Δ*picC C. rodentium* at 25° C in LB (no salt), as assessed using the Congo red binding assay. Asterisks indicate statistical significance (* $p < 0.05$ by the Mann-Whitney test).

4.2.10 Δ*picC C. rodentium* induces significantly greater TLR2 activation than WT *C. rodentium*

Based on the aberrant *in vivo* and *in vitro* behaviour of Δ*picC C. rodentium,* and since SPATES have been shown to modulate inflammatory responses, we tested whether the exaggerated inflammatory response elicited against Δ*picC C. rodentium* could reflect an abnormal activation of the host immune system. To investigate this hypothesis, we used HEK293 cell lines expressing either TLR2 or TLR4, as these are the primary innate receptors that recognize *C. rodentium*. These cell lines were then exposed to diluted overnight cultures of WT *C. rodentium* (contains PicC) and *C. rodentium* Δ*picC* (no PicC), and the activation of these TLRs was measured using a SEAP (secreted alkaline phosphatase) reporter assay. Interestingly, we noted that while there was no difference in TLR4 activation by the two strains (Figure 4.17A), TLR2 showed significantly more activation with the Δ*picC C. rodentium* as compared to WT *C. rodentium* (Figure 4.17B). Notably, preincubating an exogenous TLR2 ligand PAM3CSK4 with WT *C. rodentium* and Δ*picC C. rodentium* respectively had no effect on the ligands ability to activate TLR2 signalling (Figure 4.17C). Interestingly the differences in TLR2 activation between WT and Δ*pic C. rodentium* were lost upon lysing the bacteria (Figure 4.17B). Overall, these results suggest that PicC is likely modulating the surface structure of *C. rodentium* in a manner that typically limits TLR2 activation.

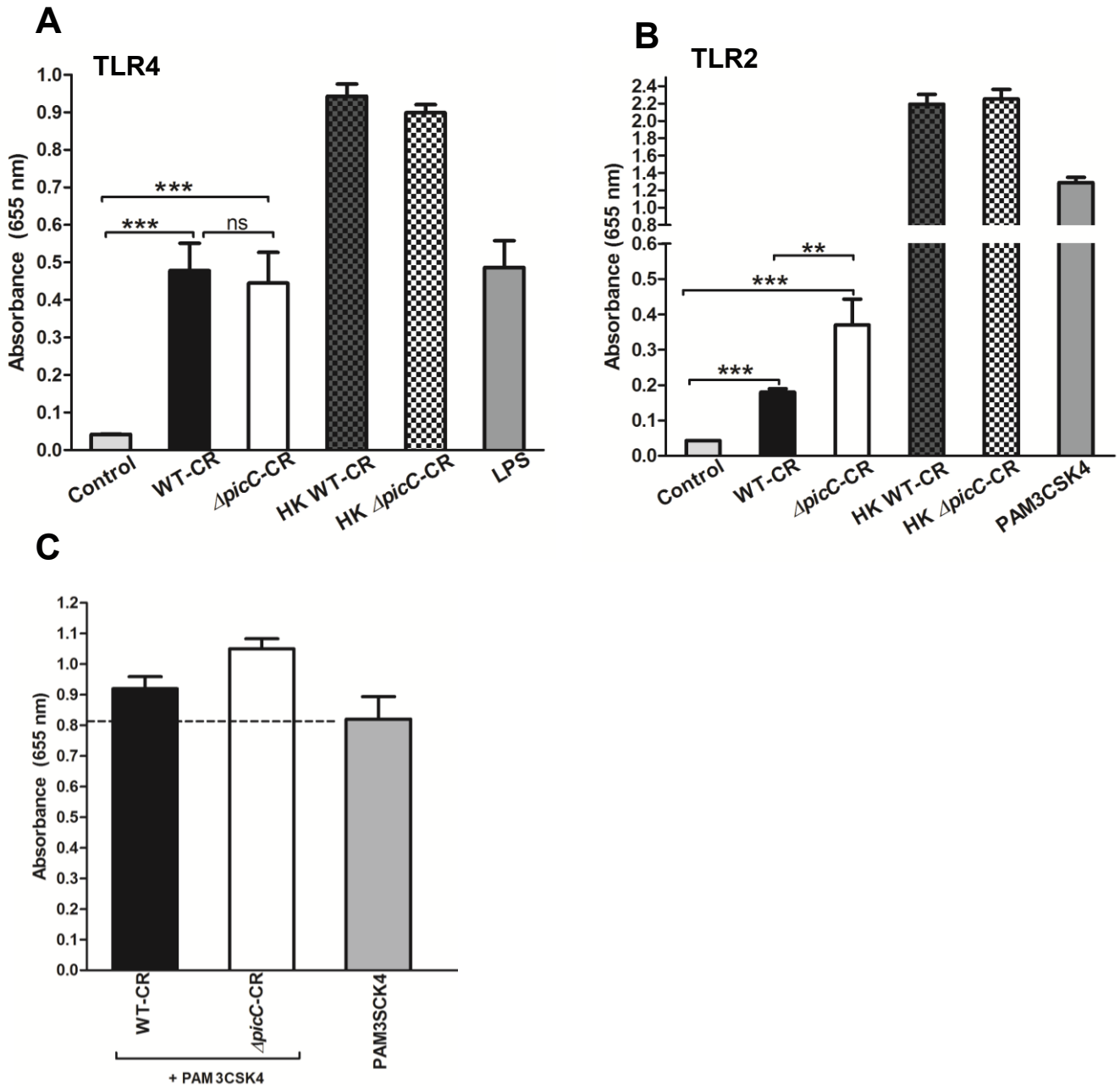

Figure 4.17 PicC plays a role in innate immune recognition through TLR2.
(A) TLR Reporter Assay. (A) HEK-BlueTM hTLR4 (B) HEK-BlueTM hTLR2 (A), were exposed to supernatants from either live or heat-killed (HK) WT *C. rodentium* and Δ*picC C. rodentium* for 4 hours. Δ*picC C. rodentium* significantly increased the stimulation of TLR2 compared to WT *C. rodentium.* Heat-killed (HK) bacteria maxed out the TLR4 and TLR2 stimulation under tested conditions. (C) Preincubation of an exogenous TLR2 ligand PAM3CSK4 with WT *C. rodentium* and Δ*picC C. rodentium* respectively had no effect on the ligands ability to activate TLR2 signalling (i.e. no additive effect was seen on TLR2 activation). Errors bars= SEM; ***, $p< 0.0005$, ** $p < 0.01$ by the Mann-Whitney test; ns- not significant. Values represent the mean of three independent experiments.

4.2.11 The exaggerated colitis caused by Δ*picC C. rodentium* in C57BL/6 mice is largely TLR2 dependent

The higher (*in vitro*) stimulation of TLR2 by Δ*picC C. rodentium* compared to WT *C. rodentium* suggested a potential mechanism by which Δ*picC C. rodentium* could be causing exaggerated colitis. To further investigate this finding *in vivo*, we infected *Tlr2 -/-* mice with WT *C. rodentium* and Δ*picC C. rodentium*, to clarify whether the exaggerated pathology caused by Δ*picC C. rodentium* would be reduced in the absence of TLR2. While *Tlr2-/-* mice have already been shown to be moderately more susceptible to WT *C. rodentium* infection than C57BL/6 mice, the susceptibility tends to exhibit only at later stages of infection. Notably, at 8 DPI we found that Δ*picC C. rodentium* infected *Tlr2 -/-* mice showed similar magnitudes of histological and macroscopic damage as *Tlr2 -/-* mice infected with WT *C. rodentium*. Weight loss and histologic measures of colonic pathology were also similar between WT and Δ*picC C. rodentium* infection (Figure 4.18). Taken together, these findings indicate that the autotransporter PicC impacts *C. rodentium* virulence primarily through its role in controlling innate recognition of *C. rodentium*, rather than its actions as a mucinase.

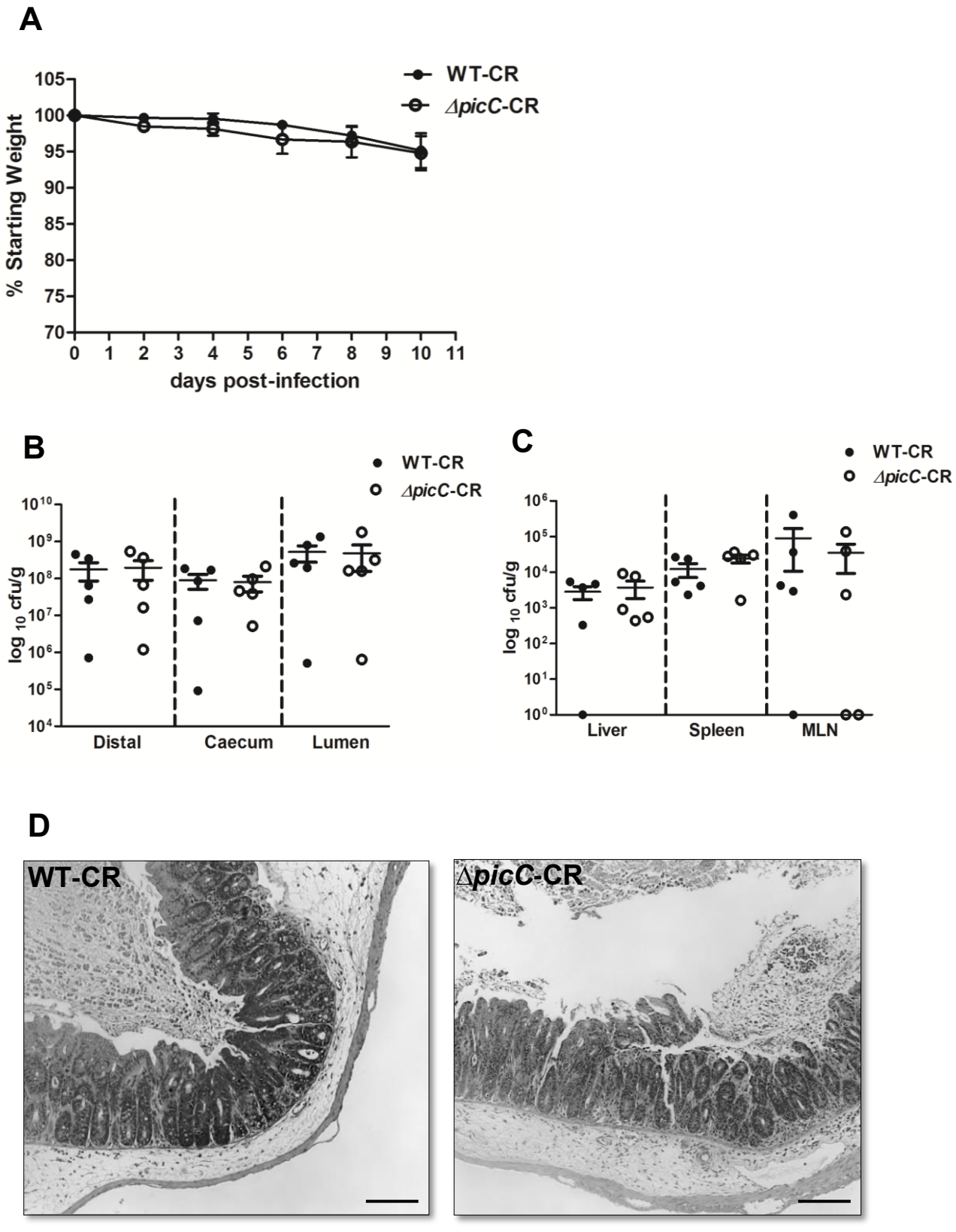
A
WT-CR
ΔpicC-CR
% Starting Weight
105
100
95
90
85
80
75
70
0 1 2 3 4 5 6 7 8 9 10 11
days post-infection
B
WT-CR
ΔpicC-CR
log 10 cfu/g
Distal
Caecum
Lumen
C
WT-CR
ΔpicC-CR
log 10 cfu/g
Liver
Spleen
MLN
D
WT-CR
ΔpicC-CR

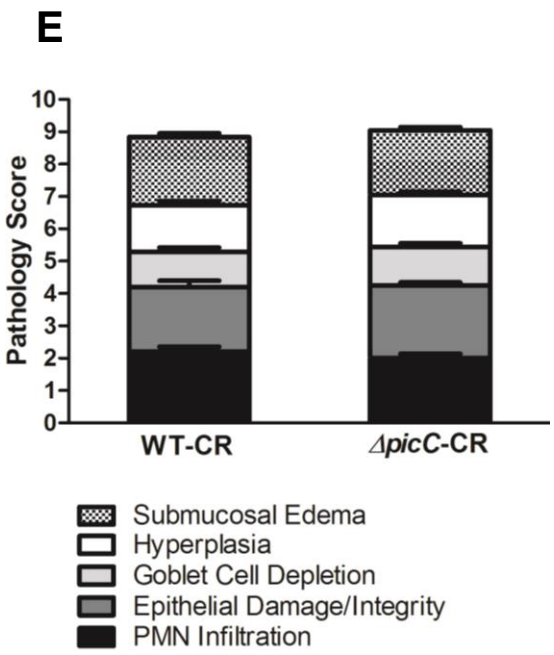

Figure 4.18 Exaggerated colitis caused by Δ*picC C. rodentium* is primarily dependent on TLR2.
(A) Body weights of *Tlr2 -/-* mice infected with WT *C. rodentium* and Δ*picC C. rodentium*, plotted as % of starting body weight. (B) Pathogen burdens enumerated in colonic sites (distal, caecum) and in the lumen of *Tlr2 -/-* mice infected with WT *C. rodentium* and Δ*picC C. rodentium respectively.* (C) Quantification of viable *C. rodentium* recovered from systemic sites of WT *C. rodentium* and Δ*picC C. rodentium* infected *Tlr2 -/-* mice day 8 PI. (D) H&E stained representative images showing histological damage to distal colon of WT *C. rodentium* and Δ*picC C. rodentium* infected *Tlr2 -/-* mice day 8 PI (original magnification 200X). (E) Pathology scores comparing damage to distal colon in *Tlr2 -/-* mice infected with WT *C. rodentium* and Δ*picC C. rodentium* respectively, scored under blinded conditions. Overall, no differences were detected between the 2 groups. Each bar represents an average score of 6 tissues, scored under blinded conditions. Error bars represent SEM and results from 3 independent experiments are pooled.

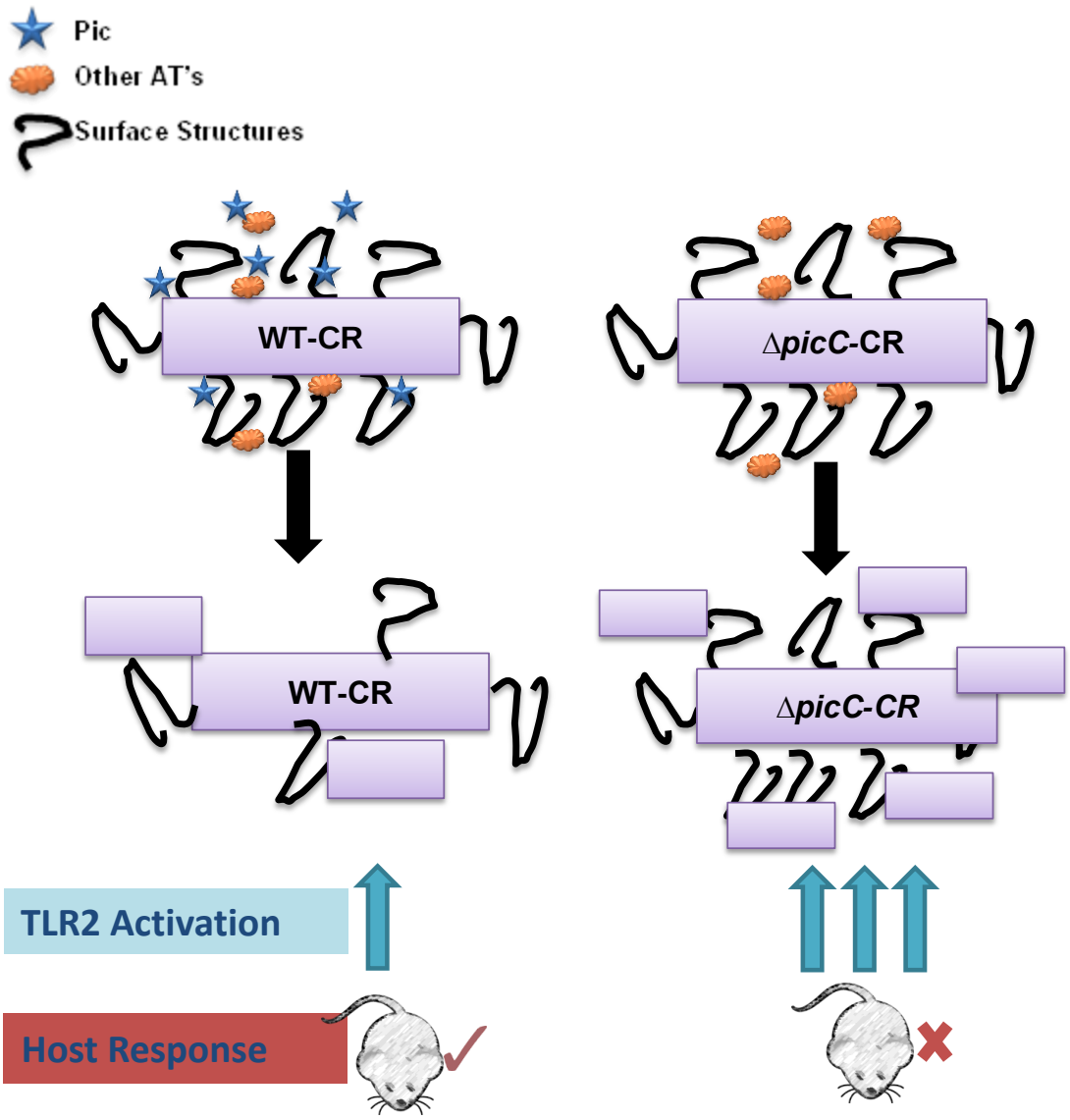

Figure 4.19 Graphic representation suggesting how *C. rodentium* PicC impacts the severity of host responses through modulation of TLR2 activation.
Δ*picC C. rodentium* aggregation *in vivo* may be attributed to PicC's ability to alter bacterial surface structures. Differences in surface structures may ultimately contribute towards differential TLR2 activation by WT *C. rodentium* and Δ*picC C. rodentium*. Increased TLR2 activation results in higher inflammatory responses *in* Δ*picC C. rodentium*, a contributing factor towards increased mortality in Δ*picC C. rodentium* infected mice. Absence of TLR2 (*Tlr2 -/-* mice) ameliorated the pathological differences between the two strains (as shown in Figure 4.17), providing further evidence that *C. rodentium* Pic's ability to modulate virulence can be attributed to its role to modulate innate immune regulation through TLR2 activation.

4.3 Discussion

SPATES are large extracellular proteases secreted by Gram-negative bacteria that have been implicated in bacterial pathogenesis. At present, more than 25 SPATES with phylogenetically diverse functions have been identified. In the last few decades, numerous studies have performed *in vitro* characterization of SPATES secreted by pathogens such as *Shigella*, EPEC, EAEC and UPEC[204,206,259]. While SPATES have been shown to impact bacterial virulence through cytotoxic effects on intestinal epithelial cells (Class 1 SPATES) and immunomodulatory properties (Class 2 SPATES), virtually all these studies have been performed under *in vitro, in situ* or *ex vivo* conditions[244,246,255]. There is now significant interest in understanding how these proteases interact with their hosts, but the lack of appropriate animal models has limited our understanding of how SPATES can modulate bacterial pathogenesis *in vivo*.

C. rodentium is widely used as an *in vivo* model for studying A/E infections and is a natural mouse pathogen. Recently, a study was published reporting 19 putative autotransporters in *C. rodentium*, five of these were SPATES showing close homology to previously reported /characterized SPATES expressed by pathogenic *E. coli* strains[260]. A putative homolog of Pic, a Class 2 SPATE was also reported (ROD_p1411, YP_003368482.1), confirming our bioinformatics analysis. Pic, a Class 2 SPATE has been shown to target extracellular factors that include glycoproteins in the mucus layer and leukocyte surface glycoproteins involved in diverse immune functions, suggesting that Class 2 SPATES, such as Pic are bacterial virulence factors with immunomodulatory properties[257,258].

Our initial interest in studying PicC was in regards to its predicted mucinolytic activity. Previous studies have shown that *C. rodentium* can bind to intestinal mucins, potentially as an

early step in its colonization of host intestines[190]. While it is clear that *C. rodentium* is able to cross the mucus layer to reach and infect the underlying intestinal epithelium, we previously showed that the presence of the mucin Muc2, the main constituent of the intestinal mucus significantly delayed the rate at which *C. rodentium* reached and infected the intestinal epithelium. Moreover, *Muc2 -/-* mice were highly susceptible to *C. rodentium* infection, carrying higher pathogen burdens, and suffering exaggerated intestinal pathology and epithelial barrier damage[144]. Thus Muc2 is a protective host barrier that *C. rodentium* must overcome; however little is known about how this and other bacterial pathogens accomplish this task. While motile microbes like *Salmonell*a[243] and *Campylobacter* species[314] likely swim through mucus to reach the epithelium, non-motile pathogens such as *Shigella* and *C. rodentium* potentially use proteases to degrade the mucus layer[121].

We demonstrated that WT *C. rodentium* is able to cleave bovine submaxillary mucin whereas loss of PicC significantly reduced this ability. In order to determine the role of PicC in *C. rodentium* pathogenesis, we infected C57BL/6 mice with WT and Δ*picC C. rodentium*. Surprisingly, the Δ*picC C. rodentium* was far more virulent than WT, heavily colonizing the host's intestine and causing exaggerated inflammation and tissue damage that often required early euthanization of infected mice. These results indicate that *C. rodentium* does not require PicC to colonize, suggesting that either other proteases can compensate in the absence of PicC to degrade the intestinal mucus barrier, or that *C. rodentium* is able to colonize without overtly degrading the mucus layer. At present, we cannot rule out either possibility.

Another striking finding was the heavier pathogen burdens seen in the Δ*picC C. rodentium* infected mice. Notably, these mice only showed increased tissue adherent pathogen burdens, with the luminal burdens similar to WT levels. Upon further investigation, it was found

that the tissue adherent burdens reflected aggregates of Δ*picC C. rodentium* on the epithelial surface as well as in the overlying mucus layer and deep in colonic crypts. While showing no overt defect in infecting the intestinal epithelium, the aggregation of Δ*picC C. rodentium* appeared to impair the pathogen's ability to leave the mucus layer and reach the lumen. Moreover, Δ*picC C. rodentium* showed a severe impairment in its ability to transmit from an infected host to new hosts, suggesting PicC plays an important role in pathogen transmission/shedding. An increased propensity of Δ*picC C. rodentium* to aggregate *in vivo* may be linked to its *in vitro* ability to produce the RDAR morphotype. As previously suggested, the RDAR phenotype represents an aggregative state due in part to the production of extracellular matrix components such as curli and cellulose[310,311,313]. Δ*picC C. rodentium's* RDAR morphotype (potentially linked to its ability to produce higher levels of cellulose and a modest increase in its ability to form biofilms *in vitro*) may be analogous to the pathogen's ability to form *in vivo* microcolony-like structures associated with the intestinal mucus layer, thereby decreasing the ability of pathogen to shed into the lumen. It should be noted however that our current understanding of the RDAR morphotype is far from complete, and almost nothing is known about how it may be expressed in an *in vivo* situation.

While the exaggerated colitis suffered during Δ*picC C. rodentium* infection may in part reflect their heavier pathogen burdens, the dramatic weight loss and high mortality rates suffered by infected mice suggested other factors might be at play. In previous studies, using *in vitro* reporter assays, we showed that like other Gram-negative bacteria, *C. rodentium* predominantly activates TLR2 and TLR4. These findings were supported by *in vivo* studies, where TLR4 signalling was highly pro-colitic during *C. rodentium* infection[218], whereas TLR2 signalling drove both pro-inflammatory as well as tissue protective effects, including promoting

expression of the cytokine IL-6[217]. Notably, we found that Δ*picC C. rodentium* hyper-stimulates the innate receptor TLR2, but induces normal activation of TLR4. Moreover, the ability of *ΔpicC C. rodentium* to cause greater damage than wild-type *C. rodentium* was lost in the TLR2 deficient mice, suggesting that TLR2 signalling plays a role in regulating the pathology seen during *ΔpicC C. rodentium* infection. In fact, it is possible that exaggerated TLR2 activation may play a role in limiting the survival of *ΔpicC C. rodentium* within the lumens of infected C57BL/6 mice.

This finding could suggest that PicC directly or indirectly helps *C. rodentium* evade the host immune system. In fact, we recently used a novel mouse model of *Campylobacter jejuni* infection to show that the capsule that surrounds this pathogen played an important role in limiting the innate recognition of *C. jejuni*, potentially as a means to evade host inflammatory/anti-microbial responses. While the *ΔkpsM* (capsule) mutant strain also triggered exaggerated gut inflammation, it stimulated both TLR2 and TLR4 reporter cell lines to a significantly higher degree than the wild-type 81–176 strain, since LPS as well as lipoproteins and other TLR2 ligands were more exposed[315]. Since Δ*picC C. rodentium* only shows enhanced activation of TLR2, this might instead suggest the Δ*picC* mutant shows increased expression of TLR2 ligands. Interestingly, the RDAR morphotype is associated with increased expression of curli and cellulose, and bacterial curli have been shown to activate TLR2[66,316–318]. While it remains unclear how loss of PicC promotes the RDAR phenotype, secreted SPATES like EspP and EspC have been reported to be associated with macroscopic-rope like structures (extracellular matrix) that promote aggregative phenotypes[319]. Furthermore, a genome-wide transposon mutagenesis study revealed a link between EspP and biofilm formation[320]. Taken together, these studies suggest an intriguing link between the ability of secreted SPATES to

interact with components of extracellular matrix and the ability of the microbes secreting them to aggregate. We speculate that loss of PicC may affect the surface structure of *C. rodentium* through direct interactions with bacterial extracellular components (e.g. curli fibrils, cellulose) or indirectly by affecting other autotransporters that are directly involved in bacterial aggregation. Our findings thus indicate a previously unsuspected role for Class 2 SPATES like Pic in affecting host immune responses by altering bacterial surface structures, and modulating TLR2 activation. Ascertaining a definitive link between SPATES and the surface structure of bacteria in the future will however require significant in-depth investigation.

It is notable that several Class 2 SPATES (Pic, Tsh/Hbp) have been described to have immunomodulatory properties due to their ability to cleave broad range of human leukocyte O-linked glycoproteins. Pic homologs from *Shigella*, UPEC and EAEC have also been hypothesized to suppress inflammation through the cleavage of leukocyte surface signalling glycoproteins[257,258]. However, these studies have only been performed *in vitro,* limiting our understanding of whether these actions occur *in vivo*. Interestingly, a recent study examined the role of a Class 1 SPATE in *C. rodentium*[261], finding that *Δcrc1 C. rodentium* infection led to a hyper-inflammatory phenotype, similar to what we noted with *ΔpicC C. rodentium*. Unfortunately the basis for the exaggerated inflammatory response elicited against *Δcrc1 C. rodentium* was not defined, but it is tempting to speculate that different SPATES may play common roles in regulating host recognition of the microbes that produce them, perhaps by controlling their surface structures.

Taken together, it appears that PicC ultimately modulates both the function of *C. rodentium* as well as its ability to activate the host's immune system in ways that benefit the pathogen and its host. For *C. rodentium* infection, it has been previously shown that virulence is

positively selected by successful transmission to new hosts (fecal-oral route transmission)[309]. During Δ*picC C. rodentium* infection, increased host mortality, as well as reduced transmission to new hosts confer significant disadvantages to this pathogen. From an evolutionary perspective, host to host transmission of an enteric pathogen ensures its successful propagation. This suggests that Pic is potentially acting as an "anti-virulence" factor, modulating *C. rodentium*'s morphotype so that it does not aggregate or hyper-stimulate the host immune system. These results shed light on novel functions of SPATEs during enteric infections. Moreover, the lack of a distinct impairment in Δ*picC C. rodentium's* ability to colonize the mouse intestine suggests either that *C. rodentium* uses other mucinases to cross the mucus barrier, or that this pathogen uses other as yet undiscovered mechanisms to cross the intestinal mucus barrier.

Chapter 5: Investigating the role of core O-derived glycosylation(s) of Muc2, as well as intestinal fucosylation during *C. rodentium* infection

5.1 Introduction

As previously discussed, type O-glycans are the major component of the mucin, Muc2 which forms the protective gel-like intestinal mucus layer. Absence of the mucin Muc2 has been shown to increase host susceptibility to enteric pathogens such as *C. rodentium* and *S.* Typhimurium[144,145]. However, little is known about the functional significance of different forms of Muc2 glycosylation. It is well documented that the status of Muc2 glycosylation varies between healthy and diseased states and there are notable changes in the terminal modifications of Muc2 glycans commonly observed in intestinal diseases[130,321]. Increased amounts of smaller glycans, reduction in complex glycan structures, decreased sulfation and the increased presence of sialyl-Tn antigen are some of the glycan alterations implicated in intestinal inflammatory disorders such as ulcerative colitis[130,157,184,322,323]. Core 1 derived O-glycans and core 3 derived O-glycans are the major O- glycans found on the mouse Muc2 protein and they are likely candidates for studying the role of protein glycosylation in the pathogenesis of intestinal disorders such as IBD. Recent studies have shown the important role played by mucin-derived O-glycans (specifically core 1 and core 3) in promoting intestinal mucus barrier function[152]. Lack of core 1 derived O- glycans resulted in a dramatic thinning of the intestinal mucus layer, correlated with defective mucosal barrier function, increased translocation of bacteria into the intestinal tissues and development of spontaneous colitis[324]. Similarly, lack of core 3 derived O-glycans resulted in increased susceptibility to experimental colitis (DSS) and impaired mucosal barrier integrity[140].

While core 1 and core 3 glycosylation have the greatest impact in terms of overall changes to protein structure, the terminal changes in glycosylation may also have large effects on Muc2 function. Post-translational modifications of intestinal glycans are important for

controlling the maturity and stability of the mucin molecules and protecting mucins from enzymatic degradation[122,158]. Furthermore, terminal sulfated and fucosylated carbohydrate moieties are found to be associated with murine Muc2 mucin and contribute towards the protective function of the Muc2 mucin as studies have revealed that reductions in mucin sulfation and fucosylation are implicated in increased susceptibility to colitis[154,160,325].

Recent studies have also examined the role of intestinal fucosylation in promoting host defense during systemic exposure of TLRs to LPS as well as the role of intestinal fucose, a sugar found abundantly in the gut[326], in modulating enteric pathogen virulence and metabolic gene transcription[161,167,173,327,328]. It is important to note that while the intestinal mucus layer is the primary site for the presence of fucosylated glycans, fucosylated glycoconjugates can also be associated with epithelial surface structures (glycolipids) and ABO blood antigens[159].

Since Muc2 is a heavily O-glycosylated glycoprotein, we sought to test whether the critical role it plays in host defense against enteric pathogens reflected the actions of the Muc2 protein itself, or instead some aspects of its glycosylation. We also conducted preliminary studies examining the role of terminal branch modification of the Muc2 mucin, fucose in affecting *C. rodentium* virulence *in vitro* and *in vivo*. To better define the role of these glycosylations during A/E bacterial infection, WT, *C3GnT -/-* (lacking core 3 β1,3-N-acetylglucosaminyltransferase C3GnT, an enzyme predicted to be important in the synthesis of core 3 derived O-glycans) and IEC (intestinal epithelial cell specific KO) *C1galt1 -/-* mice (lacking core 1 β1,3-galactosyltransferase C1galt1, an important enzyme for core1 derived structures) were infected with *C. rodentium* and monitored over the course of infection. We found that IEC *C1galt1 -/-* mice were dramatically more susceptible to *C. rodentium* infection as compared to *C3GnT -/-* and WT mice as measured by weight loss and signs of morbidity

(hunched posture, inactivity, blood in the stool, diarrhea) and required euthanization by day 6 PI. IEC *C1galt1 -/-* carried significantly higher pathogen burdens in their colon, caecum, lumen and also showed greater translocation to systemic sites (liver, spleen, MLN), whereas *C3GnT -/-* mice had similar levels of pathogen colonization to that seen in WT mice. IEC *C1galt1 -/-* showed impaired barrier integrity (as measured by higher FITC- Dextran reading in the serum) compared to *C3GnT -/-* and B6 mice and suffered from greater histopathological and macroscopic damage. Interestingly, *C3GnT -/-* and WT mice displayed comparable levels of damage to mucosal integrity and histopathologic scores. Overall, these preliminary data suggests an important role for core 1 derived O-glycans in host defense against A/E pathogens.

Our preliminary findings also suggest that *C. rodentium* infection results in upregulation of intestinal fucosyltransferases, fut1 and fut2, potentially as a means to promote host defense against *C. rodentium* infection. Causing an inability of *C. rodentium* to sense fucose (Δ*fucK*) was shown to affect the localization and virulence of this mouse pathogen. Fucose was also found to inhibit *C. rodentium* biofilm formation (*in vitro*) as well as its aggregation in *C1galt1 -/-* mice *in vivo*. The exact mechanisms underlying the role of intestinal fucose/fucosylation in *C. rodentium* pathogenesis have yet to be fully elucidated but preliminary results provide a promising direction to assess the molecular interactions between mucin glycosylation pathways, terminal sugars, intestinal microbiota and enteric pathogens.

5.2 Results

5.2.1 *C1galt1 -/-* mice display heightened susceptibility to *C. rodentium* infection

To assess the role of core 1 versus core 3 glycosylation during *C. rodentium* infection, we first infected WT, *C3GnT -/-* and *C1galt1 -/-* mice with *C. rodentium* and monitored their body weights over a 2 week infection period. While WT and *C3GnT -/-* mice did not show any significant body weight loss, *C1galt1 -/-* mice displayed dramatic susceptibility to *C. rodentium* infection. *C1galt1 -/-* mice developed steady weight loss over the course of infection and by day 6 PI, had lost ~15-20% of their initial/starting body weight and were euthanized (Figure 5.1A). At this point, *C1galt1 -/-* mice displayed clinical signs of morbidity such as hunched posture, piloerection and inactivity. Since *C1galt1 -/-* developed such severe disease by day 6 PI, further studies focused on characterization at day 6 PI.

To investigate the basis for their increased susceptibility, we measured *C. rodentium* burdens via bioluminescent imaging of live mice using a luciferase-expressing *C. rodentium* at day 6 PI. We noted that *C1galt1 -/-* mice displayed stronger signal intensity in their lower GI tract, in comparison to *C3GnT -/-* and WT mice respectively, indicative of significantly greater pathogen burdens at the indicated sites (Figure 5.1B). To validate these findings, we enumerated *C. rodentium* burdens in the stool samples of these mice over the course of *C. rodentium* infection. While there were no significant differences in *C. rodentium* burdens between WT and *C3GnT -/-* mice, *C1galt1 -/-* mice showed significantly greater pathogen burdens (10-100 fold greater) starting at day 2 and this trend was maintained at day 4 and day 6 PI (Figure 5.1C). Overall, these findings suggested that *C1galt1 -/-* mice were highly susceptible to *C. rodentium* infection and were colonized with (as well as shedding) *C. rodentium* at much higher levels during infection.

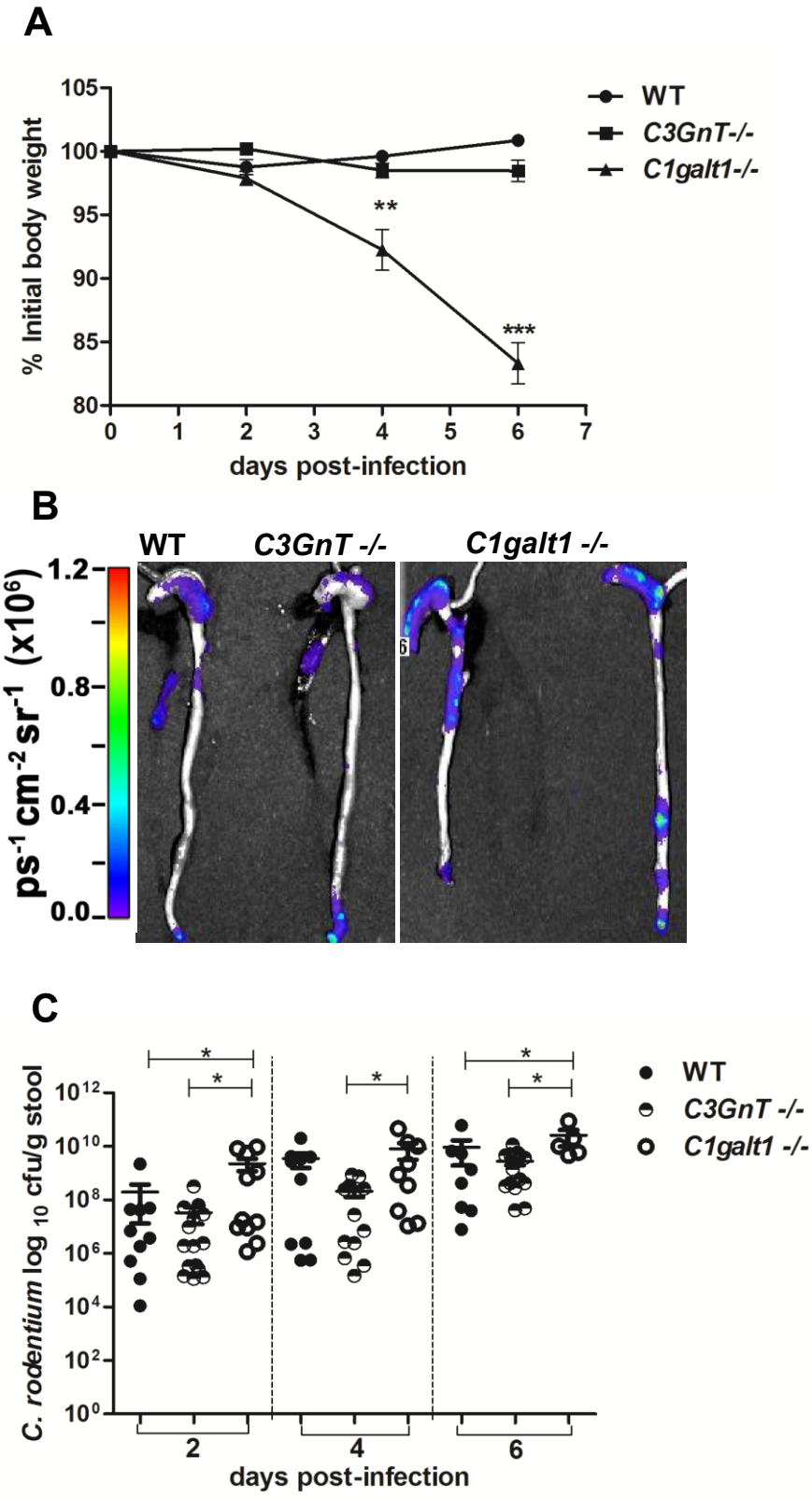
A
% Initial body weight
105
100
95
90
85
80
0
1
2
3
4
5
6
7
days post-infection
**
***
WT
C3GnT-/-
C1galt1-/-
B
WT
C3GnT -/-
C1galt1 -/-
ps-1 cm-2 sr-1 (x10^6)
1.2
0.8
0.4
0.0
C
C. rodentium log 10 cfu/g stool
10^12
10^10
10^8
10^6
10^4
10^2
10^0
2
4
6
days post-infection
*
WT
C3GnT -/-
C1galt1 -/-

Figure 5.1 *C1galt1-/-* mice display higher susceptibility to *C. rodentium* infection.
(A) Weight loss of WT, *C3GnT -/-* and *C1galt1 -/-* mice, plotted as % of the initial body weight during *C. rodentium* infection. While WT and *C3GnT -/-* mice did not display any significant weight loss, *C1galt1 -/-* mice exhibited rapid weight loss, starting at day 2 PI and losing15-20% of their starting body weight by day 6 PI. (B) Bioluminescent imaging showing *C. rodentium* localization in WT, *C3GnT -/-* and *C1galt1 -/-* mice on day 6 PI, performed using a luciferase-expressing *C. rodentium* construct. *C1galt 1-/-* displayed greater signal intensity in the caecum and the colon. The color bar represents the signal intensity, red corresponding to the highest color intensity and blue to the lowest signal intensity. (C) Enumeration of *C. rodentium* burdens shed in the stool samples. *C1galt1 -/-* mice displayed significantly greater *C. rodentium* burdens at day 2, day 4 and day 6, as compared to WT and *C3GnT -/-* mice. There were no differences noted between WT and *C3GnT -/-* mice. Results are representative of 3 independent infections (n=9 for each group). Error bars represent SEM, and asterisks indicate significant differences (**, $P < 0.01$, ***, $P < 0.0005$) by the Mann-Whitney test.

5.2.2 *C1galt1 -/-* mice carry greater *C. rodentium* intestinal and systemic burdens

Considering that increased susceptibility of *C1galt1 -/-* mice to *C. rodentium* may be attributed to increased *C. rodentium* burdens at specific sites within these mice, we next enumerated *C. rodentium* burdens within the GI tract, and at systemic sites. *C1galt1 -/-* mice had significantly greater pathogen loads (10-100 fold higher) at all intestinal sites (caecum, distal, mid and proximal colon), with these microbes considered to be adherent (or directly infecting the underlying epithelium). Luminal burdens, representing non-adherent *C. rodentium* collected from *C1galt1 -/-* mice were also significantly greater as compared to WT and *C3GnT -/-* mice (Figure 5.2A). Interestingly, no differences were found in the number of CFU recovered from intestinal sites and in the luminal contents of the *C3GnT -/-* and WT mice. These findings were consistent with bioluminescent imaging showing the intensity of *C. rodentium* signals between the three groups (Figure 5.1B).

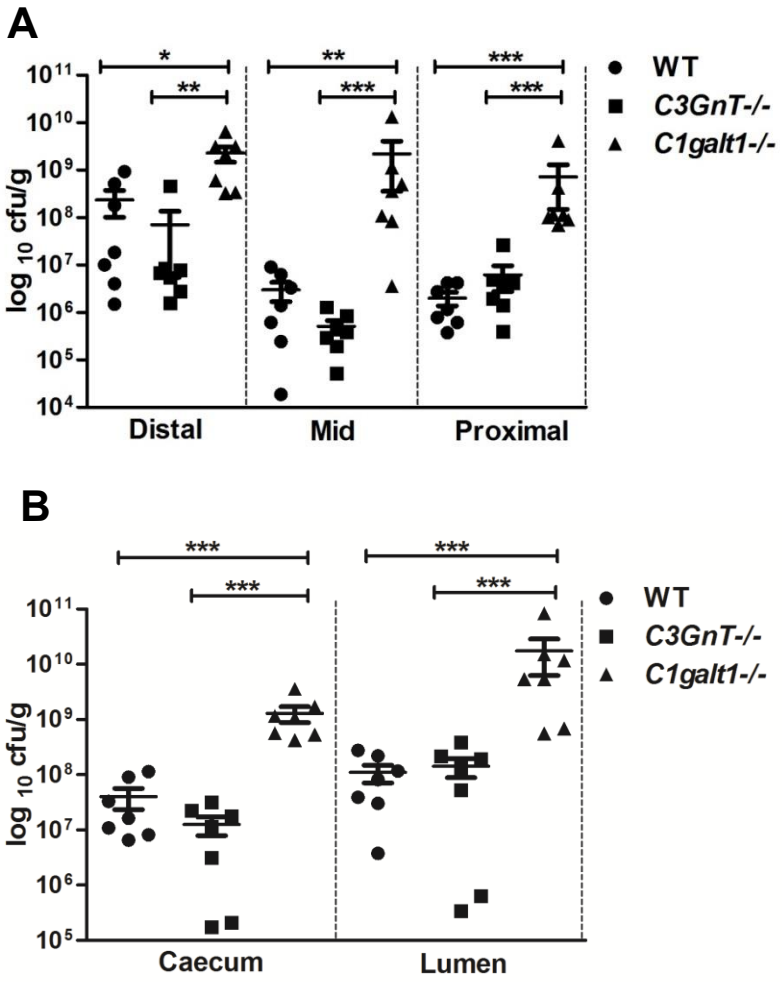

Figure 5.2 *C1galt1 -/-* mice carry heavier intestinal pathogen burdens.
(A) Adherent *C. rodentium* burdens enumerated from the distal, mid and proximal colon at day 6 PI. *C1galt1 -/-* carried significantly higher pathogen burdens than WT and *C3GnT -/-* mice. (B) Adherent *C. rodentium* burdens recovered from the caecum were significantly higher in *C1galt1 -/-* mice. Non-adherent luminal *C. rodentium* were also 100 fold higher in *C1galt1 -/-* mice than WT and *C3GnT -/-* mice. Note that *C3GnT -/-* mice had comparable pathogen burdens to WT mice, with no noticeable/significant differences. Results represent the mean of 3 independent infections (n=7 per group). Errors bar represent SEM and asterisks indicate significant difference (*, $P < 0.05$; **, $P < 0.01$; ***, $P < 0.0005$) by the Mann-Whitney test.

5.2.3 *C1galt1 -/-* mice develop exaggerated tissue damage and colitis during *C. rodentium* infection

Consistent with their increased pathogen burdens, *C1galt1 -/-* mice showed greater macroscopic intestinal damage, characterized by shrunken ceca, thickening of the descending (distal) colon, absence of solid stool contents throughout their large intestine and shortened colon lengths. Focal ulcerations were also noted in the caecum of at least 50% of the *C. rodentium* infected *C1galt1 -/-* mice. No such phenotype was observed in WT mice infected with *C. rodentium*. While *C3GnT -/-* mice also displayed signs of *C. rodentium* infection (pus filled cecal tip), there were no overt differences when compared to WT mice (Figure 5.3A).

To further examine the extent of this damage and assess the severity of colitis, H&E stained tissues (distal and cecum) were examined for pathology (Figure 5.3B). *C1galt1 -/-* mice suffered from exaggerated damage to the cecal tissues, characterized by edema, increased PMN infiltration, excessive damage to epithelial integrity, including ruffling of the epithelial surface and disruption of crypt organization and architecture, mucosal hyperplasia (increased colonic crypt heights) and goblet cell depletion, with overall scores averaging 13.2 ± 1.0. Similar features were also seen in the distal colons of *C1galt1 -/-* mice (average score of 10.5 ± 0.3). While WT mice suffered minimal damage in the caecum (scores averaging 5.9 ± 1.1), *C3GnT -/-* mice showed diffuse damage to the mucosal surface, submucosal edema and PMN infiltration, displaying an intermediate phenotype (average score of 10.7 ± 1.0), whereas there were no differences seen in the distal colon of the two groups and they were scored similarly (6.6± 1.2, 6.5 ± 0.7 respectively) (Figure 5.3C). Since *C. rodentium* infection is most prominent in the distal colon, the rest of the study focused on characterizing differences in the distal colon of *C. rodentium* infected WT, *C3GnT -/-* and *C1galt1 -/-* mice.

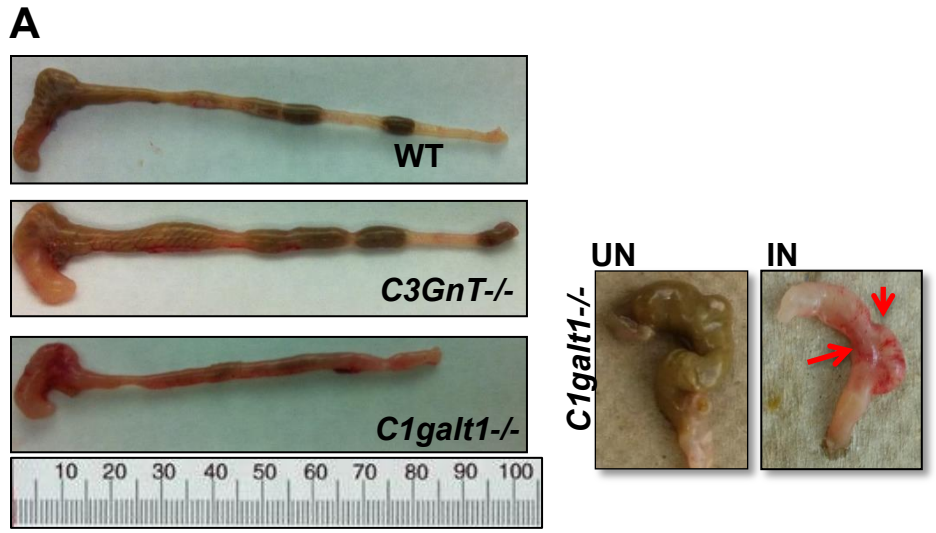
A
WT
C3GnT-/-
C1galt1-/-
10 20 30 40 50 60 70 80 90 100
UN
IN
C1galt1-/-

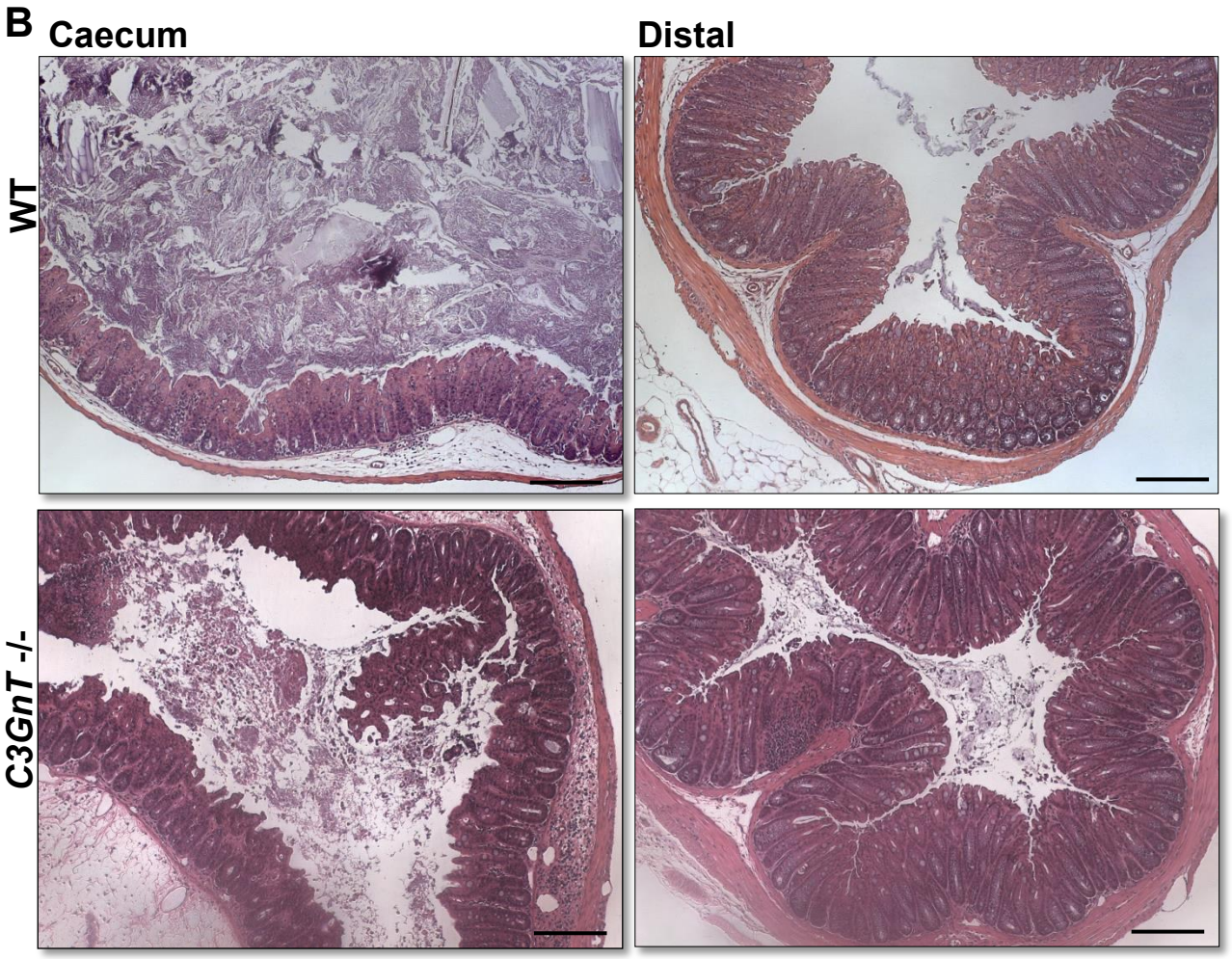
B
Caecum
Distal
WT
C3GnT -/-

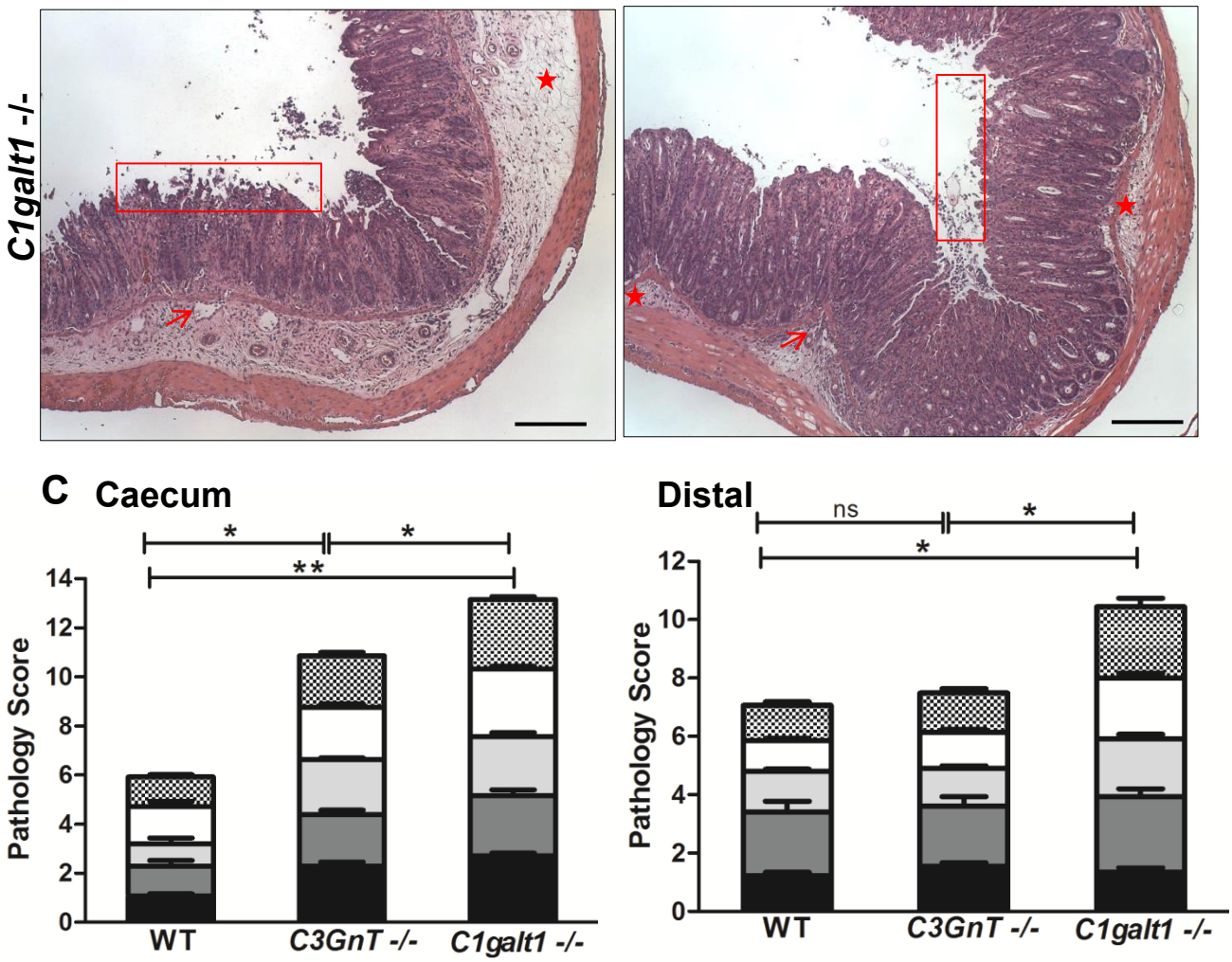

Figure 5.3 *C1galt1 -/-* mice suffer more severe colitis during *C. rodentium* infection.
(A) Macroscopic images of large intestines harvested from WT, *C3GnT -/-* and *C1galt1 -/-* mice on day 6 post *C. rodentium* infection. Note the shrunken ceca, and shortening in the length of the colon, devoid of solid contents in *C1galt 1 -/-* mice, in comparison to other 2 groups. Focal ulceration is shown (right panel) where red arrows point to the ulcers noted in the cecum of *C1galt1 -/-* mice.(B) Representative H&E stained cecal and distal tissues (original magnification 100x, scale bar 50 µm) of *C. rodentium* infected WT, *C3GnT -/-* and *C1galt 1 -/-* mice. *C1galt1 -/-* mice develop exaggerated damage to the mucosal surface. Box highlights damage to epithelial integrity, as seen by ruffling and loss of crypt structure. Arrow points to the immune cell infiltration, whereas asterisks denote edema. (C) Cumulative pathology scores, assessing the tissue damage caused during *C. rodentium* infection. Bars represent the average values for 9 mice per group, pooled from 3 independent experiments. The asterisk indicates a significant difference (**, $P < 0.01$, *, $P < 0.05$) by the Mann-Whitney test (ns- not significant).

5.2.4 *C1galt1 -/-* mice suffer heightened barrier disruption and hyper-proliferative epithelial response during *C. rodentium* infection

Due to the heightened mucosal damage caused by *C. rodentium* infection in *C1galt1 -/-* mice, we next investigated if the intestinal mucosal barrier was impaired in *C1galt1 -/-* mice and whether infection induced barrier disruption and bacterial translocation to systemic sites contributed to the increased susceptibility of *C1galt1 -/-* mice to *C. rodentium.* We assayed epithelial barrier function using the oral FITC-Dextran assay. Briefly, mice were orally gavaged with FITC Dextran at day 6 PI and 4 hours post-inoculation, serum was collected using cardiac puncture and levels of FD4 translocated into the serum were measured. We found no significant differences in the levels of FITC-dextran translocated into the serum between uninfected WT, *C3GnT -/-* and *C1galt1 -/-* mice (i.e. the baseline levels), while each group of mice showed a significant impairment in mucosal barrier function after *C. rodentium* infection, as noted by increased translocation of FD4 from the gut lumen into the serum, compared to uninfected controls. However, *C1galt1 -/-* mice showed a dramatic and significant increase in the amount of FD4 in the serum compared to infected WT and *C3GnT -/-* infected mice, suggesting that *C1galt1 -/-* mice developed increased gut barrier permeability during *C. rodentium* infection. Interestingly, *C. rodentium* infection caused a modest, but significant worsening in epithelial barrier function in *C3GnT -/-* mice when compared to WT counterparts (Figure 5.4A). Overall this data suggests that Muc2 glycosylation plays a role in protecting intestinal barrier function, while core 1 derived O-glycans seem to have a larger impact than core 3 glycosylation.

To determine the impact of the increased gut barrier permeability on systemic translocation of *C. rodentium*, we enumerated pathogen burdens at systemic sites (liver, spleen, MLN) day 6 PI. *C1galt1 -/-* mice carried significantly greater pathogen burdens at all systemic

sites in comparison to WT and *C3GnT -/-* mice. In contrast, there were no significant differences in pathogen burdens recovered from WT and *C3GnT -/-* mice (Figure 5.4B). Since *C. rodentium* is known to induce IEC proliferation, we next looked at the proliferation marker Ki67. Although there were no differences in IEC proliferation between mouse strains under uninfected conditions, infection induced upregulation of IEC proliferation was significantly accelerated in *C1galt1 -/-* mice compared to *C3GnT -/-* and WT mice, likely reflective of the rapid pathogen colonization and increased inflammation these mice suffer (Figure 5.4C).

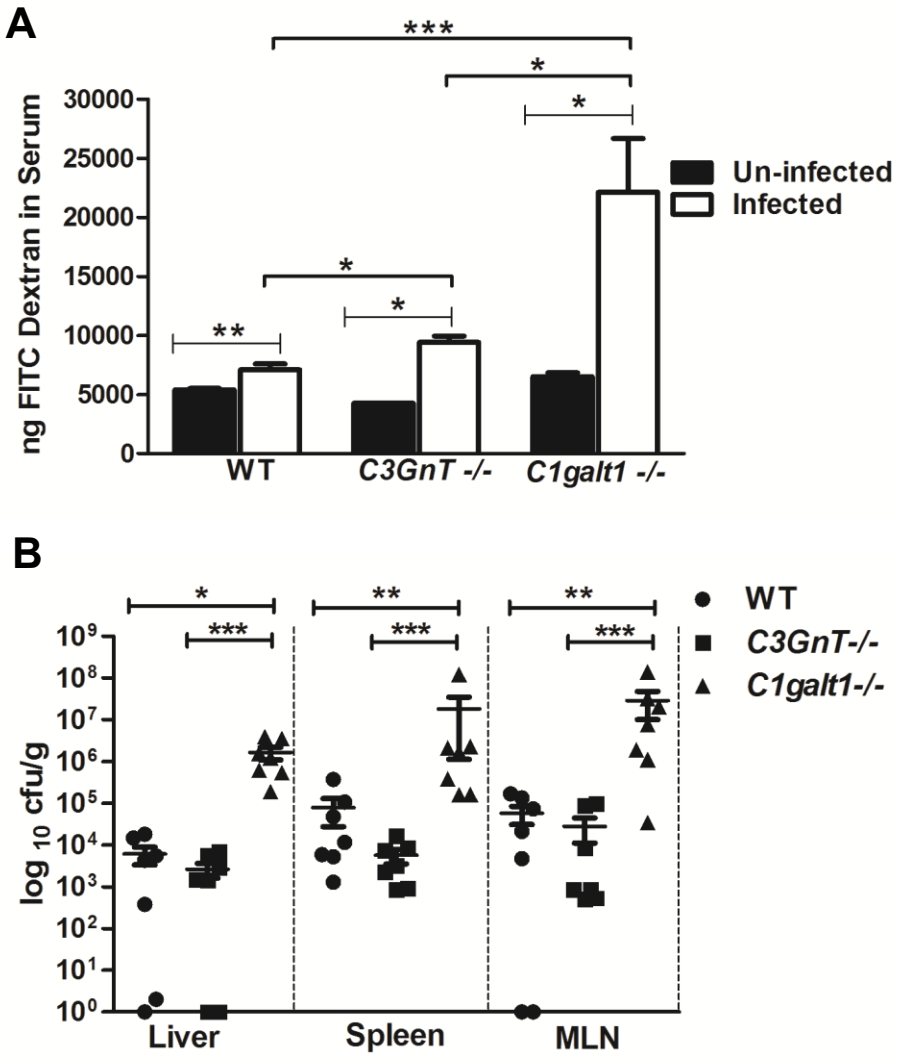

C

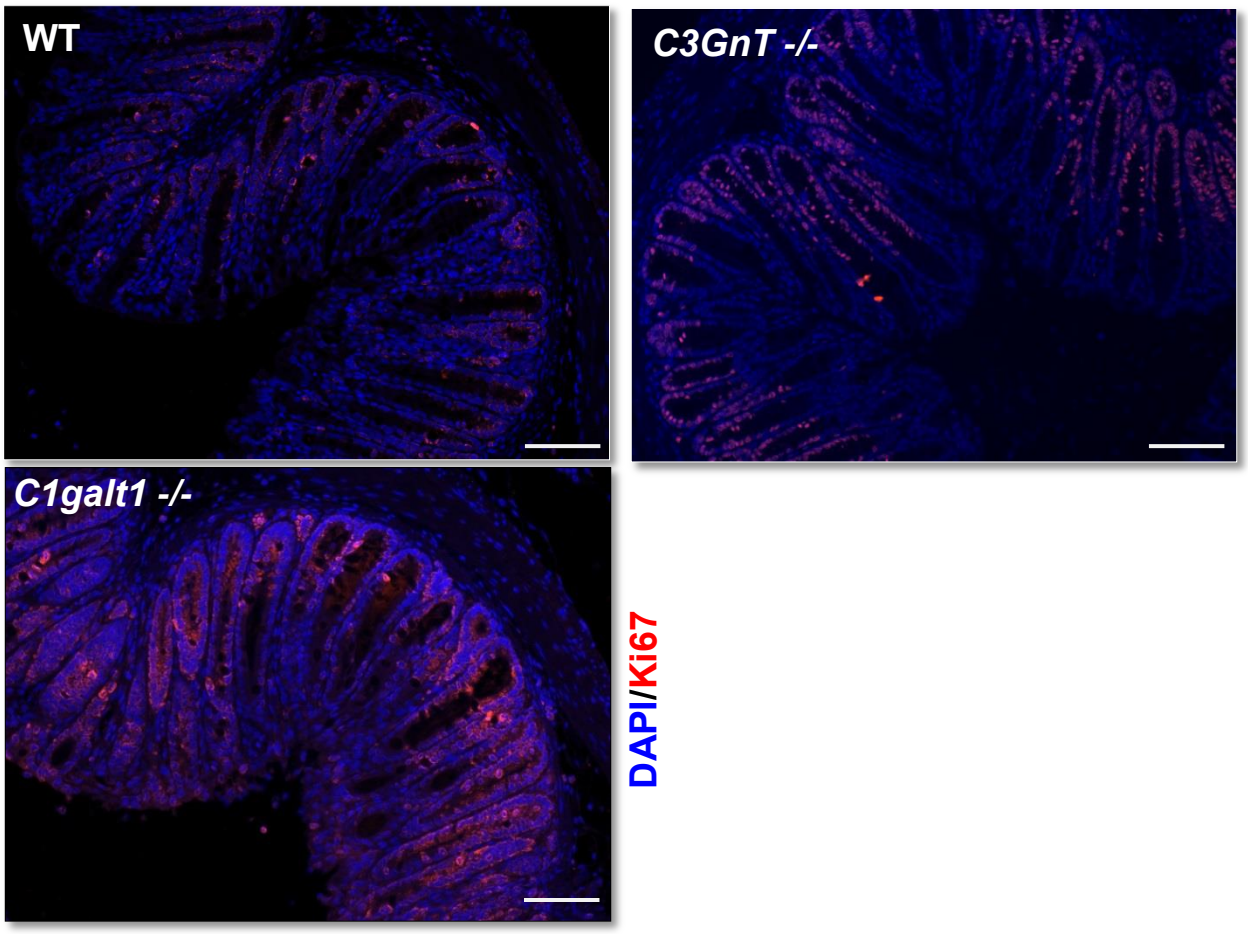

Figure 5.4 *C1galt1 -/-* mice display defects in epithelial barrier function and increased translocation of pathogenic bacteria.
(A) *C1galt1 -/-* mice display increased FD4 flux into serum at day 6 PI in comparison to WT and *C3GnT -/-* counterparts. Note that although *C. rodentium* infection causes barrier disruption in all groups, there was much greater FITC-dextran flux within *C1galt1 -/-* mice during *C. rodentium* infection, indicative of greater impairment in their gut barrier in comparison to the other groups. (B) Quantification of viable *C. rodentium* burdens recovered from systemic sites (liver, spleen, MLN). *C1galt1 -/-* had significantly greater *C. rodentium* translocation to systemic sites that WT and *C3GnT -/-* mice. Results are pooled from at least 3 independent experiments (n=9). Error bars = SEM; asterisks indicate significant difference (*, $P < 0.05$; **, $P < 0.01$; ***, $P < 0.0005$) by the Mann-Whitney test. (C) Immunostaining for proliferation marker Ki67 (red) in the distal colon of WT, *C3GnT -/-* and *C1galt1 -/-* mice. *C1galt1 -/-* mice had greater IEC proliferation at day 6 PI in comparison to other groups.

5.2.5 *C1galt1 -/-* mice display heavier and altered localization/colonization of *C. rodentium* in distal colon

As previously discussed, *C1galt1 -/-* carried greater *C. rodentium* burdens at colonic sites. As increased intestinal pathology is often associated with significantly greater epithelium associated pathogen burdens, we next examined the localization of *C. rodentium* by immunostaining for *C. rodentium*-derived translocated intimin receptor (Tir) (focusing on the distal colon). In WT and *C3GnT -/-* mice, *C. rodentium* was predominantly localized to the mucosal surface with patchy distribution (Figure 5.5A and 5.5B respectively). In contrast, Tir staining of tissue from *C1galt1 -/-* mice showed a greater mucosal surface area positively staining for Tir. In addition to its localization to the mucosal surface, *C. rodentium* could be seen penetrating deeper into colonic crypts. Furthermore, *in C1galt1 -/-* mice, *C. rodentium* appeared to form large aggregates in close proximity to epithelial surfaces as well as within the lumens of colonic crypts. Overall, *C1galt1 -/-* mice displayed altered localization as well as heavier colonization of *C. rodentium*, which was consistent with pathogen burdens enumerated from the distal colons of these mice (Figure 5.2A).

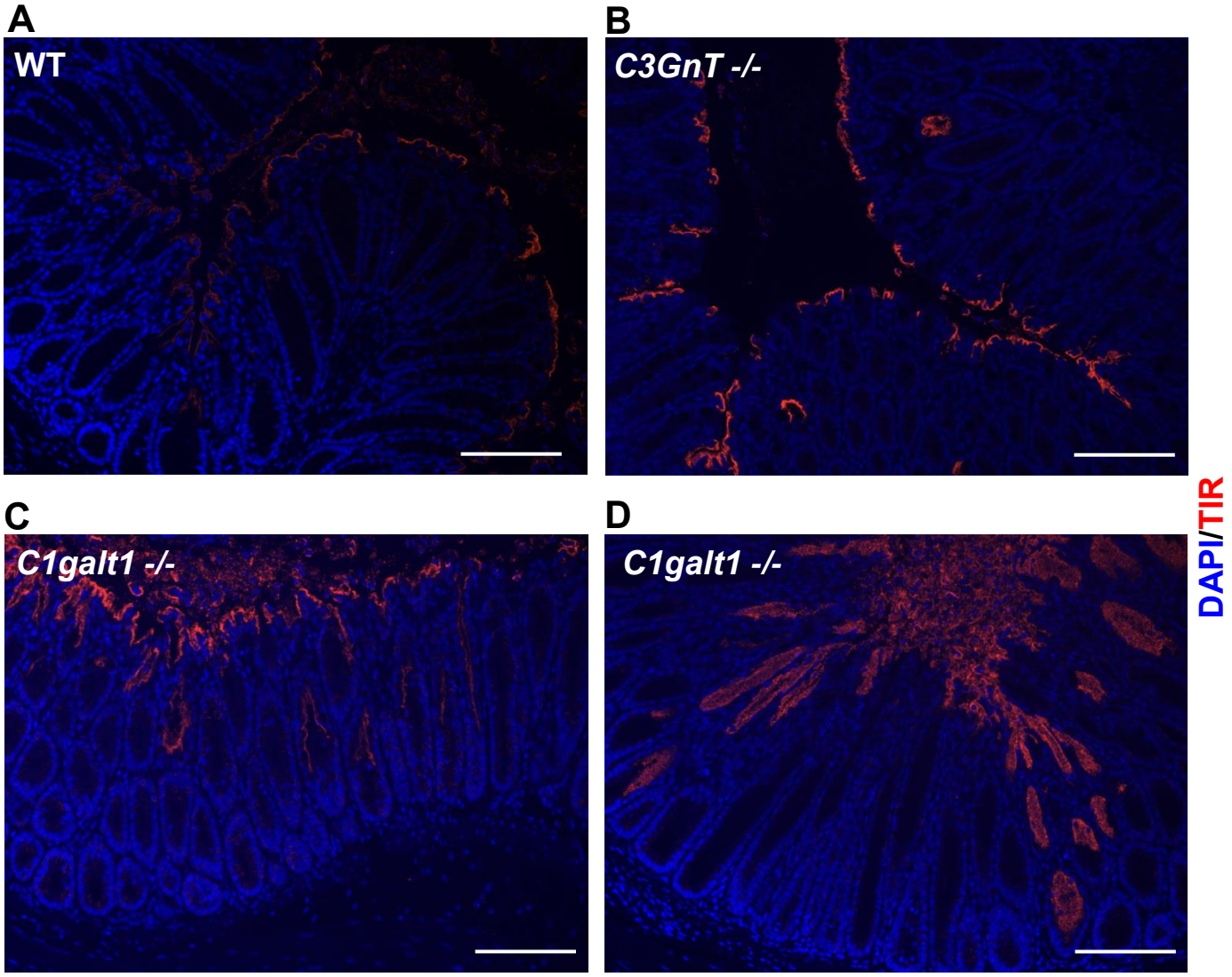

Figure 5.5 Disease severity in *C1galt1 -/-* mice is associated with altered localization of *C. rodentium*.
Representative images from distal colon, showing *C. rodentium* localization as seen via staining for Tir (*C. rodentium* infection marker, Red) and DAPI (nuclei specific, counterstain, Blue). (A/B) *C. rodentium* can be mostly seen localized to the mucosal surface, with patchy distribution in WT and *C3GnT -/-* mice respectively. (C/D) *C1galt1 -/-* distal colons display greater regions of mucosal surface stained positively for Tir. *C. rodentium* can be seen penetrating deeper into the crypts as well as aggregating along the mucosal surface, indicative of greater *C. rodentium* burdens in these mice. Original magnification 200x, scale bar 50 µm.

5.2.6 Absence of core 1 or core 3 derived O- glycosylation does not cause overt alterations in gut microbiota composition

The composition of intestinal microbiota can play an important role in influencing host susceptibility to *C. rodentium* infection[171,329,330]. To check for any significant alterations in the baseline gut microbiota of WT, *C3GnT -/-* and *C1galt1 -/-* mice, we analyzed the microbial composition in the fecal pellets. While comparing the overall microbiota composition, we found that Bacteroidetes was the dominant phyla (~60-70%) whereas Firmicutes represented ~ 10-20% of the total commensal population. Not surprisingly, γ-proteobacteria represented ~ 1% of the population, with other microbes making up the remainder of the commensal population. There were no dramatic differences in the relative proportions of the 2 major bacterial phylas found in the murine intestine- i.e. Firmicutes and Bacteroidetes. However, the proportion of Firmicutes was significantly lower in *C1galt1 -/-* mice (~20% lower) and *C3GnT -/-* mice (~5% lower, not significant) in comparison to WT mice, as previously reported (Figure 5.5A). While deficiency of core 3 glycosylation had no effect on microbiota composition, core 1 derive O-glycans seemed to affect the makeup of the gut microbiome.

Furthermore, *C. rodentium* infection is characterized by rapid depletion of commensals, largely mediated by host-driven processes[221]. To further characterize the commensal dynamics during *C. rodentium* infection in *C1galt1 -/-* mice, we quantified the total commensal numbers in fecal pellets. We found that commensal numbers were rapidly depleted in WT mice and by day 6PI, ~70% of the total commensals had been depleted. In *C1galt1 -/-* mice, ~50% of the commensals were depleted which was significantly lower than WT mice. There were no significant differences in commensal depletion at earlier time points (day 2 and day 4) between the two groups (Figure 5.5B). Overall, these findings suggest that commensal microbes are

unlikely to fully underlie the increased susceptibility of *C1galt1 -/-* mice to *C. rodentium* infection.

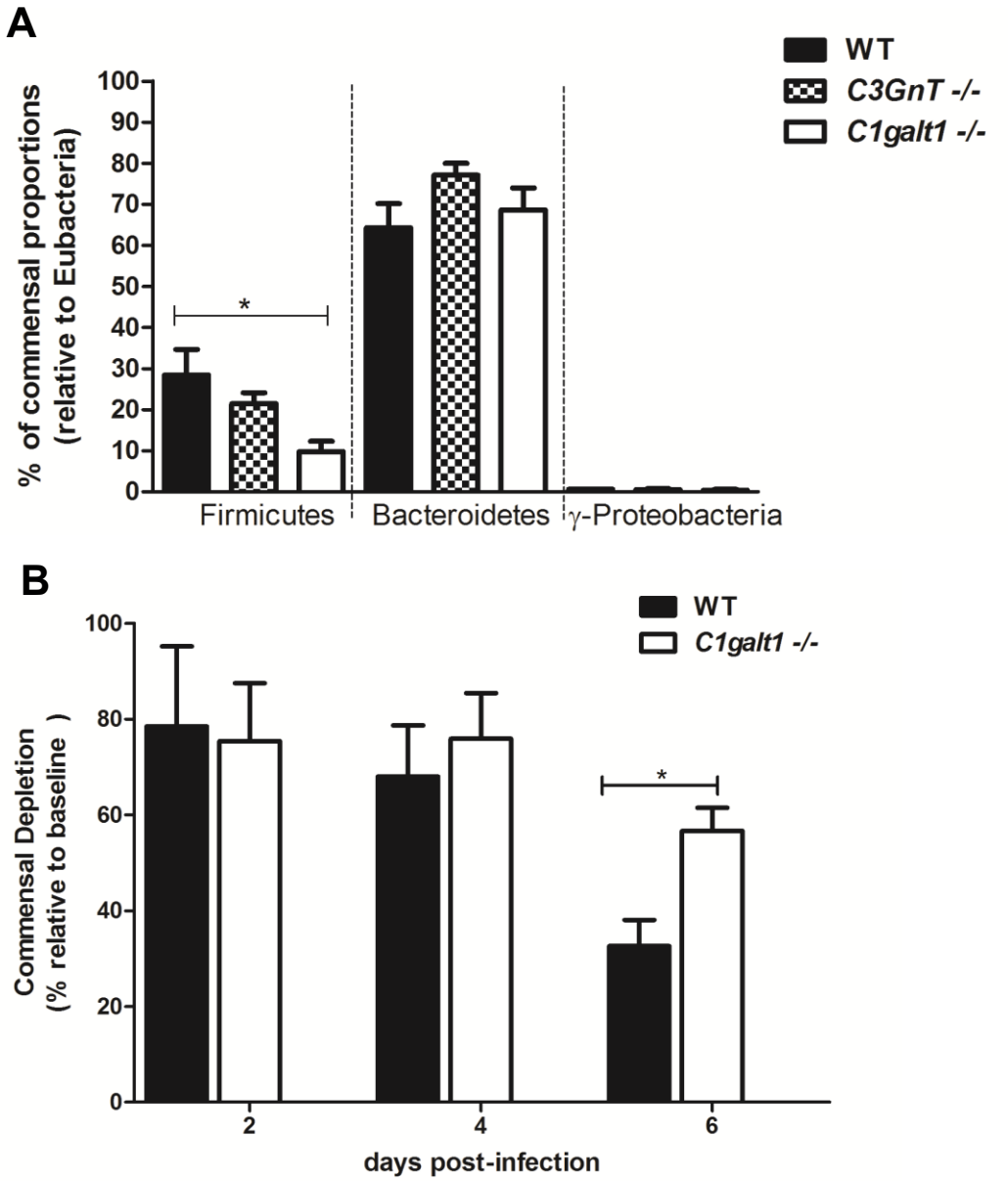

Figure 5.6 Mucus glycosylation alters gut microbiota composition.
(A) Commensal microbiota composition in WT, *C3GnT -/-* and *C1galt1 -/-* mice, under baseline (uninfected) conditions, assessed by qPCR analysis. Subtle, but significant differences in Firmicutes composition were seen between WT and *C1galt1 -/-* mice. (B) Commensal depletion on day 2, day 4 and day 6 post *C. rodentium* infection in WT and *C1galt1 -/-* mice. Data was normalized to uninfected (day 0) baseline values. Results are pooled from 3 independent infections (n=9 per group) while error bars represent SEM (*, $P < 0.05$, Mann-Whitney test).

5.2.7 *C1galt1 -/-* mice show altered goblet cell function at baseline as well as during *C. rodentium* infection

Since absence of glycosylation has been shown to alter the mucus barrier, primarily affecting the mucin Muc2[150,331], we next assessed the goblet cell readouts in WT, *C3GnT -/-* and *C1galt1 -/-* mice at baseline levels to determine if they showed any dramatic differences in these baseline measurements which might affect their susceptibility to *C. rodentium* infection. There were no dramatic differences in the staining profile of the Muc2 mucin, the proinflammatory mediator Relm-β, and the reparative trefoil factor 3 (TFF3) between WT and *C3GnT -/-* mice under baseline and infection conditions. However, we noted that *C1galt1 -/-* mice had reduced staining for Muc2 as well as fewer Muc2 +ve goblet cells, when compared to the other groups (Figure 5.7A, left panel). The goblet cell mediator Tff3 showed less positive staining in the *C1galt1 -/-* mice at the base of their colonic crypts whereas for Relm-β, there was little positive staining (Figure 5.7B, 5.7C, left hand panels). We decided to further assess the changes in these mediators during infection and if these factors played a role in altering host susceptibility during infection. As previously described, we used immunostaining to determine whether there was differential induction of Muc2, Tff3 and Relm-β. Consistent with previous findings, *C. rodentium* infection induced secretion of Muc2 mucin, as seen by the presence of luminal Muc2 in WT and *C3GnT -/-* mice at day 6 PI. In contrast, *C1galt1 -/-* mice appeared to have significantly reduced levels of the secreted Muc2 mucin in the lumen as well as fewer Muc2 +ve goblet cells (Figure 5.7A, left hand panels). Furthermore, there was decreased detection of Tff3 and Relm-β in *C1galt1 -/-* mice in comparison to WT and *C3GnT -/-* mice (5.7B, 5.7C, right hand panels).

To quantify if there was any impaired transcriptional differences in *C1galt1 -/-* mice in comparison to their WT and *C3GnT -/-* counterparts, we performed quantitative PCR analysis (RT-PCR) on the distal colon tissues. We found that *C. rodentium* infection leads to increased *Muc2*, *Tff3* and *Relm-β* gene transcription, as compared to uninfected tissues in all mouse groups (WT, *C3GnT -/-* and *C1galt1 -/-* mice), however the gene induction during infection was significantly impaired in *C1galt1 -/-* mice. At the gene transcript level, while there were no differences in *Muc2*, *Tff3* and *Relm-β* between WT and *C3GnT -/-* mice at baseline as well as under infected conditions (day 6), whereas *C1galt1 -/-* mice had lower gene transcription under uninfected and infection conditions when compared to the other two groups (Figure 5.17D). Overall, these findings reveal that absence of core 1 derived O-glycosylation alters the goblet cell responses at baseline levels and impairs goblet cell responses during *C. rodentium* infection, potentially contributing to the heightened susceptibility of *C1galt1 -/-* mice.

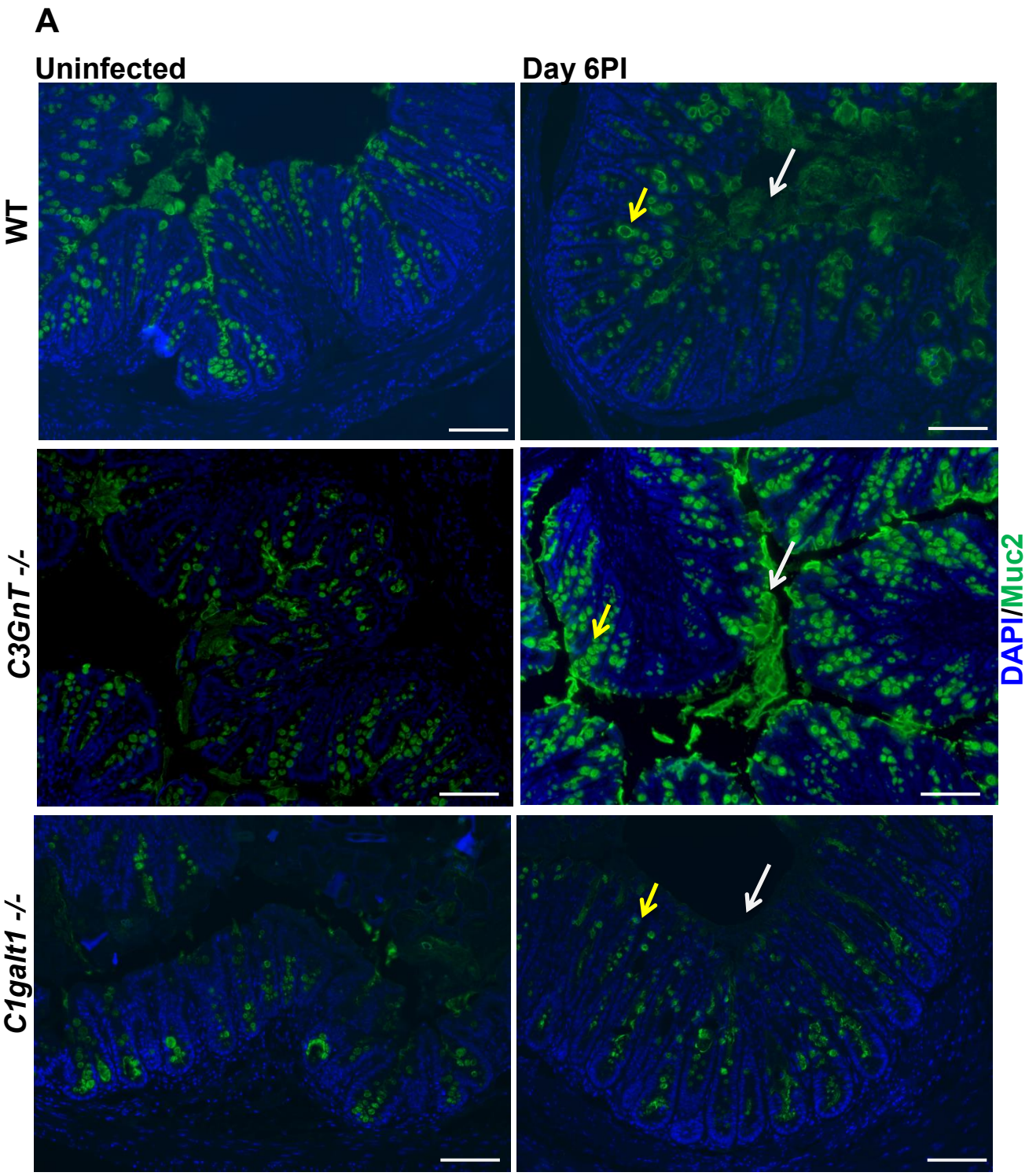
A
Uninfected
Day 6PI
WT
C3GnT -/-
C1galt1 -/-
DAPI/Muc2

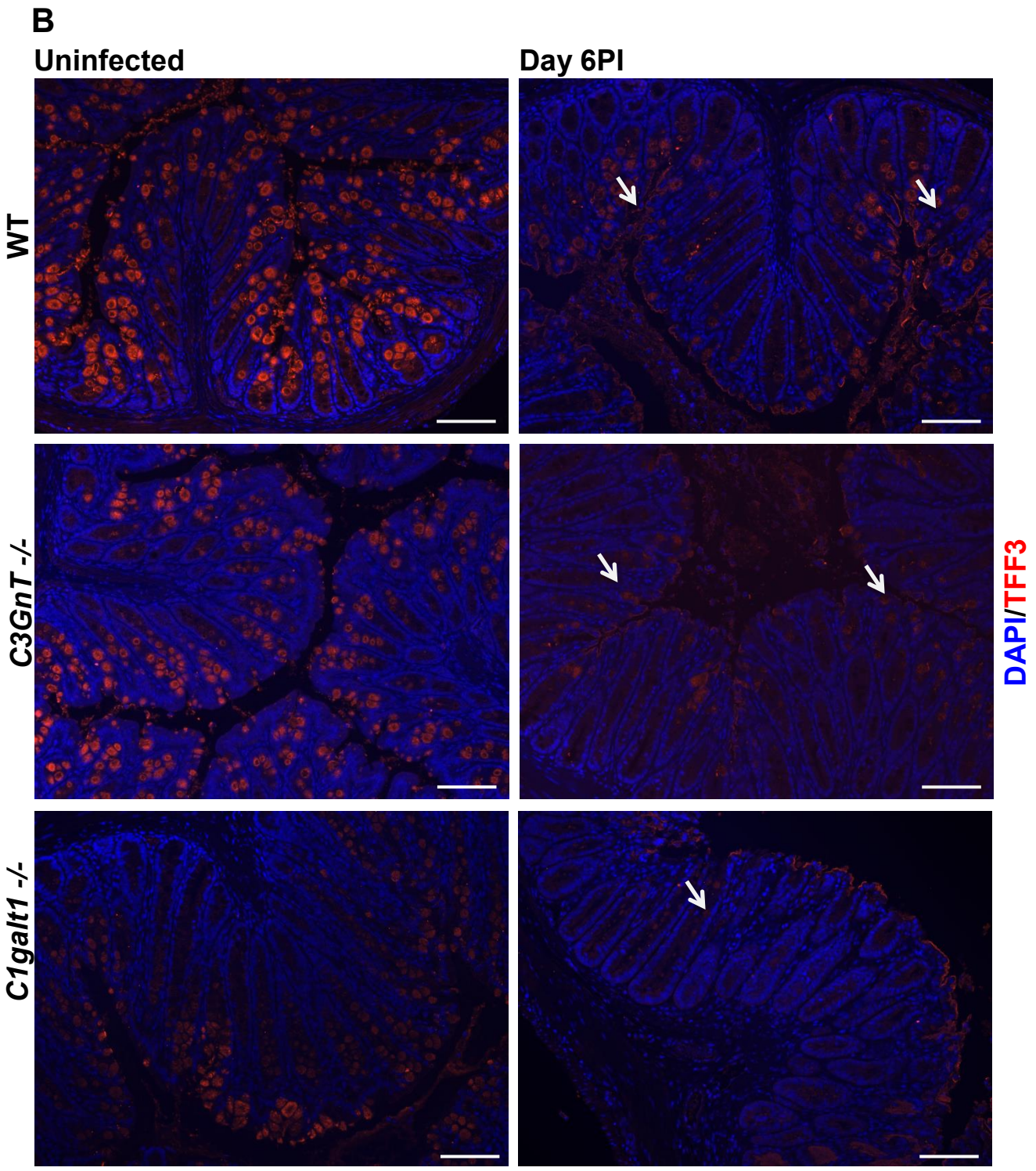
B
Uninfected
Day 6PI
WT
C3GnT -/-
C1galt1 -/-
DAPI/TFF3

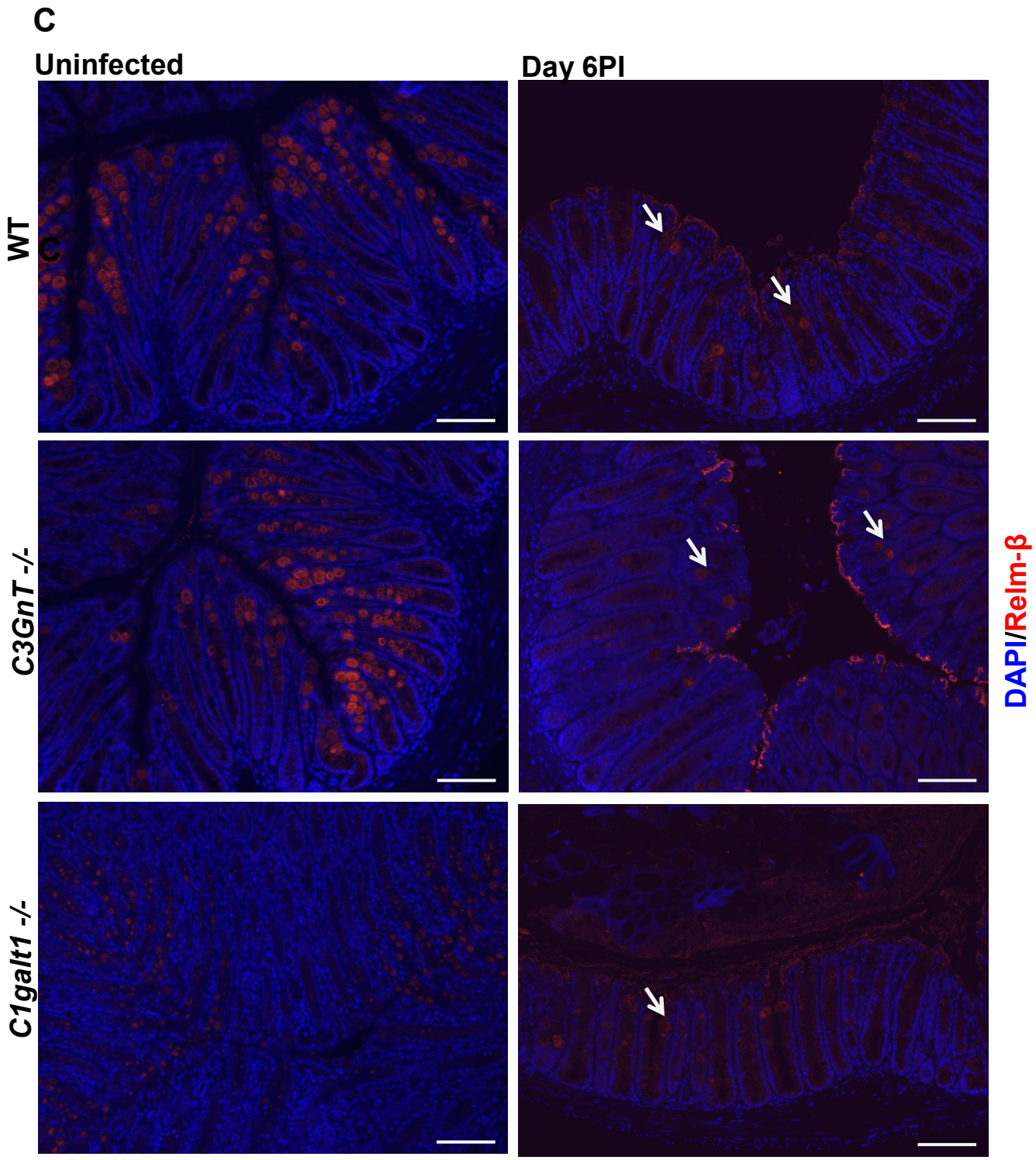

Figure 5.7 Goblet cell responses during *C. rodentium* infection.
Representative immunostaining images examining the changes in (A) Muc2 (white arrow- secreted/luminal Muc2 mucin, yellow arrow- mucus- filled goblet cells) (B) Tff3 (C) Relm-β under baseline and infected conditions (day 6 PI) in the distal colon of WT, *C3GnT -/-* and *C1galt1 -/-* mice. Tff3 and Relm-β positive staining is indicated using white arrows.

D

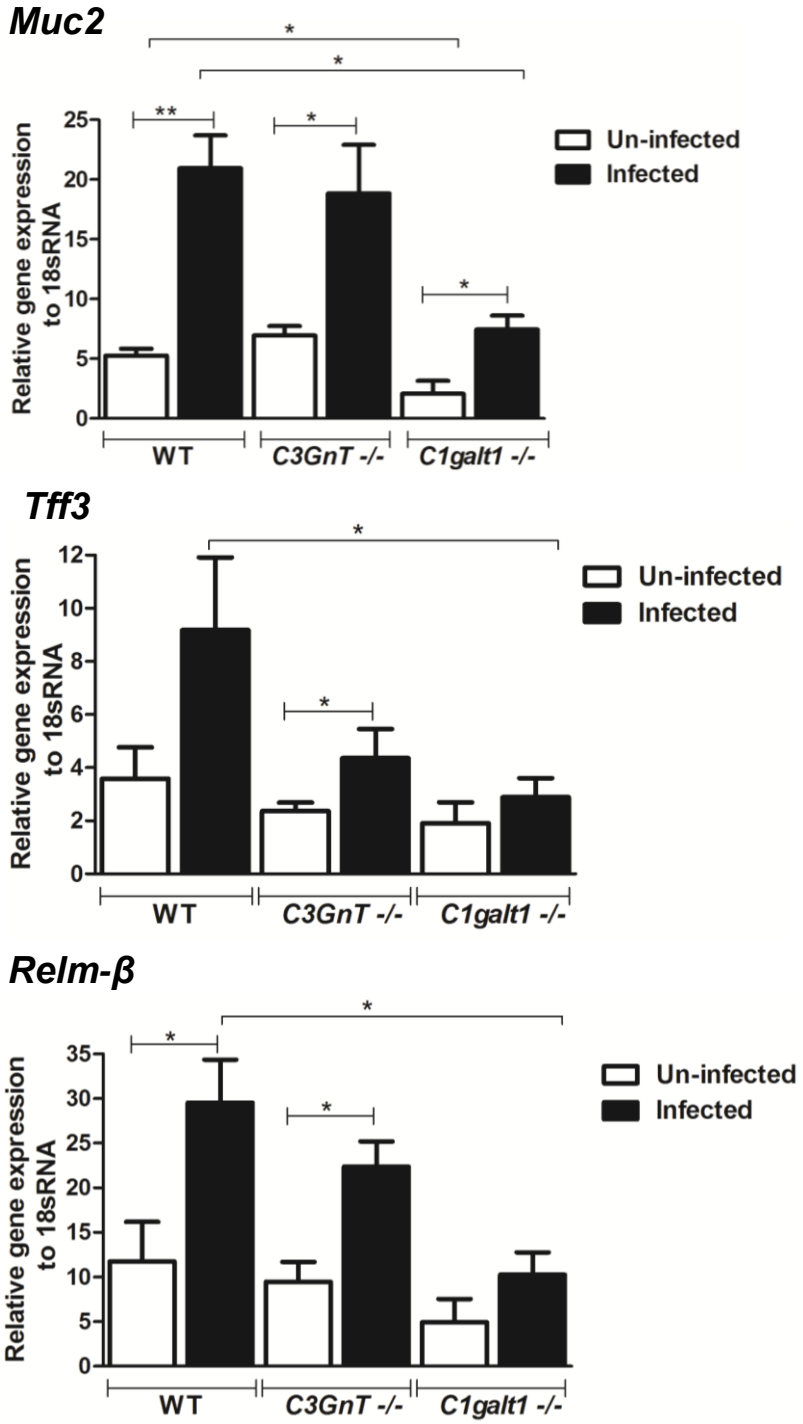

Figure 5.7D: Transcriptional profile of goblet cell mediators during *C. rodentium* infection
C. rodentium infection induces upregulation of goblet cell mediators, Muc2, Tff3 and Relm-β is impaired in *C1galt1 -/-* mice, in comparison to WT and *C3GnT -/-* mice. *C1galt1 -/-* mice had impaired goblet cell responses under baseline as well as infection conditions. Error bars represent SEM from 3 independent experiments (n=9 per group), asterisks indicate significance (*, $P < 0.05$; **, $P < 0.01$; ***, $P < 0.0005$) by the Mann-Whitney test.

5.2.8 *C1galt1 -/-* mice exhibit altered antimicrobial IEC responses

We next wondered if exaggerated pathogen burdens in *C1galt1 -/-* mice could be attributed to impaired antimicrobial responses**.** Upon assessment of two antimicrobial peptides, mCRAMP and RegIII-γ, we found that these AMPs were expressed similarly in the distal colons of WT, *C3GnT -/-* and *C1galt1 -/-* mice under uninfected conditions. As expected, *C. rodentium* infection significantly upregulated the expression of mCRAMP and RegIII-γ in all three groups of mice. While WT and *C3GnT -/-* mice showed a modest increase in the expression of these AMP's, *C1galt1 -/-* mice developed dramatically greater transcription of mCRAMP and RegIII-γ, likely reflecting the accelerated pathogen colonization they suffered.

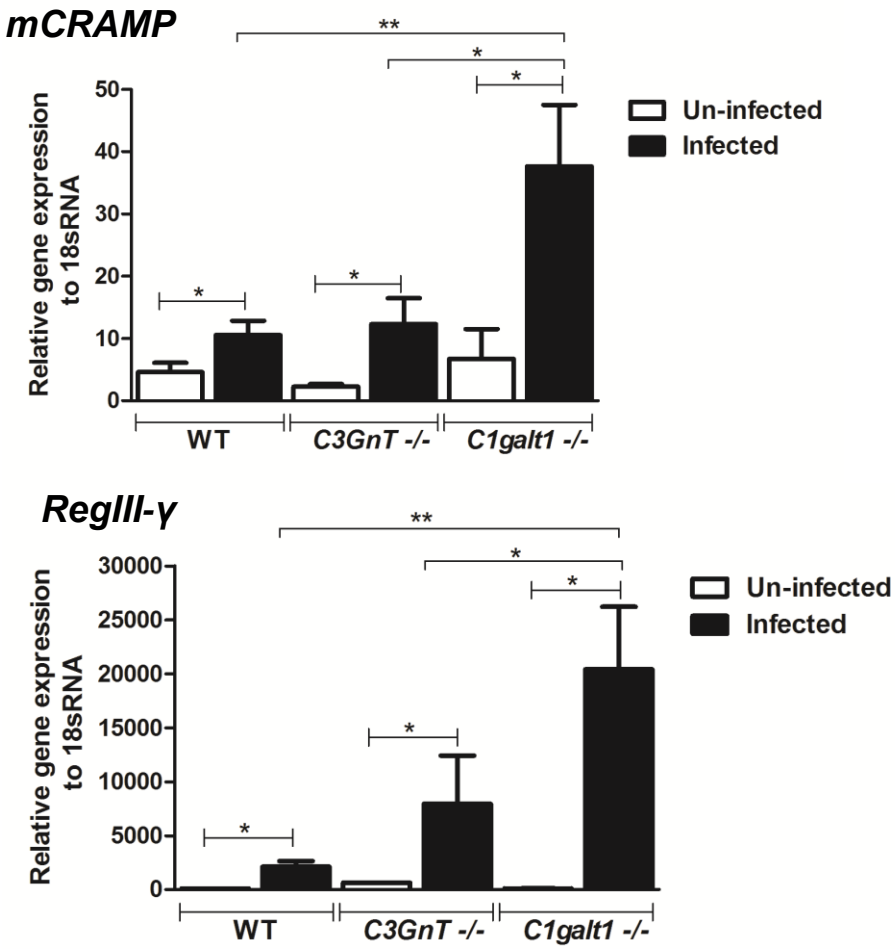

Figure 5.8 *C1galt1 -/-* display altered antimicrobial responses during *C. rodentium* infection.
C. rodentium infection induces significantly greater transcription of two AMPs, mCRAMP and RegIII-γ in WT, *C3GnT -/-* and *C1galt1 -/-* mice, when compared to uninfected tissues. Exaggerated antimicrobial responses were seen in *C1galt1 -/-* mice. Error bars represent SEM from 3 independent experiments (n=9 per group), with asterisks indicating significance (*, $P < 0.05$; **, $P < 0.01$) by the Mann-Whitney test.

5.2.9 Evidence for altered Muc2 fucosylation during *C. rodentium* infection

We next examined the dynamics of fucosylation changes during *C. rodentium* infection in the WT, *C3GnT -/-* and *C1galt1 -/-* mice, through Ulex europaeus agglutinin UEA-1 lectin staining, which binds to α (1,2) fucosylated residues, and glycoproteins found abundantly in the mucus layer and is a strong indicator of Muc2 fucosylation[163,332]. In WT mice, there was abundant UEA-1 positive staining in goblet cells under baseline conditions and *C. rodentium* infection resulted in more positive staining along the crypt lumen as well as the epithelial surface, indicative of increased mucus secretion and fucosylation of O-glycan structures present on the secreted mucin Muc2 during *C. rodentium* infection. A similar response was noted in *C3GnT -/-* mice, where *C. rodentium* infection led to increased UEA-1 positive staining along the epithelial surface as well as in the regions where mucus was secreted into the lumen (Figure 5.9A, 5.9B). *C1galt1 -/-* mice, however, were largely devoid of UEA-1 positive staining in the lumen as well as along the epithelial surface under infected conditions. Interestingly, UEA-1 positive staining was seen in hypertrophic goblet cells in *C1galt1 -/-* mice which appeared to be induced during *C. rodentium* infection (Figure 5.9C). Overall, an infection induced increase in fucosylation was evident in all groups of mice. Although *C1galt1 -/-* mice were not completely devoid of UEA-1 staining, these mice had significantly reduced staining in comparison to WT and *C3GnT -/-* groups, suggesting that *C1galt1 -/-* mice are impaired in mucus responses during *C. rodentium* infection, and perhaps also in the levels of Muc2 fucosylation. Since core 1 derived

O-glycans offer multiple glycosylation sites, it is possible that absence of core 1 derived O-glycans on the Muc2 results in reduction of the number of potential fucosylation sites present on the mucus layer.

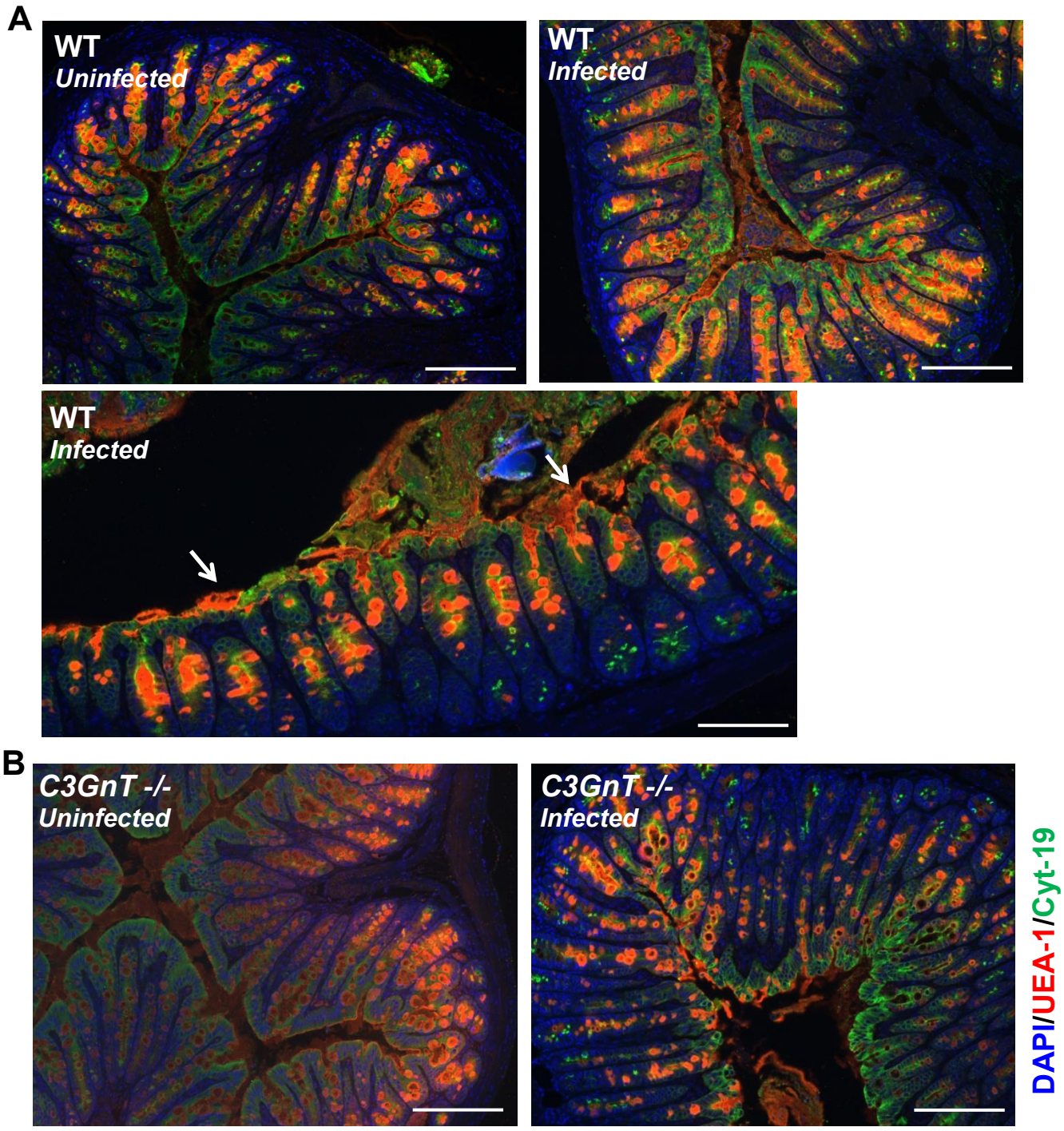

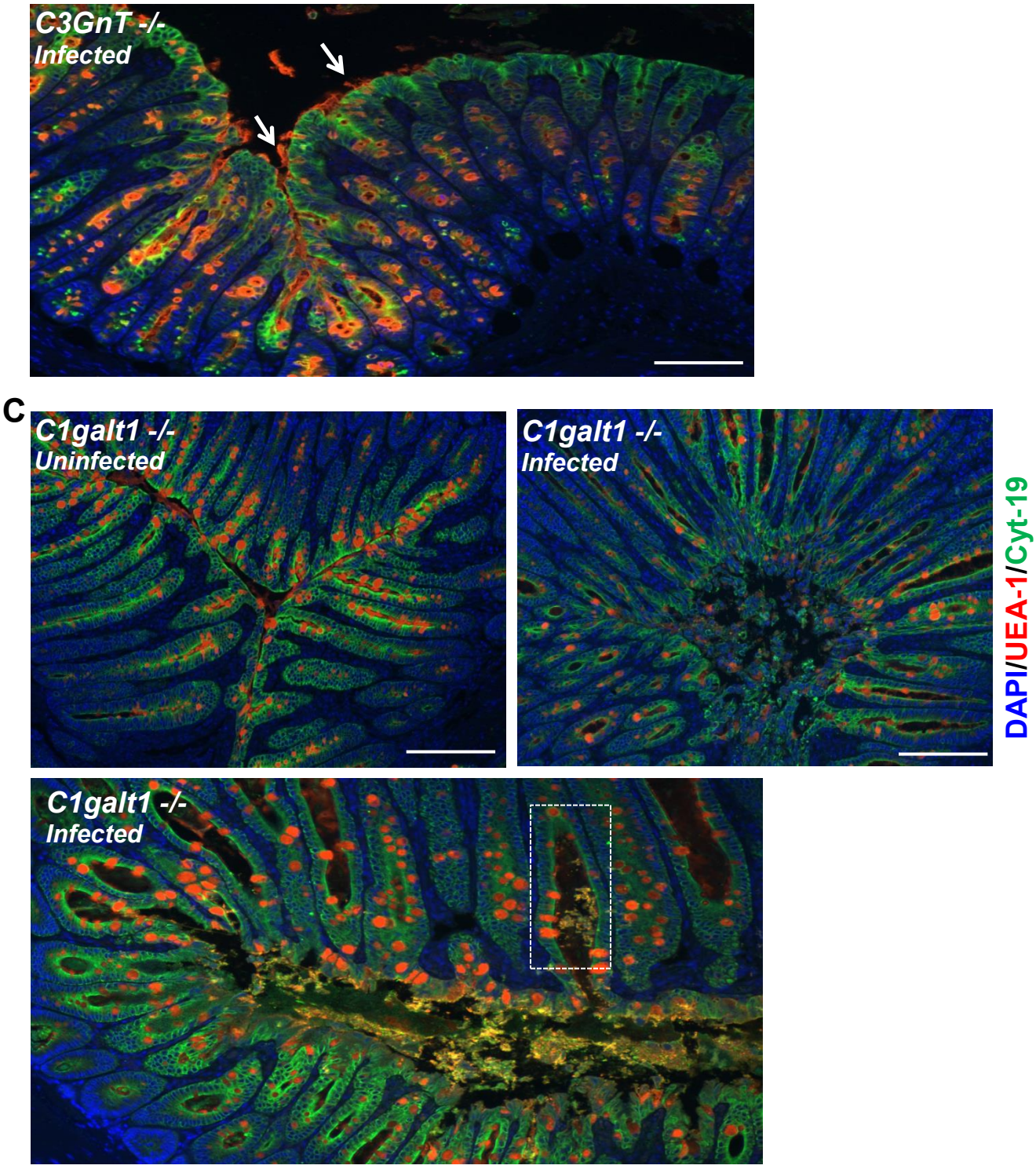

Figure 5.9 UEA-1 (fucosylated mucus) staining profile during *C. rodentium* infection. Representative images showing UEA-1 staining (red), cytokeratin-19 staining (green, outlines the epithelial cells and is a marker for structural integrity of IEC) and DAPI staining (counterstain) (A/B) In WT and *C3GnT* -/- mice, UEA-1 staining is mostly restricted to the base

of the crypts in uninfected tissues. When infected with *C. rodentium*, there is localization of UEA-1 staining throughout the crypts as well as in close proximity to the mucosal surface and in the secreted mucus in the intestinal lumen (white arrows). *C1galt1 -/-* mice appear to have reduced UEA-1 staining under baseline conditions, and smaller mucus granules. Note that in *C1galt1 -/-* tissues, there is no significant UEA-1 positive staining in the intestinal lumen and the majority of the staining is seen in mucus filled goblet cells. Also note that in *C1galt1 -/-* mice, some crypt lumens are largely devoid of mucus contents with some UEA-1 positive staining noted in the hypertrophic goblet cells (representative crypt outlined in white box).

5.2.10 Examining the IL-22/fucosylation axis during *C. rodentium* infection

We hypothesized that the decreased fucosylation noted in *C1galt1 -/-* mice may be attributed to differential levels of expression of fut1 and fut2, α(1,2)fucosyltransferases that can be expressed in the mouse colon[333,334]. We therefore checked for the transcription of the genes *fut1* and *fut2* in the distal colon under baseline and infection conditions. Since *fut1* is generally expressed at low levels in comparison to *fut2*, the expression levels were dramatically different for the two enzymes. We noted that there were no dramatic differences in the baseline expression of *fut1* and *fut2* between the three hosts, although fut2 was modestly (but significantly) higher in the *C1galt1 -/-* mice at baseline. *C. rodentium* infection induced significantly greater expression of *fut1* in WT, *C3GnT -/-* and *C1galt1 -/-* mice and the level of *fut1* was upregulated to a similar degree between the three hosts, suggesting that it could be a general host defense mechanism (Figure 5.10). While *fut2* mRNA levels significantly increased in WT and *C3GnT -/-* mice during infection, there was no significant increase in *fut2* during infection in the *C1galt1 -/-* mice, however this might reflect a modestly elevated baseline transcription of *fut2* seen in these mice (Figure 5.10). Concomitant with the UEA-1 immunostaining profile, this data implies that *C1galt1 -/-* mice may vary from other hosts in terms of their intestinal fucosylation status. However, further in depth analysis of fucosylation status of the Muc2 mucin and other fucosylation targets would be needed to make definitive conclusions. The exact mechanisms of

how intestinal fucosylation contributes to the overall fitness of the host during *C. rodentium* infection still remain to be elucidated.

IL-22 has been shown to enhance host colonization resistance and promote defense during *C. rodentium* infection by inducing intestinal fucosylation[335]. To further investigate the link between IL-22 and induced fucosylation in our study, we performed q-PCR analysis checking IL-22 gene expression levels. IL-22 gene transcription was induced to a similar degree in WT, *C3GnT -/-* mice and *C1galt1 -/-* mice day 6 PI during *C. rodentium* infection (Figure 5.11), suggesting that the differences in fucosylation status are not due to intrinsic differences in IL-22/fut2 axis, but perhaps due to the differences in the available fucosylation sites in the absence of core 1 derived O- glycans.

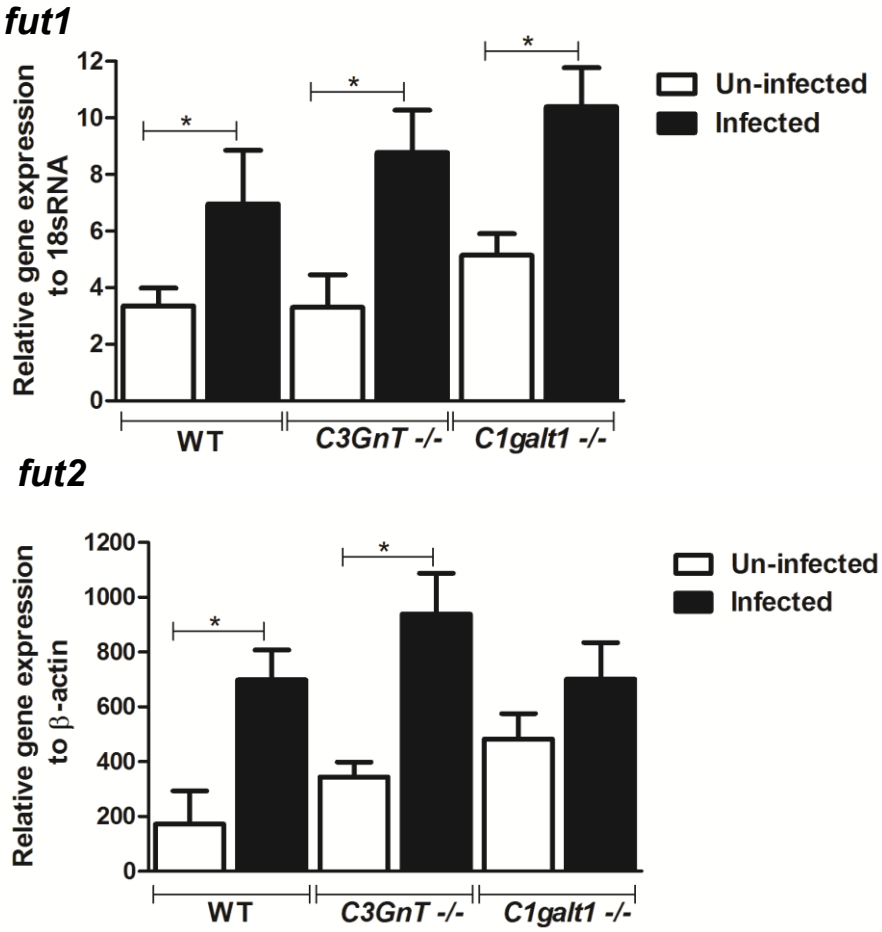

Figure 5.10 α(1,2)fucosyltransferases *fut1* and *fut2* are upregulated during *C. rodentium* infection.
Expression of mouse fucosyltranferases *fut1* and *fut2* in the distal colonic tissues for uninfected and infected (day 6 PI) mice. (A) Significantly greater induction of fut1 is induced during *C. rodentium* infection in WT, *C3GnT -/-* and *C1galt1 -/-* mice. There were no significant differences between the uninfected and infected groups (B) Infected WT and *C3GnT -/-* mice have significantly higher gene transcript levels for *fut2* when compared to uninfected counterpart. No significance difference was noted between uninfected and infected *C1galt1 -/-* samples. Results are pooled from three independent infections (n=9 per group) with asterisks indicating significance (*, $P < 0.05$), Mann-Whitney test.

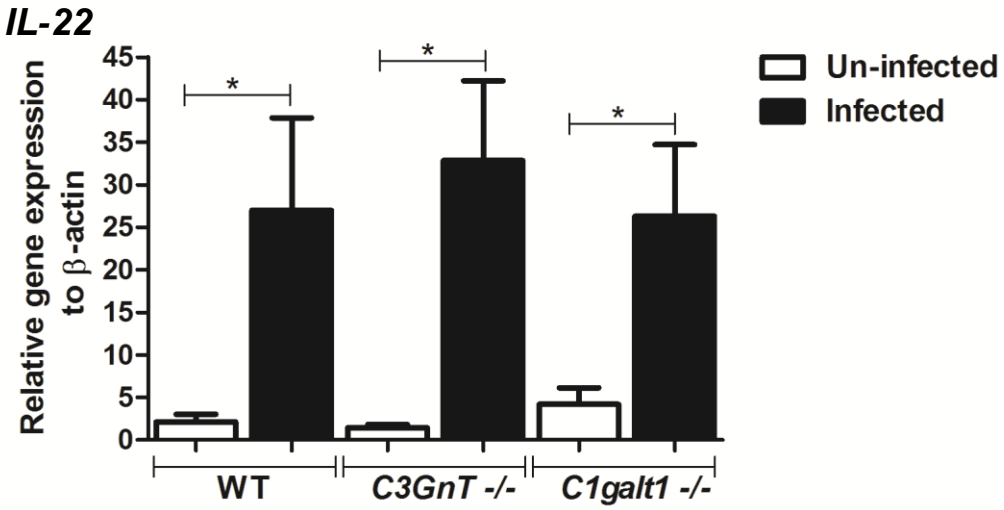

Figure 5.11 IL-22 is induced during *C. rodentium* infection.
qPCR of IL-22 in WT, *C3GnT -/-* and *C1galt1 -/-* distal colons after *C. rodentium* infection. Significantly higher IL-22 transcripts were induced in the distal colon (in comparison to un-infected samples) for all three groups following infection. Note-there were no differences detected between groups. Results are pooled from three independent infections (n=9 per group), asterisks indicate significance (*, $P < 0.05$), Mann-Whitney test.

5.2.11 Infected *C1galt1 -/-* mice display microcolony-like structures/bacterial aggregates, comprising *C. rodentium*

As previously shown, Muc2/mucus secretion is important for controlling pathogen and commensal burdens during *C. rodentium* infection[145]. Since *C1galt1 -/-* mice were impaired in goblet cell responses, we wondered if reduced Muc2 secretion would result in increased bacterial aggregation on the epithelial surface. Following staining for *C. rodentium* Tir and mucin Muc2

(dual staining), we noted that in WT mice, mucus secretion provided an important barrier to flush away *Citrobacter* away from the epithelial surface and *Citrobacter* could be seen in the mucus layer (Figure 5.10, top panel). In *C1galt1 -/-* mice, we noted distinct areas where no mucus secretion was apparent and *Citrobacter* could be seen aggregating on the epithelial surface. Although some goblet cells were seen in most of the crypts, unlike WT mice, no obvious mucus secretion response could be seen in *C1galt1 -/-* mice. In the few crypts where mucus secretion was evident, *C. rodentium* could be seen distal from the epithelial surface (Figure 5.10, bottom panel), as if it had been pushed away from the surface.

In uninfected *Muc2 -/-* mice (no mucus layer), commensal bacteria have been found in direct contact with the colonic epithelial surface as well as in the intestinal crypts whereas in WT mice, the majority of commensals are restricted to the intestinal lumen[110,134]. To look at localization of *C. rodentium* (infecting versus luminal) we performed LPS (stains *C. rodentium*, green) and Tir (red, *C. rodentium* marker of epithelial infection) dual staining. In WT mice, *C. rodentium* could be seen in the intestinal lumen (green) as well as along the epithelial surface (yellow). In *C1galt1 -/-* tissues, we noted several Tir negative, LPS positive (green) *C. rodentium* microcolonies in close proximity of the epithelial surface as well as directly interacting with the mucosa. In addition to significantly greater adherent pathogen burdens, *C1galt1 -/-* mice also appeared to have higher non-adherent, luminal pathogen burdens associated with the mucosal surface (Figure 5.13).

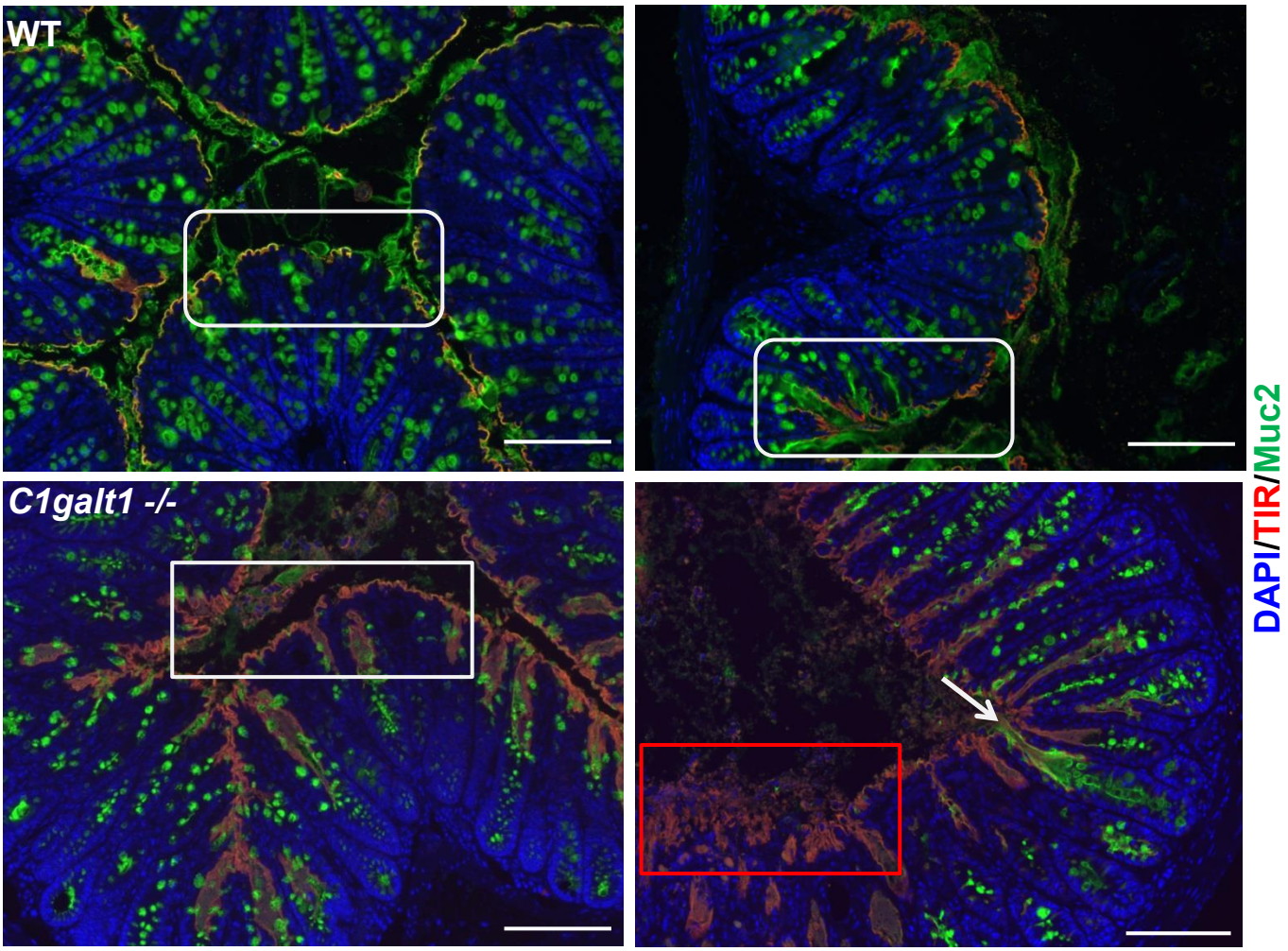

Figure 5.12 *C1galt1 -/-* mice have impaired mucus secretion & increased pathogen burdens. Representative images for Muc2 and Tir dual staining from the distal colon of infected WT and *C1galt1 -/-* mice are shown. Top panel- in *C. rodentium* infected WT mice, the majority of *C. rodentium* can be seen along the epithelial surface with patchy distribution and in a single layer (no aggregation). In the majority of the crypts, mucus can be seen flushing the *C. rodentium* away from the mucosal surface. In some crypts showing luminal mucus, *C. rodentium* colonization is minimal (highlighted using white box). Bottom panel- In *C1galt1 -/-* mice, mucus secretion is not obvious and *C. rodentium* can be seen going deeper into the crypts. Lack of mucus mediated flushing potentially contributes to heavier colonization throughout the distal colon (clustered) (white box). In a few crypts with evidence of mucus secretion (white arrow), *C. rodentium* colonization is dramatically lower than in other crypts. In certain areas, *C. rodentium* clusters/aggregates can be seen in close proximity to the epithelial surface, coinciding with the absence of any mucus (red box). Original magnification 200x, scale bar 50 µm.

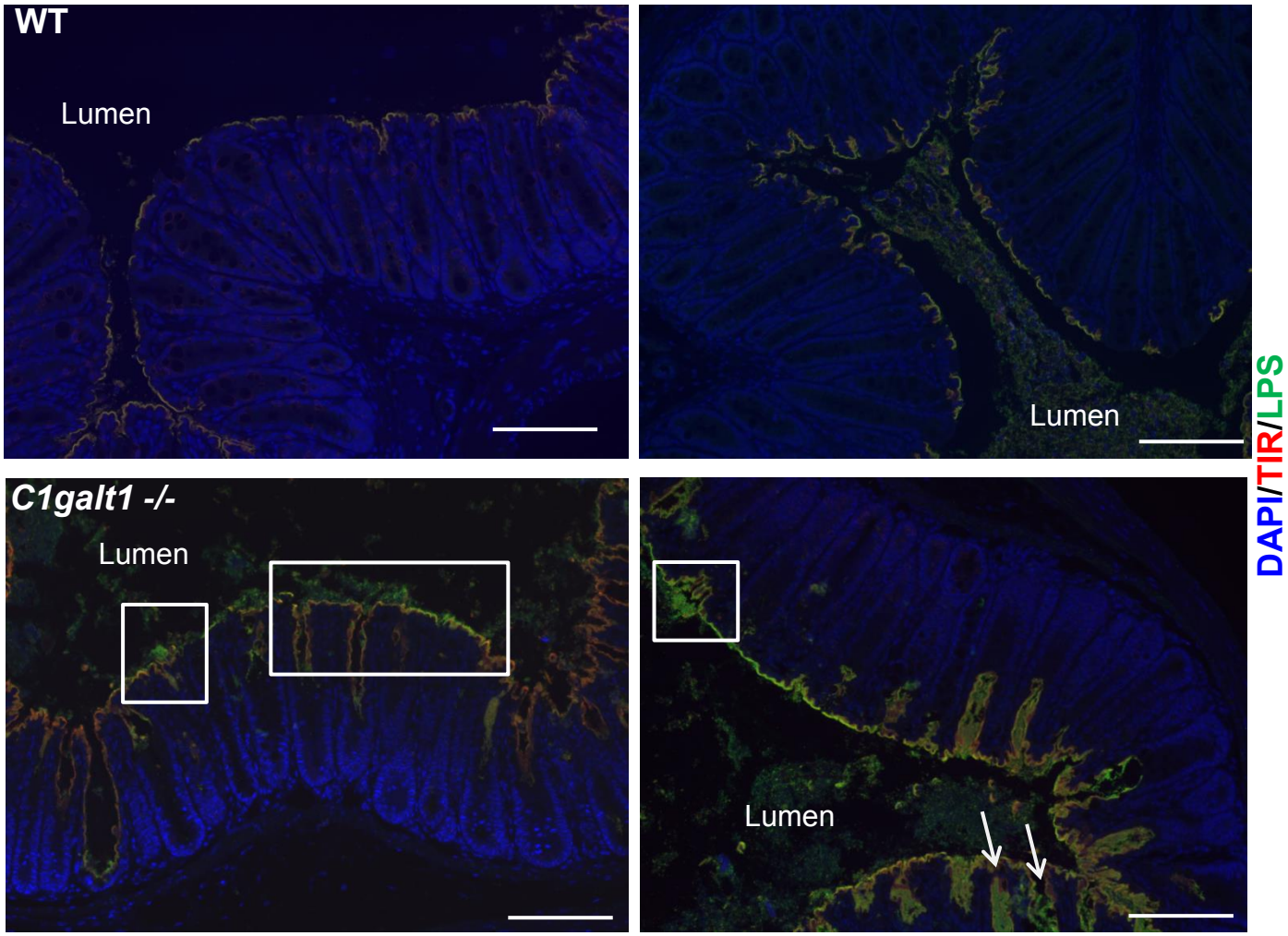

Figure 5.13 *C1galt1 -/-* mice contain microcolonies of *C. rodentium.*
Representative dual immunostaining profile (LPS- Green, *C. rodentium* infection marker Tir- Red, DAPI- counterstain, Blue). Top panel- In the distal colon of *C. rodentium* infected WT mice, the majority of *C. rodentium* (yellow, stains positive for LPS, green and Tir, red) can be seen localized along the epithelial surface (LPS positive, Tir negative) can be seen mostly in the intestinal lumen. Bottom panel- In *C1galt1 -/-* mice, the boxed areas shows the microcolony like structures (*C. rodentium*) in close proximity to the epithelial surface, and at some sites, directly interacting with the epithelium and invading the intestinal crypts. White arrows point to the clustering seen in the intestinal crypts. Original magnificantion 200x.

The role of fucose in controlling host susceptibility during *C. rodentium* infection

Fucose is an important intestinal sugar and a mediator of host-commensal symbiosis[161]. A recent study examined the role of host-induced intestinal fucosylation in providing host defense against enteric pathogens such as *C. rodentium* and *S. typhimurium*[163,335]. Furthermore, the role of fucose sensing by enteric pathogens, such as EHEC in modulating bacterial pathogenesis and metabolism has recently come to light[167]. Fucose appears to be a key player at the complex interface of interactions between the host, its microbiota and enteric pathogens. Our finding that *C. rodentium* infection induced host fucosylation of the intestinal Muc2 mucin as well as upregulated the expression of intestinal fucosyltransferases prompted us to investigate the role of fucose in *C. rodentium's* pathogenesis as well as its role in determining host susceptibility to *C. rodentium* infection. One of the key bacterial enzymes of the L-fucose metabolic pathway is the l-fuculose kinase encoded by the *fucK* gene[159,162]. Deletion of the *fucK* gene in *C. rodentium* results in *C. rodentium* being unable to utilize the fucose pathway. We began our investigations by constructing a non-polar *C. rodentium fucK* mutant. We also assessed the impact of L-fucose *in vitro* and *in vivo* on *C. rodentium* growth and virulence.

5.2.12 Fucose induces *C. rodentium* T3SS and affects biofilm formation *in vitro*

It has been recently shown that fucose sensing regulates the expression of the LEE pathogenicity island in EHEC[167]. We wondered if fucose would impact the expression of the T3SS in the related mouse pathogen *C. rodentium*. For the functional assessment of their type III secretion system, the bacterial strains were grown in DMEM with and without fucose. The secretion-deficient *C. rodentium ΔescN* mutant was used as a negative control. Notably there were no differences in the T3SS effector profile between the WT *C. rodentium* and Δ*fucK C. rodentium*, suggesting that the Δ*fucK* strain suffered no intrinsic defects in T3SS effector

secretion. We also noted that in presence of fucose, there was relatively more expression of T3SS virulence proteins, EspB and EspA in both WT *C. rodentium* and Δ*fucK*, implying that the presence of fucose induces T3SS system (Figure 5.14A), likely reflecting that fucose can still be sensed by the Δ*fucK C. rodentium*. We next assessed the role of fucose in biofilm formation and found that the presence of fucose significantly inhibited biofilm formation in WT *C. rodentium* (Δ0.23 OD_{595} units). However, the inhibition was to a much lesser degree (Δ0.03 OD_{595} unit) for the Δ*fucK* mutant, potentially due to its inability to utilize available fucose. Furthermore, the Δ*fucK* mutant displayed moderately but significantly lower biofilm formation in comparison to WT *C. rodentium* (Figure 5.14B). To confirm the specificity of response to L-fucose, we tested two other sugars, D-glucose and D-ribose and noted that the *fucK* mutant was only impacted when exposed to fucose (Figure 5.14C). Overall, this data suggested that fucose had subtle, but significant effects on the behaviour and virulence of *C. rodentium.*

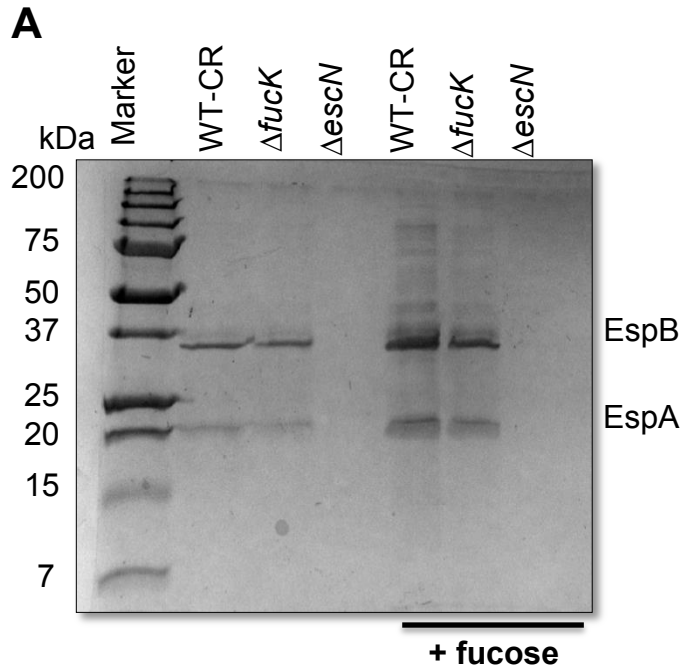

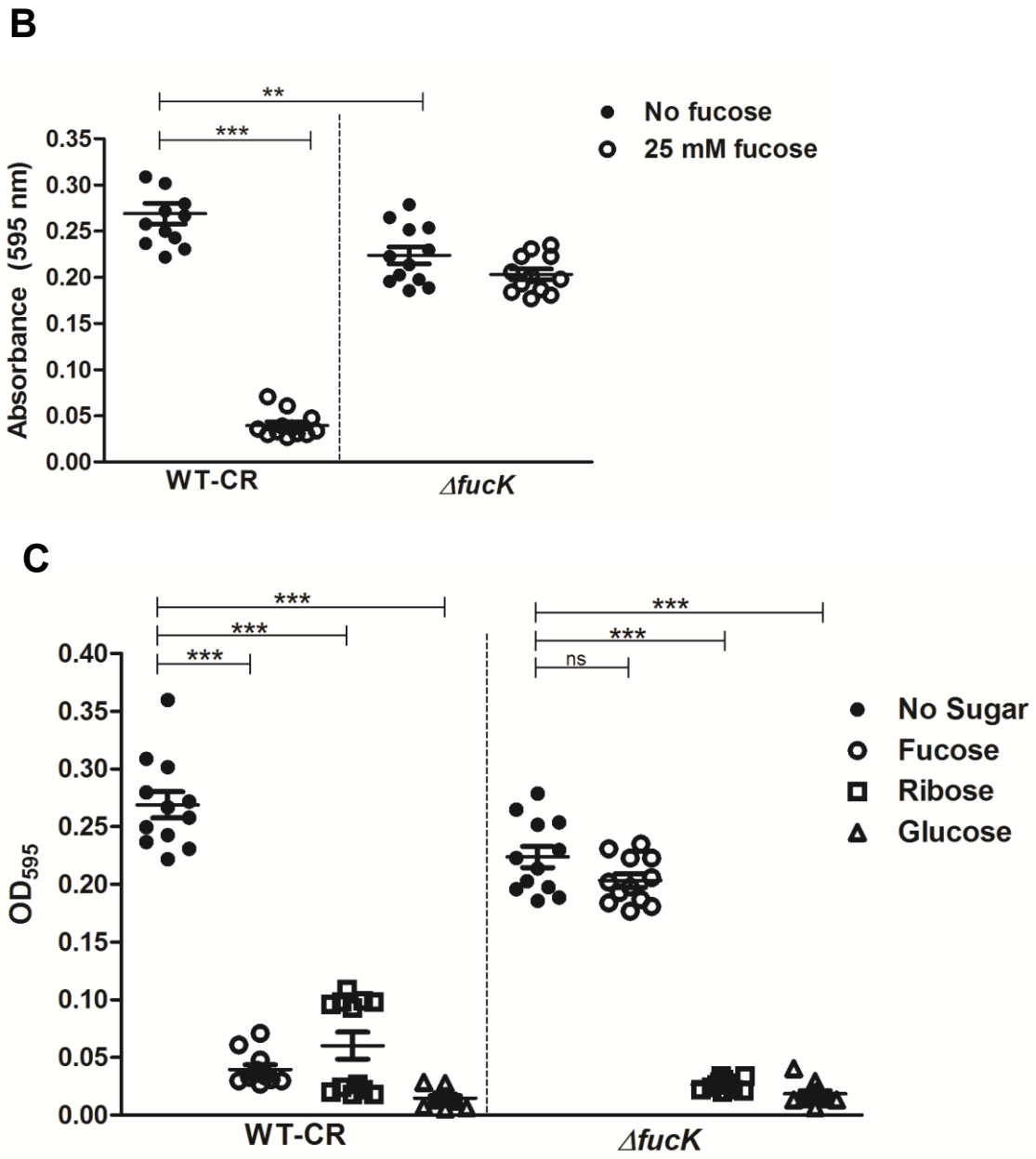

Figure 5.14 Assessing the impact of fucose on *C.rodentium*.
(A) WT *C. rodentium* and the Δ*fucK* mutant did not display any significant differences in their T3SS secretion profile after growth in DMEM with and without fucose. The presence of fucose resulted in increased secretion of T3SS dependent factors for both strains. *ΔescN C. rodentium* is a negative control strain that is T3SS-deficient. (B) Biofilm formation in LB (no salt) at 25° C for WT *C. rodentium* vs Δ*fucK C.rodentium* as measured using the Crystal violet assay with and without fucose. Fucose inhibited biofilm formation in WT *C. rodentium* whereas no impact was seen for Δ*fuck C.rodentium.* (C) Biofilm formation in WT *C. rodentium* and Δ*fucK C.rodentium* in the presence of L-fucose, and other carbon sources, D-glucose or D-ribose. This panel shows that *fucK* is only impacted by L-fucose, showing the specificity of its response to fucose. The asterisk indicates a significant difference (***, $P < 0.0005$, **, $P < 0.01$) by the Mann-Whitney test (ns- no significance difference).

5.2.13 Assessing the *in vivo* impact of fucose feeding on *C. rodentium* induced colitis

It has been previously shown that gavaging mice with exogenous L-fucose resulted in higher production of SCFA and played a role in increased host fitness under infection-induced stress[163,336]. To assess the impact of L-fucose on the course of *C. rodentium* infection, WT and *C1galt1 -/-* mice were infected with *C. rodentium* and gavaged with 1.23 mg of L-fucose for the first 5 days of the infection and then euthanized on day 6 PI. In WT mice, although there were no significant differences in pathogen burdens in the distal colon of mice infected with *C. rodentium* (no fucose) and *C. rodentium*(fucose supplemented) groups , there were significantly greater pathogen burdens in both cecal tissues (100 fold higher) and lumen (10 fold higher) in the fucose-fed group.

Curiously, we found no significant differences in the intestinal *C. rodentium* burdens for infected *C1galt1 -/-* with or without fucose treatment (Figure 5.15A). To determine whether exogenous fucose would impact the systemic translocation of *C. rodentium*, we analyzed systemic sites for pathogen burdens. In fucose-fed WT and *C1galt -/-* mice, there was a trend towards lower systemic pathogen burdens when compared to vehicle -treated counterparts at all systemic sites (Figure 5.15B). To assess if L-fucose affected bacterial aggregation/biofilm like structures *in vivo*, we examined *C. rodentium* localization using immunostaining in *C1galt1 -/-* mice, which have been previously shown to contain *C. rodentium* aggregates *in vivo* (Figure 5.12 and 5.13). In *C1galt1 -/-* mice, fucose treatment appeared to modestly alter the distribution of *C. rodentium* in the distal colon. While the mucosal surface area stained positive for *C. rodentium* was still comparable, in contrast, in the fucose-fed mice, *C. rodentium* was not seen deep in colonic crypts and there appeared to be less pathogen aggregates in the crypts as well along the mucosal surface (Figure 5.15D). Overall this finding suggests that exogenous fucose (which

potentially mimics the state of increased intestinal fucosylation and increased fucose level during an infection- induced stress) may be playing a role in modulating *C. rodentium* infection.

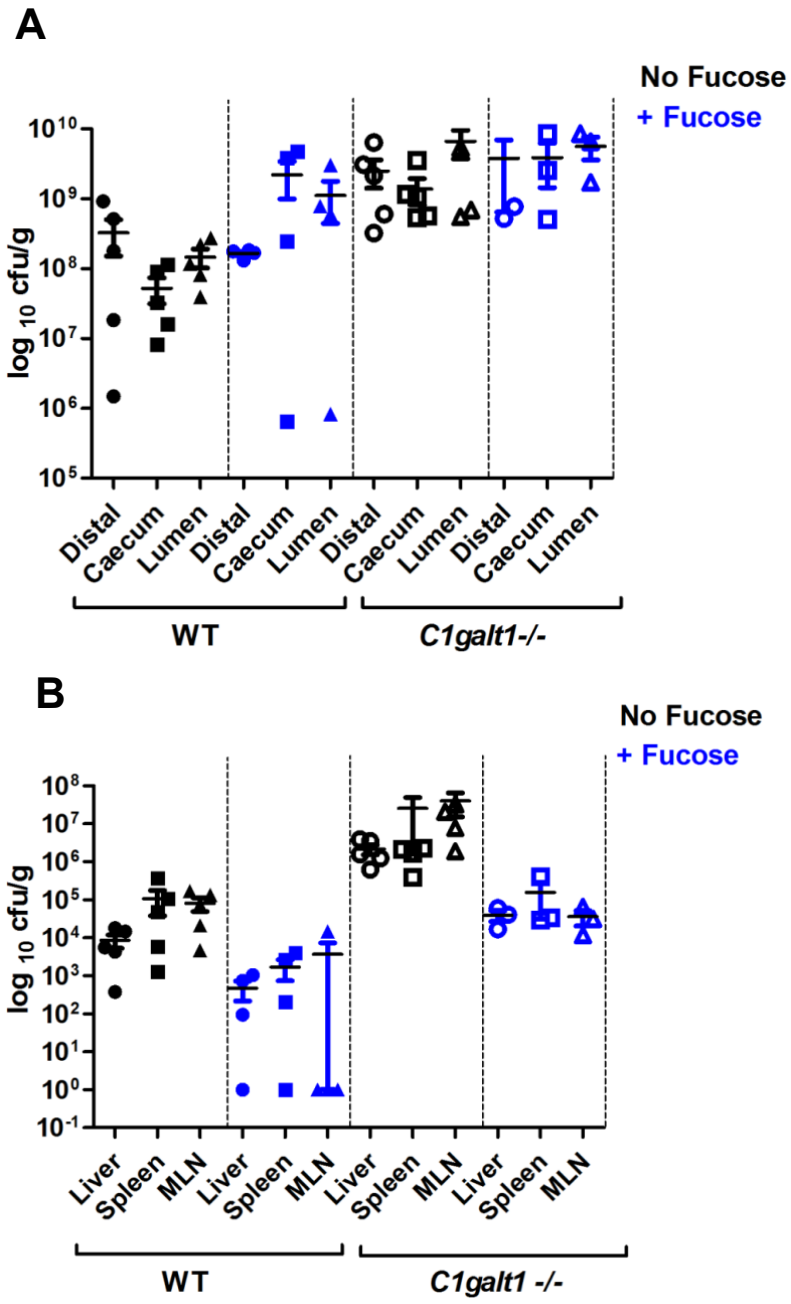

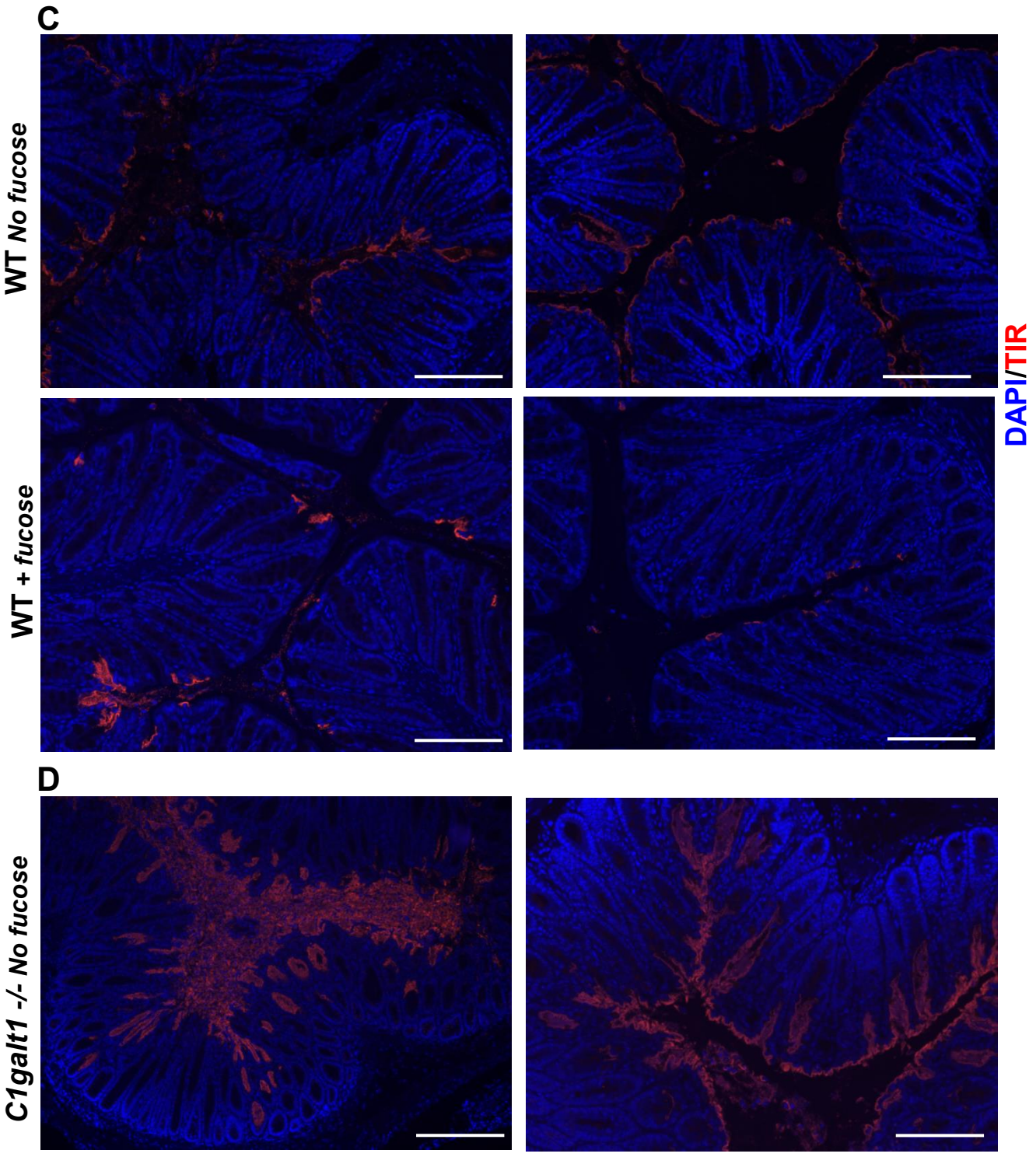
C
WT No fucose
WT + fucose
DAPI/TIR
D
C1galt1 -/- No fucose

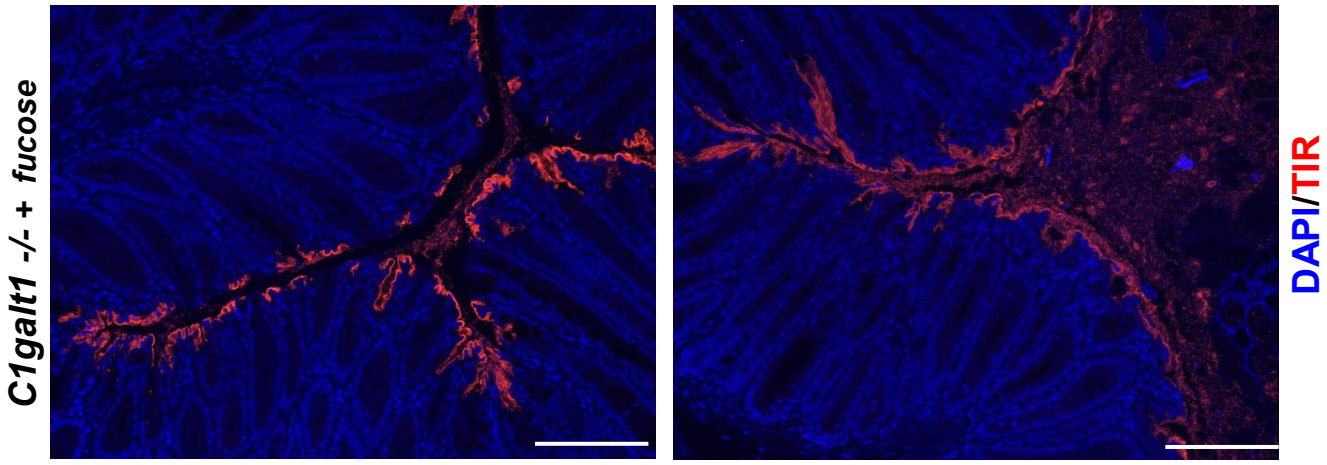

Figure 5.15 Exogenous fucose alters *C. rodentium* burdens and localization.
(A) Quantification of viable adherent *C. rodentium* burdens recovered from distal and cecal tissues and luminal, non-adherent burdens from WT and *C1galt1 -/-* mice, vehicle or fucose treated. No significant differences were detected in *C1galt1 -/-*. WT mice displayed higher *C. rodentium* burdens after fucose treatment. (B) Systemic pathogen burdens enumerated from liver, spleen and MLN. Fucose-fed groups had lower *C. rodentium* burdens at all systemic sites. Results are pooled from 2 independent infections (n=6 per group). (C) Representative images showing *C.rodentium* localization, using Tir staining in the distal colon. Note the altered *C. rodentium* colonization along the epithelial surface with fucose treatment. (D) *C. rodentium* localization as seen in *C1galt1 -/-* mice with and without fucose treatment. When infected with *C. rodentium* (without fucose), *C. rodentium* was seen aggregating along the surface and intestinal crypts as well as penetrating deep into the crypts. Fucose treatment appeared to dissipate such colonization pattern to some extent. Original magnification 200x.

5.2.14 *In vivo* characterization of Δ*fucK C. rodentium*

Based on the observation that fucose affects *C. rodentium* characteristics *in vitro* and the impact of fucose on *C. rodentium* colonization *in vivo*, we next looked at whether the inability of *C. rodentium* to utilize fucose in the murine gut would alter pathogen burdens and disease susceptibility. We infected WT mice with WT *C. rodentium* and Δ*fucK* (lacking l-fuculose kinase, impaired in utilization of the fucose pathway) *C. rodentium* and followed the course of infection. Mice were euthanized at day 6 PI. While infected WT mice displayed almost no weight loss with WT *C. rodentium* infection, they exhibited significantly greater weight loss (~10%) when infected with Δ*fucK C. rodentium* (Figure 5.16A). Δ*fucK C. rodentium* infected WT mice also showed greater macroscopic damage, as seen by loss of stool contents and edema

throughout the colon. *C1galt1 -/-* mice on other hand, displayed similar weight loss with both strains and there were no significant differences in susceptibility (Figure 5.16A), potentially because there is little fucose in *C1galt1 -/-* mice, thereby minimizing the impact that the presence of FucK signalling would have during *C. rodentium* infection

While there were no significant differences in pathogen burdens between WT *C. rodentium* and Δ*fucK* mutant when infecting *C1galt1 -/-* mice, WT mice carried significantly greater pathogen burdens when infected with Δ*fucK C. rodentium* in comparison to WT *C. rodentium* (Figure 5.16B). At day 6 PI, Δ*fucK* infected WT mice showed significantly greater pathology scores, as reflected by crypt epithelial cell hyperplasia and inflammatory cell infiltration, greater damage to the epithelial surface in the distal colon and goblet cell depletion in comparison to WT *C. rodentium* infected counterparts. *C1galt1 -/-* mice showed no significant differences in the pathology score for both strains (Figure 5.16C, 5.16D). Next we measured the comparative fitness between the WT *C. rodentium* and Δ*fucK C. rodentium* in WT mice using competitive index (CI) studies. CI provides a more sensitive measure of bacterial virulence. We found that Δ*fucK* had a CI index of 1.435 ± 0.22, suggesting that Δ*fucK* outcompeted WT *C. rodentium* in the murine distal colon, the predominent site of infection by *C. rodentium*.

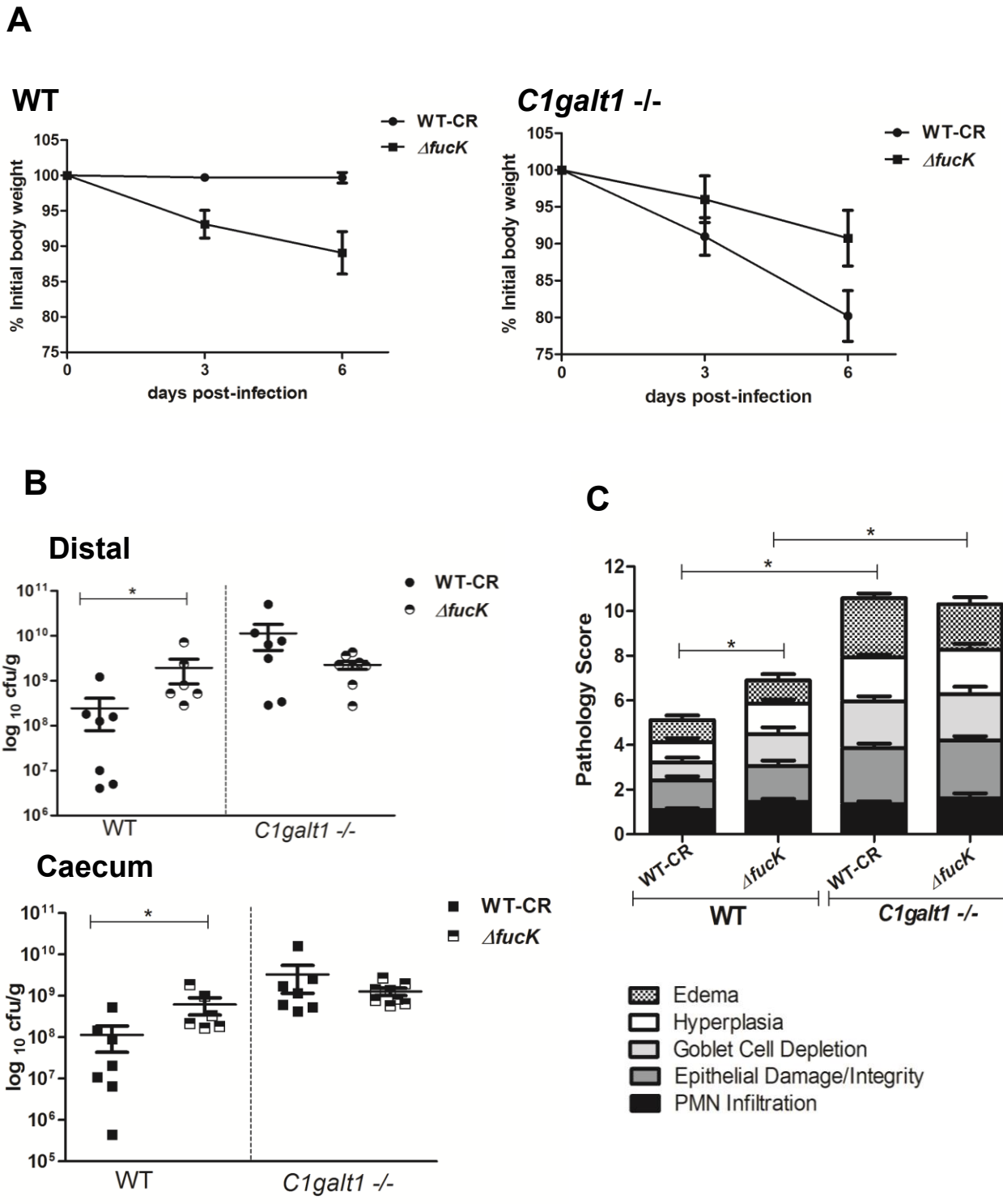
A
WT
C1galt1 -/-
WT-CR
ΔfucK
% Initial body weight
days post-infection
B
Distal
Caecum
log 10 cfu/g
WT
C1galt1 -/-
C
Pathology Score
Edema
Hyperplasia
Goblet Cell Depletion
Epithelial Damage/Integrity
PMN Infiltration

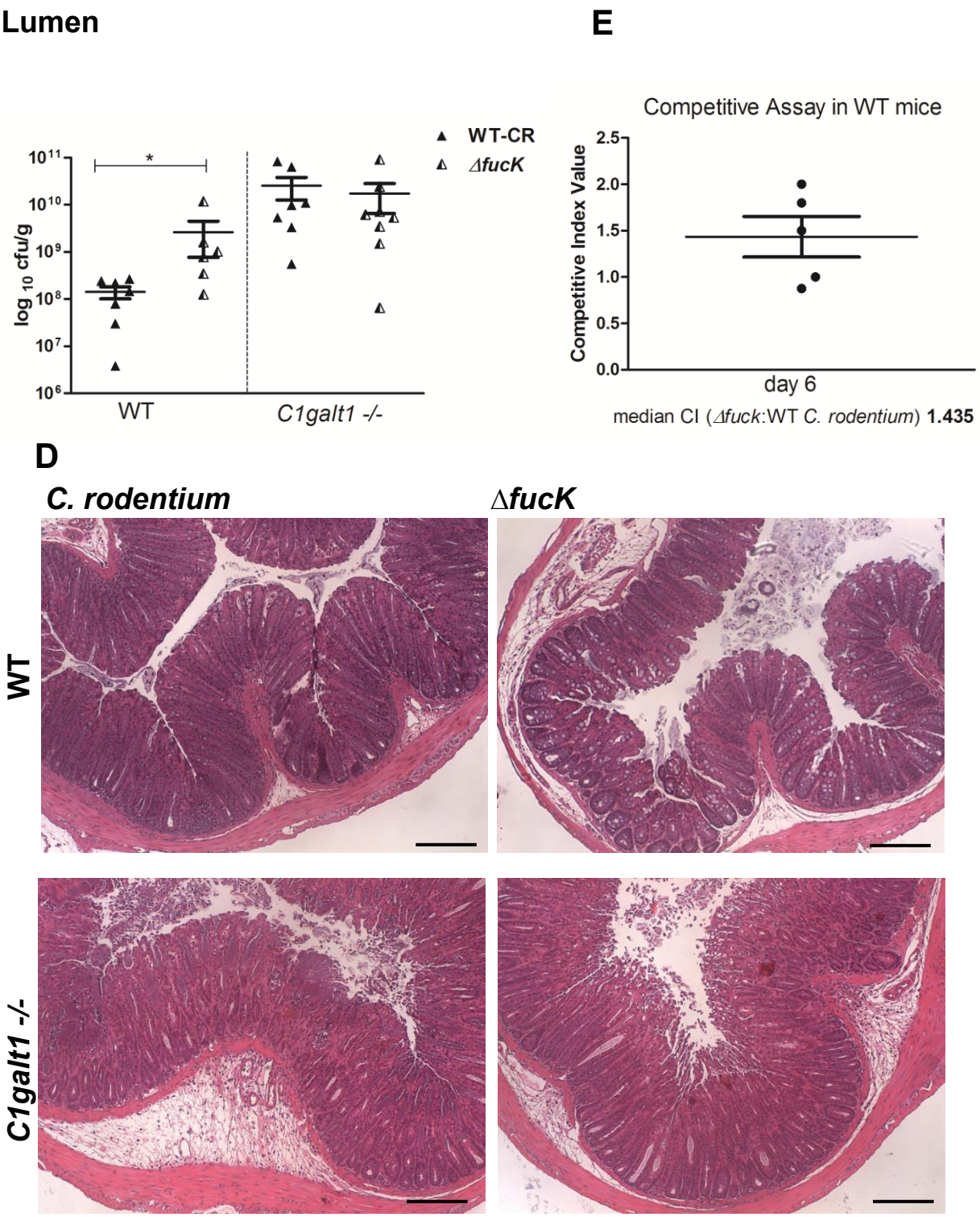

Figure 5.16 *C. rodentium* Δ*fucK* causes exaggerated damage and heavier colonization in WT mice.

(A) Weight loss of WT and *C1galt1 -/-* mice infected with WT *C. rodentium* (●) and Δ*fucK* (■), plotted as % of initial body weight and normalized to day 0 weight. (B) Adherent (distal and cecal tissues) and non-adherent luminal *C. rodentium* burdens at day 6 PI enumerated from WT and *C1galt1 -/-* mice, infected with WT or Δ*fucK C. rodentium*. Error bars represent SEM, and

asterisks indicate significant differences (*, $P < 0.05$), Mann-Whitney test). Results are pooled from 2 independent infections (n=6/7 mice per group). (C/D) Histopathological analysis of WT and *C1galt1 -/-* mice infected with WT *C.rodentium* or Δ*fucK. C. rodentium* Δ*fucK* caused heightened histopathological damage in WT mice in comparison to WT *C. rodentium* whereas the pathology scores were similar for both strains in *C1galt1 -/-* mice. Original magnification 100x. Results are representative of 2 independent experiments. (E) Competitive index (CI) of simultaneous WT and *C. rodentium* Δ*fucK* infection day 6 PI in the distal colon of WT mice. A CI > 1 indicates that *C. rodentium* Δ*fucK* outcompeted WT *C. rodentium* in a competitive assay.

5.2.15 *C. rodentium* Δ*fucK* causes exaggerated mucus secretion in WT mice

C. rodentium infection has been shown to induce mucus secretion at the peak of infection (day 6-day 10). As a consequence of this induced mucus secretory response, goblet cells often appear depleted of mucin, which is a hallmark of *C. rodentium* infection[145,190,321]. While analyzing H&E stained slides, we noted that in the Δ*fucK* infected WT mice; there were greater numbers of mucus filled goblet cells in comparison to WT *C. rodentium* infected mice. To test whether Δ*fucK*altered the mucus secretion responses during infection, we checked for mucin secretion responses in the distal colon using Muc2 immunostaining. While WT *C. rodentium* infection was associated with an increase in mucin secretion, there was notably higher mucus secretion seen with the Δ*fucK* infection, where mucus could be seen accumulating in the intestinal lumen, suggesting that the host might be releasing more mucus in an effort to reduce pathogen virulence, but it does not work with the *fucK* mutant that can't use the fucose. There were no obvious differences in the mucus secretion responses in *C1galt1 -/-* mice infected with WT *C. rodentium* and Δ*fucK C. rodentium*.

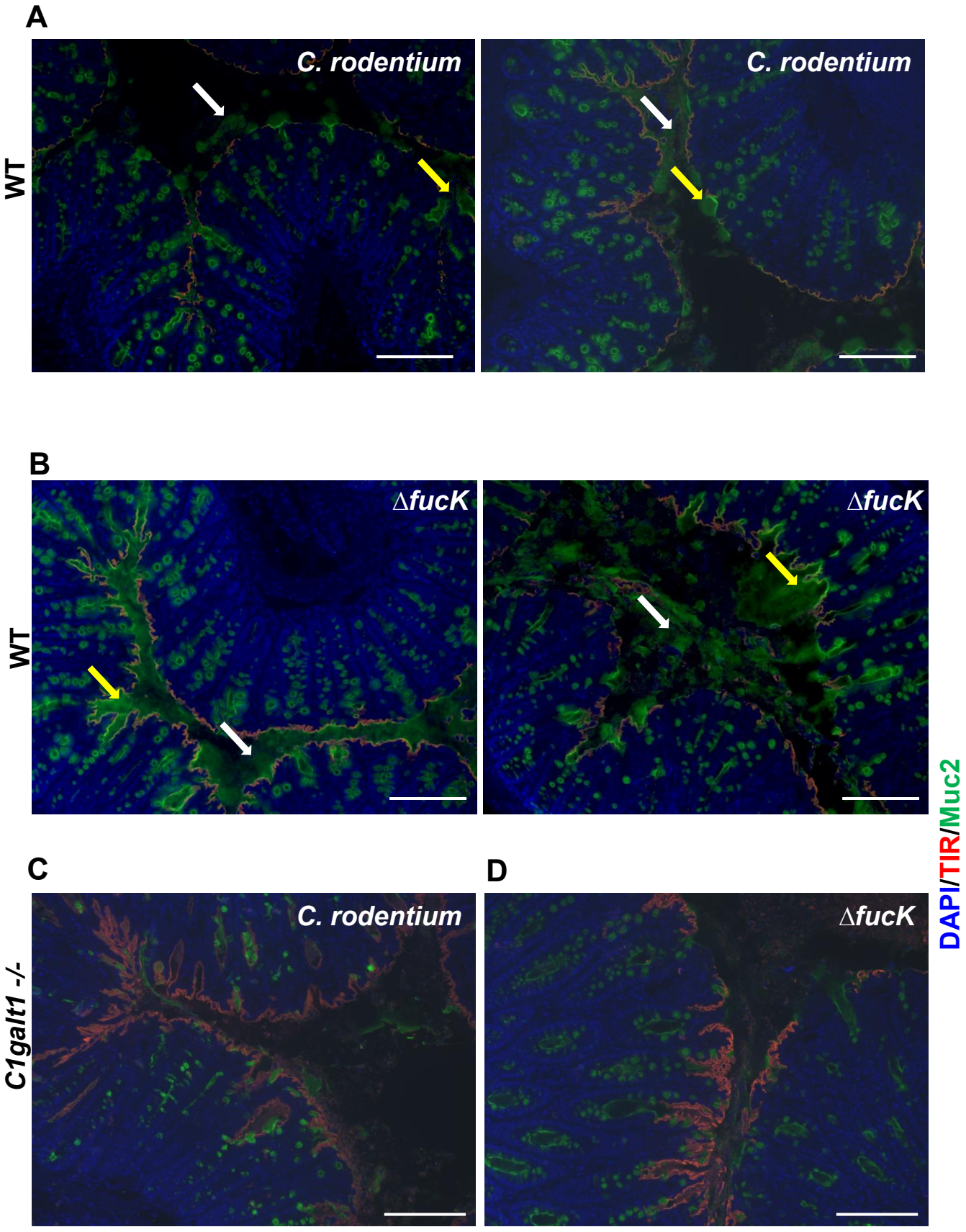
A
C. rodentium
C. rodentium
WT
B
ΔfucK
ΔfucK
WT
C
D
C. rodentium
ΔfucK
C1galt1 -/-
DAPI/TIR/Muc2

Figure 5.17 *C. rodentium* Δ*fucK* causes mucus hyper secretion response in WT mice. Mucin Muc2 (green), Tir (red); shows the association of *C. rodentium* with Muc2-positive crypts), and DAPI (nuclei; counterstain) are shown. (A) Mucus responses induced during WT *C. rodentium* infection, as seen by secreted mucus in the lumen and mucus filled goblet cells in WT mice. (B) Increased mucus release caused by Δ*fucK C. rodentium* infection. White arrow points to the luminal mucus whereas yellow arrowhead denotes the release of the Muc2 mucin from the intestinal crypts. (C/D) Mucus secretion responses during WT *C. rodentium* and Δ*fucK C. rodentium* in *C1galt1 -/-* mice. No obvious differences were noted in terms of the mucus release between the two strains infecting the *C1galt1 -/-* mice. Original magnification 200x.

5.2.16 *C. rodentium* Δ*fucK* display altered localization in the distal colon of WT mice

Next we examined WT *C. rodentium* localization in the distal colon by staining for the translocated intimin receptor (Tir) and LPS. WT *C. rodentium* primarily infected the mucosal surface (stained positive for Tir) but did not show any invasion/deeper penetration of the intestinal crypts. However, in the Δ*fucK* infected mice, there was significantly more staining for *C. rodentium* on the mucosal surface. Δ*fucK C. rodentium* was also seen invading crypts which is usually not seen with WT *C. rodentium*. *C1galt1 -/-* mice, on the other hand, did not reveal any dramatic differences in *C. rodentium* localization with WT or Δ*fucK* mutant. Thus WT mice displayed increased susceptibility to Δ*fucK C. rodentium* in comparison to WT *C. rodentium.*

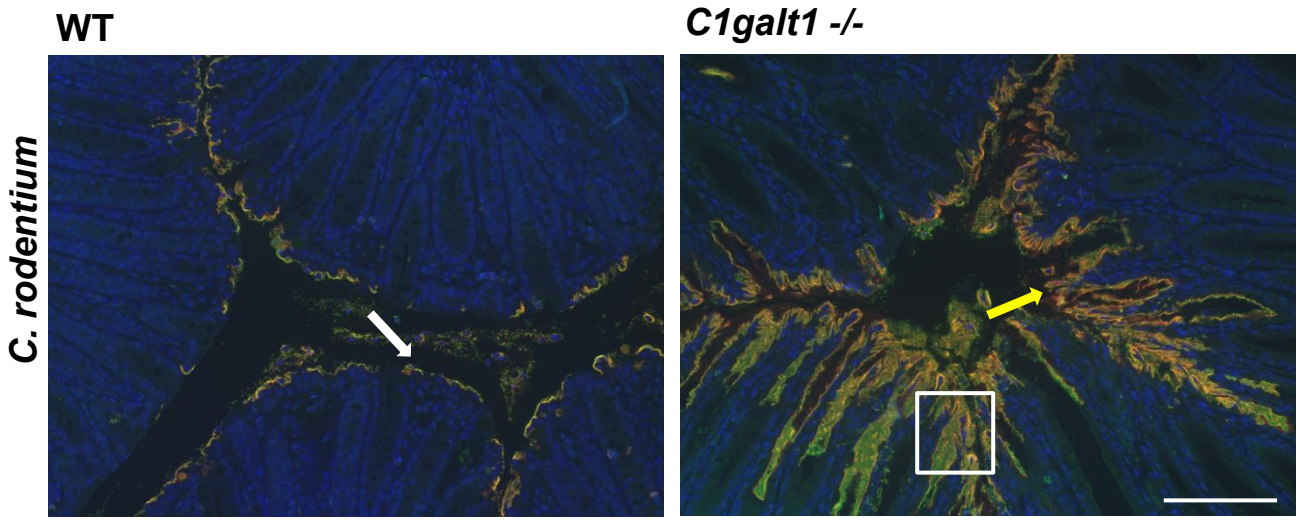

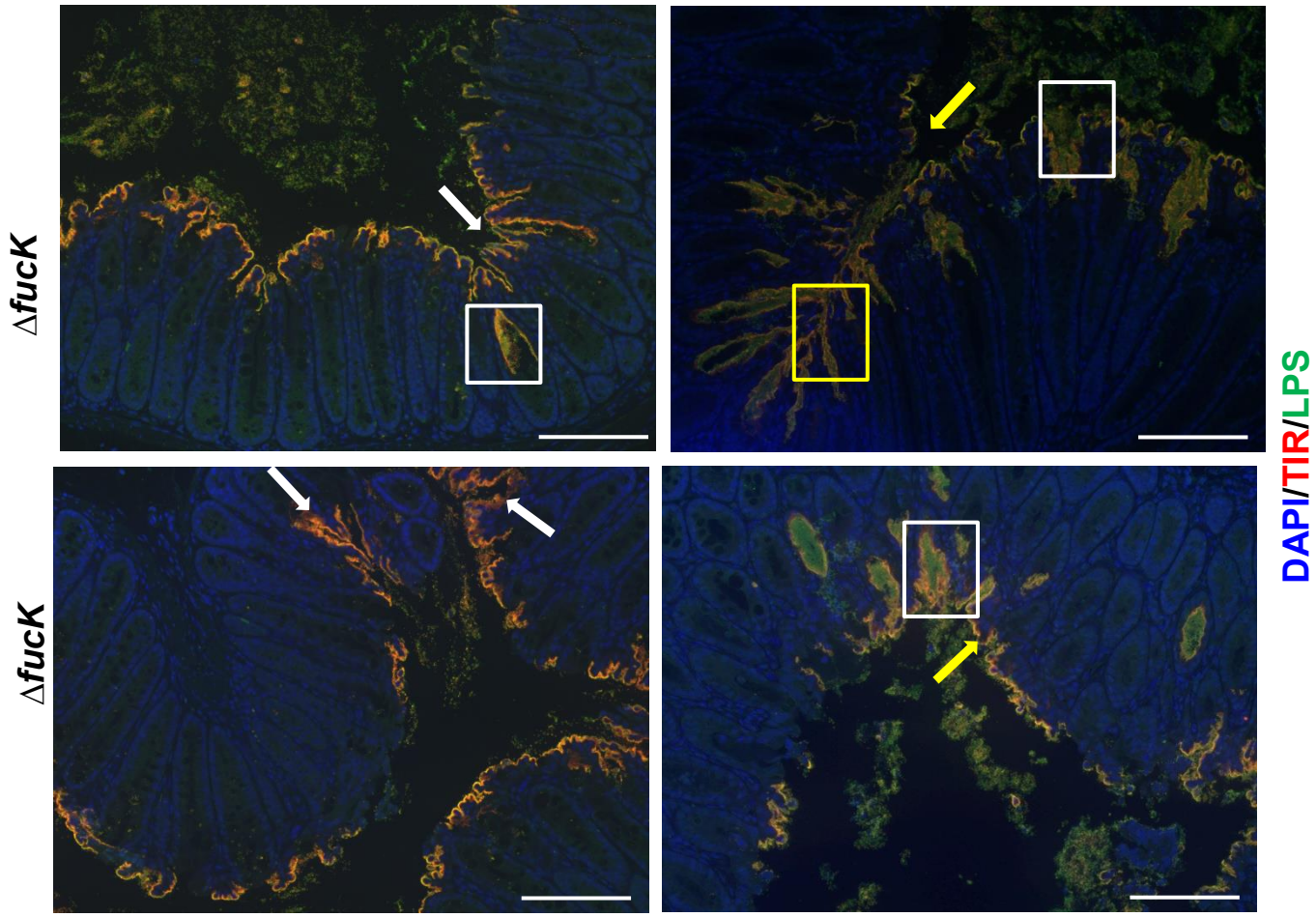

Figure 5.18 Δ*fucK C. rodentium* display altered localization in the distal colon. Representative combined immunostaining images for *C. rodentium* LPS (green), *C. rodentium*-specific effector Tir (red) and DAPI (blue, nuclei, and counterstain) in distal colon of infected WT and *C1galt1-/-* mice with WT and Δ*fucK C. rodentium*. (Left panel) *C. rodentium* Δ*fucK* colonizes a greater surface area of the intestinal mucosa and shows deeper penetration into intestinal crypts (white arrow). (Right panel) In addition to heavier colonization on the mucosal surface (yellow arrowhead and yellow box), *C1galt1 -/-* mice also have greater non-adherent luminal bacterial burdens, which can be seen invading the intestinal crypts along with *C. rodentium* (white box) Note that while there were no dramatic differences between the WT *C. rodentium* and Δ*fucK* non-adherent luminal burdens (green), Δ*fucK C. rodentium* had lesser surface area staining positive for Tir when compared to WT *C. rodentium* in *C1galt1 -/-* mice.

5.2.17 L-fucose transport provides advantage to *C.rodentium in vivo*

As previously mentioned, exogenous L- fucose provided a colonization advantage to WT *C. rodentium in vivo* as seen by higher colonization levels in the colonic sites when compared to the infected group without exogenous L-fucose. To further assess the basis for the advantage of fucose transport and fucose metabolism to *C. rodentium in vivo*, we infected WT and

C1galt1 -/- mice with *C. rodentium* Δ*fucK* with and without L-fucose supplementation and euthanized mice day 6 PI. In the presence of exogenous L-fucose, *C. rodentium* Δ*fucK* infected mice displayed reduced weight loss when compared to the groups infected with *C. rodentium* Δ*fuck* without fucose supplementation. *C. rodentium* Δ*fucK* showed significantly lower pathogen burdens at colonic sites (distal, caecum and lumen) in the presence of exogenous L-fucose (Figure 5.19B). Furthermore, there was no systemic translocation noted in the fucose fed group, suggesting that in the presence of excess L-fucose, *C. rodentium's* inability to utilize L-fucose conferred a colonization disadvantage (Figure 5.19C), potentially through the impact of fucose on the host, or on commensal bacteria that can use it. Interestingly, there were no overt differences noted with and without fucose supplementation in the infected *C1galt1 -/-* mice (Figure 5.19B and 5.19C).

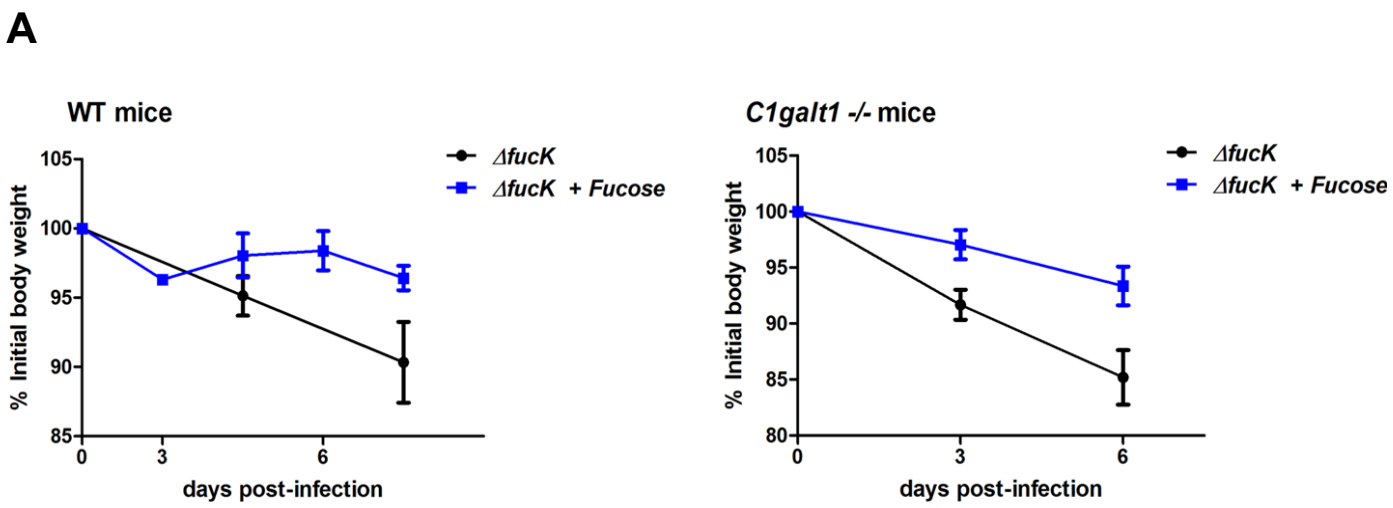

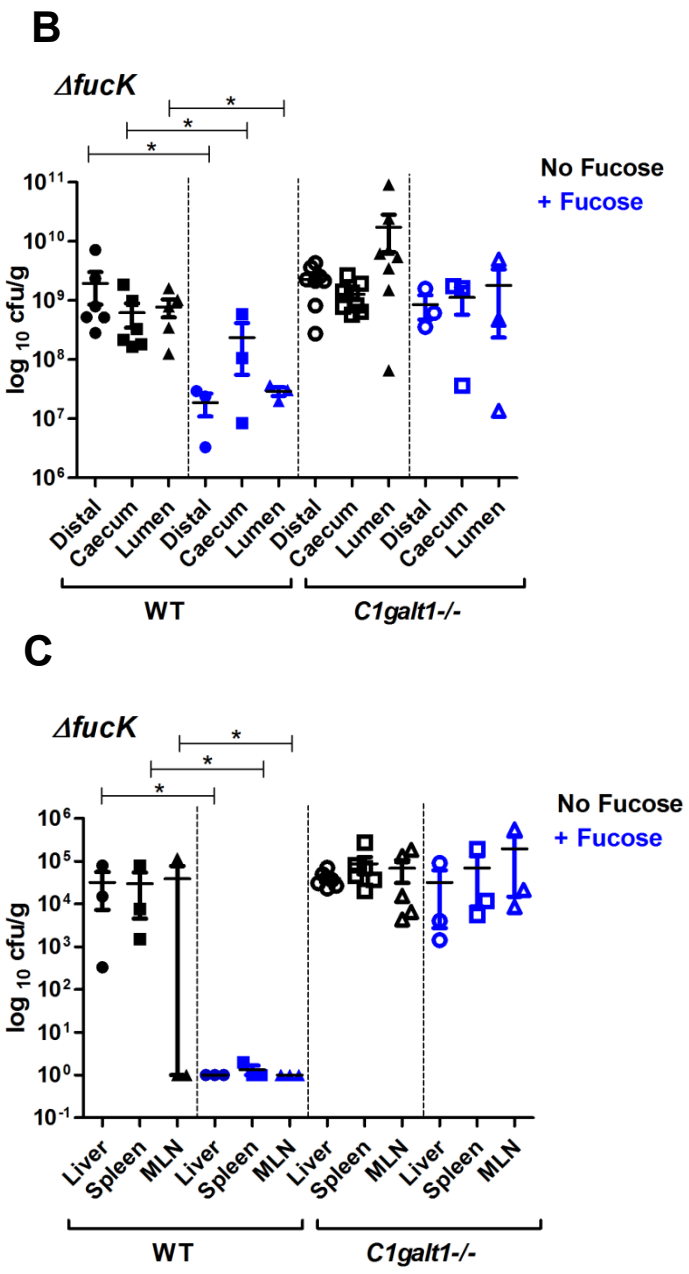

Figure 5.19 *C. rodentium* Δ*fucK* shows decreased colonization in the presence of exogenous L-fucose.
(A) Weight loss data with and without fucose supplementation in WT (left) and *C1galt1 -/-* (right) mice infected with Δ*fucK* C. *rodentium.* (B/C) C. *rodentium* burdens enumerated from colonic sites (distal, caecum, lumen) and systemic sites (liver, spleen, MLN) respectively on day 6 PI. WT and *C1galt1 -/-* mice were infected with Δ*fucK* C. *rodentium* with (blue) or without exogenous L-fucose inoculation (black). Fucose fed WT group had significantly lower pathogen burdens at all sites. (*, $P < 0.05$), Mann-Whitney test, error bars represent standard error mean (SEM). Results are representative of 2 independent infections (n=6 mice per group).

5.3 Discussion

The intestinal mucus layer is the primary defense barrier against noxious agents such as pathogens, food toxins, and bacterial products/antigens. Absence of the glycoprotein Muc2 in the intestine has been linked to increased susceptibility to enteric pathogens, such as *C. rodentium* and *S. typhimurium*[133,144,145,321]. We now understand that the Muc2/mucus layer has multifaceted roles in host defense. Despite the fact that the Muc2 mucin is 80% carbohydrates by mass and is decorated by several different glycans, thereby providing a functional integrity and complexity to the mucus layer, our understanding of the role and the importance of these glycosylations is fairly limited. To our knowledge, this is the first study to investigate the role of core 1 and core 3 derived O- glycosylation using an infectious colitis model. In this study, we provide evidence that while both core 1 and core 3 derived O-glycans are crucial in providing host defense, the absence of core 1 derived O- glycans dramatically increases host susceptibility to the A/E pathogen *C. rodentium*. Impaired goblet cell responses, a thinner intestinal mucus barrier, increased systemic translocation of the pathogen, development of *C. rodentium* microcolonies and deeper invasion into the crypts resulted in dramatically increased susceptibility of *C1galt1 -/-* mice to *C. rodentium*. Overall these findings suggest that core 1 derived-O glycans are an important component for maintaining the integrity of the mucus layer, and providing host defense by at least partially controlling luminal and mucosal pathogen burdens. However, the importance of robust host innate and adaptive responses in regulating the bacterial burdens at the mucosal surface cannot be ignored. $CD4^+$ T cells and B cells are required for *C. rodentium* clearance[213,219] and the production of several host mediators such as AMPs and cytokines[74] can play an important role in limiting bacterial colonization during *C. rodentium* infection. Rather than focusing on all different host responses, for the purpose of this

study, we focused on characterizing the role of the frontline defense barrier, Muc2 and its glycosylation in host defense.

Overall, *C1galt1 -/-* mice (thinner mucus layer) displayed a similar susceptibility phenotype to *Muc2 -/-* mice (no mucus layer), suggesting that the absence of the predominant type of glycosylation of the Muc2 mucin has effects similar to loss of the entire mucus layer. While *Muc2 -/-* mice have minimal mucin secretion responses[145], *C1galt1 -/-* mice demonstrated altered goblet cell responses (such as significantly reduced mucus flushing), implying that the underlying basis of their heightened susceptibility may be dependent on the integrity of the mucus barrier and mucus-mediated flushing. Furthermore, mucin secretion responses appeared to be important for regulating pathogen burdens and preventing the formation of bacterial aggregates (microcolony-like structures). In both *Muc2 -/-* and *C1galt1 -/-* mice, there was evidence of the increased presence of invasive microcolonies which were virtually absent in WT and *C3GnT -/-* mice. Furthermore, their altered mucus barriers (thickness, glycosylation status) ultimately contributed to increased translocation of *C. rodentium* into the mucosa and increased pathogen burdens at systemic sites. Consistent with previous studies, our data supports the concept that Muc2 production and secretion are critical host defense mechanisms that regulate the interactions of *C. rodentium* with the intestinal mucosal surface[145]. It was equally intriguing to note that the induction of goblet cell mediator (Tff3 and Relm-β) responses was also affected in *C1galt1 -/-* mice. It has been previously shown that impaired O-glycosylation and the presence of non-modified glycoconjugates (due to altered activity of glycosyltransferases) in a goblet cell's golgi apparatus can cause endoplasmis reticulum (ER) stress[150,337,338]. Although this would require further examination, it is possible that ER stress responses could be triggered in

C1galt1 -/- mice due to the presence of the biosynthetic intermediate Tn antigen, ultimately affecting the protein translation of Tff3 and Relm-β.

Although loss of core 3 derived O-glycans has been shown to cause a ~40% reduction in their Muc2 protein levels[140], *C3GnT -/-* mice did not display dramatically heightened susceptibility to *C. rodentium* infection, as compared to the susceptible *C1galt1 -/-* mice. *C3GnT -/-* mice carried comparable *C. rodentium* burdens at their colonic and systemic sites and suffered similar histopathological damage in the distal colon, but modest, yet significantly greater intestinal barrier permeability than WT mouse counterparts. *C3GnT -/-* mice displayed greater signs of infection in their ceca, as assessed by histology scoring, when compared to WT counterparts. This finding is consistent with our earlier study looking at Muc2 and *Salmonella* (Chapter 3) where lack of core 3 O-glycosylation (*C3GnT-/-* mice) did not impact pathogen burdens but resulted in epithelial barrier dysfunction[144]. Overall, this implies that core 3 derived O-glycans could be playing a generic role in controlling epithelial barrier function induced by enteric pathogens, such as *C. rodentium* and *Salmonella*. The modest impact on pathology may be attributed to the fact that core 3 derived O- glycans make up to only 1% of the total Muc2 O-glycome in mice whereas core 1 derived O-glycans are the predominant component of the Muc2 O-glycome[124]. Absence of the C3GnT enzyme, a key enzyme solely responsible for the synthesis of core 3 derived O-glycans in the intestinal tract, still allowed for the retention of core 1 derived O-glycans. Furthermore, *C3GnT -/-* mice showed comparable induction of all goblet cell responses to their WT counterparts. Overall, these findings suggest that although core 3 derived O-glyosylation is important in controlling maintenance of mucosal barrier integrity, it had little effect on other readouts during infection such as pathogen burdens and mucosal responses.

Absence of core 1 derived O- glycans in mice can result in the eventual development of spontaneous colitis (not seen at our facility however), which has largely been attributed to a thin mucus layer, accompanied by a breached inner mucus barrier (commensals can be seen interacting with the epithelial surface) and altered intestinal mucosal barrier function[150]. To better define the role of core 1 derived O-glycosylation during *C. rodentium* pathogenesis, we infected mice lacking *C1galt1*, an enzyme responsible for the synthesis of core 1 derived-O glycans[339]. Interestingly, *C1galt1 -/-* mice proved highly susceptible to *C. rodentium* infection and showed a strikingly similar phenotype to that observed in infected *Muc2 -/-* mice. In addition to heavier pathogen burdens at all colonic sites, these mice developed exaggerated damage to their epithelial barrier, as indicated by increased intestinal barrier permeability and subsequently greater translocation of *C. rodentium* to systemic sites. We also noted that infected *C1galt1 -/-* mice were prone to the development of mucosal ulcers. It is likely that the ulcerated regions represent the site of increased pathogen translocation into the tissues, resulting in greater infiltration of PMN (neutrophils), ultimately leading to exaggerated inflammation. This was further supported by staining for Ki67, a cell proliferation marker. We noted that while *C. rodentium* infection induced crypt hyperplasia and IEC proliferation in both WT and *C3GnT -/-* mice, there was a greater induction of IEC proliferation in *C1galt1 -/-* mice, indicative of accelerated inflammation in these mice.

The presence of microcolonies/bacterial aggregates in close proximity to the epithelial surface as well as inside the intestinal crypts in *C1galt1 -/-* mice was intriguing. This phenotype has been previously observed in *Muc2 -/-* mice infected with *C. rodentium* as well as in WT mice infected with *C. rodentium ΔpicC* (lacking Pic, a class 2 SPATE, characterized in Chapter 4) suggesting that this phenotype can be mediated by host as well as pathogen factors[145,340].

Interestingly, in *C1galt1 -/-* mice, while the regions lacking Muc2 showed heavier bacterial aggregation, the intestinal crypts where mucus secretion was evident did not demonstrate significant bacterial aggregation of adherent *C. rodentium*. We also noted that *C1galt1 -/-* mice had impaired commensal depletion as well as greater luminal burdens of *C. rodentium* as enumerated using stool counts over the course of infection, suggesting that overall these mice carried heavier pathogen burdens when compared to their WT counterparts. We propose that in the absence of Muc2-mediated luminal flow, bacteria are able to aggregate in close proximity to the epithelial surface as well as inside intestinal crypts. Muc2-mediated flushing is also thought to play an important role in host protection by regulating commensal burdens on the mucosal surface[145]. *C1galt1 -/-* were impaired in commensal depletion (~20% reduced commensal depletion in comparison to WT counterparts), providing further evidence that impaired Muc2 function in these mice potentially contributed to reduced host-mediated bacterial clearance from the epithelial surface and greater bacterial burdens in their GI tract. Mucins have been shown to inhibit EPEC adherence to intestinal cells and have been shown to limit the binding of pathogens such as *Campylobacter* to the cell surface[195,197,341]. Therefore it is possible that loss of core 1 O-derived glycans limits such protection and exposes the underlying mucosa to invasive *C. rodentium* burdens, ultimately contributing to heightened tissue damage. It is also likely that absence of the mucus layer (*Muc2 -/-* mice) and/or reduction in the thickness of the mucus layer (*C1galt1 -/-* mice) may create an environment of nutritional deprivation for the pathogens as they have limited supply of nutrients. Under these circumstances, biofilm formation may assist in persistence of pathogens inside the host[342–344].

Mucus glycosylation is thought to play an important role in maintaining intestinal homeostasis as well as microbial ecology. A previous study outlined gut microbiota composition

in WT and *C1galt1 -/-* mice and identified few differences in their intestinal microbiota at baseline levels[345]. In accordance with their results, we also noted only subtle changes in the baseline microbiota composition of these mice. While there were no notable differences in Bacteriodetes and γ-proteobacteria phyla, O-glycosylation may be playing a role in regulating the Firmicutes phyla as the proportions of Firmicutes were significantly lower in *C1galt1 -/-* mice while they only showed a trend towards reduced numbers in the *C3GnT -/-* mice. At this point, the link between O-glycosylation and Firmicutes levels is not clear, but it might reflect that the absence of predominant core O- derived glycosylation alters the microenvironment (nutrients/food source) and hence sustainability of certain bacterial populations and may thus limit the presence of certain bacterial populations[346,347]. This may ultimately result in skewed intestinal homeostasis and altered host responses during infection. A recent paper reported the relative abundance of Firmicutes phyla associated with the intact colonic mucus layer, as determined by 16S microbial amplicon sequencing[348]. Therefore, it is possible that alterations in the mucus layer (i.e. absence of core 1 derived O-glycans) have a significant impact on Firmicutes abundance.

α-linked L-fucose comprises up to 14% of the total oligosaccharide content of intestinal mucin Muc2 and hence represents a predominant oligosaccharide component of this mucin[349]. Fucose utilization has been reported for both commensals as well as enteric pathogens[173,344,350]. While a systemic LPS challenge has been shown to induce host fucosylation in the small bowel as a defense mechanism to support fucose-feeding commensals which in turn produce more SCFA to strengthen the epithelial barrier[163], some enteric pathogens like EHEC are known to utilize their fucose sensing operon to regulate their expression of virulence and metabolic genes[167]. Addition of fucose to predominant core 1 derived O-glycans in mice was shown to be

exclusively attached to galactose residues which also form the basis for more complex mucin derived structures. Therefore, the absence of core 1 derived O-glycans may result in significant alterations in the dynamics of these modifications of the Muc2 mucin. Host fucosylation is mediated by specific intestinal fucosyltransferases. We noted that the expression of two predominant mouse α(1,2)fucosyltransferase genes, *fut1* and *fut2* was significantly upregulated during *C. rodentium* infection suggesting that IEC fucosylation could be a general host-induced defense response. This is consistent with findings from a previous study showing that bacterial challenge induces the expression of these fucosyltransferases[163]. Further mechanistic insights into how fucosylation can play a role in host defense provided a link between IL-22 and fucosylation, where IL-22 mediated activation of IL-22RI receptors in the intestinal epithelium enhanced host-microbiota mutualism by promoting fucosylation[335]. In our study, IL-22 was significantly upregulated during *C. rodentium* infection, further supporting a link between IL-22 and fucosylation at the epithelial surface. Furthermore, since intestinal dysbiosis is a key characteristic *of C. rodentium* infection marked by significant reduction in commensal numbers and diversity[74,221], induction of host fucosylation could be a key strategy used by the host to preserve commensal populations. This is the first study to document the fucosylation responses during *C. rodentium* infection.

In terms of the mucus-associated fucosylation responses- there was a proportional reduction in the positive UEA-1 staining in *C3GnT -/-* mice and *C1galt1 -/-* mice. Since it is estimated that 74% of the fucose in the intestine is mucin-derived[351,352], this may suggest that the status of fucose availability may vary between WT, *C3GnT -/-* and *C1galt1 -/-* mice, as the mucus thickness varies between each host. Although the exact implications are not well understood, it is plausible that fucosylation status may alter the intestinal microbiota, as there is

an intricate and complex nutrient controlled network in the intestine controlling the microbiota composition. Assessment of L-fucose levels in the mucus layer of WT, *C3GnT -/-* and *C1galt1 -/-* mice and fucosylation status of O-linked glycans in the intestine of these hosts will provide further evidence to support a correlation between mucus thickness and fucosylation levels.

L-fucose (the readily available form of fucose) appeared to have an effect on *C. rodentium* fitness, behaviour and pathogenesis, as suggested by its impact on T3SS secretion profiles and biofilm formation. The ability of fucose to inhibit biofilm formation *in vitro* was supported by reduced bacterial aggregation in *C1galt1 -/-* mice when infected with *C. rodentium* and subsequently fed exogenous L-fucose. The fact that WT *C. rodentium* showed greater intestinal colonization (as reflected by higher luminal and adherent tissue burdens) with fucose supplementation in WT mice suggests that *C. rodentium* is potentially using exogenous L-fucose for metabolism as a carbon source. Overall, these findings suggest a role for fucose availability on bacterial fitness and colonization success *in vivo*. Furthermore, host induced fucosylation during *C. rodentium* may play a role in affecting the fucose availability in the murine intestine.

This work also provides some insights into the complexity of the nutrient pool in the gut. We found that *C. rodentium* Δ*fucK* had a competitive advantage over WT *C. rodentium* when colonizing the murine intestine (competitive index analysis). This suggests that in a limited fucose environment, the ability to utilize fucose is not a requirement by *C. rodentium*, and it can rely on other monosaccharide food sources in the gut, such as L-ribose and D-galactose, food sources commonly not used by competing commensals[169,346,353]. Furthermore, *C. rodentium* Δ*fuck* was not impaired in intestinal colonization, suggesting that fucose sensing may not be necessary for promoting *C. rodentium* colonization in the murine intestine. However, when

excessive (exogenous) L-fucose was available, *C. rodentium* could potentially utilize L-fucose since the *C. rodentium* genome was annotated to contain all three key enzymes responsible for L-fucose degradation pathway- L-fucose isomerase (fucI), L-fuculokinase (fucK), L-fuculose phosphate aldolase (fucA) and the strain lacking the ability to do so (Δ*fuck)* suffered a colonization disadvantage. Metabolic versatility under nutrient constraints and exploiting available resources is an important prerequisite for successful colonization by enteric pathogens[350]. Impaired fucose metabolism may change nutrient accessibility, and the colonization niches (in mucus layer vs in close proximity of the epithelial surface) for *C. rodentium*, in contrast to excess L-fucose which alters the growth dynamics and bacterial fitness in the gut. It is also plausible to hypothesize that the presence of fucose metabolism operon may allow *C. rodentium* to effectively compete with commensals when there is an excess of L-fucose. It is also important to note that these are energy dependent process (active transport dependent on ATP utilization) and tight regulation (potentially dictated by environmental cues) may be necessary for enteric pathogens such as *C. rodentium* to invest energy and resources for efficient colonization[167,354]. In addition to its role in nutrional dynamics in the GI tract, L-fucose may also act as competitive inhibitor for the bacteria by binding to the bacteria cell surface antigens/lectin structures present on the bacterial cell surfaces and reduce its interactions with the epithelial surface or the intestinal mucus layer.

Overall these findings highlight the complex role played by mucus glycosylation and host fucosylation in host defense against A/E pathogen *C. rodentium*. Future studies will clarify the specific mechanisms regulating host glycosylation as well as the glycosylation dynamics during *C. rodentium* infection. Moreover these topics warrant further investigation into how these changes impact host susceptibility during an infection and host-microbiota homeostasis in the

gut. Further insights ascertaining the role of a specific glycosylation in host protection may assist in developing novel therapies and translational opportunities.

Chapter 6: Conclusions and future directions

6.1 Summary and contribution to the field

Until recently, the intestinal mucus layer has largely been viewed as a static, physical barrier and has been relatively ignored when it comes to intestinal host defense as well as exploring its impact on the ability of pathogens to infect their host's intestinal mucosal surface. Over the last few years however, there has been a revolutionary shift in our understanding that the mucus layer plays a key role in controlling intestinal disease progression and pathophysiology. This is not entirely surprising since for most enteric bacterial infections, mucus is the first line of defense as well as an important first point of contact between the pathogen and its host[106]. Reports documenting the effects of mucus in protecting the underlying mucosa from mechanical abrasion and keeping undesirable macromolecules and noxious agents away from the epithelial surface through barrier and flushing actions date back to the 1900s[355–358](reviewed in [359]). The 20th century saw several important, cutting edge discoveries in understanding of the mucus layer, such as the discovery of mucus secreting goblet cells, the role of bicarbonate ions in mucus expansion and mucus-mediated flushing responses. However it was not until the development of mucin deficient mice that the field truly began to appreciate the protective role of mucus and the field started shifting towards studying physiological responses and developing profound mechanistic insights into the protective roles of mucus.

As discussed in Chapter 1 (*Topic- Mucus and Disease*), any defects in the mucus barrier ranging from changes in the expression of glycosyltransferases and/or changes in mucin glycosylation status, or mutations affecting the assembly and processing of the mucins can have debilitating effects on the host[39,152,360]. They can also have profound effects on the exacerbation and/or perpetuation of a wide spectrum of human diseases such as colorectal cancer, Inflammatory Bowel Disease (IBD) and lung disorders[158,361–363]. Thus, despite the complex

nature of the mucus layer (chemical and structural complexity defined by extensive glycosylation), it is necessary that we continue to further our understanding of the dynamics of the mucus layer.

The work described in this dissertation provides an important, novel understanding of the multifaceted role of the intestinal mucin Muc2 as well as its intestinal glycosylation in providing host defense against enteric bacterial pathogens. This work also highlights the complexity of host mucus-enteric pathogen interactions and how intestinal mucus can play a dual role, both by promoting host innate immune and IEC responses, and by modulating bacterial virulence and pathogenesis strategies as well as altering commensal microbial homeostasis. The majority of my work concentrated on studying the role of the mucin Muc2 and its glycosylation (core 1 and core 3 derived O-glycans). However, I also examined intestinal fucosylation responses elicited during enteric bacterial infections, and I examined how enteric pathogens cross the mucus layer and how bacterial effector proteins that impact microbial interactions with the mucus layer can also play a role in modulating bacterial virulence and host immune responses. I also looked at the role of the predominant intestinal sugar, L-fucose in affecting bacterial behaviour and virulence, in the context of nutrition dynamics.

It has been documented that Muc2 deficiency resulted in heightened susceptibility to the A/E pathogen *C. rodentium*[144]. We wondered how the same deficiency would affect host susceptibility to the human pathogen *Salmonella* typhimurium. Consistent with the *C. rodentium* studies, we found that Muc2 provided a distinct barrier between the epithelial surface and luminal *Salmonella* burdens. During our investigations into the basis for the increased susceptibility of *Muc2 -/-* mice to *Salmonella*, we found that *Muc2 -/-* mice had impaired IAP activity in their intestinal tissues and there was no IAP retained in close proximity to the

epithelial surface, ultimately resulting in increased translocation of bacterial LPS (a potent TLR4 stimulus), and potentially other bacterial factors into systemic sites. This contributed towards exaggerated systemic inflammation and heightened susceptibility to *Salmonella.* This was the first study to show a link between intestinal mucus and IAP and how this can affect disease susceptibility during an infection. Furthermore, we also found that the absence of Muc2 resulted in a significant impairment in the ability of *ΔinvA Salmonella* to cause any pathology, suggesting that mucus interactions may modulate *Salmonella* pathogenicity[144]. This is an important finding and proposes a novel role for the mucus layer in modulating bacterial pathogenesis. Therefore in addition to supporting the conventional barrier function of Muc2, mucus interactions appear to play a novel role in modulating bacterial pathogenesis and in limiting systemic disease.

These findings prompted us to take a step back and look at the mechanisms by which enteric pathogens cross the protective mucus barrier in the first place. While enteric pathogens like *Salmonella* and other motile pathogens uses flagellar motility to swim through the mucus barrier[242,243,364], it is unclear how non-motile pathogens like *C. rodentium* cross the mucus barrier. Using *C. rodentium* as a model organism, we characterized a class 2 SPATE termed PicC, which has homologs in several clinically important enteric pathogens and is characterized by its mucinase activity[176,206,256]. While our *in vitro* findings that *C. rodentium* PicC can cleave mucins suggested it might be required for *C. rodentium* to overcome the mucus barrier, in contrast, we found no overt role for PicC in intestinal colonization suggesting that either absence of PicC resulted in upregulation of other compensatory proteases/mucinases/specific glycosidases which can cleave mucus or that *C. rodentium* does not require overt mucus digestion for effective colonization. However, we discovered an unprecedented role for PicC in altering the surface of *C. rodentium* and its behaviour *in vivo*. Absence of PicC resulted in a

hyper-aggregative bacterial phenotype within the mucus layer and intestinal crypts and also surprisingly led to increased activation of TLR2. Furthermore, aggregation of the PicC mutant within intestinal mucus potentially contributed to its decreased shedding in the stool and correlated with reduced commensal depletion, affecting the infection outcome. This study also highlights the complexity of *in vivo* dynamics of an enteric bacterial infection and is the first study to elucidate that bacterial class 2 SPATES can modulate host immune responses[340].

Looking at the evolutionary perspective, enteric pathogens have evolved strategies for effective host to host transmission, as virulence is thought to help promote transmission between hosts[309,365]. In fact, the ability of an enteric pathogen to successfully transmit to a new susceptible host is by definition an important criteria for a successful pathogen[366]. We found the deletion of PicC significantly attenuated the ability of *C. rodentium* to transmit to naïve hosts, and resulted in increased virulence (tissue damage and mortality), suggesting that enteric pathogens like *C. rodentium* must regulate their virulence to ensure successful transmission through the oral-fecal route. Thus our study provides novel insights into the pathogenicity cycle of *C. rodentium*. Since the pathogen factors that facilitate successful transmission to new hosts and the exact relationships between pathogen virulence and disease transmission are not well characterized, this finding provides an important step towards furthering our understanding of these concepts in the *C. rodentium* model.

Upon review of Chapter 3 and Chapter 5, their key themes addressed the protective role of host induced glycosylation in providing defense against enteric pathogens. This work further expanded on the specific role of mucin modifications (core 1 vs core 3 derived O-glycans) and carbohydrate moieties (fucose) in host defense. We noted that while core 3 derived O-glycans appeared to modestly regulate intestinal mucosal barrier function, core 1 derived O-glycans were

crucial in regulating pathogen burdens and commensal numbers in close proximity to the epithelial surface. Although the utilization of the 1,2 fucosyltransferase (Fut2) deficient mice would be necessary to ascertain the role of host fucosylation in providing defense against enteric infections, our preliminary work suggests fucosylation to be a general host defense mechanism, that is upregulated during *C. rodentium* infection. Certain host commensal populations such as *Bacteroidetes thetaiotamicrion* contain fucosidases, which then cleave L-fucose from the mucin structures and use it as a food source[161]. Therefore, host-induced fucosylation during *C. rodentium* infection may promote host-commensal homeostasis and strengthen microbiota based colonization resistance against invading enteric pathogens[335,367]. To add to the complexity of the system, our preliminary work also suggests that the ability of *C. rodentium* to utilize excess L-fucose provides a colonization advantage when compared to a mutant not capable of utilizing L-fucose (Δ*fucK*) therefore pointing to the complex nutrient network in the gut and its influence on commensals as well as bacterial pathogenesis and behaviour.

Overall, my studies have been important in establishing the complex but central role of Muc2 O-glycosylations in providing mucosal protection. While my work supports the conventional role for Muc2 in providing host defense (physical barrier, and flushing action), my studies provided insights into novel ways that mucus-enteric bacterial interactions can modulate bacterial virulence (i.e. in the absence of mucus layer, Δ*invA Salmonella* does not cause significant pathology), ultimately affecting the outcome of an infection. Our findings expanded on the ways the mucus layer could be important in maintaining intestinal homeostasis and regulating host immune responses.

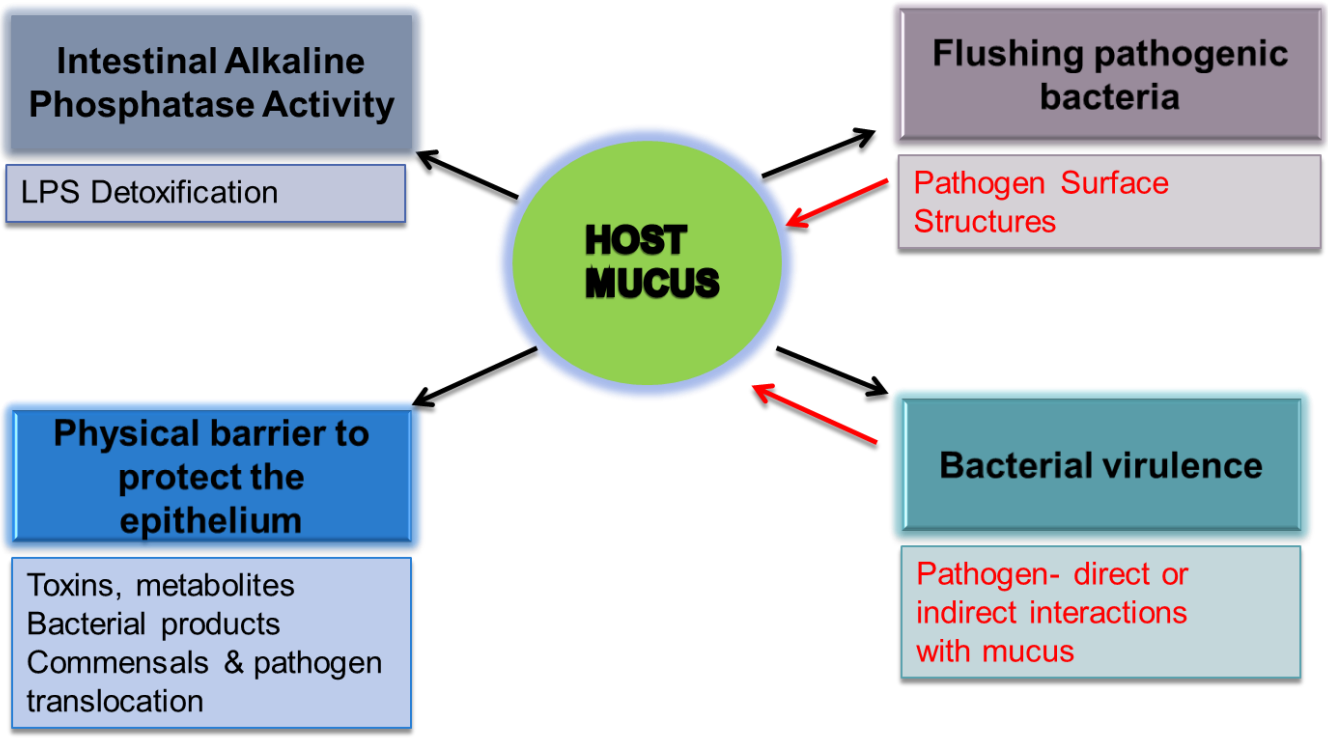

Figure 6.1 Broader overview: summary of different roles of the intestinal mucin Muc2 studied in this dissertation.
While intestinal mucus promotes host defense through conventional means (i) by acting as a physical barrier to protect the intestinal epithelium (ii) by flushing pathogenic bacteria away from the intestinal surface, host mucus can also play a role in affecting host susceptibility by (iii) regulating and retaining IAP activity at the mucosal surface (Chapter 3) (iv) by modulating bacterial virulence (Chapter 3, Chapter 5) (v) by affecting the ability of enteric pathogens to use their surface structures to interact with the mucus layer (Chapter 4). Black arrow represents the role of mucus whereas the red arrow represents the dynamic interactions between the enteric pathogens and the host mucus. Overall, this work provided insights into additional, novel ways that mucus-pathogen interactions can alter host susceptibility to infection.

6.2 Future directions

The work presented in this thesis answers some fundamental questions about the role of Muc2 O-glycosylation(s) in host defense and provides a broader overview of different functions of the intestinal mucus layer. However, this work also raises some important questions about our limited understanding of the dynamics of glycosylation changes during an enteric infection as well as further assessing the impact of mucus interactions on bacterial pathogenesis. The

following section identifies some of the key questions raised by my thesis work and the experimental approaches that can be used to move forward in the indicated direction(s).

Monitoring O-glycosylation changes in the mucus layer before and during infection

In terms of providing host defense against enteric pathogens, it is clear that Muc2 derived O-glycans can influence disease outcome and dramatically alter host susceptibility to enteric infections. However, still very little is known about the dynamics of mucus glycosylation during an infection and how the glycosylation pattern may change – presumably to increase host defense as well as potentially promote pathogen clearance from the host. As the link between the development of IBD and intestinal glycosylation becomes more evident[130,158], it is possible that understanding the dynamics of glycosylation during normal and diseased (infection) state may also further our understanding of particular glycan pathways (or pathways involving glycans) that may impact susceptibility to IBD. It is also important to develop an understanding of the molecular mechanisms underlying these complex glycosylation pathways such as the expression of glycosyltransferases, and the regulation of mucin glycosylation. Detailed O-glycomics analysis of the Muc2 mucin isolated from the colon of *C3GnT -/-* and *C1galt1 -/-* mice revealed some interesting differences in terminally differentiation modifications and the core composition (core 1,core 2, core 3 and core 4 derived O- glycans) between the indicated hosts. While the base LC/MS chromatogram was similar between WT and *C3GnT -/-* mice, it was markedly different for *C1galt1 -/-* mice, suggesting that the glycosylation profile was different[124,127]. However, to the best of our knowledge, there is only one study providing in depth analysis of glycosylation differences between these hosts but we still do not have an in-depth understanding of glycosylation changes during the course of a disease or an enteric bacterial infection.

Quantitative glycomics and glycoproteomics have emerged as powerful tools to study disease related changes in glycosylation profiles as well as assess the role of glycosylation in normal physiology and disease[368–370]. In order to develop a better understanding of how Muc2 glycosylation and fucosylation is changed during the course of infection, and whether any presumed changes are driven by the host, or alternatively by microbes, we recently initiated collaboration with Dr. Jianjun Li, National Research Council, Ottawa. We isolated mucus from the colons of uninfected and infected WT and *Muc2* -/- mice. The preliminary analysis will aim to detect differences in Muc2 glycosylation and/or fucosylation during *C. rodentium* infection in the indicated hosts using LC/MS analysis.

The TLR and IL-1R adaptor molecular MyD88 is an important component underlying host defense mechanisms during *C. rodentium* infection[74,215]. A recent study revealed that global depletion of MyD88 in mice prevented intestinal fucosylation responses during infection, suggesting that innate immune signalling mediated through MyD88-TLR activation could serve as an important signal for the induced fucosylation during a systemic bacterial challenge[163]. A caveat of using a global KO model is that typically multiple cells express the gene of interest and since we are most interested in examining intestinal epithelial and goblet cell responses, it may be difficult to ascertain whether the observed phenotypic changes reflect only the actions of these cells. In a more focused study, intestinal epithelial cell (IEC) specific *MyD88* -/- mice have been shown to display impaired goblet cell responses during *Salmonella* infection[371]. Therefore, it would be of interest to examine if any of the glycosylation changes during *C. rodentium* infection are mediated by the innate immune responses (i.e. examine glycosylation analysis in Intestinal Epithelial Cell Specific (IEC) *MyD88* -/- mice under uninfected (baseline) and infected (*C. rodentium*, day 6 post-infection) conditions.

Knowing that certain cell associated mucins (Muc1 and Muc13) can regulate inflammatory responses during infection by the A/E pathogen EPEC[372], it is reasonable to propose that in addition to providing host defense through previously discussed functions, intestinal mucins could also be playing a role in the recognition of PRR (signal through TLRs) and regulating epithelial cell inflammatory responses. Making MyD88/O-glycan double KO mice constructs could be useful in unraveling the role of O-linked glycosylations in regulating epithelial cell signalling through these innate immune pathways.

Not to be overlooked, resident/commensal microbiota can also have dramatic effects on intestinal homeostasis and the glycosylation status of the intestine[9,373]. Intestinal microbiota can produce a plethora of mucinases, glycosidases and proteases that can break down mucin O-linked glycans to release monosaccharides which are then used as food sources. Therefore, it is likely that infection-induced microbiota changes (dysbiosis) may alter the glycosylation dynamics in the intestine. To examine the role of microbiota in mediating glycosylation changes, microbiota differences between WT, *C3GnT -/-*, *C1galt1 -/-* and *Muc2 -/-* mice will need to be further assessed using a more sensitive and accurate measure, such as high-throughput 16S rRNA gene sequencing. Examination of glycosylation dynamics/changes after antibiotic-mediated depletion of the commensal microbiota (with broad spectrum antibiotics) and potentially rearing these mice in germ-free environment would also help define whether glycosylation changes are mediated by commensal microbes. For example, *Bacteroides thetaiotaomicron* is an important commensal with a plethora of enzymes that it uses to forage on intestinal mucins and as such[172], it can induce host changes such as fucosylation when intestinal levels of fucose are low. Dual-colonization studies with *B. thetaiotaomicron* and *C. rodentium*

could help in understanding of the role of commensals during *C. rodentium* infection as well as in metabolic variations during an infection.

Whole-genome transcription profiling- further exploration of mucus-enteric bacterial interactions

Muc2 has been implicated in preventing the development of biofilm-like structures in the gut due to its ability to flush away bacteria from the mucosal surface and reducing bacterial surface adhesion[145]. Notably, we previously showed that absence of Muc2 mucin (*Muc2 -/-*) resulted in the development of *C. rodentium* overgrowths on the colonic epithelial surface. A similar phenotype was noted in *C1galt1 -/-* mice further supporting the idea that an impaired mucus barrier may contribute towards microbial biofilm formation in the GI tract. It is not clear how these biofilms may contribute to the aetiology of disease. As we noted in Chapter 4, PicC mediated changes in the bacterial surface structure presumably results in altered interactions with the mucus layer and contributed to bacterial aggregation on the epithelial surface and within the mucus layer. Consistent with a previous study that implicated the synergistic role of curli and cellulose in biofilm formation in A/E *E. coli*[311,374], we noted that *C. rodentium* Δ*picC* showed increased curli and cellulose production, potentially resulting in altered interactions with the mucus layer and a hyper-aggregative phenotype. It would be of interest to identify the global transcriptional regulators of curli and cellulose production as well as biofilm formation in *C. rodentium*, to further understand the molecular mechanisms behind biofilm formation in this mouse pathogen.

Assessing the impact of the mucus layer on commensal and pathogen makeup within the intestine is another interesting area. A recent study revealed that the colonic mucus represents a dynamic environment where colonizing bacteria adapt their metabolic and nutrient requirements

to the availability of the nutrients found in the mucus[348]. Since *C. rodentium* has been shown to colonize the intestinal mucus layer and penetrate the inner mucus layer, we are interested in looking at how *C. rodentium*'s transcription of metabolic and virulence genes may differ in the presence of mucus (B6 mice) a partial mucus layer (*C1galt1 -/-* mice) and in the complete absence of the mucus layer (*Muc2 -/-* mice). We noted two distinct subpopulations of *C. rodentium* in WT mice, the first being within the outer mucus layer, while the second directly infects the epithelial cell surface. While the epithelial infecting population was still present in mucin deficient mice bacteria adherent to the mucosal surface area) the mucus dwelling population in WT mice is replaced by the aggregating, biofilm like *C. rodentium* populations. It would be interesting to examine how *C. rodentium* found in the outer mucus layer may differ from *C. rodentium* found in the biofilm-like structures/bacterial aggregates in terms of their virulence and metabolism as assessed by transcriptomics. This will provide useful insights into how mucus is playing a role in regulating microbes and their virulence in *vivo.*

Overall, these studies have the potential to cause a paradigm shift in our traditional approach of looking at bacterial pathogenesis *in vivo* – rather than focusing on one particular aspect of a disease, we need to start appreciating that enteric infections reflect a complex network of interactions between the host, pathogen and commensal microbes. A recent study revealed that commensal microbes such as *B. thetaiotaomicron* had distinct transcriptional profiles in the colonic mucus and colonic contents, potentially due to differential resource availability and utilization. Extending these findings to enteric pathogens - it may well be found that the ability of bacteria to adapt to the environment, depending on the nutrient availability and their genomics can alter host susceptibility and warrants further investigation.

Establishing a link between mucus and bacterial virulence - successful host transmission as a new read-out for virulence?

As discussed earlier in this chapter, the ability of a pathogen to successfully transmit to a new host ensures its successful propagation; it would therefore be interesting to investigate how interactions with the mucus layer can modulate/alter bacterial virulence and ultimately affect the ability of a pathogen to successfully transmit to new hosts. To test this I would propose to infect WT, *C3GnT -/-, C1galt1 -/-* and *Muc2 -/-* mice with WT *C. rodentium*. The infected host would then be introduced to naïve mice at day 3 post infection (to minimize the risk for heightened mortality in susceptible *C1galt1 -/-* and *Muc2 -/-* mice) and then co-housed for 3-6 days. Susceptibility to shed microbes in the stool of the index mouse could be assessed by examining *C. rodentium* burdens in the distal colon. An alternate approach would be to take the stool from infected WT, *C3GnT -/-*, *C1galt1 -/-* and *Muc2 -/-* mice (day 5-6 post infection, peak of the infection) and inoculate naïve WT mice with the host-adapted stool samples This experiment would be important for assessing the transmissible potential of *C. rodentium* from different hosts and determine if mucus-*C. rodentium* interactions are playing a role in determining virulence and host transmission. Consequently, it is possible that different mucus levels (thickness) and altered O-glycosylation status may affect the dynamics of how *C. rodentium* interacts with the mucus layer. This will also help determine if the virulence of host-adapted *C. rodentium* is a function of host behaviour in the intestine.

6.3 Translational opportunities and human studies

As previously discussed, there is increasing evidence that mucin alterations can predispose to the development of intestinal inflammation and inflammation-induced cancer. Use of human biopsies can be extremely useful to complement findings from animal studies and to

investigate the clinical relevance of O-glycan deficient models. Healthy and diseased human biopsies (suffering intestinal disorders like IBD) can be used for qPCR analysis, looking at potential alterations in mucin gene transcription as well as for assessing mucin glycosylation differences after the onset of the disease. Immunohistochemical staining of human biopsies from normal (healthy) controls and IBD patients for mucin glycosylation/mucin oligosaccharide changes using protein and lectin markers could prove useful in understanding if similar glycosylation pathways (mice) are implicated in human intestinal aetiologies and if their loss promotes the pathogenesis of colitis, as seen in O-glycan deficient mice.

Culturing of isolated intestinal crypts or intestinal stem cells, when supplemented with appropriate growth medium and cultured inside a three dimensional matrix, can generate intestinal organoids (a structure reminiscent of the normal intestinal crypts), offering a three dimensional cell-culture system[375–377]. Culturing of human intestinal biopsies samples into organoids offers an exciting opportunity to look at glycosylation dynamics and mucus-bacterial interactions. Organoid models derived from healthy and IBD patients could provide useful insights into the glycosylation mechanisms and their regulation in response to microbial challenges (human specific pathogens such as EPEC, EHEC) as well as commensals and will be an invaluable tool for translational studies of mucus.

6.4 Concluding remarks

Overall, the work described in this dissertation has provided numerous contributions towards the advancement of our understanding of mucus layer-enteric bacterial interactions. Furthermore, it has laid the groundwork for the beginnings of new research directions in the lab, to further expand on the role of the mucus layer in modulating bacterial virulence and biofilm formation as well as its role in maintaining host-commensal homeostasis. The continuation of the

mucin glycobiology work presented here will hopefully result in a renewed interest in the functional biology of the mucus layer and its glycosylation and terminal modifications. Since changes in glycosylation patterns/glycan composition are implicated in the pathogenesis of IBD, these studies will provide useful insights into how changes in glycosylation patterns or specific glycans can affect host susceptibility to developing intestinal inflammation and disease progression. Furthermore, ascertaining the role of specific forms of glycosylation in host protection may assist in developing novel therapies and translational opportunities.

References

1. Chow, J., Lee, S. M., Shen, Y., Khosravi, A. & Mazmanian, S. K. Host-bacterial symbiosis in health and disease. *Adv. Immunol.* **107,** 243–274 (2010).
2. O'Hara, A. M. & Shanahan, F. The gut flora as a forgotten organ. *EMBO Rep.* **7,** 688–693 (2006).
3. Dethlefsen, L., McFall-Ngai, M. & Relman, D. a. An ecological and evolutionary perspective on human-microbe mutualism and disease. *Nature* **449,** 811–818 (2007).
4. Sansonetti, P. J. To be or not to be a pathogen: that is the mucosally relevant question. *Mucosal Immunol.* **4,** 8–14 (2011).
5. Round, J. L. & Mazmanian, S. K. The gut microbiota shapes intestinal immune responses during health and disease. *Nat. Rev. Immunol.* **9,** 313–323 (2009).
6. Yu, L. C.-H., Wang, J.-T., Wei, S.-C. & Ni, Y.-H. Host-microbial interactions and regulation of intestinal epithelial barrier function: From physiology to pathology. *World J. Gastrointest. Pathophysiol.* **3,** 27–43 (2012).
7. Spees, A. M., Lopez, C. a., Kingsbury, D. D., Winter, S. E. & Bäumler, A. J. Colonization resistance: battle of the bugs or ménage à trois with the host? *PLoS Pathog.* **9,** 9–12 (2013).
8. Buffie, C. G. & Pamer, E. G. Microbiota-mediated colonization resistance against intestinal pathogens. *Nat. Rev. Immunol.* **13,** 790–801 (2013).
9. Ouwerkerk, J. P., De Vos, W. M. & Belzer, C. Glycobiome: Bacteria and mucus at the epithelial interface. *Best Pract. Res. Clin. Gastroenterol.* **27,** 25–38 (2013).
10. Hooper, L. V., Littman, D. R. & Macpherson, a. J. Interactions Between the Microbiota and the Immune System. *Science (80-.).* **336,** 1268–1273 (2012).
11. Cerf-Bensussan, N. & Gaboriau-Routhiau, V. The immune system and the gut microbiota: friends or foes? *Nat. Rev. Immunol.* **10,** 735–744 (2010).
12. Sansonetti, P. J. War and peace at mucosal surfaces. *Nat. Rev. Immunol.* **4,** 953–964 (2004).
13. Round, J. L., O'Connell, R. M. & Mazmanian, S. K. Coordination of tolerogenic immune responses by the commensal microbiota. *J. Autoimmun.* **34,** J220–5 (2010).
14. Dupont, A., Heinbockel, L., Brandenburg, K. & Hornef, M. W. Antimicrobial peptides and the enteric mucus layer act in concert to protect the intestinal mucosa. *Gut Microbes* **5,** 761–5 (2014).
15. Victorino, F. & Alper, S. Identifying novel spatiotemporal regulators of innate immunity. *Immunol. Res.* **55,** 3–9 (2013).
16. Macpherson, A. J. & Harris, N. L. Interactions between commensal intestinal bacteria and the immune system. *Nat. Rev. Immunol.* **4,** 478–485 (2004).

17. Berkes, J., Viswanathan, V. K., Savkovic, S. D. & Hecht, G. Intestinal epithelial responses to enteric pathogens: effects on the tight junction barrier, ion transport, and inflammation. *Gut* **52,** 439–451 (2003).

18. Sirard, J. C., Bayardo, M. & Didierlaurent, A. Pathogen-specific TLR signaling in mucosa: Mutual contribution of microbial TLR agonists and virulence factors. *Eur. J. Immunol.* **36,** 260–263 (2006).

19. Peterson, L. W. & Artis, D. Intestinal epithelial cells: regulators of barrier function and immune homeostasis. *Nature reviews. Immunology* **14,** 141–53 (2014).

20. Yen, T.-H. & Wright, N. a. The gastrointestinal tract stem cell niche. *Stem Cell Rev.* **2,** 203–212 (2006).

21. Shen, L. Functional Morphology of the Gastrointestinal Tract. *Curr. Top. Microbiol. Immunol.* **337,** 1–35 (2009).

22. van der Flier, L. G. & Clevers, H. Stem cells, self-renewal, and differentiation in the intestinal epithelium. *Annu. Rev. Physiol.* **71,** 241–260 (2009).

23. Schonhoff, S. E., Giel-Moloney, M. & Leiter, A. B. Minireview: Development and differentiation of gut endocrine cells. *Endocrinology* **145,** 2639–2644 (2004).

24. Bevins, C. L. & Salzman, N. H. Paneth cells, antimicrobial peptides and maintenance of intestinal homeostasis. *Nat. Rev. Microbiol.* **9,** 356–368 (2011).

25. Specian, R. D. & Oliver, M. G. Functional biology of intestinal goblet cells. *Am. J. Physiol.* **260,** C183–C193 (1991).

26. Karam, S. M. Lineage commitment and maturation of epithelial cells in the gut. *Front. Biosci.* **4,** 286–298 (1999).

27. Snoeck, V., Goddeeris, B. & Cox, E. The role of enterocytes in the intestinal barrier function and antigen uptake. *Microbes Infect.* **7,** 997–1004 (2005).

28. Barker, N. Adult intestinal stem cells: critical drivers of epithelial homeostasis and regeneration. *Nat. Rev. Mol. Cell Biol.* **15,** 19–33 (2014).

29. Barker, N., van de Wetering, M. & Clevers, H. The intestinal stem cell. *Genes Dev.* **22,** 1856–1864 (2008).

30. Sato, T. *et al.* Single Lgr5 stem cells build crypt-villus structures in vitro without a mesenchymal niche. *Nature* **459,** 262–5 (2009).

31. Barker, N. *et al.* Identification of stem cells in small intestine and colon by marker gene Lgr5. *Nature* **449,** 1003–1007 (2007).

32. van Es, J. H. *et al.* Notch/gamma-secretase inhibition turns proliferative cells in intestinal crypts and adenomas into goblet cells. *Nature* **435,** 959–963 (2005).

33. Fre, S. *et al.* Notch signals control the fate of immature progenitor cells in the intestine. *Nature* **435,** 964–968 (2005).

34. Fevr, T., Robine, S., Louvard, D. & Huelsken, J. Wnt/beta-catenin is essential for intestinal homeostasis and maintenance of intestinal stem cells. *Mol. Cell. Biol.* **27,** 7551–7559 (2007).

35. Pinto, D. & Clevers, H. Wnt control of stem cells and differentiation in the intestinal epithelium. *Exp. Cell Res.* **306,** 357–363 (2005).

36. Nakamura, T., Tsuchiya, K. & Watanabe, M. Crosstalk between Wnt and Notch signaling in intestinal epithelial cell fate decision. *J. Gastroenterol.* **42,** 705–710 (2007).

37. Suzuki, K. *et al.* Hes1-deficient mice show precocious differentiation of Paneth cells in the small intestine. *Biochem. Biophys. Res. Commun.* **328,** 348–52 (2005).

38. Yang, Q., Bermingham, N. a, Finegold, M. J. & Zoghbi, H. Y. Requirement of Math1 for secretory cell lineage commitment in the mouse intestine. *Science* **294,** 2155–2158 (2001).

39. Kim, Y. S. & Ho, S. B. Intestinal goblet cells and mucins in health and disease: recent insights and progress. *Curr. Gastroenterol. Rep.* **12,** 319–30 (2010).

40. Ayabe, T., Ashida, T., Kohgo, Y. & Kono, T. The role of Paneth cells and their antimicrobial peptides in innate host defense. *Trends Microbiol.* **12,** 394–8 (2004).

41. Deplancke, B. & Gaskins, H. R. Microbial modulation of innate defense: goblet cells and the intestinal mucus layer. *Am. J. Clin. Nutr.* **73,** 1131S–1141S (2001).

42. Dignass, A., Lynch-Devaney, K., Kindon, H., Thim, L. & Podolsky, D. K. Trefoil peptides promote epithelial migration through a transforming growth factor beta-independent pathway. *J. Clin. Invest.* **94,** 376–83 (1994).

43. Albert, T. K. *et al.* Human Intestinal TFF3 Forms Disulfide-Linked Heteromers with the Mucus-Associated FCGBP Protein and Is Released by Hydrogen Sulfide. *J. Proteome Res.* **9,** 3108–3117 (2010).

44. Kindon, H., Pothoulakis, C., Thim, L., Lynch-Devaney, K. & Podolsky, D. K. Trefoil peptide protection of intestinal epithelial barrier function: cooperative interaction with mucin glycoprotein. *Gastroenterology* **109,** 516–523 (1995).

45. Bergstrom, K. S. B. *et al.* Goblet Cell Derived RELM-β Recruits CD4+ T Cells during Infectious Colitis to Promote Protective Intestinal Epithelial Cell Proliferation. *PLOS Pathog.* **11,** e1005108 (2015).

46. Artis, D. *et al.* RELMbeta/FIZZ2 is a goblet cell-specific immune-effector molecule in the gastrointestinal tract. *Proc. Natl. Acad. Sci. U. S. A.* **101,** 13596–13600 (2004).

47. Muniz, L. R., Knosp, C. & Yeretssian, G. Intestinal antimicrobial peptides during homeostasis, infection, and disease. *Front. Immunol.* **3,** 1–13 (2012).

48. Meyer-Hoffert, U. *et al.* Secreted enteric antimicrobial activity localises to the mucus surface layer. *Gut* **57,** 764–71 (2008).

49. Antoni, L. *et al.* Human colonic mucus is a reservoir for antimicrobial peptides. *J. Crohn's Colitis* **7,** e652–e664 (2013).

50. Jepson, M. a, Schlecht, H. B. & Collares-Buzato, C. B. Localization of dysfunctional tight junctions in Salmonella enterica serovar typhimurium-infected epithelial layers. *Infect. Immun.* **68,** 7202–8 (2000).

51. Schulzke, J. D. *et al.* Epithelial tight junctions in intestinal inflammation. *Ann. N. Y. Acad. Sci.* **1165,** 294–300 (2009).

52. Guttman, J. a. & Finlay, B. B. Tight junctions as targets of infectious agents. *Biochim. Biophys. Acta - Biomembr.* **1788,** 832–841 (2009).

53. Turner, J. R. Intestinal mucosal barrier function in health and disease. *Nat. Rev. Immunol.* **9,** 799–809 (2009).

54. Kucharzik, T. *et al.* Role of M cells in intestinal barrier function. *Ann. N. Y. Acad. Sci.* **915,** 171–183 (2000).

55. Rimoldi, M. *et al.* Intestinal immune homeostasis is regulated by the crosstalk between epithelial cells and dendritic cells. *Nat. Immunol.* **6,** 507–14 (2005).

56. Pott, J. & Hornef, M. Innate immune signalling at the intestinal epithelium in homeostasis and disease. *EMBO Rep.* **13,** 684–698 (2012).

57. Abreu, M. T. Toll-like receptor signalling in the intestinal epithelium: how bacterial recognition shapes intestinal function. *Nat. Rev. Immunol.* **10,** 131–44 (2010).

58. Rakoff-Nahoum, S., Paglino, J., Eslami-Varzaneh, F., Edberg, S. & Medzhitov, R. Recognition of commensal microflora by toll-like receptors is required for intestinal homeostasis. *Cell* **118,** 229–241 (2004).

59. Fukata, M., Vamadevan, A. S. & Abreu, M. T. Toll-like receptors (TLRs) and Nod-like receptors (NLRs) in inflammatory disorders. *Semin. Immunol.* **21,** 242–253 (2009).

60. Abreu, M. T., Fukata, M. & Arditi, M. TLR signaling in the gut in health and disease. *J. Immunol.* **174,** 4453–4460 (2005).

61. Akira, S. & Takeda, K. Toll-like receptor signalling. *Nat. Rev. Immunol.* **4,** 499–511 (2004).

62. Abreu, M. T. *et al.* TLR signaling at the intestinal epithelial interface. *J. Endotoxin Res.* **9,** 322–30 (2003).

63. Ostaff, M. J., Stange, E. F. & Wehkamp, J. Antimicrobial peptides and gut microbiota in homeostasis and pathology. *EMBO Mol. Med.* **5,** 1465–1483 (2013).

64. Podolsky, D. K., Gerken, G., Eyking, A. & Cario, E. Colitis-associated variant of TLR2 causes impaired mucosal repair because of TFF3 deficiency. *Gastroenterology* **137,** 209–20 (2009).

65. Vaishnava, S., Behrendt, C. L., Ismail, A. S., Eckmann, L. & Hooper, L. V. Paneth cells directly sense gut commensals and maintain homeostasis at the intestinal host-microbial interface. *Proc. Natl. Acad. Sci. U. S. A.* **105,** 20858–20863 (2008).

66. Tükel, C. *et al.* Toll-like receptors 1 and 2 cooperatively mediate immune responses to

curli, a common amyloid from enterobacterial biofilms. *Cell. Microbiol.* **12,** 1495–505 (2010).

67. Fukata, M. & Abreu, M. T. TLR4 signalling in the intestine in health and disease. *Biochem Soc Trans* **35,** 1473–1478 (2007).

68. Gewirtz, A. T., Navas, T. A., Lyons, S., Godowski, P. J. & Madara, J. L. Cutting edge: bacterial flagellin activates basolaterally expressed TLR5 to induce epithelial proinflammatory gene expression. *J. Immunol.* **167,** 1882–1885 (2001).

69. Tallant, T. *et al.* Flagellin acting via TLR5 is the major activator of key signaling pathways leading to NF-kappa B and proinflammatory gene program activation in intestinal epithelial cells. *BMC Microbiol.* **4,** 33 (2004).

70. Kawai, T. & Akira, S. The role of pattern-recognition receptors in innate immunity: update on Toll-like receptors. *Nat Immunol* **11,** 373–384 (2010).

71. Kumar, H., Kawai, T. & Akira, S. Toll-like receptors and innate immunity. *Biochem. Biophys. Res. Commun.* **388,** 621–625 (2009).

72. Mabbott, N. A., Donaldson, D. S., Ohno, H., Williams, I. R. & Mahajan, A. Microfold (M) cells: important immunosurveillance posts in the intestinal epithelium. *Mucosal Immunol.* **6,** 666–77 (2013).

73. Hathaway, L. J. & Kraehenbuhl, J. P. The role of M cells in mucosal immunity. *Cell. Mol. Life Sci.* **57,** 323–332 (2000).

74. Collins, J. W. *et al.* Citrobacter rodentium: infection, inflammation and the microbiota. *Nat. Rev. Microbiol.* **12,** 612–623 (2014).

75. Lebeis, S. L., Bommarius, B., Parkos, C. a, Sherman, M. a & Kalman, D. TLR signaling mediated by MyD88 is required for a protective innate immune response by neutrophils to Citrobacter rodentium. *J. Immunol.* **179,** 566–577 (2007).

76. Wong, A. R. C. *et al.* Enteropathogenic and enterohaemorrhagic Escherichia coli: Even more subversive elements. *Mol. Microbiol.* **80,** 1420–1438 (2011).

77. Deng, W., Li, Y., Vallance, B. a & Finlay, B. B. Locus of enterocyte effacement from Citrobacter rodentium: sequence analysis and evidence for horizontal transfer among attaching and effacing pathogens. *Infect. Immun.* **69,** 6323–35 (2001).

78. Vallance, B. A. & Finlay, B. B. Exploitation of host cells by enteropathogenic Escherichiacoli. *Proc Natl Acad Sci U S A* **97,** 8799–8806 (2000).

79. Gruenheid, S. *et al.* Enteropathogenic E. coli Tir binds Nck to initiate actin pedestal formation in host cells. *Nat. Cell Biol.* **3,** 856–859 (2001).

80. de Grado, M., Rosenberger, C. M., Gauthier, A., Vallance, B. A. & Finlay, B. B. Enteropathogenic Escherichia coli infection induces expression of the early growth response factor by activating mitogen-activated protein kinase cascades in epithelial cells. *Infect Immun* **69,** 6217–6224 (2001).

81. Crane, J. K. & Vezina, C. M. Externalization of host cell protein kinase C during

enteropathogenic Escherichia coli infection. *Cell Death Differ.* **12,** 115–27 (2005).

82. Rosenshine, I., Donnenberg, M. S., Kaper, J. B. & Finlay, B. B. Signal transduction between enteropathogenic Escherichia coli (EPEC) and epithelial cells: EPEC induces tyrosine phosphorylation of host cell proteins to initiate cytoskeletal rearrangement and bacterial uptake. *EMBO J.* **11,** 3551–3560 (1992).

83. Vallance, B. a & Finlay, B. B. Exploitation of host cells by enteropathogenic Escherichia coli. *Proc. Natl. Acad. Sci. U. S. A.* **97,** 8799–8806 (2000).

84. Nataro, J. P. & Kaper, J. B. Diarrheagenic Escherichia coli. *Clin. Microbiol. Rev.* **11,** 142–201 (1998).

85. Schulze-Osthoff, K., Ferrari, D., Riehemann, K. & Wesselborg, S. Regulation of NF-kappa B activation by MAP kinase cascades. *Immunobiology* **198,** 35–49 (1997).

86. Silva, M. J. *et al.* The Multifaceted Role of Commensal Microbiota in Homeostasis and Gastrointestinal Diseases. *J Immunol Res* **2015,** 321241 (2015).

87. Hooper, L. V, Bry, L., Falk, P. G. & Gordon, J. I. Host-microbial symbiosis in the mammalian intestine: exploring an internal ecosystem. *Bioessays* **20,** 336–343 (1998).

88. Krajmalnik-Brown, R., Ilhan, Z.-E., Kang, D.-W. & DiBaise, J. K. Effects of Gut Microbes on Nutrient Absorption and Energy Regulation. *Nutr. Clin. Pract.* **27,** 201–214 (2012).

89. Lawley, T. D. & Walker, A. W. Intestinal colonization resistance. *Immunology* **138,** 1–11 (2013).

90. Kamada, N., Chen, G. Y., Inohara, N. & Núñez, G. Control of pathogens and pathobionts by the gut microbiota. *Nat. Immunol.* **14,** 685–90 (2013).

91. Xu, J. *et al.* A genomic view of the human-Bacteroides thetaiotaomicron symbiosis. *Science* **299,** 2074–2076 (2003).

92. Gern, J. E. The Antibacterial Lectin RegIII-Gamma Promotes the Spatial Segregation of Microbiota and Host in the Intestine. *Pediatrics* **130,** S48–S49 (2012).

93. Natividad, J. M. M. *et al.* Differential induction of antimicrobial REGIII by the intestinal microbiota and Bifidobacterium breve NCC2950. *Appl. Environ. Microbiol.* **79,** 7745–7754 (2013).

94. Brandl, K., Plitas, G., Schnabl, B., DeMatteo, R. P. & Pamer, E. G. MyD88-mediated signals induce the bactericidal lectin RegIII gamma and protect mice against intestinal Listeria monocytogenes infection. *J. Exp. Med.* **204,** 1891–900 (2007).

95. Talham, G. L., Jiang, H. Q., Bos, N. A. & Cebra, J. J. Segmented filamentous bacteria are potent stimuli of a physiologically normal state of the murine gut mucosal immune system. *Infect Immun* **67,** 1992–2000 (1999).

96. Goto, Y. *et al.* Segmented filamentous bacteria antigens presented by intestinal dendritic cells drive mucosal Th17 cell differentiation. *Immunity* **40,** 594–607 (2014).

97. Ivanov, I. I. *et al.* Induction of intestinal Th17 cells by segmented filamentous bacteria. *Cell* **139,** 485–98 (2009).

98. Stecher, B. Finding a sugary foothold: How antibiotics pave the way for enteric pathogens. *Cell Host Microbe* **14,** 225–227 (2013).

99. Ng, K. M. *et al.* Microbiota-liberated host sugars facilitate post-antibiotic expansion of enteric pathogens. *Nature* **502,** 96–9 (2013).

100. Van der Waaij, D., Berghuis-de Vries, J. M. & Lekkerkerk-van der Wees, J. E. C. Colonization resistance of the digestive tract in conventional and antibiotic-treated mice. *J. Hyg. (Lond).* **69,** 405 (1971).

101. Stecher, B., Berry, D. & Loy, A. Colonization resistance and microbial ecophysiology: Using gnotobiotic mouse models and single-cell technology to explore the intestinal jungle. *FEMS Microbiol. Rev.* **37,** 793–829 (2013).

102. Stecher, B. *et al.* Like will to like: abundances of closely related species can predict susceptibility to intestinal colonization by pathogenic and commensal bacteria. *PLoS Pathog.* **6,** e1000711 (2010).

103. Manichanh, C., Borruel, N., Casellas, F. & Guarner, F. The gut microbiota in IBD. *Nat. Rev. Gastroenterol. Hepatol.* **9,** 599–608 (2012).

104. Sartor, R. B. & Mazmanian, S. K. Intestinal Microbes in Inflammatory Bowel Diseases. *Am. J. Gastroenterol. Suppl.* **1,** 15–21 (2012).

105. Nell, S., Suerbaum, S. & Josenhans, C. The impact of the microbiota on the pathogenesis of IBD: lessons from mouse infection models. *Nat. Rev. Microbiol.* **8,** 564–77 (2010).

106. Liévin-Le Moal, V. & Servin, A. L. The front line of enteric host defense against unwelcome intrusion of harmful microorganisms: mucins, antimicrobial peptides, and microbiota. *Clin. Microbiol. Rev.* **19,** 315–37 (2006).

107. Ashida, H., Ogawa, M., Kim, M., Mimuro, H. & Sasakawa, C. Bacteria and host interactions in the gut epithelial barrier. *Nat. Chem. Biol.* **8,** 36–45 (2011).

108. Atuma, C., Strugala, V., Allen, a & Holm, L. The adherent gastrointestinal mucus gel layer: thickness and physical state in vivo. *Am. J. Physiol. Gastrointest. Liver Physiol.* **280,** G922–G929 (2001).

109. Matsuo, K., Ota, H., Akamatsu, T., Sugiyama, A. & Katsuyama, T. Histochemistry of the surface mucous gel layer of the human colon. *Gut* **40,** 782–789 (1997).

110. Johansson, M. E. V, Larsson, J. M. H. & Hansson, G. C. The two mucus layers of colon are organized by the MUC2 mucin, whereas the outer layer is a legislator of host-microbial interactions. *Proc. Natl. Acad. Sci. U. S. A.* **108 Suppl ,** 4659–4665 (2011).

111. Kesimer, M. *et al.* Molecular organization of the mucins and glycocalyx underlying mucus transport over mucosal surfaces of the airways. *Mucosal Immunol.* **6,** 379–92 (2013).

112. Linden, S. K., Sutton, P., Karlsson, N. G., Korolik, V. & McGuckin, M. a. Mucins in the

mucosal barrier to infection. *Mucosal Immunol.* **1,** 183–197 (2008).

113. Hattrup, C. L. & Gendler, S. J. Structure and function of the cell surface (tethered) mucins. *Annu. Rev. Physiol.* **70,** 431–457 (2008).

114. Dharmani, P., Srivastava, V., Kissoon-Singh, V. & Chadee, K. Role of intestinal mucins in innate host defense mechanisms against pathogens. *J. Innate Immun.* **1,** 123–135 (2009).

115. Gum, J. R., Hicks, J. W., Toribara, N. W., Siddiki, B. & Kim, Y. S. Molecular Cloning of Human Intestinal Mucin (MUC2) cDNA: Identification of the Amino Terminus and Overall Sequence Similarity to Prepro-Von Willebrand Factor. *J. Biol. Chem.* **269,** 2440–2446 (1994).

116. Tytgat, K. M. *et al.* Biosynthesis of human colonic mucin: Muc2 is the prominent secretory mucin. *Gastroenterology* **107,** 1352–1363 (1994).

117. Quinton, P. M. Cystic fibrosis: impaired bicarbonate secretion and mucoviscidosis. *Lancet* **372,** 415–417 (2008).

118. Yu, K., Lujan, R., Marmorstein, A., Gabriel, S. & Hartzell, H. C. Bestrophin-2 mediates bicarbonate transport by goblet cells in mouse colon. *J. Clin. Invest.* **120,** 1722–35 (2010).

119. Carlstedt, I. *et al.* Characterization of two different glycosylated domains from the insoluble mucin complex of rat small intestine. *J. Biol. Chem.* **268,** 18771–18781 (1993).

120. Ferez-Vilar, J. & Hill, R. L. The structure and assembly of secreted mucins. *J. Biol. Chem.* **274,** 31751–31754 (1999).

121. McGuckin, M. a, Lindén, S. K., Sutton, P. & Florin, T. H. Mucin dynamics and enteric pathogens. *Nat. Rev. Microbiol.* **9,** 265–278 (2011).

122. Ferguson, M. A., Kinoshita, T. & Hart, G. W. *Essentials of Glycobiology. 2nd edition*. *Essentials of Glycobiology. 2nd edition. Cold Spring Harbor (NY): Cold Spring Harbor Laboratory Press; 2009. Chapter 11. Figure 11.6* (2009). doi:10.1016/S0962-8924(00)01855-9

123. Johansson, M. E. V *et al.* Composition and functional role of the mucus layers in the intestine. *Cell. Mol. Life Sci.* **68,** 3635–3641 (2011).

124. Thomsson, K. a. *et al.* Detailed O-glycomics of the Muc2 mucin from colon of wild-type, core 1- and core 3-transferase-deficient mice highlights differences compared with human MUC2. *Glycobiology* **22,** 1128–1139 (2012).

125. Bennett, E. P. *et al.* Control of mucin-type O-glycosylation: A classification of the polypeptide GalNAc-transferase gene family. *Glycobiology* **22,** 736–756 (2012).

126. Brockhausen, I., Schachter, H. & Stanley, P. in *Essentials of Glycobiology* 1–16 (2009). doi:NBK1896 [bookaccession]

127. Larsson, J. M. H., Karlsson, H., Sjövall, H. & Hansson, G. C. A complex, but uniform O-glycosylation of the human MUC2 mucin from colonic biopsies analyzed by nanoLC/MSn. *Glycobiology* **19,** 756–66 (2009).

128. Johansson, M. E. V, Sjövall, H. & Hansson, G. C. The gastrointestinal mucus system in health and disease. *Nat. Rev. Gastroenterol. Hepatol.* **10,** 352–61 (2013).

129. Raouf, A. H. *et al.* Sulphation of colonic and rectal mucin in inflammatory bowel disease: reduced sulphation of rectal mucus in ulcerative colitis. *Clin. Sci. (Lond).* **83,** 623–6 (1992).

130. Larsson, J. M. H. *et al.* Altered O-glycosylation profile of MUC2 mucin occurs in active ulcerative colitis and is associated with increased inflammation. *Inflamm. Bowel Dis.* **17,** 2299–2307 (2011).

131. Podolsky, D. K. & Isselbacher, K. J. Composition of human colonic mucin. {Selective} alteration in inflammatory bowel disease. *J. Clin. Invest.* **72,** 142–153 (1983).

132. Heazlewood, C. K. *et al.* Aberrant mucin assembly in mice causes endoplasmic reticulum stress and spontaneous inflammation resembling ulcerative colitis. *PLoS Med.* **5,** e54 (2008).

133. Renes, I. B. *et al.* Alterations in Muc2 biosynthesis and secretion during dextran sulfate sodium-induced colitis. *Am. J. Physiol. Gastrointest. Liver Physiol.* **282,** G382–G389 (2002).

134. Van der Sluis, M. *et al.* Muc2-Deficient Mice Spontaneously Develop Colitis, Indicating That MUC2 Is Critical for Colonic Protection. *Gastroenterology* **131,** 117–129 (2006).

135. Rigottier-Gois, L. Dysbiosis in inflammatory bowel diseases: the oxygen hypothesis. *ISME J.* **7,** 1256–61 (2013).

136. Triantafillidis, J. K., Nasioulas, G. & Kosmidis, P. a. Colorectal cancer and inflammatory bowel disease: Epidemiology, risk factors, mechanisms of carcinogenesis and prevention strategies. *Anticancer Res.* **29,** 2727–2737 (2009).

137. Byrd, J. & Bresalier, R. Mucins and mucin binding proteins in colorectal cancer. *Cancer Metastasis Rev.* **23,** 77–99 (2004).

138. Holst, S., Wuhrer, M. & Rombouts, Y. in *Advances in Cancer Research* **126,** 203–256 (2015).

139. Iwai, T. *et al.* Core 3 synthase is down-regulated in colon carcinoma and profoundly suppresses the metastatic potential of carcinoma cells. *Proc. Natl. Acad. Sci. U. S. A.* **102,** 4572–7 (2005).

140. An, G. *et al.* Increased susceptibility to colitis and colorectal tumors in mice lacking core 3-derived O-glycans. *J. Exp. Med.* **204,** 1417–1429 (2007).

141. Fleming, M., Ravula, S., Tatishchev, S. F. & Wang, H. L. Colorectal carcinoma: Pathologic aspects. *J. Gastrointest. Oncol.* **3,** 153–73 (2012).

142. Kaser, A. & Blumberg, R. S. Endoplasmic reticulum stress in the intestinal epithelium and inflammatory bowel disease. *Semin. Immunol.* **21,** 156–163 (2009).

143. Johansson, M. E. V *et al.* The inner of the two Muc2 mucin-dependent mucus layers in colon is devoid of bacteria. *Proc. Natl. Acad. Sci. U. S. A.* **105,** 15064–9 (2008).

144. Zarepour, M. *et al.* The mucin muc2 limits pathogen burdens and epithelial barrier dysfunction during salmonella enterica serovar typhimurium colitis. *Infect. Immun.* **81,** 3672–3683 (2013).

145. Bergstrom, K. S. B. *et al.* Muc2 protects against lethal infectious colitis by disassociating pathogenic and commensal bacteria from the colonic mucosa. *PLoS Pathog.* **6,** 1–25 (2010).

146. Rogier, E. W., Frantz, A. L., Bruno, M. E. C. & Kaetzel, C. S. Secretory IgA is Concentrated in the Outer Layer of Colonic Mucus along with Gut Bacteria. *Pathog. (Basel, Switzerland)* **3,** 390–403 (2014).

147. Moss, A. K. *et al.* Intestinal alkaline phosphatase inhibits the proinflammatory nucleotide uridine diphosphate. *Am. J. Physiol. Gastrointest. Liver Physiol.* **304,** G597–604 (2013).

148. Bates, J. M., Akerlund, J., Mittge, E. & Guillemin, K. Intestinal Alkaline Phosphatase Detoxifies Lipopolysaccharide and Prevents Inflammation in Zebrafish in Response to the Gut Microbiota. *Cell Host Microbe* **2,** 371–382 (2007).

149. Yang, K. *et al.* Interaction of Muc2 and Apc on Wnt signaling and in intestinal tumorigenesis: potential role of chronic inflammation. *Cancer Res.* **68,** 7313–22 (2008).

150. Fu, J. *et al.* Loss of intestinal core 1-derived O-glycans causes spontaneous colitis in mice. *J. Clin. Invest.* **121,** 1657–66 (2011).

151. Stone, E. L., Lee, S. H., Ismail, M. N. & Fukuda, M. Characterization of mice with targeted deletion of the gene encoding core 2 ??1,6-N-acetylglucosaminyltransferase-2. *Methods Enzymol.* **479,** 155–172 (2010).

152. Bergstrom, K. S. B. & Xia, L. Mucin-type O-glycans and their roles in intestinal homeostasis. *Glycobiology* **23,** 1026–1037 (2013).

153. Robbe, C. *et al.* Evidence of regio-specific glycosylation in human intestinal mucins: presence of an acidic gradient along the intestinal tract. *J. Biol. Chem.* **278,** 46337–48 (2003).

154. Tobisawa, Y., Imai, Y., Fukuda, M. & Kawashima, H. Sulfation of colonic mucins by N-acetylglucosamine 6-O-sulfotransferase-2 and its protective function in experimental colitis in mice. *J. Biol. Chem.* **285,** 6750–60 (2010).

155. Ju, T., Otto, V. I. & Cummings, R. D. The Tn antigen-structural simplicity and biological complexity. *Angew. Chem. Int. Ed. Engl.* **50,** 1770–91 (2011).

156. Berger, E. G. Tn-syndrome. *Biochim. Biophys. Acta - Mol. Basis Dis.* **1455,** 255–268 (1999).

157. Ta, A. *et al.* Sialyl-tn antigen expression in Crohn's colitis. *Inflamm Bowel Dis* **3,** 254–259 (1997).

158. Theodoratou, E. *et al.* The role of glycosylation in IBD. *Nat. Rev. Gastroenterol. Hepatol.* **11,** 588–600 (2014).

159. Becker, D. J. & Lowe, J. B. Fucose: biosynthesis and biological function in mammals.

Glycobiology **13,** 41R–53R (2003).

160. Hurd, E. A., Holmén, J. M., Hansson, G. C. & Domino, S. E. Gastrointestinal mucins of Fut2-null mice lack terminal fucosylation without affecting colonization by Candida albicans. *Glycobiology* **15,** 1002–7 (2005).

161. Pickard, J. M. & Chervonsky, A. V. Intestinal Fucose as a Mediator of Host-Microbe Symbiosis. *J. Immunol.* **194,** 5588–5593 (2015).

162. Hooper, L. V, Xu, J., Falk, P. G., Midtvedt, T. & Gordon, J. I. A molecular sensor that allows a gut commensal to control its nutrient foundation in a competitive ecosystem. *Proc. Natl. Acad. Sci. U. S. A.* **96,** 9833–9838 (1999).

163. Pickard, J. M. *et al.* Rapid fucosylation of intestinal epithelium sustains host–commensal symbiosis in sickness. *Nature* **514,** 638–641 (2014).

164. Kamada, N. *et al.* Regulated Virulence Controls the Ability of a Pathogen to Compete with the Gut Microbiota. *Science (80-.).* **336,** 1325–1329 (2012).

165. Kato, K. & Ishiwa, A. The role of carbohydrates in infection strategies of enteric pathogens. *Trop. Med. Health* **43,** 41–52 (2015).

166. Iversen, H. *et al.* The gut bacterium Bacteroides thetaiotaomicron influences the virulence potential of the enterohemorrhagic Escherichia coli O103:H25. *PLoS One* **10,** e0118140 (2015).

167. Pacheco, A. R. *et al.* Fucose sensing regulates bacterial intestinal colonization. *Nature* **492,** 113–7 (2012).

168. Snider, T. a., Fabich, A. J., Conway, T. & Clinkenbeard, K. D. E. coli O157:H7 catabolism of intestinal mucin-derived carbohydrates and colonization. *Vet. Microbiol.* **136,** 150–154 (2009).

169. Chang, D.E. *et al.* Carbon nutrition of Escherichia coli in the mouse intestine. *Proc. Natl. Acad. Sci. U. S. A.* **101,** 7427–32 (2004).

170. Barthel, M. *et al.* Pretreatment of mice with streptomycin provides a Salmonella enterica serovar Typhimurium colitis model that allows analysis of both pathogen and host. *Infect. Immun.* **71,** 2839–2858 (2003).

171. Wlodarska, M. *et al.* Antibiotic treatment alters the colonic mucus layer and predisposes the host to exacerbated Citrobacter rodentium-induced colitis. *Infect. Immun.* **79,** 1536–1545 (2011).

172. Sonnenburg, J. L. *et al.* Glycan foraging in vivo by an intestine-adapted bacterial symbiont. *Science* **307,** 1955–1959 (2005).

173. Scott, K. P., Martin, J. C., Campbell, G., Mayer, C.-D. & Flint, H. J. Whole-genome transcription profiling reveals genes up-regulated by growth on fucose in the human gut bacterium 'Roseburia inulinivorans'. *J. Bacteriol.* **188,** 4340–9 (2006).

174. Oliver, M. G. & Specian, R. D. Cytoskeleton of intestinal goblet cells: role of actin filaments in baseline secretion. *Am. J. Physiol.* **259,** G991–7 (1990).

175. Giblin, J. P., Hewlett, L. J. & Hannah, M. J. Basal secretion of von Willebrand factor from human endothelial cells. *Blood* **112,** 957–64 (2008).

176. Navarro-Garcia, F. *et al.* Pic, an autotransporter protein secreted by different pathogens in the Enterobacteriaceae family, is a potent mucus secretagogue. *Infect. Immun.* **78,** 4101–4109 (2010).

177. Specian, R. D. & Neutra, M. R. Mechanism of rapid mucus secretion in goblet cells stimulated by acetylcholine. *J. Cell Biol.* **85,** 626–640 (1980).

178. Specian, R. D. & Neutra, M. R. Regulation of intestinal goblet cell secretion. I. Role of parasympathetic stimulation. *Am. J. Physiol.* **242,** G370–9 (1982).

179. Dabbagh, K. *et al.* IL-4 induces mucin gene expression and goblet cell metaplasia in vitro and in vivo. *J. Immunol.* **162,** 6233–6237 (1999).

180. Jarry, A. *et al.* Interferon-gamma modulates cAMP-induced mucin exocytosis without affecting mucin gene expression in a human colonic goblet cell line. *Eur J Pharmacol* **267,** 95–103. (1994).

181. Neutra, M. R., O'Malley, L. J. & Specian, R. D. Regulation of intestinal goblet cell secretion. II. A survey of potential secretagogues. *Am. J. Physiol.* **242,** G380–G387 (1982).

182. Hoskins, L. C. Mucin degradation in the human gastrointestinal tract and its significance to enteric microbial ecology. *Eur. J. Gastroenterol. Hepatol.* **5,** 205–213 (1992).

183. Van Klinken, B. J., Van der Wal, J. W., Einerhand, a W., Büller, H. a & Dekker, J. Sulphation and secretion of the predominant secretory human colonic mucin MUC2 in ulcerative colitis. *Gut* **44,** 387–393 (1999).

184. Morita, H., Kettlewell, M. G., Jewell, D. P. & Kent, P. W. Glycosylation and sulphation of colonic mucus glycoproteins in patients with ulcerative colitis and in healthy subjects. *Gut* **34,** 926–32 (1993).

185. Linden, S. K. & Mcguckin, M. A. Microbes at the host surface. *Most* 591–596 (2010).

186. Ng, G. Z. *et al.* The MUC1 mucin protects against Helicobacter pylori pathogenesis in mice by regulation of the NLRP3 inflammasome. *Gut* (2015). doi:10.1136/gutjnl-2014-307175

187. Lindén, S. K. *et al.* MUC1 limits Helicobacter pylori infection both by steric hindrance and by acting as a releasable decoy. *PLoS Pathog.* **5,** e1000617 (2009).

188. Tanaka, S. *et al.* H. pylori decreases gastric mucin synthesis via inhibition of galactosyltransferase. *Hepatogastroenterology.* **50,** 1739–1742 (2003).

189. McAuley, J. L. *et al.* MUC1 cell surface mucin is a critical element of the mucosal barrier to infection. *J. Clin. Invest.* **117,** 2313–2324 (2007).

190. Lindén S. K., Florin, T. H. J., McGuckin, M. A. Mucin dynamics in intestinal bacterial infection. *PLoS One* **3,** e3952–e3952 (2008).

191. Vimal, D. B., Khullar, M., Gupta, S. & Ganguly, N. K. Intestinal mucins: the binding sites for Salmonella typhimurium. *Mol. Cell. Biochem.* **204,** 107–117 (2000).

192. Ramos, H. C., Rumbo, M. & Sirard, J. C. Bacterial flagellins: Mediators of pathogenicity and host immune responses in mucosa. *Trends Microbiol.* **12,** 509–517 (2004).

193. Haiko, J. & Westerlund-Wikström, B. The role of the bacterial flagellum in adhesion and virulence. *Biology (Basel).* **2,** 1242–67 (2013).

194. Celli, J. P. *et al.* Helicobacter pylori moves through mucus by reducing mucin viscoelasticity. *Proc. Natl. Acad. Sci. U. S. A.* **106,** 14321–14326 (2009).

195. Zautner, A. E., Tareen, A. M., Groß, U. & Lugert, R. Chemotaxis in Campylobacter jejuni. *Eur. J. Microbiol. Immunol. (Bp).* **2,** 24–31 (2012).

196. Hermans, D. *et al.* Colonization factors of Campylobacter jejuni in the chicken gut. *Vet. Res.* **42,** 82 (2011).

197. Tu, Q. V, McGuckin, M. a & Mendz, G. L. Campylobacter jejuni response to human mucin MUC2: modulation of colonization and pathogenicity determinants. *J. Med. Microbiol.* **57,** 795–802 (2008).

198. Aristoteli, L. P. & Willcox, M. D. P. Mucin degradation mechanisms by distinct Pseudomonas aeruginosa isolates in vitro. *Infect. Immun.* **71,** 5565–75 (2003).

199. Martens, E. C., Roth, R., Heuser, J. E. & Gordon, J. I. Coordinate regulation of glycan degradation and polysaccharide capsule biosynthesis by a prominent human gut symbiont. *J. Biol. Chem.* **284,** 18445–18457 (2009).

200. Lewis, W. G., Robinson, L. S., Gilbert, N. M., Perry, J. C. & Lewis, A. L. Degradation, foraging, and depletion of mucus sialoglycans by the vagina-adapted actinobacterium Gardnerella vaginalis. *J. Biol. Chem.* **288,** 12067–12079 (2013).

201. Lidell, M. E., Moncada, D. M., Chadee, K. & Hansson, G. C. Entamoeba histolytica cysteine proteases cleave the MUC2 mucin in its C-terminal domain and dissolve the protective colonic mucus gel. *Proc. Natl. Acad. Sci. U. S. A.* **103,** 9298–303 (2006).

202. Slomiany, B. L. *et al.* Campylobacter pyloridis degrades mucin and undermines gastric mucosal integrity. *Biochem. Biophys. Res. Commun.* **144,** 307–14 (1987).

203. Silva, A. J., Pham, K. & Benitez, J. a. Haemagglutinin/protease expression and mucin gel penetration in El Tor biotype Vibrio cholerae. *Microbiology* **149,** 1883–1891 (2003).

204. Henderson, I. R., Czeczulin, J., Eslava, C., Noriega, F. & Nataro, J. P. Characterization of pic, a secreted protease of Shigella flexneri and enteroaggregative Escherichia coli. *Infect. Immun.* **67,** 5587–96 (1999).

205. Behrens, M., Sheikh, J. & Nataro, J. P. Regulation of the overlapping pic/set locus in Shigella flexneri and enteroaggregative Escherichia coli. *Infect. Immun.* **70,** 2915–25 (2002).

206. Harrington, S. M. *et al.* The pic protease of enteroaggregative Escherichia coli promotes intestinal colonization and growth in the presence of mucin. *Infect. Immun.* **77,** 2465–2473

(2009).

207. Nicoletti, C. Unsolved mysteries of intestinal M cells. *Gut* **47,** 735–739 (2000).

208. Lelouard, H., Reggio, H., Mangeat, P., Neutra, M. & Montcourrier, P. Mucin-Related Epitopes Distinguish M Cells and Enterocytes in Rabbit Appendix and Peyer's Patches. *Infect. Immun.* **67,** 357–367 (1999).

209. Gopal, A., Iyer, S. C., Gopal, U., Devaraj, N. & Halagowder, D. Shigella dysenteriae Modulates BMP Pathway to Induce Mucin Gene Expression In Vivo and In Vitro. *PLoS One* **9,** e111408 (2014).

210. Songhet, P. *et al.* Stromal IFN-γR-signaling modulates goblet cell function during Salmonella Typhimurium infection. *PLoS One* **6,** e22459 (2011).

211. Luperchio, S. a. & Schauer, D. B. Molecular pathogenesis of Citrobacter rodentium and transmissible murine colonic hyperplasia. *Microbes Infect.* **3,** 333–340 (2001).

212. Petty, N. K. *et al.* The Citrobacter rodentium genome sequence reveals convergent evolution with human pathogenic Escherichia coli. *J. Bacteriol.* **192,** 525–38 (2010).

213. Maaser, C. *et al.* Clearance of Citrobacter rodentium requires B cells but not secretory immunoglobulin A (IgA) or IgM antibodies. *Infect Immun* **72,** 3315–3324 (2004).

214. Koroleva, E. P. *et al.* Citrobacter rodentium-induced colitis: A robust model to study mucosal immune responses in the gut. *J. Immunol. Methods* **421,** 61–72 (2015).

215. Gibson, D. L. *et al.* MyD88 signalling plays a critical role in host defence by controlling pathogen burden and promoting epithelial cell homeostasis during Citrobacter rodentium-induced colitis. *Cell. Microbiol.* **10,** 618–631 (2008).

216. Vallance, B. A. *et al.* Modulation of inducible nitric oxide synthase expression by the attaching and effacing bacterial pathogen citrobacter rodentium in infected mice. *Infect. Immun.* **70,** 6424–6435 (2002).

217. Gibson, D. L. *et al.* Toll-like receptor 2 plays a critical role in maintaining mucosal integrity during Citrobacter rodentium-induced colitis. *Cell. Microbiol.* **10,** 388–403 (2008).

218. Khan, M. A. *et al.* Toll-like receptor 4 contributes to colitis development but not to host defense during Citrobacter rodentium infection in mice. *Infect. Immun.* **74,** 2522–2536 (2006).

219. Bry, L., Brigl, M. & Brenner, M. B. CD4+-T-cell effector functions and costimulatory requirements essential for surviving mucosal infection with Citrobacter rodentium. *Infect. Immun.* **74,** 673–681 (2006).

220. Shiomi, H. *et al.* Gamma interferon produced by antigen-specific CD4+ T cells regulates the mucosal immune responses to Citrobacter rodentium infection. *Infect. Immun.* **78,** 2653–2666 (2010).

221. Lupp, C. *et al.* Host-Mediated Inflammation Disrupts the Intestinal Microbiota and Promotes the Overgrowth of Enterobacteriaceae. *Cell Host & Microbe* **2,** 119–129

(2007).

222. Coburn, B., Grassl, G. a & Finlay, B. B. Salmonella, the host and disease: a brief review. *Immunol. Cell Biol.* **85,** 112–118 (2007).

223. Ohl, M. E. & Miller, S. I. Salmonella: a model for bacterial pathogenesis. *Annu. Rev. Med.* **52,** 259–274 (2001).

224. Vidal, S. *et al.* The Ity/Lsh/Bcg locus: natural resistance to infection with intracellular parasites is abrogated by disruption of the Nramp1 gene. *J. Exp. Med.* **182,** 655–66 (1995).

225. Chatfield, S. N. *et al.* Evaluation of Salmonella typhimurium strains harbouring defined mutations in htrA and aroA in the murine salmonellosis model. *Microb Pathog* **12,** 145–151 (1992).

226. Månsson, L. E. *et al.* MyD88 signaling promotes both mucosal homeostatic and fibrotic responses during Salmonella-induced colitis. *Am. J. Physiol. Gastrointest. Liver Physiol.* **303,** G311–23 (2012).

227. Kaur, J. & Jain, S. K. Role of antigens and virulence factors of Salmonella enterica serovar Typhi in its pathogenesis. *Microbiol. Res.* **167,** 199–210 (2012).

228. Hansen-Wester, I., Hansen-Wester, I., Hensel, M. & Hensel, M. Salmonella pathogenicity islands encoding type III secretion systems. *Microbes Infect.* **3,** 549–59 (2001).

229. Deiwick, J., Nikolaus, T., Erdogan, S. & Hensel, M. Environmental regulation of Salmonella pathogenicity island 2 gene expression. *Mol. Microbiol.* **31,** 1759–1773 (1999).

230. Coburn, B., Li, Y., Owen, D., Vallance, B. A. & Finlay, B. B. Salmonella enterica serovar Typhimurium pathogenicity island 2 is necessary for complete virulence in a mouse model of infectious enterocolitis. *Infect. Immun.* **73,** 3219–27 (2005).

231. Arpaia, N. *et al.* TLR signaling is required for salmonella typhimurium virulence. *Cell* **144,** 675–688 (2011).

232. Talbot, S. *et al.* Toll-like receptor 4 signalling through MyD88 is essential to control Salmonella enterica serovar Typhimurium infection, but not for the initiation of bacterial clearance. *Immunology* **128,** 472–483 (2009).

233. Simon, R. & Samuel, C. E. Activation of NF-??B-dependent gene expression by Salmonella flagellins FliC and FljB. *Biochem. Biophys. Res. Commun.* **355,** 280–285 (2007).

234. Hayashi, F. *et al.* The innate immune response to bacterial flagellin is mediated by Toll-like receptor 5. *Nature* **410,** 1099–1103 (2001).

235. Brinkmann, V. & Zychlinsky, A. Neutrophil extracellular traps: Is immunity the second function of chromatin? *J. Cell Biol.* **198,** 773–783 (2012).

236. Brinkmann, V. *et al.* Neutrophil extracellular traps kill bacteria. *Science (80-.).* **303,** 1532–1535 (2004).

237. Cheminay, C., Chakravortty, D. & Hensel, M. Role of neutrophils in murine salmonellosis. *Infect. Immun.* **72,** 468–77 (2004).

238. Boyle, E. C., Brown, N. F. & Finlay, B. B. Salmonella enterica serovar Typhimurium effectors SopB, SopE, SopE2 and SipA disrupt tight junction structure and function. *Cell. Microbiol.* **8,** 1946–1957 (2006).

239. Hardt, W. D., Chen, L. M., Schuebel, K. E., Bustelo, X. R. & Galán, J. E. S. typhimurium Encodes an activator of Rho GTPases that induces membrane ruffling and nuclear responses in host cells. *Cell* **93,** 815–826 (1998).

240. Patel, S. & McCormick, B. a. Mucosal inflammatory response to Salmonella typhimurium infection. *Front. Immunol.* **5,** 1–10 (2014).

241. Hallstrom, K. & McCormick, B. a. Salmonella Interaction with and Passage through the Intestinal Mucosa: Through the Lens of the Organism. *Front. Microbiol.* **2,** 88 (2011).

242. Stecher, B. *et al.* Flagella and chemotaxis are required for efficient induction of Salmonella enterica serovar Typhimurium colitis in streptomycin-pretreated mice. *Infect. Immun.* **72,** 4138–50 (2004).

243. McCormick, B. a, Stocker, B. a, Laux, D. C. & Cohen, P. S. Roles of motility, chemotaxis, and penetration through and growth in intestinal mucus in the ability of an avirulent strain of *Salmonella* typhimurium to colonize the large intestine of streptomycin-treated mice. *Infect. Immun.* **56,** 2209–17 (1988).

244. Dautin, N. Serine protease autotransporters of enterobacteriaceae (SPATEs): biogenesis and function. *Toxins (Basel).* **2,** 1179–206 (2010).

245. Dutta, P. R., Cappello, R., Navarro-Garcia, F. & Nataro, J. P. Functional Comparison of Serine Protease Autotransporters of Enterobacteriaceae. *Infect. Immun.* **70,** 7105–7113 (2002).

246. Yen, Y. T., Kostakioti, M., Henderson, I. R. & Stathopoulos, C. Common themes and variations in serine protease autotransporters. *Trends Microbiol.* **16,** 370–9 (2008).

247. Boisen, N., Ruiz-Perez, F., Scheutz, F., Krogfelt, K. a & Nataro, J. P. Short report: high prevalence of serine protease autotransporter cytotoxins among strains of enteroaggregative Escherichia coli. *Am. J. Trop. Med. Hyg.* **80,** 294–301 (2009).

248. Coburn, B., Sekirov, I. & Finlay, B. B. Type III secretion systems and disease. *Clin Microbiol Rev* **20,** 535–549 (2007).

249. Henderson, I. R., Navarro-Garcia, F., Desvaux, M., Fernandez, R. C. & Ala'Aldeen, D. Type V Protein Secretion Pathway: the Autotransporter Story. *Microbiol. Mol. Biol. Rev.* **68,** 692–744 (2004).

250. Van Ulsen, P., Rahman, S. U., Jong, W. S. P., Daleke-Schermerhorn, M. H. & Luirink, J. Type V secretion: From biogenesis to biotechnology. *Biochim. Biophys. Acta - Mol. Cell Res.* **1843,** 1592–1611 (2014).

251. Desvaux, M., Parham, N. J. & Henderson, I. R. The autotransporter secretion system. *Res.*

Microbiol. **155,** 53–60 (2004).

252. Dautin, N. & Bernstein, H. D. Protein secretion in gram-negative bacteria via the autotransporter pathway. *Annu. Rev. Microbiol.* **61,** 89–112 (2007).

253. Rutherford, N. & Mourez, M. Surface display of proteins by gram-negative bacterial autotransporters. *Microb. Cell Fact.* **5,** 22 (2006).

254. Yen, Y. T. *et al.* Common themes and variations in serine protease autotransporters. *Trends Microbiol.* **16,** 370–9 (2014).

255. Ruiz-Perez, F. & Nataro, J. P. Bacterial serine proteases secreted by the autotransporter pathway: Classification, specificity, and role in virulence. *Cell. Mol. Life Sci.* **71,** 745–770 (2014).

256. Gutiérrez-Jiménez, J., Arciniega, I. & Navarro-García, F. The serine protease motif of Pic mediates a dose-dependent mucolytic activity after binding to sugar constituents of the mucin substrate. *Microb. Pathog.* **45,** 115–23 (2008).

257. Ruiz-Perez, F. *et al.* Serine protease autotransporters from Shigella flexneri and pathogenic Escherichia coli target a broad range of leukocyte glycoproteins. *Proc. Natl. Acad. Sci. U. S. A.* **108,** 12881–6 (2011).

258. Ayala-Lujan, J. L. *et al.* Broad spectrum activity of a lectin-like bacterial serine protease family on human leukocytes. *PLoS One* **9,** e107920 (2014).

259. Parham, N. J. *et al.* PicU, a second serine protease autotransporter of uropathogenic Escherichia coli. *FEMS Microbiol. Lett.* **230,** 73–83 (2004).

260. Celik, N. *et al.* A bioinformatic strategy for the detection, classification and analysis of bacterial autotransporters. *PLoS One* **7,** e43245 (2012).

261. Vijayakumar, V. *et al.* Role of class 1 serine protease autotransporter in the pathogenesis of Citrobacter rodentium colitis. *Infect. Immun.* **82,** 2626–36 (2014).

262. Datsenko, K. A. & Wanner, B. L. One-step inactivation of chromosomal genes in Escherichia coli K-12 using PCR products. *Proc. Natl. Acad. Sci. U. S. A.* **97,** 6640–6645 (2000).

263. Datta, S., Costantino, N. & Court, D. L. A set of recombineering plasmids for gram-negative bacteria. *Gene* **379,** 109–15 (2006).

264. Cherepanov, P. P. & Wackernagel, W. Gene disruption in Escherichia coli: TcR and KmR cassettes with the option of Flp-catalyzed excision of the antibiotic-resistance determinant. *Gene* **158,** 9–14 (1995).

265. Lutz, R. & Bujard, H. Independent and tight regulation of transcriptional units in escherichia coli via the LacR/O, the TetR/O and AraC/I1-I2 regulatory elements. *Nucleic Acids Res.* **25,** 1203–1210 (1997).

266. Ho, S. N., Hunt, H. D., Horton, R. M., Pullen, J. K. & Pease, L. R. Site-directed mutagenesis by overlap extension using the polymerase chain reaction. *Gene* **77,** 51–59 (1989).

267. Edwards, R. a., Keller, L. H. & Schifferli, D. M. Improved allelic exchange vectors and their use to analyze 987P fimbria gene expression. *Gene* **207,** 149–157 (1998).

268. Caballero-Franco, C., Keller, K., De Simone, C. & Chadee, K. The VSL#3 probiotic formula induces mucin gene expression and secretion in colonic epithelial cells. *Am. J. Physiol. Gastrointest. Liver Physiol.* **292,** G315–G322 (2007).

269. Ma, Q. & Wood, T. K. OmpA influences Escherichia coli biofilm formation by repressing cellulose production through the CpxRA two-component system. *Environ. Microbiol.* **11,** 2735–2746 (2009).

270. Newman, J. V, Zabel, B. A., Jha, S. S. & Schauer, D. B. Citrobacter rodentium espB is necessary for signal transduction and for infection of laboratory mice. *Infect. Immun.* **67,** 6019–25 (1999).

271. Kenny, B., Abe, A., Stein, M. & Finlay, B. B. Enteropathogenic Escherichia coli protein secretion is induced in response to conditions similar to those in the gastrointestinal tract. *Infect. Immun.* **65,** 2606–2612 (1997).

272. Galán, J. E., Ginocchio, C. & Costeas, P. Molecular and functional characterization of the Salmonella invasion gene invA: homology of InvA to members of a new protein family. *J. Bacteriol.* **174,** 4338–49 (1992).

273. Galán, J. E. & Curtiss, R. Cloning and molecular characterization of genes whose products allow Salmonella typhimurium to penetrate tissue culture cells. *Proc. Natl. Acad. Sci. U. S. A.* **86,** 6383–7 (1989).

274. Santos, R. L. *et al.* Animal models of Salmonella infections: Enteritis versus typhoid fever. *Microbes Infect.* **3,** 1335–1344 (2001).

275. Pusztai, A. *et al.* Lectins and also bacteria modify the glycosylation of gut surface receptors in the rat. *Glycoconj. J.* **12,** 22–35 (1995).

276. Robbe-Masselot, C., Herrmann, A., Carlstedt, I., Michalski, J.-C. & Capon, C. Glycosylation of the two O-glycosylated domains of human MUC2 mucin in patients transposed with artificial urinary bladders constructed from proximal colonic tissue. *Glycoconj. J.* **25,** 213–24 (2008).

277. Holmén, J. M., Olson, F. J., Karlsson, H. & Hansson, G. C. Two glycosylation alterations of mouse intestinal mucins due to infection caused by the parasite Nippostrongylus brasiliensis. *Glycoconj. J.* **19,** 67–75 (2002).

278. Iwai, T. *et al.* Molecular cloning and characterization of a novel UDP-GlcNAc:GalNAc-peptide beta1,3-N-acetylglucosaminyltransferase (beta 3Gn-T6), an enzyme synthesizing the core 3 structure of O-glycans. *J. Biol. Chem.* **277,** 12802–12809 (2002).

279. Lalles, J. P. Intestinal alkaline phosphatase: multiple biological roles in maintenance of intestinal homeostasis and modulation by diet. *Nutr Rev* **68,** 323–332 (2010).

280. Poelstra, K., Bakker, W. W., Klok, P. A., Hardonk, M. J. & Meijer, D. K. F. A Physiologic Function For Alkaline Phosphatase - Endotoxin Detoxification. *Lab. Investig.* **76,** 319–327 (1997).

281. Poelstra, K. *et al.* Dephosphorylation of endotoxin by alkaline phosphatase in vivo. *Am. J. Pathol.* **151,** 1163–1169 (1997).

282. Goldberg, R. F. *et al.* Intestinal alkaline phosphatase is a gut mucosal defense factor maintained by enteral nutrition. *Proc. Natl. Acad. Sci. U. S. A.* **105,** 3551–3556 (2008).

283. Beumer, C. *et al.* Calf intestinal alkaline phosphatase, a novel therapeutic drug for lipopolysaccharide (LPS)-mediated diseases, attenuates LPS toxicity in mice and piglets. *J. Pharmacol. Exp. Ther.* **307,** 737–744 (2003).

284. Veen, S. Q. V *et al.* Bovine Intestinal Alkaline Phosphatase Attenuates the Inflammatory Response in Secondary Peritonitis in Mice. *Infect. Immun.* **73,** 4309–4314 (2005).

285. Bentala, H. *et al.* Removal of phosphate from lipid A as a strategy to detoxify lipopolysaccharide. *Shock* **18,** 561–6 (2002).

286. Ghosh, S. *et al.* Fish oil attenuates omega-6 polyunsaturated fatty acid-induced dysbiosis and infectious colitis but impairs LPS dephosphorylation activity causing sepsis. *PLoS One* **8,** e55468 (2013).

287. Mantle, M., Basaraba, L., Peacock, S. C. & Gall, D. G. Binding of Yersinia enterocolitica to rabbit intestinal brush border membranes, mucus, and mucin. *Infect. Immun.* **57,** 3292–3299 (1989).

288. Nutten, S. *et al.* Epithelial inflammation response induced by Shigella flexneri depends on mucin gene expression. *Microbes Infect.* **4,** 1121–1124 (2002).

289. Hess, J., Ladel, C., Miko, D. & Kaufmann, S. H. Salmonella typhimurium aroA- infection in gene-targeted immunodeficient mice: major role of CD4+ TCR-alpha beta cells and IFN-gamma in bacterial clearance independent of intracellular location. *J Immunol* **156,** 3321–3326 (1996).

290. Özkaya, H. *et al.* Salmonella typhimurium infections in BALB/c mice: A comparison of tissue bioluminescence, tissue cultures and mice clinical scores. *New Microbiol.* **35,** 53–59 (2012).

291. Vazquez-Torres, A. *et al.* Toll-like receptor 4 dependence of innate and adaptive immunity to Salmonella: importance of the Kupffer cell network. *J. Immunol.* **172,** 6202–6208 (2004).

292. Lillehoj, E. P. *et al.* Muc1 mucins on the cell surface are adhesion sites for Pseudomonas aeruginosa. *Am. J. Physiol. Lung Cell. Mol. Physiol.* **280,** L181–L187 (2001).

293. Rajkumar, R., Devaraj, H. & Niranjali, S. Binding of Shigella to rat and human intestinal mucin. *Mol. Cell. Biochem.* **178,** 261–268 (1998).

294. Berg, R. D. The indigenous gastrointestinal microflora. *Trends Microbiol.* **4,** 430–435 (1996).

295. Finlay, B. B. & Falkow, S. Salmonella interactions with polarized human intestinal Caco-2 epithelial cells. *J. Infect. Dis.* **162,** 1096–1106 (1990).

296. Jepson, M. a, Collares-Buzato, C. B., Clark, M. a, Hirst, B. H. & Simmons, N. L. Rapid

disruption of epithelial barrier function by Salmonella typhimurium is associated with structural modification of intercellular junctions. *Infect. Immun.* **63,** 356–9 (1995).

297. Coombes, B. K. *et al.* Analysis of the Contribution of Salmonella Pathogenicity Islands 1 and 2 to Enteric Disease Progression Using a Novel Bovine Ileal Loop Model and a Murine Model of Infectious Enterocolitis. **73,** 7161–7169 (2005).

298. Yrlid, U. *et al.* In vivo activation of dendritic cells and T cells during Salmonella enterica serovar Typhimurium infection. *Infect. Immun.* **69,** 5726–35 (2001).

299. Kalupahana, R. S., Mastroeni, P., Maskell, D. & Blacklaws, B. A. Activation of murine dendritic cells and macrophages induced by Salmonella enterica serovar Typhimurium. *Immunology* **115,** 462–472 (2005).

300. Wales, a. D., Woodward, M. J. & Pearson, G. R. Attaching-effacing bacteria in animals. *J. Comp. Pathol.* **132,** 1–26 (2005).

301. Mundy, R., MacDonald, T. T., Dougan, G., Frankel, G. & Wiles, S. Citrobacter rodentium of mice and man. *Cell. Microbiol.* **7,** 1697–706 (2005).

302. Bry, L. & Brenner, M. B. Critical role of T cell-dependent serum antibody, but not the gut-associated lymphoid tissue, for surviving acute mucosal infection with Citrobacter rodentium, an attaching and effacing pathogen. *J. Immunol.* **172,** 433–441 (2004).

303. Deng, W., Vallance, B. a., Li, Y., Puente, J. L. & Finlay, B. B. Citrobacter rodentium translocated intimin receptor (Tir) is an essential virulence factor needed for actin condensation, intestinal colonization and colonic hyperplasia in mice. *Mol. Microbiol.* **48,** 95–115 (2003).

304. Heimer, S. R., Rasko, D. A., Lockatell, C. V., Johnson, D. E. & Mobley, H. L. T. Autotransporter genes pic and tsh are associated with Escherichia coli strains that cause acute pyelonephritis and are expressed during urinary tract infection. *Infect. Immun.* **72,** 593–597 (2004).

305. Henderson, I. R., Meehan, M. & Owen, P. Antigen 43, a phase-variable bipartate outer membrane protein, determines colony morphology and autoaggregation in Escherichia coli K-12. *FEMS Microbiol. Lett.* **149,** 115–120 (1997).

306. Kjærgaard, K., Schembri, M. a., Ramos, C., Molin, S. & Klemm, P. Antigen 43 facilitates formation of multispecies biofilms. *Environ. Microbiol.* **2,** 695–702 (2000).

307. Sherlock, O., Schembri, M. A., Reisner, A. & Klemm, P. Novel roles for the AIDA adhesin from diarrheagenic Escherichia coli: cell aggregation and biofilm formation. *J. Bacteriol.* **186,** 8058–8065 (2004).

308. Sherlock, O., Vejborg, R. M. & Klemm, P. The TibA adhesin/invasin from enterotoxigenic Escherichia coli is self recognizing and induces bacterial aggregation and biofilm formation. *Infect. Immun.* **73,** 1954–1963 (2005).

309. Wickham, M. E., Brown, N. F., Boyle, E. C., Coombes, B. K. & Finlay, B. B. Virulence is positively selected by transmission success between mammalian hosts. *Curr.Biol.* **17,** 783–788 (2007).

310. Zogaj, X., Bokranz, W., Nimtz, M. & Römling, U. Production of cellulose and curli fimbriae by members of the family Enterobacteriaceae isolated from the human gastrointestinal tract. *Infect. Immun.* **71,** 4151–4158 (2003).

311. Bokranz, W., Wang, X., Tschäpe, H. & Römling, U. Expression of cellulose and curli fimbriae by Escherichia coli isolated from the gastrointestinal tract. *J. Med. Microbiol.* **54,** 1171–1182 (2005).

312. Dong, T., Coombes, B. K. & Schellhorn, H. E. Role of RpoS in the virulence of Citrobacter rodentium. *Infect. Immun.* **77,** 501–7 (2009).

313. White, a. P., Gibson, D. L., Kim, W., Kay, W. W. & Surette, M. G. Thin aggregative fimbriae and cellulose enhance long-term survival and persistence of Salmonella. *J. Bacteriol.* **188,** 3219–3227 (2006).

314. Young, K. T., Davis, L. M. & Dirita, V. J. Campylobacter jejuni: molecular biology and pathogenesis. *Nat. Rev. Microbiol.* **5,** 665–679 (2007).

315. Stahl, M. *et al.* A Novel Mouse Model of Campylobacter jejuni Gastroenteritis Reveals Key Pro-inflammatory and Tissue Protective Roles for Toll-like Receptor Signaling during Infection. *PLoS Pathog.* **10,** 9–11 (2014).

316. Oppong, G. O. *et al.* Epithelial cells augment barrier function via activation of the Toll-like receptor 2/phosphatidylinositol 3-kinase pathway upon recognition of Salmonella enterica serovar Typhimurium curli fibrils in the gut. *Infect. Immun.* **81,** 478–86 (2013).

317. Tükel, Ç. *et al.* CsgA is a pathogen-associated molecular pattern of Salmonella enterica serotype Typhimurium that is recognized by Toll-like receptor 2. *Mol. Microbiol.* **58,** 289–304 (2005).

318. Tukel, C. *et al.* Responses to amyloids of microbial and host origin are mediated through toll-like receptor 2. *Cell Host Microbe* **6,** 45–53 (2009).

319. Xicohtencatl-Cortes, J. *et al.* Bacterial macroscopic rope-like fibers with cytopathic and adhesive properties. *J. Biol. Chem.* **285,** 32336–32342 (2010).

320. Puttamreddy, S., Cornick, N. A. & Minion, F. C. Genome-wide transposon mutagenesis reveals a role for pO157 genes in biofilm development in Escherichia coli O157:H7 EDL933. *Infect. Immun.* **78,** 2377–84 (2010).

321. Kim, J. J. & Khan, W. I. Goblet cells and mucins: role in innate defense in enteric infections. *Pathog. (Basel, Switzerland)* **2,** 55–70 (2013).

322. Shirazi, T., Longman, R. J., Corfield, a P. & Probert, C. S. Mucins and inflammatory bowel disease. *Postgrad. Med. J.* **76,** 473–478 (2000).

323. McCormick, D. a, Horton, L. W. & Mee, a S. Mucin depletion in inflammatory bowel disease. *J. Clin. Pathol.* **43,** 143–146 (1990).

324. Fu, J. *et al.* Loss of intestinal core 1 – derived O -glycans causes spontaneous colitis in mice. *J. Clin. Invest.* **121,** 1657–66 (2011).

325. Corfield, a P. *et al.* Mucins and mucosal protection in the gastrointestinal tract: new

prospects for mucins in the pathology of gastrointestinal disease. *Gut* **47,** 589–594 (2000).

326. Robbe, C., Capon, C., Coddeville, B. & Michalski, J.-C. Structural diversity and specific distribution of O-glycans in normal human mucins along the intestinal tract. *Biochem. J.* **384,** 307–16 (2004).

327. Stahl, M. *et al.* L-fucose utilization provides Campylobacter jejuni with a competitive advantage. *Proc. Natl. Acad. Sci. U. S. A.* **108,** 7194–9 (2011).

328. Keeney, K. M. & Finlay, B. B. Microbiology: EHEC downregulates virulence in response to intestinal fucose. *Curr. Biol.* **23,** R108–R110 (2013).

329. Sekirov, I. *et al.* Antibiotic-induced perturbations of the intestinal microbiota alter host susceptibility to enteric infection. *Infect. Immun.* **76,** 4726–4736 (2008).

330. Ghosh, S. *et al.* Colonic microbiota alters host susceptibility to infectious colitis by modulating inflammation, redox status, and ion transporter gene expression. *Am. J. Physiol. Gastrointest. Liver Physiol.* **301,** G39–49 (2011).

331. Xia, L. *Core 3-derived O-glycans are essential for intestinal mucus barrier function. Methods in enzymology* **479,** (2010).

332. Gouyer, V., Gottrand, F. & Desseyn, J. L. The extraordinarily complex but highly structured organization of intestinal mucus-gel unveiled in multicolor images. *PLoS.One.* **6,** e18761– (2011).

333. Domino, S. E., Zhang, L., Gillespie, P. J., Saunders, T. L. & Lowe, J. B. Deficiency of reproductive tract alpha(1,2)fucosylated glycans and normal fertility in mice with targeted deletions of the FUT1 or FUT2 alpha(1,2)fucosyltransferase locus. *Mol. Cell. Biol.* **21,** 8336–45 (2001).

334. Domino, S. E., Zhang, L. & Lowe, J. B. Molecular cloning, genomic mapping, and expression of two secretor blood group alpha (1,2)fucosyltransferase genes differentially regulated in mouse uterine epithelium and gastrointestinal tract. *J. Biol. Chem.* **276,** 23748–56 (2001).

335. Pham, T. A. N. A. N. *et al.* Epithelial IL-22RA1-Mediated Fucosylation Promotes Intestinal Colonization Resistance to an Opportunistic Pathogen. *Cell Host Microbe* **16,** 504–516 (2014).

336. Meng, D. *et al.* Bacterial symbionts induce a FUT2-dependent fucosylated niche on colonic epithelium via ERK and JNK signaling. *Am. J. Physiol. Gastrointest. Liver Physiol.* **293,** G780–7 (2007).

337. Asker, N., Axelsson, M. a B., Olofsson, S. O. & Hansson, G. C. Dimerization of the human MUC2 mucin in the endoplasmic reticulum is followed by a N-glycosylation-dependent transfer of the mono- and dimers to the Golgi apparatus. *J. Biol. Chem.* **273,** 18857–18863 (1998).

338. Xu, Y.-X., Liu, L., Caffaro, C. E. & Hirschberg, C. B. Inhibition of Golgi apparatus glycosylation causes endoplasmic reticulum stress and decreased protein synthesis. *J. Biol. Chem.* **285,** 24600–8 (2010).

339. Xia, L. *et al.* Defective angiogenesis and fatal embryonic hemorrhage in mice lacking core 1-derived O-glycans. *J. Cell Biol.* **164,** 451–9 (2004).

340. Bhullar, K. *et al.* The serine protease autotransporter Pic modulates Citrobacter rodentium pathogenesis and its innate recognition by the host. *Infect. Immun.* **83,** IAI.00025–15 (2015).

341. Ye, J. *et al.* Core 2 Mucin-Type O-Glycan Is Related to EPEC and EHEC O157:H7 Adherence to Human Colon Carcinoma HT-29 Epithelial Cells. *Dig. Dis. Sci.* (2015). doi:10.1007/s10620-015-3548-5

342. Yaron, S. & Römling, U. Biofilm formation by enteric pathogens and its role in plant colonization and persistence. *Microb. Biotechnol.* **7,** 496–516 (2014).

343. Wang, X. *et al.* Impact of biofilm matrix components on interaction of commensal Escherichia coli with the gastrointestinal cell line HT-29. *Cell. Mol. Life Sci.* **63,** 2352–2363 (2006).

344. Bridier, A. *et al.* Biofilm-associated persistence of food-borne pathogens. *Food Microbiol.* **45,** 167–178 (2014).

345. Sommer, F. *et al.* Altered mucus glycosylation in core 1 O-glycan-deficient mice affects microbiota composition and intestinal architecture. *PLoS One* **9,** e85254 (2014).

346. Marcobal, A., Southwick, A. M., Earle, K. a. & Sonnenburg, J. L. A refined palate: Bacterial consumption of host glycans in the gut. *Glycobiology* **23,** 1038–1046 (2013).

347. Magalhaes, J. G., Tattoli, I. & Girardin, S. E. The intestinal epithelial barrier: How to distinguish between the microbial flora and pathogens. *Semin. Immunol.* **19,** 106–115 (2007).

348. Li, H. *et al.* The outer mucus layer hosts a distinct intestinal microbial niche. *Nat. Commun.* (2015). doi:10.1038/ncomms9292

349. Muraoka, W. T. & Zhang, Q. Phenotypic and genotypic evidence for L-fucose utilization by Campylobacter jejuni. *J. Bacteriol.* **193,** 1065–1075 (2011).

350. Staib, L. & Fuchs, T. M. From food to cell: Nutrient exploitation strategies of enteropathogens. *Microbiology* **160,** 1020–1039 (2014).

351. Lien, K. a, Sauer, W. C. & Fenton, M. Mucin output in ileal digesta of pigs fed a protein-free diet. *Z. Ernahrungswiss.* **36,** 182–90 (1997).

352. Monsma D.J., Vollendorf N.W., Marlett J.A. Determination of fermentable carbohydrate from the upper gastrointestinal tract by using colectomized rats. *Applied and Environmental Microbiology* **58,** 3330–3336 (1992).

353. Fabich, A. J. *et al.* Comparison of carbon nutrition for pathogenic and commensal Escherichia coli strains in the mouse intestine. *Infect. Immun.* **76,** 1143–52 (2008).

354. Hernandez-Doria, J. D. & Sperandio, V. Nutrient and chemical sensing by intestinal pathogens. *Microbes Infect.* **15,** 759–764 (2013).

355. Hollander, F. Some recent contributions to the physiology of gastric mucus secretion. *J. Natl. Cancer Inst.* **13,** 989–1005 (1953).

356. Johnson, P. and Rainsford, K. D. The physical properties of mucus: preliminary observations on the sedimentation behaviour of porcine gastric mucus. *Biochim. Biophys. Acta* **286,** 72–78 (1972).

357. A, A. Structure of gastrointestinal mucus glycoproteins and the viscous and gel-forming properties of mucus. *Br. Med. Bull.* **34,** 28–22 (1978).

358. Allen, a & Garner, a. Mucus and bicarbonate secretion in the stomach and their possible role in mucosal protection. *Gut* **21,** 249–262 (1980).

359. Rainsford, K. D. Aspirin and related drugs. 770 (2004). doi:10.1201/9780203646960.ch5

360. Stone, E. L. *et al.* Glycosyltransferase function in core 2-type protein O glycosylation. *Mol. Cell. Biol.* **29,** 3770–82 (2009).

361. Sheng, Y. H., Hasnain, S. Z., Florin, T. H. J. & McGuckin, M. a. Mucins in inflammatory bowel diseases and colorectal cancer. *J. Gastroenterol. Hepatol.* **27,** 28–38 (2012).

362. Rhodes, J. M. Colonic mucus and mucosal glycoproteins: the key to colitis and cancer? *Gut* **30,** 1660–1666 (1989).

363. Kufe, D. W. Mucins in cancer: function, prognosis and therapy. *Nat. Rev. Cancer* **9,** 874–885 (2009).

364. Ibarra, J. A. & Steele-Mortimer, O. Salmonella - the ultimate insider. Salmonella virulence factors that modulate intracellular survival. *Cell. Microbiol.* **11,** 1579–1586 (2009).

365. Lawley, T. D. *et al.* Host transmission of Salmonella enterica serovar Typhimurium is controlled by virulence factors and indigenous intestinal microbiota. *Infect. Immun.* **76,** 403–416 (2008).

366. Relman, D. A., Hamburg, M. A., Eileen, R. & Mack, A. *A Tribute to the Life and Scientific Legacies of Joshua Lederberg*. (2009).

367. Minton, K. Microbiota: support your friends to resist your enemies. *Nat. Rev. Immunol.* **14,** 715 (2014).

368. Pan, S., Chen, R., Aebersold, R. & Brentnall, T. a. Mass spectrometry based glycoproteomics--from a proteomics perspective. *Mol. Cell. Proteomics* **10,** R110.003251 (2011).

369. Hirabayashi, J. Lectin-based structural glycomics: glycoproteomics and glycan profiling. *Glycoconj. J.* **21,** 35–40 (2004).

370. Mechref, Y., Hu, Y., Desantos-Garcia, J. L., Hussein, A. & Tang, H. Quantitative glycomics strategies. *Mol. Cell. Proteomics* **12,** 874–84 (2013).

371. Bhinder, G. *et al.* Intestinal epithelium-specific MyD88 signaling impacts host susceptibility to infectious colitis by promoting protective goblet cell and antimicrobial

responses. *Infect. Immun.* **82,** 3753–3763 (2014).

372. Sheng, Y. H. *et al.* MUC1 and MUC13 differentially regulate epithelial inflammation in response to inflammatory and infectious stimuli. *Mucosal Immunol.* **6,** 557–68 (2013).

373. Moran, a P., Gupta, a & Joshi, L. Sweet-talk: role of host glycosylation in bacterial pathogenesis of the gastrointestinal tract. *Gut* **60,** 1412–1425 (2011).

374. Saldaña, Z. *et al.* Synergistic role of curli and cellulose in cell adherence and biofilm formation of attaching and effacing Escherichia coli and identification of Fis as a negative regulator of curli. *Environ. Microbiol.* **11,** 992–1006 (2009).

375. Grabinger, T. *et al.* Ex vivo culture of intestinal crypt organoids as a model system for assessing cell death induction in intestinal epithelial cells and enteropathy. *Cell Death Dis.* **5,** e1228 (2014).

376. Schumacher, M. a *et al.* The use of murine-derived fundic organoids in studies of gastric physiology. *J. Physiol.* **0,** 1–19 (2015).

377. McCracken, K. W. *et al.* Modelling human development and disease in pluripotent stem-cell-derived gastric organoids. *Nature* **516,** 400–404 (2014).